

Electronic Theses and Dissertations, 2004-2019

2017

An Analytical Investigation of Prestressed Beam Bridge Performance Before and After Widening

Chris ORiordan Adjah
University of Central Florida

 Part of the [Civil Engineering Commons](#)
Find similar works at: <https://stars.library.ucf.edu/etd>
University of Central Florida Libraries <http://library.ucf.edu>

This Doctoral Dissertation (Open Access) is brought to you for free and open access by STARS. It has been accepted for inclusion in Electronic Theses and Dissertations, 2004-2019 by an authorized administrator of STARS. For more information, please contact STARS@ucf.edu.

STARS Citation

Adjah, Chris ORiordan, "An Analytical Investigation of Prestressed Beam Bridge Performance Before and After Widening" (2017). *Electronic Theses and Dissertations, 2004-2019*. 5601.
<https://stars.library.ucf.edu/etd/5601>

AN ANALYTICAL INVESTIGATION OF PRESTRESSED BEAM
BRIDGE PERFORMANCE BEFORE AND AFTER WIDENING

by

CHRIS A. O'RIORDAN-ADJAH
B.S. Principia College, 1999
B.S. University of Central Florida, 2002
M.S. University of Central Florida, 2004
M.S. University of Central Florida, 2010

A dissertation submitted in partial fulfillment of the requirements
for the degree of Doctor of Philosophy
in the Department of Civil and Environmental Engineering
in the College of Engineering and Computer Science
at the University of Central Florida
Orlando, Florida

Summer Term
2017

Major Professor: F. Necati Catbas

© 2017 Chris A. O’Riordan – Adjah

ABSTRACT

As traffic and congestion increase, so does the likelihood of collisions. The solution to this problem is usually through a rehabilitation process with two primary options: (1) widening/expansion of existing roadway and bridges and (2) complete replacement (new construction) of roadway and bridges. The first option is the most feasible and cost-effective. While roadway widening/expansion pose minimal issues, the same cannot be said of bridge widening. An existing bridge presents a multitude of challenges during the planning and design phases, during construction, and throughout the structure's—service life. Special attention is required in both the design and detailing of the widening in order to minimize construction and maintenance problems.

The primary objective of this dissertation is to present a better understanding of structural behavior and capacity by studying an existing widened structure: a bridge that has been in service for over 40 years (constructed in 1972 and widened in 2002). The load demand on this bridge has doubled over the years. Consequently, the widened structural system is composed of four-span continuous prestressed concrete bridge segments.

To better understand the widened 2002 bridge used in this—study, an initial comparative analysis was—performed, comparing the original 1972 bridge and the 2002 widened—bridge. This comparative analysis included a determination of bridge capacity, distribution factors, and load-rating factors using current American Association of State Highway and Transportation Officials (AASHTO) Load and Resistance Factor Design (LRFD) Specifications design codes. However, the original codes used for the two bridges should also be noted, as follows: (1) the

AASHTO Load Factor Design (LFD) Code was used for the original bridge; and (2) a combination of the AASHTO LFD and AASHTO LRFD Specifications were used for the existing widened bridge. Linear three-dimensional finite element models were developed for both bridges to obtain the maximum moment and shear values with varying HL-93 load cases for these analyses.

To develop models that describe the possible existing condition of the 2002 widened bridge, a nonlinear model of one of the critical members in the structure was developed by changing the most critical parameters. The critical parameters are categorized as material properties and prestress losses. Sensitivity studies were conducted using parametric models for simulations with moving loads for the different load cases using the HL-93 truck.

The load-rating and reliability indexes were computed for all the cases under different loading conditions. The parameters that have the most influence on load rating and reliability are also presented in the analyses. The information generated from these analyses can be used for better-focused visual inspection and widened bridge load rating criteria, and can also be used for developing a long-term widening structural monitoring plan. Additionally, this study will be used as a benchmark for future studies, and to establish a procedure and methodology for future bridge widening projects.

Dedicated to;

My wife, Simonetta Dacia

My daughter, Hope Maadee

My son, Edzah Noah

And my parents Evelyn and late father Chris

ACKNOWLEDGMENTS

I wish to acknowledge and thank Dr. F. Necati Catbas for the research opportunity under his direction and vision, for exposure and involvement in the important fields of bridge widening and bridging the gap of code specifications through this analytical investigation and for his support in my continuing education and understanding the opportunities that this experience and successful completion of this research will bring.

To my committee members, Dr. Kevin Mackie, Dr. Manoj Chopra and Dr. Petros Xanthopoulos, for their time and valuable feedback; our student research team, especially Ozan Celik and Enes Karaaslan.

To my great friends, Mr. Edward Severino for his tremendous support and interest in the bridge industry, Mr. Caesar Cabral and Mr. Kevin Fischer for an amazing support and provision of documents, data and abundant relentless needed information.

I want to thank my family for their timeless and priceless support and encouragement through many months of personal, professional, and academic challenges; especially to my lovely wife Simonetta for being there to support our family when I was not there, my children Hope and Edzah for being obedient to their mother in my absence, my mother Evelyn for her support with the children and my late father Chris for his continuous prayerful support and admiration for my persistence – “Dad thank God we did it.”

TABLE OF CONTENTS

LIST OF FIGURES.....	xii
LIST OF TABLES.....	xvii
LIST OF ACRONYMS.....	xix
LIST OF VARIABLES	xx
CHAPTER ONE: INTRODUCTION.....	1
Structural Concept	4
Pre-tensioning	8
Design Specifications.....	12
Inspection and Maintenance Practice.....	15
Service Life and Life – Cycle	20
Increased Loads and Load Effects	23
Objectives & Motivation.....	24
Methodology, Scope, and Tasks.....	26
Novelty and Long-Term Vision of the Research	29
CHAPTER TWO: LITERATURE REVIEW AND FUNDAMENTAL CONCEPTS.....	31
Condition Assessment.....	31
Structural Modeling & Analysis	38

Simulations and Load Rating.....	39
Model Updating	40
Finite – Element Analysis	44
Finite – Element Methods for Concrete Structures.....	46
Fundamental Concepts in Bridge Widening	49
Prestressed Concrete Bridges.....	55
CHAPTER THREE: PRELIMINARY MODEL DEVELOPMENT	60
Bridge Segment Selection.....	60
Primary Selection Criteria.....	61
Secondary Selection Criteria.....	63
Software Considerations	63
Preliminary Models and Benchmark Studies.....	67
Benchmark Background Information and Input	68
Benchmark Three – Span Model	71
Benchmark Modal Analysis.....	77
Benchmark Discussion.....	80
CHAPTER FOUR: FOUR – SPAN FINITE – ELEMENT MODEL (1972)	81
Introduction.....	81
Superstructure	82

Objective.....	93
Discussion.....	95
CHAPTER FIVE: FOUR – SPAN FINITE ELEMENT MODEL (2002).....	96
Introduction.....	96
Objective.....	100
Discussion.....	103
CHAPTER SIX: MODAL ANALYSIS AND PARAMETER SENSITIVITY.....	104
Introduction.....	104
Selection of Modes	104
Results.....	105
Discussion.....	107
CHAPTER SEVEN: LIVE LOAD DISTRIBUTION FACTORS ANALYSIS	109
Benchmark Live Load Distribution Factors	110
1972 and 2002 Live Load Distribution Factors	113
Discussion.....	118
CHAPTER EIGHT: SIMULATIONS AND LOAD RATING (FULL BRIDGE)	121
Objective.....	121
Simulations	121
Load Rating.....	121

Design vs. Load Rating.....	125
Relationship between Load Rating and Reliability	126
Benchmark Verification	127
1972 Bridge Load Rating Under Aging.....	128
Results.....	128
CHAPTER NINE: MODAL ANALYSIS AND LOAD RATINGS.....	130
Introduction.....	130
Results.....	132
Discussion.....	136
CHAPTER TEN: LOAD RATING AND RELIABILITY ANALYSIS (SINGLE SPAN)	
.....	138
Introduction.....	138
Reliability Index and Probability of Failure	138
Simulations, Load Rating and Reliability.....	141
Benchmark	143
Discussion.....	144
Sensitivity – Load Rating & Reliability Analysis.....	145
Introduction.....	145
Results.....	146

Discussion.....	148
CHAPTER ELEVEN: NONLINEAR SIMULATION & RELIABILITY ANALYSIS .	150
Introduction.....	150
Model	150
Benchmark	152
Analysis.....	152
Results.....	154
Discussion.....	157
CONCLUSIONS AND RECOMMENDATIONS	159
Highlights.....	159
Details	159
APPENDIX A: FREQUENCIES AND MODE SHAPES	163
APPENDIX B: LIVE LOAD DISTRIBUTION FACTORS ANALYSIS	170
APPENDIX C: CAPACITY ANALYSIS	186
APPENDIX D: MODULUS OF ELASTICITY ANALYSIS	190
APPENDIX E: PRESTRESS LOSS ANALYSIS	195
APPENDIX F: LOAD RATING & RELIABILITY ANALYSIS.....	199
LIST OF REFERENCES	223

LIST OF FIGURES

Figure 1: Model of Original Bridge	5
Figure 2: Bridge Cross Section at Mid – Span	5
Figure 3: Model Illustration of Bridge Widening	6
Figure 4: Top View Schematics of Widening	7
Figure 5: Model Components & Cross – Section of Widened Bridge.....	8
Figure 6: I – 4 Ultimate Project showing potential bridge widenings	25
Figure 7: Investigation Framework for Bridge – Widening Analysis.....	29
Figure 8: Research Contribution Focus Flow Chart	30
Figure 9: Widening/Rehabilitation Load – Rating Flow Chart Illustrating Mixed Coding	34
Figure 10: Existing and Widened Bridge for Capacity and Performance Analysis	35
Figure 11: The Bridge Structure	50
Figure 12: The Rehabilitation Structure	50
Figure 13: Bridge Widening Classification.....	50
Figure 14: Option I – Ext. Bridge Widening Exp. (Inside Widening)	52
Figure 15: Option II – Ext. Bridge Widening Exp. (Inside and Outside Widening).....	52
Figure 16: Option III – Bridge Ht. (Proposed Bridge Ht. over Ext. Bridge)	52
Figure 17: Option IV – One – Side Widening (New Bridge Expansion)	52
Figure 18: Option V – Inside & Outside Widening (New Bridge Expansion)	52
Figure 19: Bridge Plan indicating significant segment.....	61

Figure 20: Bridge Cross – Section indicating New and Existing Girders	62
Figure 21: Simplified Structure (NAP).....	65
Figure 22: NAP Classes	66
Figure 23: Benchmark Bridge – Framing Plan.....	69
Figure 24: Benchmark Bridge Typical Cross Section.....	69
Figure 25: Benchmark AASHTO Type V Girder Section Dimensions & Properties	69
Figure 26: Benchmark Strand Layout.....	70
Figure 27: Benchmark Analytical Investigation Flow Chart	71
Figure 28: Benchmark Continuous Three – Span Model	72
Figure 29: Benchmark Model – Tendons.....	72
Figure 30: Benchmark Cross – Section Model & Line Loads.....	73
Figure 31: Benchmark Study Dead – Load Moment & Shear Envelopes	74
Figure 32: Benchmark Study Live – Load Moment & Shear Envelopes	74
Figure 33: Benchmark Live – Load Distribution Factors Schematics.....	75
Figure 34: Benchmark Single – Span Moment Comparison	76
Figure 35: Benchmark Single – Span Shear Comparison.....	76
Figure 36: Benchmark Single – Span Maximum Points.....	77
Figure 37: Dynamic Analysis Effects & Modes	78
Figure 38: Benchmark End – Connection for Modal Analysis.....	79
Figure 39: Benchmark Eigen Value Analysis First Modes	80
Figure 40: Four – Span Continuous Bridge FEM.....	81
Figure 41: Beam Cross – Section Pre-defined in Program.....	83

Figure 42: Bridge Object Definitions	84
Figure 43: Material Property Data	87
Figure 44: Plot of Long – Term Modulus of Elasticity Aging.....	89
Figure 45: Plot of Long – Term Concrete Compressive Strength Aging.....	89
Figure 46: Prestress Losses Analysis Map.....	90
Figure 47: Plot of Long – Term Elastic Shortening Losses	91
Figure 48: Plot of Long – Term Effective Prestress.....	92
Figure 49: Single – Span 1972 Bridge Model	94
Figure 50: 1972 Bridge Single – Span Illustration	95
Figure 51: Four – Span Continuous Widened FEM.....	96
Figure 52: Bridge – Widening Connection	99
Figure 53: Existing and Targeted Girder in Widened Bridge	100
Figure 54: Single – Span 2002 Widened Bridge.....	102
Figure 55: 2002 Widened Bridge Single – Span Illustration	102
Figure 56: Aging Progression Schematics of Widened Bridge Members.....	103
Figure 57: Modal Behavior of 1972 Bridge.....	106
Figure 58: Modal Behavior of 2002 Widened Bridge	106
Figure 59: Live Load Distribution Factors Analysis Illustration	109
Figure 60: Benchmark Live Load Distribution Factors.....	113
Figure 61: 1972 Bridge Live Load Distribution Factors (Moment)	115
Figure 62: 1972 Bridge Live Load Distribution Factors (Shear).....	115
Figure 63: Critical Case Selection for Targeted Components.....	116

Figure 64: 2002 Bridge Live Load Distribution Factors (Moment)	117
Figure 65: 2002 Bridge Live Load Distribution Factors (Shear).....	117
Figure 66: Moment Live – Load Distribution Factors Comparison	119
Figure 67: Shear Live – Load Distribution Factors Comparison.....	119
Figure 68: Load Rating Flow Chart	123
Figure 69: Benchmark Critical Component Rating	127
Figure 70: 1972 Bridge Load Ratings.....	129
Figure 71: Benchmark Bridge Dynamic Modes and Load Ratings	130
Figure 72: 1972 Bridge Dynamic Modes and Load Ratings (aging not considered)	131
Figure 73: 2002 Bridge Dynamic Modes and Load Ratings	131
Figure 74: Plot of Loading Ratings Versus Eigen Values (All Structures)	133
Figure 75: Plot of Load Ratings Versus Eigen Values (1972 and 2002 Bridges)	135
Figure 76: Plot of Load Ratings and Eigen Value Differences (1972 and 2002 Bridges)	135
Figure 77: Load Rating & Eigen Value Analysis Flow Chart.....	137
Figure 78: Reliability Index Equation.....	139
Figure 79: 1972 Single Span Bridge for Load Ratings and Reliability Analysis	144
Figure 80: Hand Calculations and FEM Comparison.....	145
Figure 81: Case I – Sensitivity Analysis (No Losses).....	146
Figure 82: Case II – Sensitivity Analysis (Losses – All Members).....	147
Figure 83: Case III: Sensitivity Analysis (Losses – Selected Members)	148
Figure 84: Detailed Schematics of Nonlinear Model	151

Figure 85: Virtual Loading Schematics	154
Figure 86: Virtual Load Testing Plots	157
Figure 87: Benchmark Modes.....	165
Figure 88: 1972 Bridge Modes	167
Figure 89: 2002 Bridge Modes	169

LIST OF TABLES

Table 1: 1972 Model Components Summary	4
Table 2: 2002 Model Components Summary	7
Table 3: Traffic Data on Research Bridge.....	24
Table 4: Bridge Widening Options	51
Table 5: Benchmark Composite Section Properties.....	70
Table 6: Summary – Benchmark Material Properties.....	70
Table 7: Benchmark Line Load Analysis.....	73
Table 8: Benchmark Hand Calculations for Distribution Factors.....	110
Table 9: Moment & Shear Controlling Live Load Distribution Factors.....	113
Table 10: 1972 and 2002 Bridge Hand Calculations for Distribution Factors	114
Table 11: Moment and Shear Controlling Live Load Distribution Factors (1972 Bridge)	116
Table 12: Moment and Shear Controlling Live – Load Distribution Factors (2002 Bridge)	118
Table 13: Moment Live – Load Distribution Factors Analysis.....	118
Table 14: Shear Live – Load Distribution Factors Analysis	118
Table 15: Eigen Values and Load Ratings Results.....	134
Table 16: Statistical Parameters for Load and Resistance	142
Table 17: Hand Calculation Load Rating and Reliability Results for Single and Multiple HL93	143
Table 18: Case I & II Load – Rating Summary Chart	149

Table 19: Case III Load Rating Summary Chart	149
Table 20: Benchmark Results and Comparison	152
Table 21: Single and Multiple Lanes Distribution Factors (AASHTO/FEM)	154
Table 22: Nominal Parameters Load Analysis Results	155
Table 23: Variable Parameters Load Analysis Results	155
Table 24: Linear and Nonlinear Limit State Function Reliability Indices	156
Table 25: Virtual Load Rating Results	156

LIST OF ACRONYMS

AASHTO	American Association of State Highway and Transportation Officials
ACI	American Concrete Institute
DOF	Degree of Freedom
FEM	Finite Element Model
FHWA	Federal Highway Administration
LRFD	Load and Resistance Factor Design (of Highway Bridges)
LRFR	Load and Resistance Factor Rating (of Highway Bridges)
PC	Personal Computer
RF	Rating Factor

LIST OF VARIABLES

A_c	gross area of concrete member cross-section, in ² .
A_{ps}	area of prestressed reinforcement in tension zone, in ² .
A_v	area of shear reinforcement within a distance, s , in ² .
a	depth of equivalent uniformly stressed compression zone assumed for concrete in the strength limit state, in. b width of compressive face of member, in.
b_w	web width, in.
COV	coefficient of variation
c	distance from extreme compression fiber to neutral axis, in.
DC	subscript referring to dead load from structural components and attachments
DW	subscript referring to superimposed dead load (wearing surfaces, utilities)
d	distance from compression face to centroid of tension reinforcement, in.
d_v	effective shear depth, in.
E_c	modulus of elasticity of concrete (general), ksi; modulus for precast beams, ksi.
E_{CIP}	modulus of elasticity of concrete, cast-in-place connection, ksi.
E_{cLT}	long-term modulus of elasticity of concrete, ksi.
E_{cn}	ultimate effective modulus of elasticity of concrete, ksi.
E_{COL}	modulus of elasticity of concrete, precast columns, ksi.
E_s	modulus of elasticity of reinforcing bars, ksi.
E_p	modulus of elasticity of prestressing reinforcement

e	eccentricity of load parallel to axis of member measured from centroid of cross-section, in.
f_c	specified 28-day compressive strength of concrete, psi.
f_{ps}	stress in prestressed reinforcement at nominal strength, psi.
f_{pu}	specified tensile strength of prestressing tendons, psi.
f_{py}	specified yield strength of prestressing tendons, psi.
f_y	specified yield strength of nonprestressed reinforcement, ksi.
h	overall beam thickness of member, in.
I_c	moment of inertia of concrete section, in ⁴ .
IM	dynamic load allowance (impact factor)
K	prestress loss (wobble) coefficient, 1/ft.
LL	subscript referring to live load
M_n	nominal flexural resistance, kip-ft. M_u factored moment at the section, kip-ft.
n	modular ratio of elasticity, E_{ps}/E_c .
P_f	probability of failure
RF	load rating factor
S	section modulus of concrete section, in ⁴ .
s	spacing of shear reinforcement in the direction parallel to longitudinal reinforcement, in. t time, days.
w_c	unit weight of concrete, pcf.
β	reliability index
β_1	ratio of depth of the equivalent uniformly stressed compression zone

assumed for concrete in the strength limit state to the depth of the actual compression zone.

γ	load factor
Δf_{CR}	prestress loss due to creep, psi.
Δf_{ES}	prestress loss due to elastic shortening, psi.
Δf_R	prestress loss due to relaxation of steel, psi.
Δf_{SH}	prestress loss due to shrinkage, psi.
Δf_T	total prestress loss, psi.
μ	prestress loss (curvature) coefficient; also mean value.
σ	standard deviation
ϕ	resistance factor

CHAPTER ONE: INTRODUCTION

A high-quality transportation network is vital to a top performing economy. Investments by previous generations of Americans – from the Erie Canal in 1807, to the Transcontinental Railroad in 1869, to the Interstate Highway System in the 1950s and 1960s – were instrumental in putting the country on a path for sustained economic growth, productivity increases, an unrivalled national market for goods and services, and international competitiveness. But today, current estimates indicate that America's transportation infrastructure is not keeping pace with demands or the needs of our growing economy, for today or for future generations – An Economic Analysis of Transportation Infrastructure Investment (A report prepared by the National Economic Council and the President's Council of Economic Advisers – July 2014) [1].

With over 600,000 bridges in the U.S., as documented in the National Bridge Inventory (NBI), it is very clear that they are a major component in the civil infrastructure system, and are ranked as such; they are the backbone of the U.S. infrastructure system. People and vehicles use bridges every day, allowing them to pass-over obstacles such as bodies-of water, valleys, or other roads in congested areas. And as stated above, bridges are part of the country's-infrastructure system, contributing to economic growth or decline. For example, in a regional economy, a new bridge can bring prosperity, while an older damaged or collapsed bridge can-cause severe adverse impacts such as detours, re-routings and traffic jams, which increase the cost of transportation (through time delays, extra fuel and more driving time). Consequently, bridges become a sustaining commodity which, also requires production and inventory control (maintenance and prevention inventory). Therefore, in the field of civil engineering, bridges are critical structures. They must work under extremely difficult conditions, including heavy daily

loads and harsh weather conditions.

Although there is a consensus in admitting the importance of infrastructure systems, with 614,387 bridges across the nation many drastically in need of repair or replacement -- we can see that the future picture for bridges in the United States is not bright. The most recent report published this year by the American Society of Civil Engineers (ASCE) issued a report card for America's infrastructure, giving it a grade of C+ for bridges. Below is a summary of the report's findings on the status of bridges in the U.S.

“The U.S. has 614,387 bridges, almost four in 10 of which are 50 years or older. 56,007 – 9.1% - of the nation’s bridges were structurally deficient in 2016; and on average there were 188 million trips across a structurally deficient bridge each day. While the number of bridges that are in such poor condition as to be considered structurally deficient is decreasing, the average age of America’s bridges keeps going up, and many of the nation’s bridges are approaching the end of their design life. The most recent estimate puts the nation’s backlog of bridge rehabilitation needs at \$123 billion.” [2]

This information proves that if we do not have effective methods for inspection and maintenance of the nation’s bridges, the goal for eliminating the deficient bridges will never be accomplished, because the budget is always limited. Just as detecting and repairing initial damage (including cracks, rusted members, and loss of sections in structures) will cost much less than replacing girders, supports or other main components, so the cost of widening bridges to reduce traffic congestion and collision will be less than completely replacing the structure. Thus, one of the most cost-effective approaches for addressing aged aging bridges with limited funds is bridge widening.

The primary objective of this research work is to present a study to better understand the structural behavior and capacity of a bridge that has been in service for over 40 years. The original bridge was constructed in 1972 and was widened in 2002.

Preliminary investigation between the original bridge (hereafter referred to as the 1972 bridge) and the existing widened bridge (hereafter referred to as the 2002 bridge) will involve a 3D model to capture structural demand (shear and flexure) for different loads and capacity for resistance analysis along with distribution factors and load ratings.

A detailed finite–element model of the structure is developed and various possible conditions are simulated to bound the existing condition, since there is only very limited experimental data (no access to data). The parameters are selected based on evaluation of the entire structure. These parameters exhibit uncertainty, and the structural response is also sensitive to variations of these parameters. Models will also be used to determine the load-carrying capacity of the widened structure for the initial and current load demand. Verification of analytical results with special codes considerations for widened structures will also be examined, as well as the investigation of the load rating and reliability of the widened structure at the time of initial and current load demands. A comparison of the reliability of the current structure with the target reliability index will also be considered. Results and discussions are included for the various analyses. The final chapter includes conclusions and recommendations for future research. This research will provide comparative evaluation of a bridge load-carrying capacity in a more thorough manner, along with an understanding of ultimate load levels and reliability based nonlinear analysis.

Structural Concept

As stated earlier, the original bridge used for this research was constructed in 1972. It has an east-west orientation with two lanes in each direction. Both the eastbound and the westbound bridge have four spans, with lengths 37.0, 60.3, 60.3 and 37.0 ft. (11.3, 18.4, 18.4 and 11.3 m), and an out-to-out width of 43.3 ft. (13.2 m). The four-span bridge is supported by three piers where the girders with half-inch diameter and 270 kips per-square-inch low relaxation strands are supported on elastometric bearings. The girders have a compressive strength of 6 kips per-square-inch, and the 7-inch (177.8 mm) supporting deck slab that forms a composite with the girder has a compressive strength of 4.5 kips per-square-inch. A combination of AASHTO Type II and Type III girders was used for this bridge. The shorter spans (1 & 4) have both Type II and Type III girders, whereas the longer spans (2 & 3) have all Type III. The bridge was modeled with 844, 3090 and 120 tendon, shell and support elements, respectively. The model had 4,242 joints, 19 restraints and 1,185 constraints. A summary of the model components is provided in Table 1, and the model is shown in Figure 1. The cross-sections of the bridge spans, illustrating the girder configurations, are shown in Figure 2.

Table 1: 1972 Model Components Summary

Model Components	Quantity
Joints	4242
Restraints	19
Frame/Cable/Tendon Elements	844
Shell Elements	3090
Link/Support Elements	120
Constraints/Welds	1185

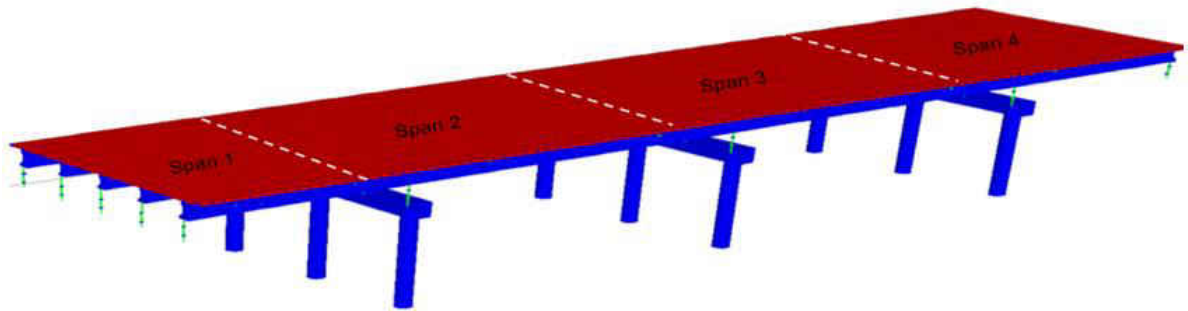


Figure 1: Model of Original Bridge

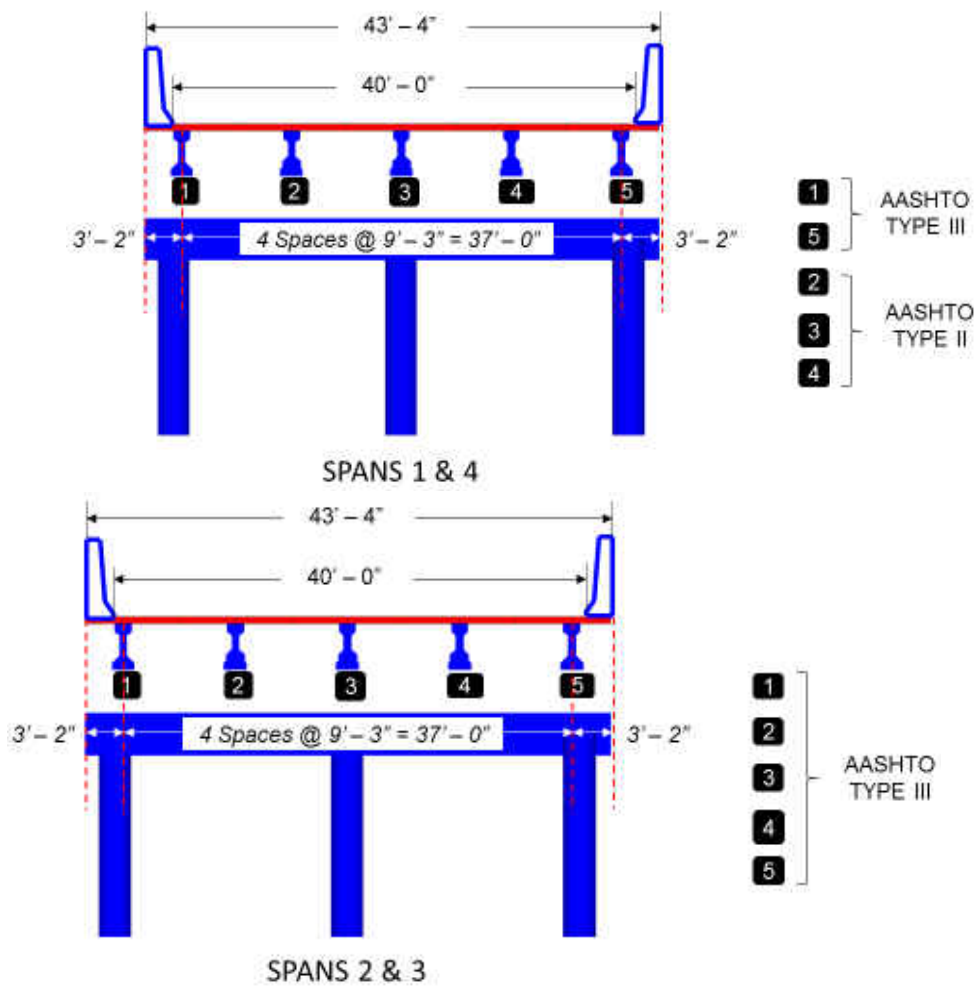


Figure 2: Bridge Cross Section at Mid - Span

Due to increase in traffic there was an initiative to widen the original 1972 bridges in 2002. Improvements included converting mainline toll plazas and tolled ramps to include Express Lanes, and adding cash and receipt lanes. The projects also resulted in additional through-lanes, expanded interchanges, aesthetically pleasing sound walls, decorative bridge columns and pylons, planter walls, and landscaping [3].

The widening involved adding two new through-lanes between the two original bridges and connecting them with the bridges, as shown in the “before and after” model illustration in Figure 3.

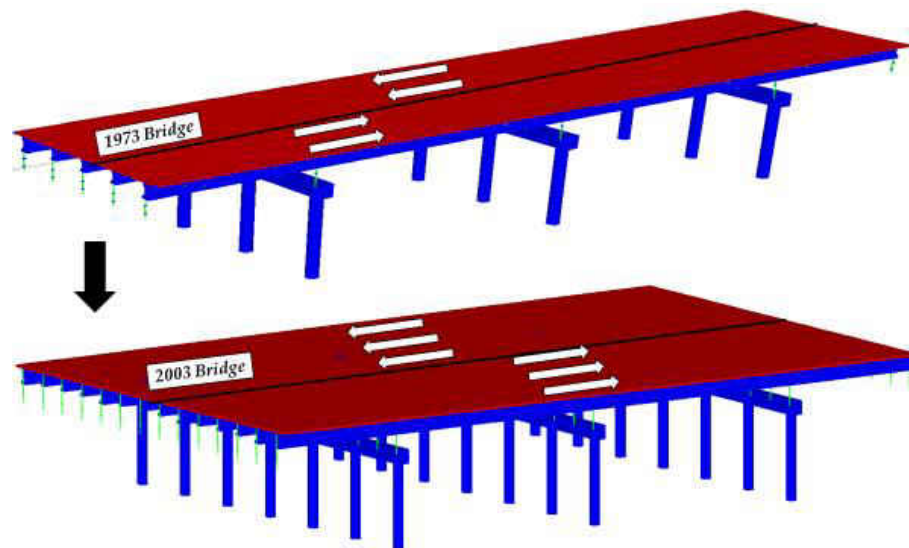


Figure 3: Model Illustration of Bridge Widening

The widening, which maintained the same bridge length of 196.5 ft. (59.9 m), had a new roadway and deck, with edge-to-edge widths of 110.9 ft. (33.8 m) and 117.1 ft. (35.7 m), respectively [4]. The prestressed concrete girder-widened bridge, with concrete cast-in-place deck and monolithic concrete wearing surface, was widened in the median as well as the right

(east-bound) side, to accommodate three lanes each way (eastbound and westbound). Figure 4 and Figure 5 present detailed schematics top view, as well as cross-sections, to illustrate the widening process. A summary of the model components is provided in Table 2.

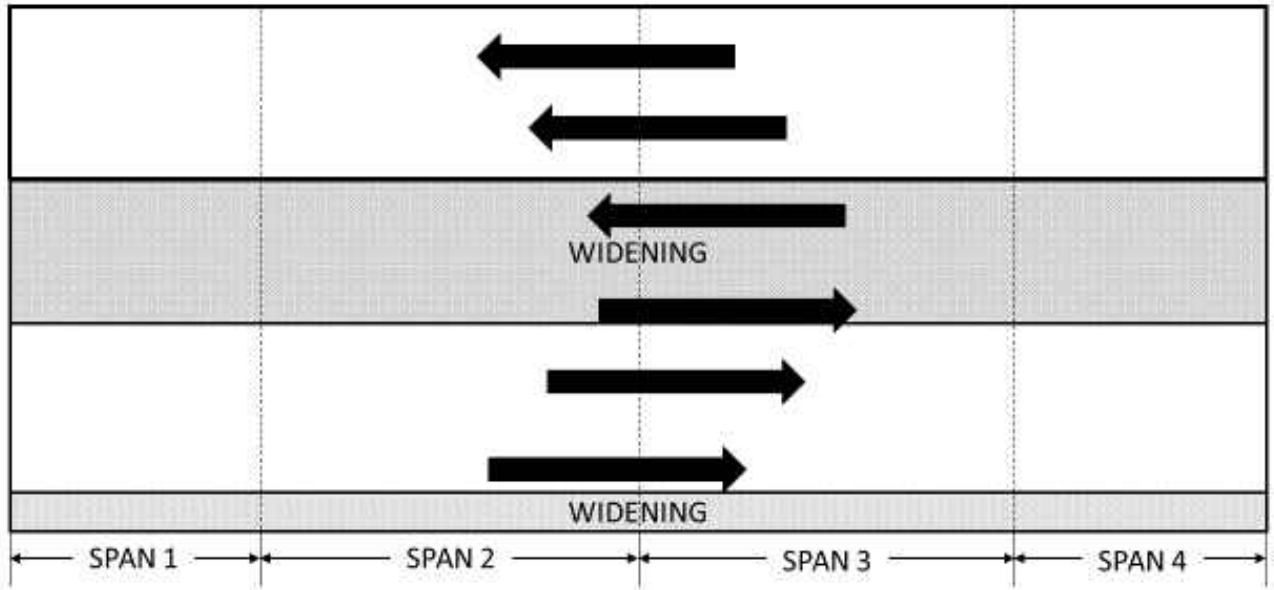


Figure 4: Top View Schematics of Widening

Table 2: 2002 Model Components Summary

Model Components	Quantity
Joints	11881
Restraints	161
Frame/Cable/Tendon Elements	2348
Shell Elements	8736
Link/Support Elements	336
Constraints/Welds	4176

**Aging Effect Incorporated in Existing Girders (1972)*

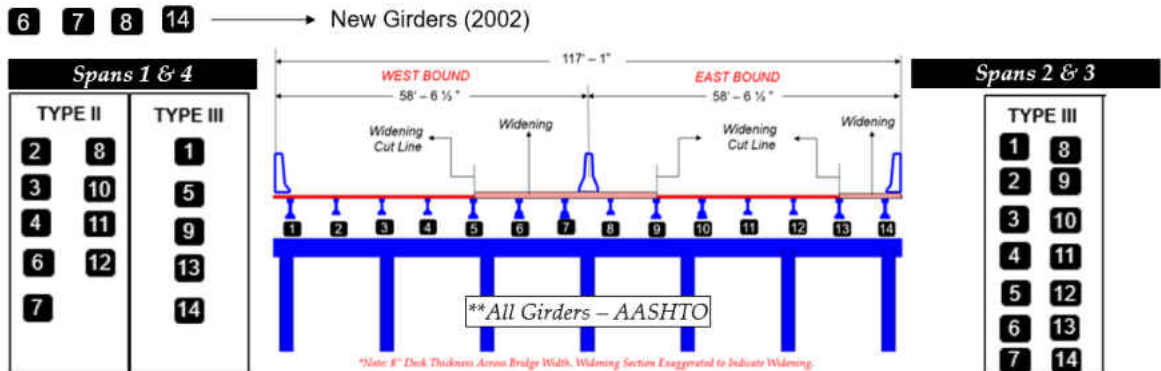


Figure 5: Model Components & Cross – Section of Widened Bridge

The bridge chosen for this research was unique in the sense that it fit the criteria for the analysis and investigation required for the performance of a prestressed beam before and after widening. Some of the key components include;

- An existing bridge that was widened (1972 – 2002).
- A widening process and procedure falls into the two widening conditions considered in this research (*see Fundamental Concepts in Bridge Widening – Chapter 2*).
- Geometry & Materials
 - o Straight (no skew)
 - o Prestressed beams

Pre-tensioning

The AASHTO (American Association of State Highway and Transportation Officials) I-beam and bulb I-beam are commonly used in the State of Florida and other states as well. The use of ASTM A416, Grade 270, low-relaxation, straight, prestressing strands is preferred for the

design of prestressed beams.

Typically, the Florida bridge beams are pre – tensioned (prestressed) compared to post – tensioned beams. Prestressed, pre-tensioned, tendons are tensioned by a jack without any concrete. Then, concrete is poured, allowed to set and bond, at which time the ends are cut and the beam becomes instantly stressed by the tendons. Service loads can then be applied. Pre – tensioning is normally performed at precasting plants, where a precasting stressing bed of a long-reinforced concrete slab is cast on the ground with vertical anchor bulkheads or walls at its ends. The steel strands are stretched and anchored to the vertical walls, which are designed to resist the large eccentric prestressing forces.

Prestressed, post-tensioned, tendons are tensioned by a jack after the concrete has already cured (but a duct is installed such that the concrete is unbonded to the prestressing), at which time the tendons are tensioned by means of a hydraulic jack, and the beam becomes stressed. Grout may or may not then infill the ducts. Grouting should typically be performed, to minimize the chance of a single tendon rupture causing catastrophic failure of the member. Service loads can then be applied [5].

Post-tensioning is a method of reinforcing (strengthening) concrete or other materials with high-strength steel strands or bars, typically referred to as tendons. The two main types of post tensioning consist of unbonded and bonded tendons.

An unbonded tendon is one in which the prestressing steel is not actually bonded to the concrete that surrounds it except at the anchorages. In bonded systems, two or more strands are inserted into a metal or plastic duct that is embedded in the concrete. The strands are stressed with a large, multi-strand jack and anchored in a common anchorage device. The duct is then

filled with a cementitious grout that provides corrosion protection to the strand and bonds the tendon to the concrete surrounding the duct [6].

Research has also shown that partially prestressed concrete beams with bonded tendons provide better behavior than those of unbonded tendons such as increase ductility, initial stiffness and the ultimate deflection up to 265%, 13% and 199% respectively. Additionally, increasing the nominal compressive strength from 72 to 97 MPa for bonded prestressed beams led to a slight increase in the ultimate and cracking loads by 4% and 18% respectively whereas increasing the nominal compressive strength from 72 to 97 MPa for unbonded prestressed beams decreased the maximum deflections at the failure loads by 16% and 23% respectively [7].

Consequently, pre – tensioned bridge beams can have some of the strands bonded and deboned. Strand debonding in a pretensioned prestressed beam is similar to the bar curtailment technique usually used in reinforced concrete beams. Both methods incorporate the intermediate anchorage technique, which induces high stress concentrations at the point of bar cutoff in reinforced concrete members or strand debonding in pretensioned beams. This may cause an adverse effect on the ultimate strength of the beam.

A research on strand debonding in pretensioned beams mainly at the ends where moment is not critical revealed the following results;

- Strand debonding reduces flexure – shear cracking capacity of pretensioned beams compared to that of fully bonded members.
- The debonded strands developed the required prestressing force at the point load.

- Strand development length specified by the ACI/AASHTO codes for fully bonded strands is not adequate if web – shear cracking penetrates the transfer length of the strand, or if flexure – shear cracking occurs within the current full anchorage length l_a of the strand.
- Adequate anchorage length for the prestressing strand in pretensioned beams is of critical importance in reaching the full ultimate capacity both in flexure and shear.
- The flexure and shear design of both bonded and debonded pretensioned I – beams, where the flexural capacity controls, based on current ACI/AASHTO design provisions would be adequate if the fully bonded strands in the member have anchorage length of a least $1.7 l_a$.
- The findings from this study indicate that the degree of conservatism decreases as the percentage of debonding increases. It is recommended that no more than 67% of the strands be debonded. The current limit of 50% was shown to be conservative provided the anchorage length of the fully bonded strand is at least $1.7 l_a$, with l_a based on current ACI/AASHTO requirements [8].

The pre-tensioned beams have a parabolic soffit, or haunched beam profile. The haunched beam profile was developed for camber control. The bottom edges of the Type II prestressed beams are chamfered $\frac{3}{4}$ " at sides and $1 \frac{1}{2}$ " by $1 \frac{1}{2}$ " continuous wood chamfer at ends (typical). The bottom edges of the other types of prestressed beams were chamfered $\frac{3}{4}$ " at sides and $1 \frac{1}{2}$ " by $1 \frac{1}{2}$ " continuous wood block out at ends (typical).

In typical pre-tensioned beams, the tendons are straight but can be harped or draped to match the dead load moment.

Design Specifications

The moment demand for a girder depends on the magnitude and location of the imposed loads and on the properties of the bridge. The design moment in the girder will vary with girder spacing, span, flexural stiffness, torsional stiffness, and on the properties of the deck and diaphragms [10]. To simplify the design process, many bridge codes, such as the AASHTO Load and Resistance Factor Design (LRFD) Specifications (1998), the AASHTO Standard Specifications (1996), and the Ontario Highway Bridge Design Code (1992), treat the longitudinal and transverse effects of wheel loads as uncoupled phenomena. The design live-load moment caused by a truck (or lane of traffic) is first estimated by obtaining the maximum truck (or lane of traffic) moment on a single girder. A designer then obtains the design moments for each girder by multiplying the maximum single girder moment by a factor, which is usually referred to as the live-load distribution factor [10].

Live load distribution is important for the design of new bridges, as well as for the evaluation of existing bridges, and has been the basis for design in the United States for over seven decades. The AASHTO Standard Specifications for Highway Bridges have contained live load distribution factors since 1931. The early values were based on the work done by Westergaard (1930) and Newmark (1948), but the factors were modified as new research results became available. For a bridge constructed with a concrete deck on prestressed concrete girders and carrying two or more lanes of traffic, the current distribution factor (AASHTO 1996) is $S/5.5$, where S is the girder spacing in feet. This factor, multiplied by the moment on a single girder, caused by one line of wheels, gives the girder design moment. The applicability of the

procedures in the Standard Specifications is limited by the fact that they were developed considering only non-skewed, simply supported bridges. Piecemeal code changes over the years have also created inconsistencies [11]. In 1994, AASHTO adopted the LRFD Bridge Design Specifications (AASHTO 1994) as an alternative to the Standard Specifications. The LRFD expressions for live-load distribution are based on the results of a parameter study by Zokaie et al. [12], which considered variations in girder spacing, girder stiffness, span length, skew, and slab stiffness. The resulting LRFD expressions account for many parameters that were neglected previously, including skew. Per Zokaie et al., the LRFD code distribution factors lie within 5% of the distribution factors calculated with detailed finite-element models.

The finite-element models used to develop the AASHTO LRFD (1994) code equations were detailed, but the models did not include all the components of a typical bridge. For example, Zokaie et al. considered the effects of diaphragms in a pilot study but not in the main parameter study. In addition, the factor that Zokaie et al. proposed to account for girder continuity was not included in the LRFD Specifications. Consequently, the LRFD code expressions are based on the results of analyses for HS20 loading of simply supported bridges without lifts, intermediate diaphragms, or end diaphragms.

The AASHTO LRFD equations for the distribution factors are more accurate than those provided in the Standard Specifications [12]. However, Chen and Aswad [13] found that the LRFD code distribution factors can be uneconomically conservative for bridges with large span-to depth ratios. Based on the results of finite-element analysis, Chen and Aswad found that this conservatism could be as much as 23% for interior beams and 12% for exterior beams [13]. A reduction in the conservatism of the code would lead to more economical bridge designs.

Further research was needed to evaluate the accuracy of the code live-load distribution factors and to quantify the effects of parameters not considered in the codes or most previous analyses.

The AASHTO Standard Specifications and AASHTO LRFD Specifications contain simplified methods currently used to compute live load effects. The National Cooperative Highway Research Program (NCHRP) is one program that develops LRFD equations which have been used in modern design.

These equations include limited ranges of applicability that, when exceeded, require a refined analysis to be used. The ranges of applicability and complexity of the equations have been viewed by some as weaknesses since their adoption into the LRFD specifications. NCHRP recently developed an even *simpler* live load distribution factor equations for moment and shear to replace those in the current LRFD specifications. These equations are expected to be straightforward to apply and easily understood and yield results comparable to rigorous analysis results. NCHRP used rigorous analysis as the basis for establishing the target distribution factors for their research; which helped their research team to better delineate the effects (i.e., contributions) of multiple-vehicle presence, of variability associated with the simplified analysis, and of the calibration (tuning the simple method to better match the rigorous results) [14].

Usually the parametric analyses are based on the application of a single point load in the investigation of shear. However, such a load configuration does not realistically appear in practice. Thus, to confirm shear capacity, loads on a selection of model beams are applied representative of vehicular traffic.

Consequently, research by Eamon et al., [11] showed that for every analysis (two legal

Michigan vehicle configurations applied to the FEA bridge model), moment failure occurred at a load level much below that required for a shear failure (i.e. development of shear cracks). It was also not possible to fail the beams in shear (before a moment failure) using reasonable vehicle configurations. Thus, as expected, typical vehicle configurations on a reasonably designed and undamaged prestressed concrete beam will generally result in moment failures rather than shear failures, especially for longer vehicles and spans [16].

For the original bridge used in this research, the 1966 specifications and special provisions for the State of Florida Department of Transportation Standard Specifications for Road and Bridge Construction was used. The design code used was in accordance with the 1969 Edition of the AASHTO Standard Specifications for Highway Bridges with approved revisions. The loading truck was an HS 20 – 44 (Modified for Military Loading as required). However, the Florida Department of Transportation (FDOT) Structures Design Guidelines which makes provision for mixed coding for the bridge widening was used for the widened bridge as is elaborated in this section under “Condition Assessment.”

Inspection and Maintenance Practice

In general, regular maintenance and inspections are performed on the study bridge, since it is part of the Florida Department of Transportation (FDOT) bridge network. Engineering technicians perform visual inspections on a biennial basis. Through its Office of Maintenance, Structure Operations and Bridge Inspection, FDOT manages consultant contracts to inspect local government bridges. Participation in the local government bridge inspection program is

voluntary on the part of the local governments, but does not relieve them of their responsibility to inspect, maintain, impose and enforce weight restrictions, repair, rehabilitate, or replace the bridges in their jurisdictions. The Federal Highway Administration (FHWA) holds FDOT administratively responsible for ensuring that all qualified bridges in the state are inspected and load-rated in accordance with state statutes and federal codes. In addition, FDOT is required to report to FHWA that all publicly-owned bridges are inspected in accordance with these standards.

Sample inspection methods for protecting public safety and safeguarding the public's investment in bridge structures are listed below:

1. Visual Inspection.
2. Non-destructive Testing.
3. Material Sampling (Coring, removal and testing).

During the initial inspection of a structure, the bridge inventory data is verified in the field to reflect the "as built" conditions. Before making subsequent inspections, the previous bridge inspection reports and the bridge record file are reviewed.

Visual Inspections being the most common methods requires that dirt and debris be removed to permit visual observation and precise measurements. Careful visual inspection is supplemented with appropriate special equipment and techniques. Usually the use of mirrors is employed to increase visual access to many bridge components. Tools and equipment needed for the inspection of bridges vary with the type of inspection being made. Refer to the current FHWA Bridge Inspector's Reference Manual, for a list of equipment that may be used for inspection. Sketches, photographs and video cameras are used as required to record significant

or unusual details. The procedures for “visual inspections” are outlined as follows;

1. Sequence – Whenever practical, inspection should proceed from substructure to superstructure to deck. The cause of superstructure and deck deficiencies may be more apparent if the substructure was inspected initially.
2. Thoroughness – All surface areas of each bridge member must be examined. To ensure that no surface is overlooked, each inspection team should develop a standard and methodical order for examining the surfaces of each member. The minimum distance the inspector needs to be from each surface varies depending on what is being inspected and the condition of the structure. Typically, items such as bearing areas, fatigue prone details, areas where debris accumulates and other areas known to be prone to deterioration should be inspected at arm’s length. Areas like mid span portions of prestressed girder bridges in good condition can typically be inspected from the ground. As the condition of the structure worsens, the effort required for the inspection will increase.
3. Completeness – Inspection of all components of the bridge during every inspection. If, for any reason, a specific component or member cannot be inspected, it must be noted in the bridge inspection report. Features that are not of a structural nature, such as approach guard rails, lighting, and signs should also be inspected since they have a significant impact on bridge performance and public safety. The elements listed in the bridge inspection report should be used as a guide to assure complete inspections. There are also items that are incidental to the elements that need to be inspected.

4. Discovery of Serious Safety Concerns – When critical deficiencies are discovered which pose a definite threat to public safety, the inspection team leader shall initiate actions to correct these deficiencies. In extreme cases when the structure is in imminent danger of collapse, the inspector shall close the bridge to traffic. The district structures maintenance engineer shall be notified immediately of the critical deficiency, and the following steps shall be taken:
- a. Coordinate the traffic restrictions for public safety.
 - b. Visit the site to evaluate the critical deficiency. During this phase personnel, may be brought to the site to aid in the evaluation of the critical deficiency.
 - c. Determine the action to correct the critical deficiency.

5. Questionable Conditions – During the inspection, conditions may be encountered which require evaluation beyond the knowledge and experience of the bridge inspector. When this occurs, engineers from the district structures maintenance office shall visit the site and personally examine the situation before determining the course of action. The district structures maintenance engineer shall determine if experts from the district, the central office, the state materials office, universities, federal agencies, or other state agencies need to be consulted to aid in evaluating the questionable conditions.

Non-destructive testing (NDT) can be used to augment or supplement visual inspection. Generally, NDT is not practical for large scale use on a bridge unless a defect has first been detected by visual means. NDT can be used to highlight or define the extent of the defect.

Since most types of NDT require special equipment, and detailed instructions to perform

the various tests, and correctly interpret the results, it is essential to have the NDT performed and interpreted by qualified personnel.

Last but not the least, material sampling (destructive testing) must be done. Destructive testing can be used in evaluating bridge materials. This requires taking samples from the various bridge components. Samples from low-stress areas of steel beams can help the engineer determine the type and strength of the steel. Taking samples out of concrete members can be useful for identifying hidden defects, as well as determining the strength of the concrete. Taking small samples from timber members using an incremental boring may be performed, but the hole should be plugged with a treated wood plug, or by some other suitable method, afterward.

Destructive testing is not usually recommended, except in cases where it is necessary to evaluate the structure before major rehabilitation, or to determine material properties for analysis. It is imperative that sample holes be patched or plugged to prevent future deterioration.

Consequently, a bridge inspection could lead to a more thorough and detailed structural investigation. The purpose, notification and preliminary actions for such an investigation are described below;

- Purpose - When a failure or condition threatening structural integrity is discovered on a bridge, culvert, overhead sign, high-mast light pole, retaining wall, mast arm traffic signal, or other significant structure, the failure or condition shall be investigated to determine its cause. Based on the investigation, action can be taken to prevent future similar failures or conditions.

- Notification - The district structures maintenance engineer must be notified when a failure or near failure occurs. When possible, the failed structure should not be ~~moved~~ removed until an investigation can be performed. When traffic or safety concerns dictate immediate removal of the failed structure, it should be stored where it will be available for future investigation.
- Preliminary Actions - The initial phase of the investigation should be a documentation of the condition. Extensive videos, photographs, sketches and measurements should be used to document the failed structure. During the preliminary phase of the investigation, the district structures maintenance engineer will notify the following:
 1. State maintenance office
 2. District structures design office
 3. District general counsel, if the incident involves the public

As stated earlier, each bridge is to be inspected at regular intervals, with no interval exceeding 24 months. An inspection will not be delinquent if it is conducted in the month it is due. If a bridge is inspected *after* the month it is due, the reason must be documented in the communications section of the bridge record file, and in the inspection notes section of the bridge management system.

Service Life and Life – Cycle

The AASHTO LRFD Specifications provides these definitions:

Service Life — “The period that the bridge is expected to be in operation.”

Design Life — “Period on which the statistical derivation of transient loads is based: 75

years for these Specifications.”

Since service life involves consideration of many environmental, design, materials, and construction factors, the LRFD definition of design life obviously does not represent a basis for service life. Accordingly, the AASHTO LRFD Specifications does not recommend any specific period for service life [15].

AASHTO specification provisions not being able to predict or approximate the length of service life is an obvious obstacle to the implementation of extended service life for bridge projects in the United States. Development of specific service life recommendations for bridges would probably involve an effort by the AASHTO Subcommittee on Bridges and Structures and the Federal Highway Administration, extending over several years.

The most problematic component of life-cycle calculations may be maintenance costs. Nearly all states experience chronic deficiencies in the amount of funding available for maintenance. The lack of adequate maintenance funding may be a significant factor contributing to the structural deficiency of bridges. Proper maintenance is essential to achieving extended service life, as well as a sustainable bridge infrastructure [15].

Design options that have been used to extend service life include:

1. Use of high-performance concrete (HPC) to reduce permeability.
2. Pretensioning and/or post-tensioning to control or eliminate cracking.
3. Minimizing the use of expansion joints and bearings. (Integral bridges should be used where feasible.)
4. Use of integral deck overlays on precast concrete segmental bridges in aggressive environments.

There is a sense of urgency in the United States for achieving the goals of extended service life and a sustainable bridge infrastructure. However, reaching these goals involves incorporating details in the design process necessary for extended service life, as well as providing consistent funding necessary for bridge maintenance. Probabilistic, performance-based durability design of concrete structures is now available. Extended service life of major bridges is recommended, even if some marginal increase in initial cost is required. Service life of 150 years is recommended for major urban bridges or bridges on critical highways. Eventually, extended service life is recommended for application to all bridges. Development of an AASHTO specification with specific service life periods would be beneficial to bridge infrastructure sustainability in the United States.

Considering the complexities of the design and the uncertainty associated with the materials -- including their initial and time-dependent properties, the changes in loading from design values, as well as the comprehensive bridge maintenance and inspection programs -- there is no simple answer to the question of how long the bridge will last, or how that service life will be affected by certain maintenance activities or future changes in loading. However, this could be relevant information that the bridge owner could use to make better decisions and business plans.

Life-cycle cost analysis (LCCA) is an engineering economic analysis tool used to compare the relative merit of competing project alternatives. The Federal Highway Administration (FHWA) defines five major steps in the LCCA process [20], as listed below:

1. Establish design alternatives
2. Determine activity time

3. Estimate activity costs (agency and user)
4. Compute the life-cycle costs
5. Analyze the results

By considering all owner costs over a finite time, the LCCA can help the owner make objective business decisions about new construction and maintenance. Transit infrastructure continually ages, while population and load demands increase. These events precipitate the need for maintenance or improvement projects coupled with the use of objective information derived from analytical simulations, along with experimental data.

The analytical investigation in this research can provide information to the first step of the process, which is outlined by FHWA. The analytical investigation may also increase knowledge about the effects of increased loads on an existing bridge and provide better decision-making. Information used to determine a conventional bridge condition rating comes from visual inspections and load ratings based on design assumptions [15]. Design assumptions are based on simplified models of resistance and load effects. It is widely understood that engineers try to make conservative assumptions when uncertainty in these assumptions exists. Consequently, the first analysis of an aging civil infrastructure system may be based on conservative assumptions to facilitate a rapid design [15]. This research may demonstrate additional capacity, in which case the bridge condition rating would be improved.

Increased Loads and Load Effects

State Road 408 – SR 408 (Spessard L. Holland East-West Expressway) is the backbone

of the Central Florida Expressway Authority’s 109-mile network. The 22-mile toll road runs east-west, connecting Ocoee from Florida’s Turnpike in west Orange County to SR 50 (Colonial Drive) east of Alafaya Trail near the University of Central Florida in east Orange County. At its peak, more than 164,000 vehicles a day travel the 408 as it crosses downtown Orlando.

The bridge used in this research is one of the bridges that constitute the 109 network. The loads on this bridge have increased significantly from those assumed in the original design as is shown in Table 3 provided by the Tallahassee Democrat part of the USA Today Network [18].

Table 3: Traffic Data on Research Bridge

Year Built	1973
Average Daily Traffic (Year)	65,000 (2014) with 14% of truck traffic
Year Reconstructed	2005
Future Average Daily Traffic (Year)	112,775 (2036)

The finite element models developed may be used to determine if the bridge has the capacity to handle these increased loads.

Objectives & Motivation

A key motivation to this research is a new major project involving a 21-mile expansion roadway and bridge improvements, including direct access to the express lanes and a few bridge widenings (Figure 6). One of the bridges to be widened on this project was chosen for analysis in this research.

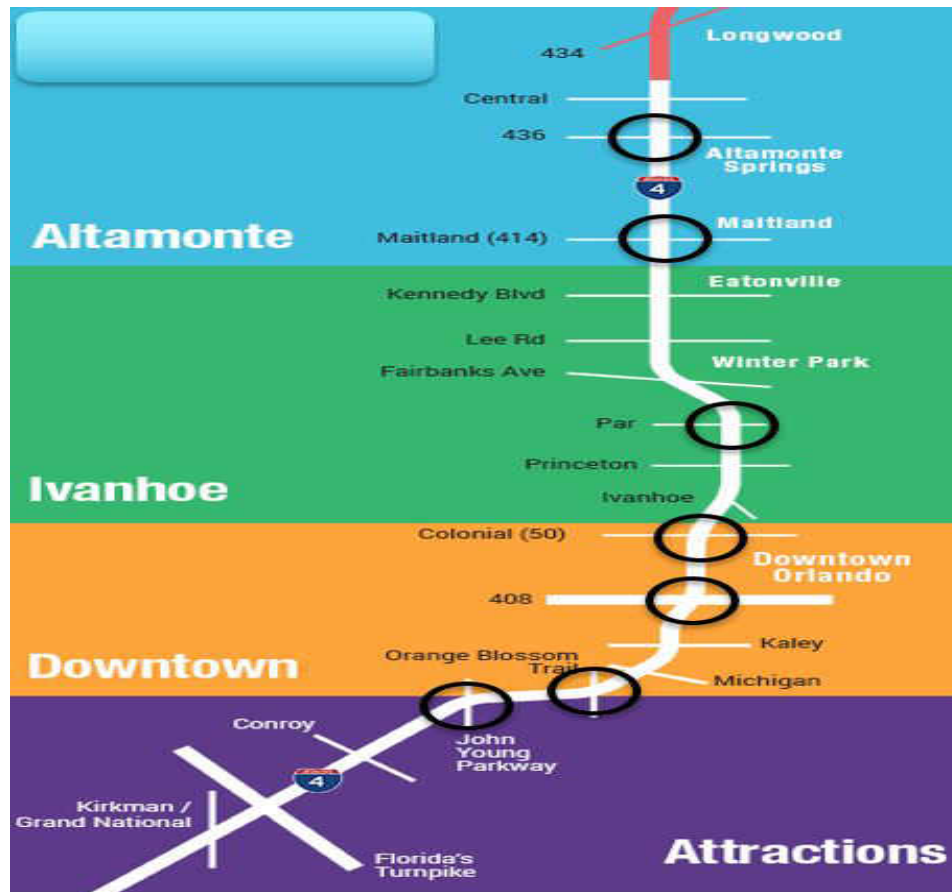


Figure 6: I – 4 Ultimate Project showing potential bridge widenings

Consequently, considering the key points indicated in the problem statement, the objectives of the research are defined as follows:

- Provide a better understanding of the capacity and performance of a widened bridge.
- Provide a better understanding of the bridge widening current design code and practices.
- Provide a better understanding of the load-rating process for widened bridges.
- Explore changes in bridge dynamics before and after widening.
- Conduct a reliability analysis before and after widening.
- Conduct a nonlinear analysis for load-carrying capacity

This research will provide a better understanding of the capacity and performance of a widened bridge by exploring and modeling uncertainties with a finite element model, which will be quantified in terms of load-rating and reliability, and by studying the live-load distribution factors for the bridge before and after widening. Additionally, a nonlinear finite element reliability analysis that provides analytical reliability indices to be compared against design code reliability indices for widened bridges will be investigated.

The results will then be compared with the current state-of-practice index using a case study of a widened bridge in Florida. Thus, the goal of this analytical investigation of prestressed beam bridge performance before and after widening is to provide a better understanding of load-rating and reliability.

Additionally, the motivation for this research stems from general bridge practice involvement and experience, which has led to the opportunity of improving current bridge-widening practices through introduction of an effective bridge-widening framework, as well as a contribution to the widening specification approach (Inspection and Load-Rating).

Methodology, Scope, and Tasks

An analytical investigation is a comprehensive parametric study (a series of simulations where one or more parameters of the problem are varied to investigate the sensitivity of the solution to the parameters) conducted to investigate the range of validity of a concept and to identify combinations of key parameters essential to ensure adequate performance under certain

conditions.

The process in this analytical investigation consists of generating a benchmark finite element model (FEM) and calibrating that model using existing results. The results from the calibrated model are then used to rate the condition of the bridge or investigate new loadings. The process will also include a comprehensive association and comparison of existing results, data, and established code values and estimates.

Since the structure under investigation was a widening of an original structure, the original structure is also investigated in this research. Design assumptions are based on simplified models of resistance and load effects. Sensitivity studies are conducted to identify critical parameters and are verified by comparison with other analyses. The verification process optimizes the model in terms of the critical parameters. After verification, the FEM may be used for simulation of existing or proposed loads, damage, retrofit, or improvement schemes. Results from the simulations may be combined with resistance calculations to determine load ratings. A reliability analysis can give an objective measure of structural reliability and probability of failure.

The state-of-practice approach to an analytical investigation of bridges commonly involves research teams, with each researcher focused on one or more subdivided portions of the study, such as FEM development, experimental design and data processing, model calibration, and/or simulations and rating. These processes can take researchers many years to complete on the various aspects of the bridge.

The scope of this research study is to generate a four-span continuous prestressed bridge finite element model that is representative of the original structure before and after

widening. In developing the FEM, boundary conditions, modal analysis, and dynamic behavior are considered. The FEM is used for simulations of different vehicle loads. AASHTO load ratings are conducted and examined for future widening. Reliability analyses are performed to identify a reliability index, and recommendations for experimental verification are presented.

Study tasks include the following:

1. Literature search
2. Bridge segment selection for analysis
3. FEA software evaluation and acquisition
4. Preliminary models and benchmark studies
5. Model visualization
6. Four-span FEM development
7. Critical parameter identification and bounding
8. Eigenvalue analysis and parameter sensitivity studies
9. Simulations, load ratings, and reliability analysis

For these objectives to be fulfilled, a roadmap is constructed explaining the main steps of the research framework, as shown in Figure 7.

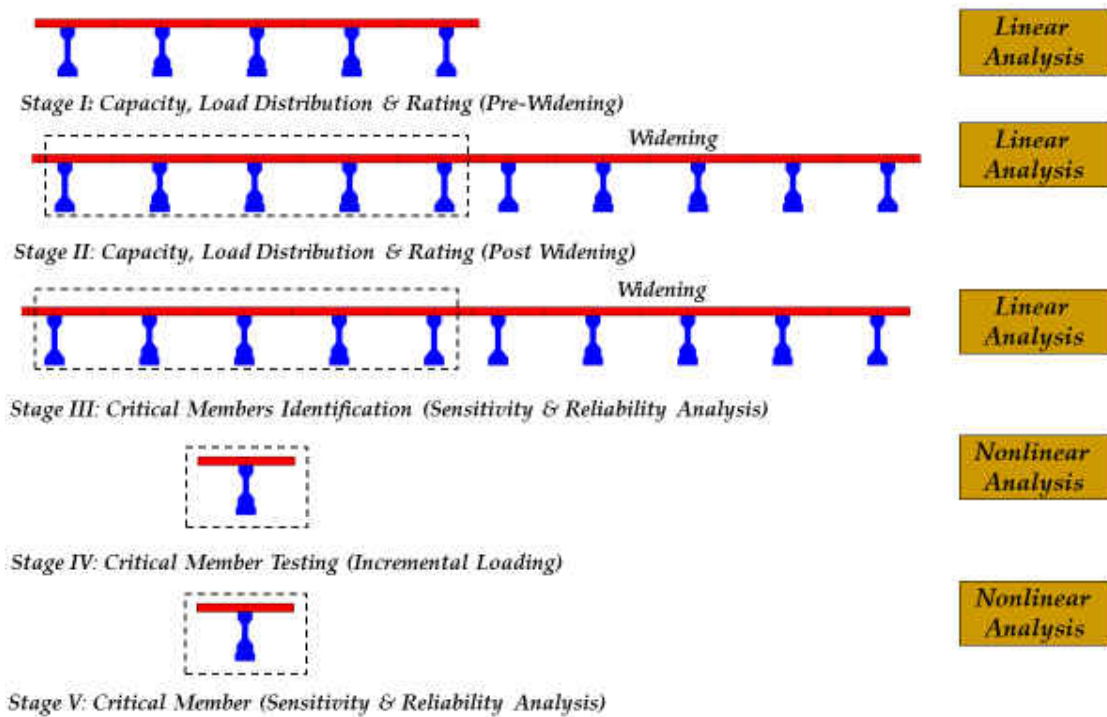


Figure 7: Investigation Framework for Bridge – Widening Analysis

The framework proposed in this study is expected to be implemented broadly because of its simple and inexpensive deployment in real life on bridge type structures. The broad implementation of the framework with this new approach to bridge widening criteria conditions could be of use to both inspectors and owners.

Novelty and Long-Term Vision of the Research

After a thorough literature search, it can be stated that further work is required at all stages of the bridge-widening process and implementation. This research, which aims to provide

a better understanding of the bridge-widening process and the suggested methods for analysis and investigation, is undertaken in three stages. The first stage is the capacity and performance analysis, which focuses on the linear analysis investigation of the bridge before and after widening. The second stage is the nonlinear analysis of a component of the widened bridge. Finally, the third stage is a reliability analysis of the bridge before and after widening.

Overall, the schematic shown below (Figure 8) highlights the contribution of this research.

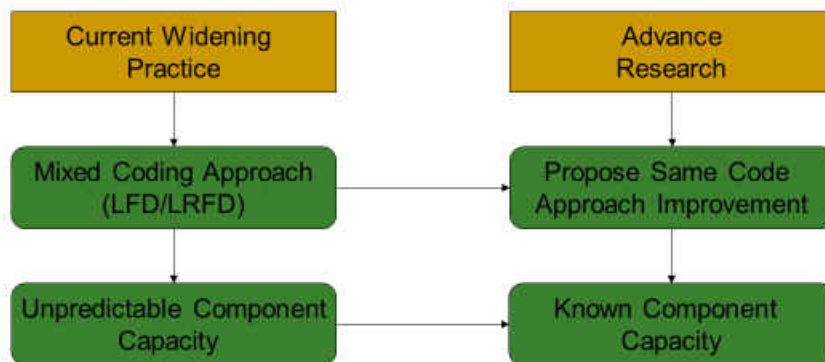


Figure 8: Research Contribution Focus Flow Chart

Current widening practice requires that the existing bridge under investigation for widening be load-rated using design codes and trucks that were initially used for designing if the bridge did not rate using current codes and trucks. This research will highlight the results of using the same and current code for load-rating analysis of the bridge before and after widening. Also, the capacity of a bridge and its components are usually underestimated or unpredictable, due to either a linear investigation or analysis. In this research, a nonlinear analysis aids in closely approximating the actual capacity of a component in the bridge system.

CHAPTER TWO: LITERATURE REVIEW AND FUNDAMENTAL CONCEPTS

Condition Assessment

Current widening methods and application are assumed to satisfy conditions without knowing the exact capacity of both the existing and pre-existing conditions (i.e., what is the capacity of the existing bridge? and what is the capacity of the widened bridge?) Critical inconsistencies can arise from several sources: (1) mixed used of design codes, (2) little or no knowledge of capacity and response performance between the original and widened bridge, (3) uncertainties (e.g., component level, system level, design and construction) and (4) rating and reliability computation.

AASHTO-LRFD codes achieve uniform reliability for the design components; whereas, when the LRFD limit states are calibrated against previous AASHTO design requirements to achieve component proportions, uniform reliability is not achieved. However, during widening, these codes (previous and current) are used interchangeably.

The FDOT Structures Design Guidelines (2014) make provision for this mixed coding, as follows;

- A. Before preparing widening or rehabilitation plans, review the inspection report and the existing load rating. If the existing load rating is inaccurate, or was performed using an older method (e.g., Allowable Stress or Load Factor), perform a new LRFR load rating. If any LRFR design inventory or any FL120 Permit rating factors are less than 1.0, calculate rating factors using LFR (MBE Section 6, Part B). If any LRFR or LFR

inventory load-rating factors are less than 1.0, a revised load rating may be performed using one of the additional procedures in C.1, C.2, C.3, or C.4 to obtain a satisfactory rating. If any LFR inventory rating factors remain less than 1.0, replacement or strengthening is required, unless a Design Variation is approved (see section B below). Calculate ratings for all concrete box girders (segmental) using only LRFR (MBE Section 6, Part A).

B. Design of bridge widening or rehabilitation projects must be done in accordance with SDG 7.3, and load rating must be done in accordance with SDG 1.7. Do not isolate and evaluate the widened portion of the bridge separately from the rest of the bridge. After preparing widening or rehabilitation plans, if any LRFR design inventory or any FL 120 permit rating factors (MBE Section 6, Part A) are less than 1.0, calculate rating factors using LFR (MBE Section 6, Part B). If any LFR inventory rating factors remain less than 1.0, replacement or strengthening is required, unless a Design Variation is approved. If any LRFR or LFR inventory load-rating factors are less than 1.0, a revised load rating may be performed using one of the additional procedures in C.1, C.2, C.3, or C.4 to obtain a satisfactory rating.

C. Additional procedures may be performed to obtain a satisfactory inventory load rating. Only one of the following is allowed per rating factor:

- i. **Approximate Method of Analysis:** When using LRFD approximate methods of structural analysis and live-load distribution factors, a rating factor of 0.95 may be rounded up to 1.0 for the existing portion of the bridge.

- ii. **Refined Method of Analysis:** Refined methods of structural analyses (e.g., using finite elements) may be performed to establish an enhanced live-load distribution factor and improved load rating. For continuous post-tensioned concrete bridges, a more sophisticated, time-dependent construction analysis is required to determine overall longitudinal effects from permanent loads.
- iii. **Shear Capacity - Segmental Concrete Box Girder - Crack Angle (LRFD [5.8.6]):** To calculate a crack angle more accurately than the assumed 45-degree angle used in LRFD, use the procedure found in Appendix B of "Volume 10 Load Rating Post-Tensioned Concrete Segmental Bridges" (dated Oct. 8, 2004) found on the Structures Design Office website [17].

The design summary is provided in the flow chart presented in Figure 9.

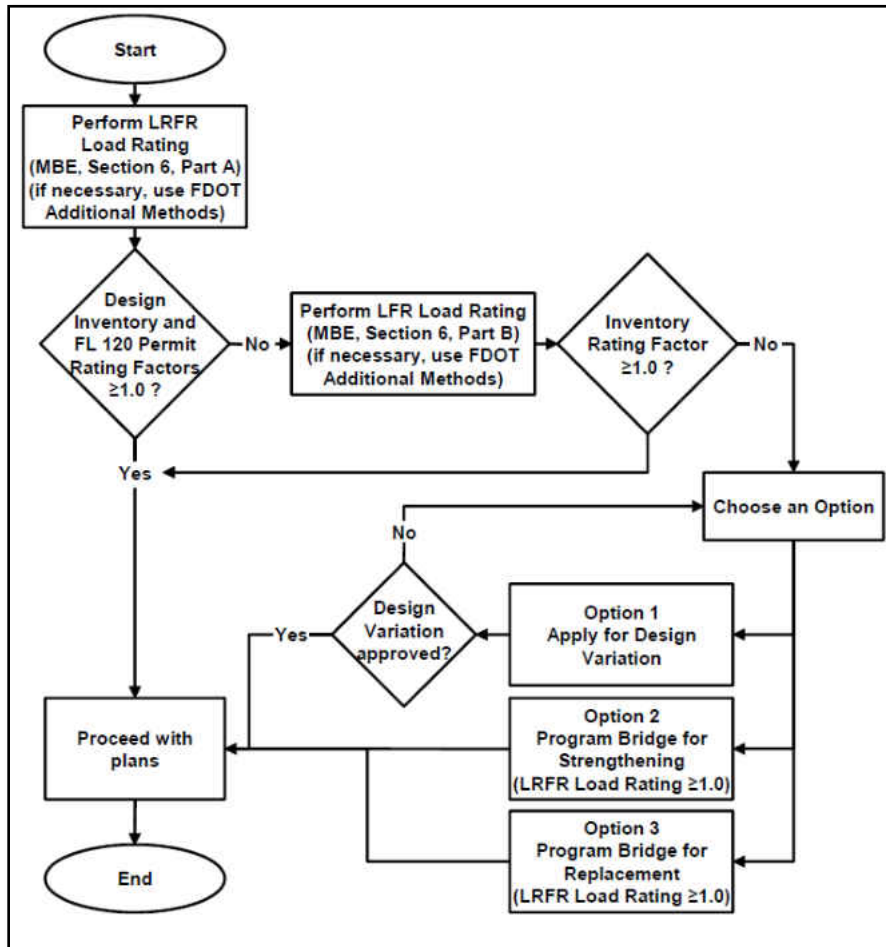


Figure 9: Widening/Rehabilitation Load – Rating Flow Chart Illustrating Mixed Coding

While there are no effective methods of determining the capacity and performance of existing bridges, there is relatively no knowledge to compare the capacity and performance of the original (existing) bridge with the widened bridge as is illustrated here in Figure 10.

The inability to adequately load rate a widened bridge stems from the initial complexity of computing the response of a bridge to live loads.

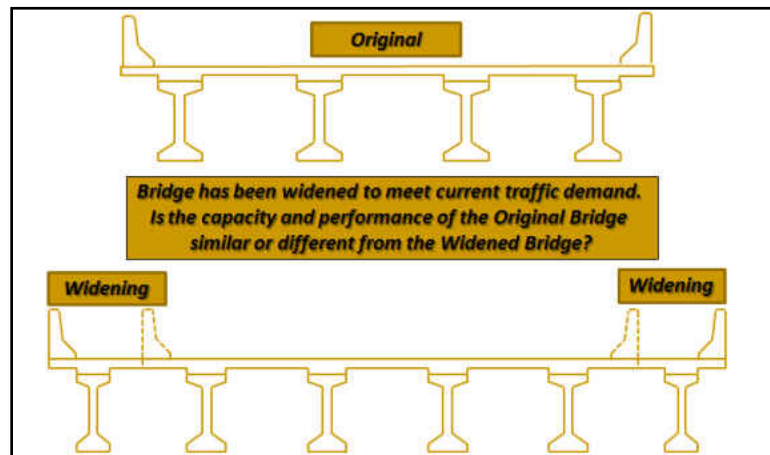


Figure 10: Existing and Widened Bridge for Capacity and Performance Analysis

In Andrew Sonnenberg's paper presented at the 2014 Small Bridges Conference, he explains the concept of assessing bridge load capacities by theoretical analysis which he breaks into two main methods: a generic assessment, and using the rating equation. The generic assessments, are economically low in cost and a good initial estimate for an asset owner in the absence of complete load-rating information [18].

And he elaborates on the second option, which is the rating equation where one is provided a rating equation that can be used to assess structures and determine a structures rating factor for a nominated rating vehicle. The rating factor is obtained by calculating the theoretical capacity of a structure and the design actions for the nominated rating vehicle.

In retrospect, researchers see the best and most effective option for determining the capacity and performance of a bridge (existing or widened) to be through reliability and load ratings.

Load ratings are a reasonable deterministic approach designed mostly to assess the safety

of a bridge and to determine the strength and allowable load on a bridge. The methodology examines the appropriate failure modes, which is consistent among different bridges, and it makes sense. However, these load ratings have some limitations that can be overcome using a reliability analysis.

The standard AASHTO HS-20 truck is a good conservative and deterministic representation of the typical truck on the highway. However, it does not account for the cumulative effect of many trucks passing over the bridge over a period of time. Using the HS-20 truck, equivalent load ratings for different failure modes do not achieve equivalent levels of safety. Load ratings do not consider redundancy in a structure or correlation between failure modes. A system reliability analysis will consider both. There are some very good probabilistic live-load models available. A reliability analysis overcomes all the listed limitations of the load-rating approach and produces a consistent level of safety for various failure modes, per Estes, et al. [19], and is in the right direction of determining the capacity and performance of a bridge.

In general, reliability-based structural performance indicators reflect the uncertainty in load, resistance, and modeling. However, they do not account for the outcome of a failure event in terms of economic losses.

Currently, the load rating is the method used by state DOTs for evaluating the safety and serviceability of existing bridges in the United States. In general, load rating of a bridge is evaluated when a maintenance, improvement work, change in strength of members, or addition of dead load alters the condition or capacity of the structure. The AASHTO-LRFD specifications provide code provisions for prescribing an acceptable and uniform safety level for the design of

bridge components. Once a bridge is designed and placed in service, the AASHTO Manual for Condition Evaluation of Bridges provides provisions for determining the safety and serviceability of existing bridge components. Rating for the bridge system is taken as the minimum of the component ratings. If viewed from a broad perspective, methods used in the state-of-the-practice condition evaluation of bridges at discrete time intervals, and in the state-of-the-art probability-based life prediction, share common goals and principles. This dissertation briefly describes a study conducted on the rating and system reliability-based lifetime evaluation of several existing bridges within a bridge network, including prestressed concrete, reinforced concrete, steel-rolled beam, and steel plate girder bridges. The approach is explained using a representative prestressed concrete girder bridge. Emphasis is placed on the interaction between rating and reliability results, to relate the developed approach to current practice in bridge rating and evaluation. The results provide a sound basis for further improvement of bridge management systems, based on system performance requirements, per Akgul, et al. [20].

Accumulation of research in the field of bridge evaluation based on structural reliability justifies the consideration of reliability index as the primary measure of safety for bridges. Furthermore, the lifetime bridge evaluation techniques are being based primarily on reliability methods. Currently, bridge safety is measured in terms of the rating factor, which reflects the live-load capacity of the structure. To investigate the reliability index of an existing bridge, and to consider its relation to the rating factor, an in-depth investigation of the interaction between these two safety measures for different limit states of different bridge types is desirable.

The paper by Akgul, et al [20] presents the results of a study in which the interaction

between rating and reliability of a group of 14 bridges in an existing bridge network was investigated. This investigation is based on advanced methods to evaluate the reliability of each bridge in the network. Rating factors for different bridge groups are identified based on bridge type, and bridge groups are compared based on mean group rating factor. Bridge rating and reliability are quantified when each bridge starts its service life. The bridge rating factor and the reliability index are evaluated for various limit states belonging to different member types within the bridge network. A correlation study between bridge rating factor and reliability index of different bridge types in an existing network reveals interesting results, per Akgul, et al. [20].

Consequently, in addition to mixed coding, unknown capacity and response performance are the uncertainties that are a major missing component in the knowledge gap. The uncertainties that can be encountered during a bridge-widening project range from component level and system level, to design and construction. A bridge-widening study is usually done prior to this process and will include, but not be limited to, examining new and existing structures, dead and live-load deflections, temperature movements, prestress deflection and shortening, and settlements.

Structural Modeling & Analysis

The analytical investigation begins with structural modeling. The state-of-practice approach to structural modeling is based on practical implementation of discrete finite element analysis methods, using conventional PC hardware and software to generate models that will accurately and completely simulate the following:

1. Three-dimensional (3D) geometry of critical regions and elements
2. Boundary conditions
3. Critical mechanisms of external loading

Recent advances in PC hardware and software have made modeling and simulation a feasible and efficient approach. After a nominal 3D FEM of the bridge has been generated, the dynamic response of the bridge is simulated to help define a comprehensive validated system. Mode shapes, natural frequencies, and modal contribution coefficients are computed by the preliminary finite element simulation, and are used to validate the efficiency and accuracy of the model behavior. Determining the natural frequencies provides the proper frequency bandwidth for a given bridge. This knowledge is used to configure the bandwidth of the data acquisition system to capture the necessary modes.

The nominal FEM represents the actual structure with limited accuracy, because of possible damage, deterioration, or structural details that behave differently than the design assumptions. Thus, the nominal model needs to be calibrated to more accurately simulate the existing data or available study and inspection results.

The critical parameters of the model are adjusted in a step-by-step process so that the analysis results match the measured static and dynamic response data. The comparisons of analytical and available design calculations and estimations give an indication of the accuracy of the model during calibration.

Simulations and Load Rating

In most cases, the final deliverable in the analytical investigation process of bridge

inspection is a bridge rating factor meeting a code criteria or specification. The calibrated FEM is used to simulate loading conditions, and the resulting load effects are recorded and analyzed to arrive at the bridge rating factors. There are several advantages to rating the bridge based on calibrated finite element results, versus static load testing. First, the FEM can rapidly produce reliable results for rating the bridge under many types of loading. In addition to the truck used for the test, standard AASHTO, FHWA, and state loading conditions can be generated for the rating procedure. A second advantage is that the rating is based on the global response of the entire bridge, rather than the local response at strain gauge locations. Ratings based on strain data rely upon the assumption that the strain gauges capture all critical behaviors. A third advantage is that calibrated finite element models can be used with damage identification technology to locate possible localized defects and failures in the bridge that go unnoticed during visual inspections and truck load testing. A fourth advantage of the using the FEM-based rating is that should an improvement or retrofit of the structure be required, engineers can use the calibrated model to quickly evaluate the alternatives [21].

To emphasize, the state-of-practice approach to analytical investigation of major bridges commonly involves multiple researchers and even multiple research teams, with different researchers focused on one or more subdivided portions of the study, such as FEM development, experimental design and data processing, model correlation, and/or simulations and load rating.

Model Updating

Finite element modeling gives a detailed description of the physical and modal characteristics of a bridge. It is desirable to measure the dynamic properties of new and existing

bridges to better understand their dynamic behavior under normal traffic loads and extreme loads, such as those caused by seismic events or high wind. Dynamic properties of interest include resonant frequencies, mode shapes, and modal damping. These measured properties can be used to update numerical models of the bridge so that the models better reflect the actual boundary conditions and as-built structural connectivity. Knowledge of the dynamic properties can be used to assess the effects of traffic loading on the fatigue life of the structure, and to determine dynamic load factors for these structures [22].

A three-dimensional dynamic FEM was developed for the Tsing Ma long suspension bridge in Hong Kong. Modal analyses were carried out to determine natural frequencies and mode shapes of lateral, vertical, torsional, and longitudinal vibrations of the bridge and to investigate the dynamic interaction between the vibrational modes, between the main span and side span, and between the deck, cables, and towers. The natural frequencies and mode shapes obtained by the numerical analysis were compared with experimental results and found to be in good agreement [23].

The combination of numerical modeling and full-scale measurement provides a comprehensive understanding of the behavior and properties of the Tsing Ma Bridge. The validated FEM, computed dynamic characteristics, and the dynamic interactions between bridge elements can serve as topics for future studies on the long-term monitoring, or for aerodynamic analysis of the Tsing Ma Bridge [23].

Model updating has developed into a practical and applicable technology in recent years. Zhang, et al. provides an excellent review of literature describing the historical development of model updating methods [24]. For a complex structure with many degrees of

indeterminacy, model updating is difficult because it involves uncertainties in many parameters, such as material properties, geometric properties, and boundary and continuity conditions. Manual calibration of the FEM should take advantage of existing knowledge from the owner, as well as knowledge of field experiments, analytical modeling, prediction and simulation of bridge response, and uncertainty associated with different types of experimental data. A flow chart that shows a procedure for manual FEM calibration using modal analysis is given in Aktan, et al. [25].

There are generally two approaches for updating the finite element model of a structure, depending on whether the system matrices or the structural parameters are selected for updating [26].

The method of system matrix updating seeks changes in stiffness and/or mass matrices by solving a system of matrix equations. This approach cannot handle the situation whereby the changes in mass and stiffness matrices are coupled together. The parametric updating method typically involves using the sensitivity of the parameters to find their changes [27].

This sensitivity-based parametric updating approach has the advantage of identifying parameters that can directly affect the dynamic characteristics of the structure. Additionally, by employing this method, one may acquire an immediate physical interpretation of the updated results. For these reasons, the updating method is chosen in the Kap Shui Mun cable-stayed bridge study [28].

Zhang, et al. describe an improved sensitivity-based parameter updating method used for model updating of the Kap Shui Mun cable-stayed bridge. This method is based on the eigenvalue sensitivity to some selected structural parameters that are assumed to be bounded

within some prescribed regions, per the degrees of uncertainty and variation existing in the parameters, together with engineering judgment. The changes of the chosen parameters are found by solving a quadratic programming problem. A comprehensive procedure for sensitivity-based model updating is given in the paper referenced [28]

Assumptions and considerations associated with the Kap Shui Mun bridge study include the following:

1. The structural parameters are grouped into major components of the structural system, including the deck, towers, connections, and boundary conditions.
2. The cross-section of the composite deck is described by equivalent homogeneous properties and a single spine passing through the shear centers of the deck.
3. The deck/tower connections, deck/pier connections, and boundary conditions are modeled using one elastic spring along each translational and rotational direction.

A total of seventeen modes, with a frequency range between 0.4 and 2.2 Hz, are selected for matching between analytical and experimental results. Thirty-one structural parameters are selected for updating, based on a comprehensive eigenvalue sensitivity study. It was found that, in general, the frequencies calculated from the updated model are closer to the measured values when compared to those calculated from the initial model. A similar result is seen even for those modes that are not included in the original updating process. The results seem to suggest that it is possible to update the FEM so that the natural frequencies are reasonably close to the measured ones. However, there is not sufficient evidence to indicate that the updated structural parameters are, or are close to, the actual values. At best, the updated model can be considered a plausible candidate to represent the real structure. Because the number of structural parameters

considered is larger than the number of modes, multiple sets of parameters that satisfy the optimality objectives may exist. The non-unique nature of the solution is an important issue that needs to be addressed in a future study [28].

The modal assurance criterion (MAC) is an objective method to quantify the correlation between mode shapes [22]. The MAC may be used to compare mode shapes measured during different tests, or to compare experimental and analytical results. The MAC makes use of the orthogonality properties of the mode shapes. If the modes are identical, a scalar value of one is calculated by the MAC.

Finite – Element Analysis

Dating back to the 1940s, since its discovery the finite element method (FEM) continues to be the predominant strategy employed by engineers to conduct structural analysis. The numerical technique for finding approximate solutions to boundary value problems for partial differential equations basically subdivides a large problem into smaller parts, called finite elements. This is also referred to as finite element analysis (FEA).

Until recently, only linear models were used to analyze structural systems composed of complex materials such as reinforced concrete. However, recently, researchers have employed many variations of the constitutive representations of the concrete component, reinforcement, and the nature of their interaction. A comprehensive summary by Darwin of 24 finite element model studies of reinforced concrete from 1985 to 1991 illustrates the wide range of options available to perform an accurate analysis [29]

The Computers and Structures, Inc. Bridge (CSiBridge) software used for the linear

analysis in this research implements a parametric object-based modeling approach when developing analytical bridge systems [30].

Per NCHRP, when using the finite element method, slab-on-girder bridges can effectively be modeled as beam/frame and shell elements. The use of shell elements to model girder bridges yields good results, and are also used to validate grillage models [13]. A shell is a three- or four-node area object used to model membrane and plate-bending behavior. Shell objects are useful for simulating floor, wall, and bridge deck systems. Shells may be homogeneous or layered throughout their thickness.

For this analysis, the CSiBridge software will be used to determine moment and shear values using area objects, and all lanes will be defined. The following are the general steps to be used for analyzing a structure using CSiBridge [31]:

- Geometry (input nodes coordinates, defined members and connections)
- Boundary conditions/ joint restraints (fixed, free, roller, pin or partially restrained with a specified spring constant)
- Material property (elastic modulus, Poisson's ratio, shear modulus, damping data, thermal properties and time-dependent properties such as creep and shrinkage)
- Loads and load cases
- Stress-strain relationship
- Analysis of the model based on analysis cases

The bridge superstructure is idealized as a two-dimensional system. The main girders and the ends diaphragm beams are modeled as space frame elements with six DOFs at each node. The bridge deck is modeled as quadrilateral shell elements with six DOFs at each node. The

center of gravity of the slab coincides with the girders center of gravity therefore, the girders' properties are transformed to the deck center of gravity. The bridge supports consist of hinges at one end of the girders and rollers at the other end [32].

Finite – Element Methods for Concrete Structures

Prestressed concrete designs have been widely used for buildings, bridges, tanks, offshore oil platforms, nuclear containment vessels, and many other structures. The design of these structures must satisfy requirements for safety, serviceability, and fatigue. While this can be accomplished with approximate or empirical procedures prescribed in codes, it is desirable to have refined analytical models and methods available which can trace the structural response of these structures throughout their service load history, under increasing loads and through elastic, cracking, inelastic, and ultimate ranges [33]. These refined analytical methods may be used to study the effects of important parameters in a systematic way, to test and improve the design codes; or they may be used directly in the analysis and design of complex structures. Many advances have occurred in recent decades with respect to the finite element analysis of reinforced and prestressed concrete structures. Three alternative approaches are used for modeling reinforcement. These are the discrete model, embedded model, and smeared model [34].

In the discrete model, first suggested by the authors Ngo and Scordelis, reinforcing bars are modeled using special elements connected to concrete through fictitious springs representing the bond. The boundaries of the concrete elements follow the reinforcing bar to achieve common nodes (DOFs). The discrete representation is the only way to account for

bond slip and dowel action directly. The main disadvantage is that the concrete element mesh patterns are restricted by the location of the reinforcement, and mesh refinement can be difficult [33]. The number of concrete elements and DOFs is increased, thereby increasing computational effort [35].

Embedded models allow an independent choice of concrete mesh. The same type of elements with the same number of nodes and DOFs are used for both concrete and steel. The stiffness matrix and internal force vector for the steel element are obtained containing only the contributions of the reinforcing bar. Bond slip and dowel action can only be modeled implicitly by modifying the constitutive relations for concrete or steel [35].

In the smeared model the reinforcement is characterized by smearing the reinforcing bar to thin layers of mechanically equivalent thickness within a concrete element. Assuming a perfect bond between concrete and steel, the constitutive relations are derived using composite theory. The smeared model accurately represents only uniformly distributed reinforcing bars [35].

The discrete model is the most general. It is the only model that uses conventional 1D elements to represent reinforcement, and the only model which can account for bond slip and dowel action directly. Different material properties for reinforcement, and different bond conditions at different nodes, can be directly and independently represented. The disadvantage to the basic discrete model is that the concrete mesh geometry depends on the reinforcement mesh [21].

To allow independent choice of the concrete mesh, authors El-Mezaini and Citipitioglu propose a special isoparametric element with movable edge nodes [34]. Reinforcing elements

are modeled independent of the concrete mesh. Reinforcing bars are commonly modeled as truss or cable elements [35]. The edge nodes of the concrete elements are moved to the points where the reinforcing layers intersect the edges of concrete elements. The concrete nodes are connected to the steel nodes.

El-Mezaini and Citipitioglu also presented a technique for the discrete representation of bonded, unbonded, and partially bonded tendons. The reinforcement nodes are constrained, depending upon the bonding assumptions. For the bonded case, the concrete and steel nodes occupy the same location and are assigned the same DOFs. The steel and concrete nodes are fully coupled, and no slip is allowed. For the unbonded case, the concrete and steel nodes are coupled in the direction perpendicular to the reinforcement axis, but are independent in the direction along the reinforcement axis. The concrete and steel have the same DOFs in the perpendicular direction and different DOFs in the tangent direction. Relative motion can occur, and the tangent direction is known as the slip degree of freedom. Partial bond is the most general method. The slip DOFs are controlled using a prescribed slip law, such as fictitious springs. The required bond model is represented by assigning appropriate properties to the fictitious springs [34].

This is the most general case, because all bond conditions can be represented by proper selection of spring properties. For example, a very stiff spring may represent perfect bond, whereas a very soft spring represents no bond. Any bond in-between can be represented. In the partially bonded method, linear or nonlinear bond models can be used to represent friction and slip. Linear or nonlinear material properties may be used for concrete and steel. Scordelis presents a unified numerical procedure for the material and geometric nonlinear

analysis of various types of reinforced and prestressed concrete structures, including planar or three-dimensional rigid frames composed of 1D elements; panels or slabs composed of 2D triangular or quadrilateral flat finite elements; thin shells composed of 2D flat or curved finite elements or axisymmetric thin-shell elements; and solids made up of 3D solid finite elements or axisymmetric solid elements. Time-dependent effects, due to load history, temperature, creep, shrinkage and aging of the concrete, and relaxation of the prestressing steel, may be included in the analysis. This work by Scordelis is based on the discrete model for reinforcement [33].

While nonlinear slip models and material properties for prestressed and reinforced concrete structures are available in the literature, the practical implementation of finite element methods may not require these advanced techniques. Elastic behavior is generally accepted as a valid assumption for analysis of prestressed concrete structures under service loads and reinforced concrete elements up to cracking, as proposed by El-Mezaini and Citipitioglu [34].

The elastic behavior concept is the approach adopted by the software used for linear analysis in this research.

Fundamental Concepts in Bridge Widening

A bridge widening which is defined as an increase of bridge deck width or modifications to the sidewalk or barrier rails of an existing bridge resulting in significant mass increase or structural component changes immediately reveals some design and construction challenges (structural component). It should also be noted here that bridge widening is a rehabilitation process defined as a “major” rehabilitation. The definition of bridge widening and its classification are illustrated in Figure 11, Figure 12 and Figure 13 below.

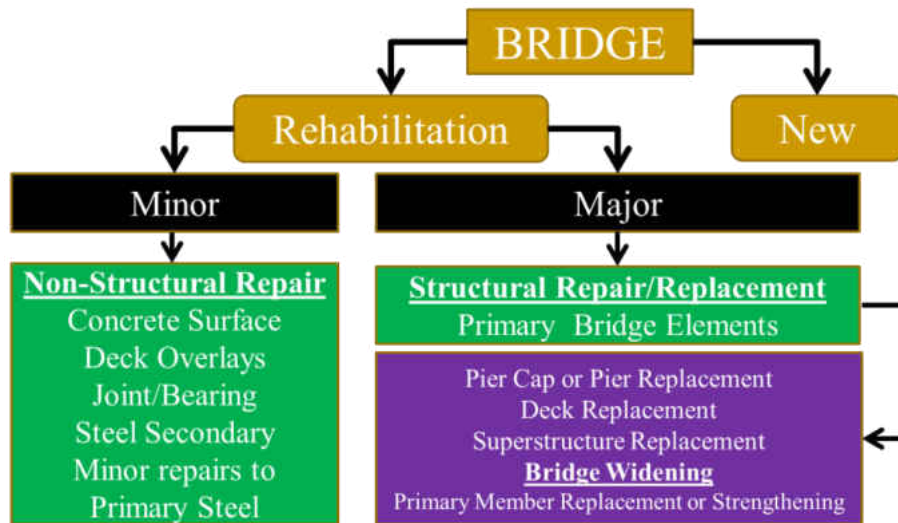


Figure 11: The Bridge Structure

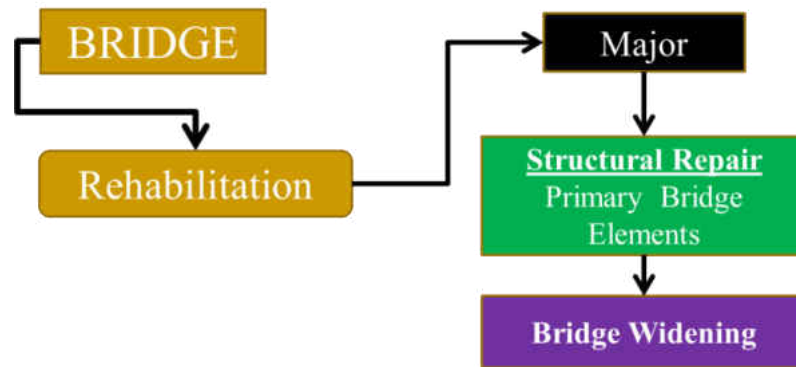


Figure 12: The Rehabilitation Structure

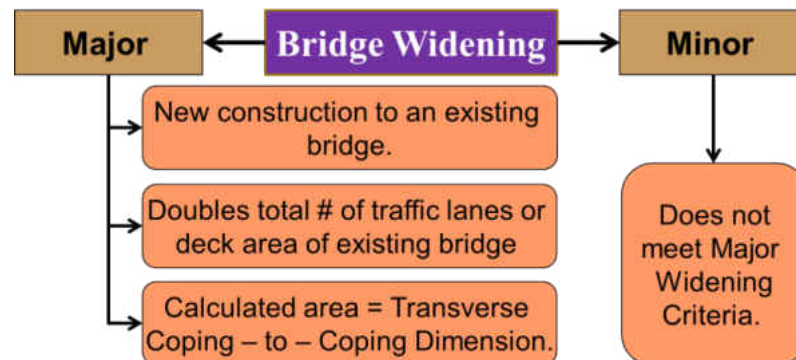


Figure 13: Bridge Widening Classification

As, it is also explained under “Bridge Widening Application,” the increase of bridge deck width can be dependent (increasing deck width of an existing bridge directly) or independent (a completely new bridge adjacent to or over the existing bridge, using separate foundation, piles, beams and caps). Bridge widening projects are common, due to the increase in traffic and safety demands on existing routes. The different bridge-widening options are summarized in Table 4, and are illustrated in Figure 14, Figure 15, Figure 16, Figure 17 and Figure 18.

Table 4: Bridge Widening Options

Option	Description
I	<i>Inside Widening (Existing Bridge Expansion)</i> – Typically in a twin bridge where widening is initiated towards the median to accommodate future increase in traffic.
II	<i>Inside and Outside Widening (Existing Bridge Expansion)</i> – This is like Option I, but includes outside widening since an inside widening only cannot and may not accommodate the traffic demand (maybe multiple lanes are required).
III	<i>Bridge Heightening</i> – Typically, when it is not feasible to widen both inside and outside of a bridge, the only alternative maybe an overhead bridge (heightened bridge) over the existing bridge that may share the same space in reference foundation.
IV	<i>One – side Widening (New Bridge Expansion)</i> – Typically when a widening is required that does not satisfy widening conditions (same girders), a completely new bridge adjacent to the existing bridge could be used (for trucks, pedestrian, bus, bicycle etc.).
V	<i>Inside and Outside Widening (New Bridge Expansion)</i> – This is similar to Option IV but widening is on both sides.

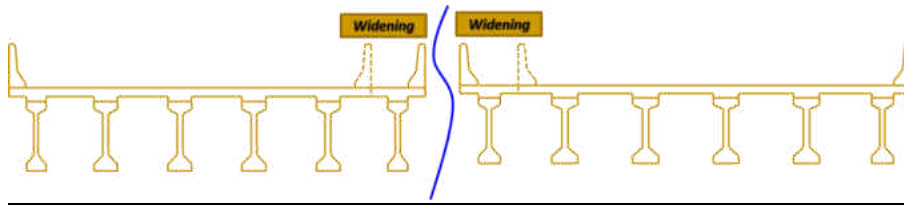


Figure 14: Option I – Ext. Bridge Widening Exp. (Inside Widening)

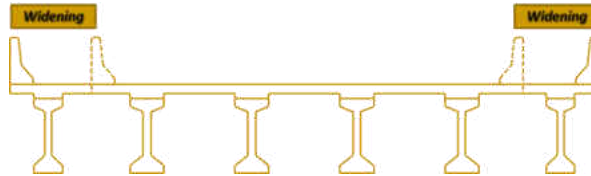


Figure 15: Option II – Ext. Bridge Widening Exp. (Inside and Outside Widening)

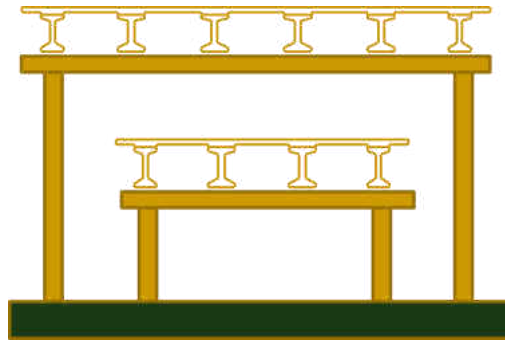


Figure 16: Option III – Bridge Ht. (Proposed Bridge Ht. over Ext. Bridge)

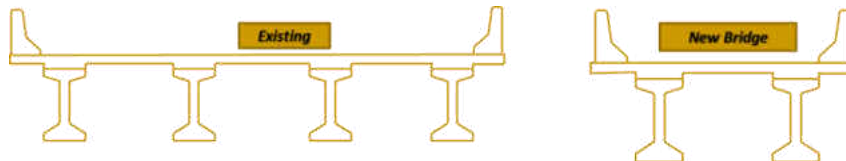


Figure 17: Option IV – One – Side Widening (New Bridge Expansion)

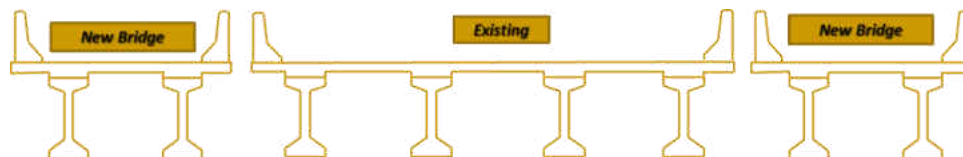


Figure 18: Option V – Inside & Outside Widening (New Bridge Expansion)

In general, a bridge widening begins with a careful study of relative movement between the new and existing structure. Dead-load and live-load deflections (both short- and long-term), temperature movements, prestress deflection and shortening, settlement, seismic movement, basic structure continuity, and stability, are all factors that must be evaluated to provide a widening that is structurally compatible with the existing bridge. The bridge widening process requires, but is not limited to, the following:

Existing Plans

Reviewing the existing plans is the first step in every bridge-widening consideration, which will include basic information concerning geometrics provided by the District's Department of Transportation (DOT), the inspection records available in the Bridge Inspection Records Information System (BIRIS), the Structures Replacement and Improvement Needs (STRAIN) report, and any additional information that can be obtained from the Area Bridge Maintenance Engineer (ABME). Additional information that can be obtained during this stage can include as-built construction drawings, photo logs from the Division of Traffic Operations (which maintains recent photos detailing approach rail, bridge rail, terrain and most likely deck overlays), and roadway as-built plans from the Document Retrieval System (DRS), which may include retaining walls, culverts and other roadway facilities information.

Preliminary Evaluation

The next step in this process is a preliminary evaluation of the bridge's substructure. This evaluation may also include a preliminary site investigation utilizing information from the following: a Preliminary Report from the Preliminary Investigations Branch (PI), and a preliminary foundation report obtained from the Geotechnical Services, which will contain

evaluations of subsurface conditions based on as-built data and preliminary boring data.

Structural Adequacy and Capacity

Once the above information is obtained, the capacity of the existing structure (bridge) is analyzed to see if it meets load-carrying capacity and current standards.

Load-Carrying Capacity for Strengthening or Replacement Requirements

- Moment and shear capacity of the girders capable of supporting the proposed design and overload vehicle loads.
- Capacity of the diaphragms to determine the adequacy of supporting the superstructure dead load in the process of replacing bridge bearings.
- Substructure components to determine the adequacy for both current and proposed vehicular live loads.
- Bridge bearings capacity to support new design loads.
- Functioning expansion joints to accommodate the bridge deck movement for the new design loads.

Current Standards

- Hydraulic – Bridge widening over water requires the development of a new hydraulic study to be approved by the Structure Hydraulics Branch and Structure Maintenance and Investigations. This study is to determine the degree of scour (degradation potential) which may increase, due to widening.
- Safety – Existing structures (bridges) which are proposed to be widened, but do not meet current geometric standards (safety deficient), are reported to the District's DOT for an alternative rehabilitation approach.

- Seismic – Where applicable, seismic evaluation will require consulting the Office of Earthquake Engineering (OEE), since a large number of factors are to be considered in a widening.
- Live Load – The American Association of State Highway and Transportation Officials (AASHTO) LRFD Bridge Design Specifications, in conjunction with the state's department of transportation, is used to assess the bridge rating and posting criteria for the design live load. The only exception for a limitation of the bridge's live load is when the limitation is directed by the Office of Structure Maintenance and Investigations [15].

Typically, in order to provide safe access and meet the needs of all users in a cost-effective manner, it is necessary to both widen the deck overhangs as much as practically possible and optimize the usable deck width by reconfiguring the traffic lanes. Usually bridge widening is done on both sides of the bridge, as previously illustrated in Figures 15 and 16.

Prestressed Concrete Bridges

In the 1930s, Eugène Freyssinet invented prestressed concrete. High-tensile steel cables were substituted for the bars. These cables were tensioned by jacks and were then locked to the concrete. Thus, they compressed the concrete, ridding it of its cracks, improving both its appearance and its resistance to deterioration. The cables could be designed to counter the deflections of beams and slabs, allowing much more slender structures to be built. As the cables were some four times stronger than the bars, many fewer were necessary, reducing the congestion within the beams, making them quicker to build and less labor-intensive. Most

concrete bridges, except for small or isolated structures, now use prestressing. It is also being used ever more widely in buildings where the very thin flat slabs it allows afford minimum interference to services and, in some circumstances, make it possible to increase the number of floors within a defined envelope [36].

The design of prestressed concrete bridge girders has changed significantly over the past several decades. Specifically, the design procedure to calculate the shear capacity of bridge girders that was used 40 years ago is very different than the procedures recommended in the current AASHTO LRFD Specifications. Thus, many bridge girders that were built 40 years ago do not meet current design standards and, in some cases, warrant replacement due to insufficient calculated shear capacity. However, despite this insufficient calculated capacity, these bridge girders have been found to function adequately in service with minimal signs of distress.

When the Utah Department of Transportation (UDOT) decided to replace the bridge at 4500 South (SR – 266) that serves southbound I-215 in Salt Lake City, it was one of the first accelerated bridge construction replacement projects in Utah, the existing bridge provided an opportunity to investigate the ultimate shear capacity of precast, prestressed bridge girders built during this era. The original bridge was built as a four-span superstructure with an overall roadway width of approximately 77 feet. The bridge had a significant change in elevation which resulted in water and de-icing salts running down the length of the bridge. Each span was constructed with a fixed support on one end and an expansion joint on the other, which allowed water and salt to enter the expansion joint and resulted in corrosion at the ends of the prestressed concrete girders.

Due to the corrosion and the insufficient calculated shear capacity, UDOT asked

researchers at Utah State University to determine the ultimate capacity of the girders, and to investigate strengthening procedures. To meet the objectives of the project, eight AASHTO Type 2 girders were salvaged during the demolition and shipped to the Systems, Materials and Structural Health (SMASH) Laboratory at Utah State University. Six girders were salvaged from one bridge, and the last two girders were salvaged from a separate bridge. Girders 1 through 6 had an in-service span length of 22-ft., 3-in. and girders 7 and 8 had an in-service span length of 34.5 ft.

The girders were simply supported and loaded at 48 inches ($d + 1\text{-ft}$) from the supports, with a single point load. Upon investigation, the shear reinforcement was found to consist of number-4 bars at a spacing of 21 inches on center. Material tests determined that the vertical stirrups were made of 33-ksi steel, and the prestressing strand was 250-ksi stress-relieved strand. Baseline ultimate shear capacities were obtained by applying a vertical load at a distance “ d ” from the face of the support. Subsequently, carbon fiber reinforced polymers that were donated by the chemical company BASF were applied to the remaining girders in five different configurations. The retrofitted girders were then tested similarly to the baseline tests, so that direct comparisons could be made. The measured data from the testing girders and the subsequent analyses lead to the following conclusions and recommendations:

1. The average measured shear capacities for girders 1 through 6, and 7 and 8, respectively, were 163.56 kips and 261.50 kips.
2. The measured capacities for the two groups of girders were compared with the calculated capacities, per procedures outlined in the AASHTO LRFD Specifications

- (2007) and the ACI 318 guidelines (2005). In general, the measured girder capacities were larger than any of the calculated values.
3. The strut-and-tie method was determined to provide the best estimate of the shear capacity of the girders. For girders 1 through 6, the strut-and-tie produced an ultimate shear capacity of 138.56 kips, which is 84.72% of the average measured value. For girders 7 and 8, the strut-and-tie method resulted in an ultimate shear capacity of 258.7 kips, which was 98.93% of the average measured value.
 4. The AASHTO LRFD and ACI methods for calculating shear capacity were much more conservative in comparison to the strut-and-tie methodology. The AASHTO LRFD general method predicted a shear capacity of 82.27 kips and 100.28 kips, which was 50.3% and 38.3% of the measured capacity for girders 1 through 6 and girders 7 through 8, respectively. The ACI-318 simplified method predicted a shear capacity of 101.74 kips and 131.09 kips, which was 62.2% and 50.1% of the measured capacity, for girders 1 through 6 and girders 7 through 8, respectively.
 5. The experimental strengthening program consisted of load testing of five different CFRP reinforcement configurations. The CFRP reinforcement was found to increase the shear capacity of the AASHTO I-shaped prestressed girders. The magnitude of the increased shear capacity was found to be highly dependent on the CFRP reinforcement configuration and anchorage system. The application of the CFRP reinforcement resulted in larger deflections before failure. Based on the recorded strain measurements, it was concluded that the CFRP fabric was not overstressed at failure, and the primary failure mode was debonding.

6. While five CFRP configurations were evaluated, the configuration on Girders 5 and 8, which consisted of vertical stirrups and a horizontal strip placed over the vertical stirrups for anchorage, was found to produce the largest consistent increase in shear capacity. This configuration was also the easiest to apply, and can be credited for its consistency. The four tests on girders 5 and 8 produced an average increased shear capacity of 55.70 kips.
7. Two analytical methods were evaluated to determine the most accurate methodology in determining the increased shear capacity of prestressed concrete I girders reinforced with CFRP. The ACI method was found to be the most accurate in predicting the increased shear capacity of the AASHTO prestressed I-shaped girders tested in this research [9].

The above analysis and results shows how conservative the AASHTO LRFD can be in evaluating the capacity of structural elements.

CHAPTER THREE: PRELIMINARY MODEL DEVELOPMENT

A full four-span continuous model was developed for this study; but before starting, consideration was given as to which segment to model, and what software to use.

1. Original bridge constructed in 1972 (Two lanes both ways, east and west)
2. Existing bridge reconstructed in 2002 (original 1972 bridge widened: three lanes both ways, east and west)

Additionally, it was important to understand the geometric and analytical details of the bridge system on a smaller scale before attempting the full four-span model. Model visualization included the process of discovering the bridge history through drawings, structural calculations, interviews, observation, and other methods. The existing drawings became the geometric basis for the finite element models. Benchmark studies were conducted to acquaint the author with the software, as well as to try different approaches to modeling aspects of the bridges.

Bridge Segment Selection

There are approximately 40 AASHTO Type II and III girders in the original bridge and 56 in the reconstructed widened bridge system (both – ways, east and west). It is important to think critically about which segment to model in order to provide maximum benefit at minimum cost, and with minimum impact to system operations. Thus, the following criteria are adapted in selecting the representative segment(s).

Primary Selection Criteria

The segment should be representative and significant, such that it (1) provides an important link in the bridge system, (2) sees significant loads, and (3) has significant (long) beam spans. This means that we can reduce the long-span (60 ft., 3 in.) interior and exterior span segments within the beam segments, as shown in the red-dotted rectangle in Figure 19, and consider the oldest segments in the system as most significant, as shown in Figure 20.

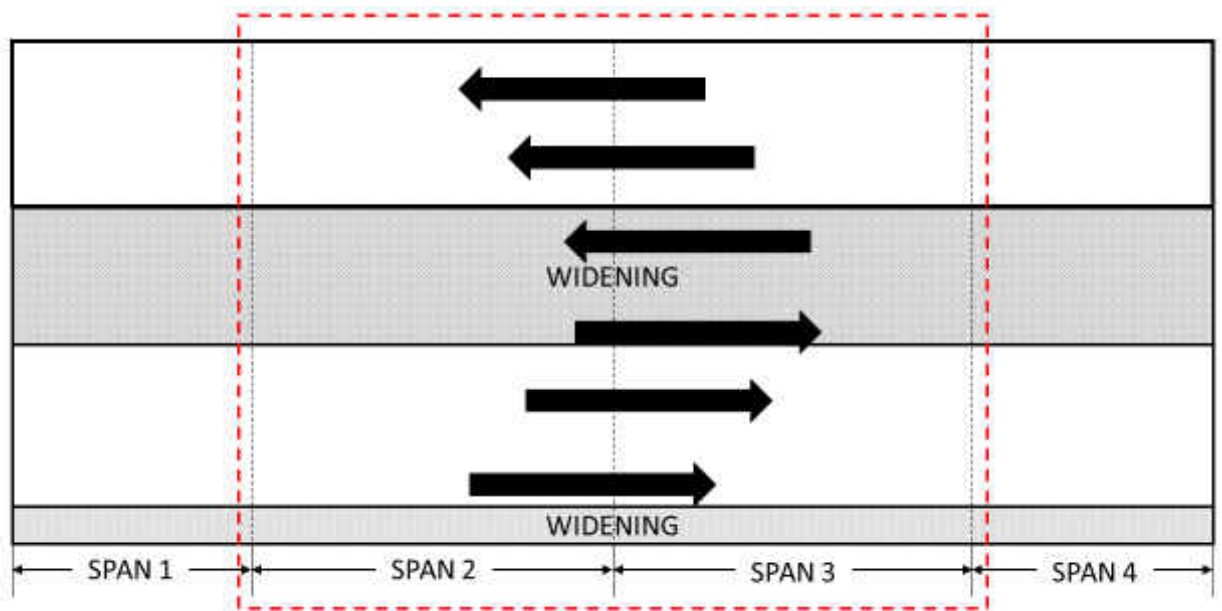
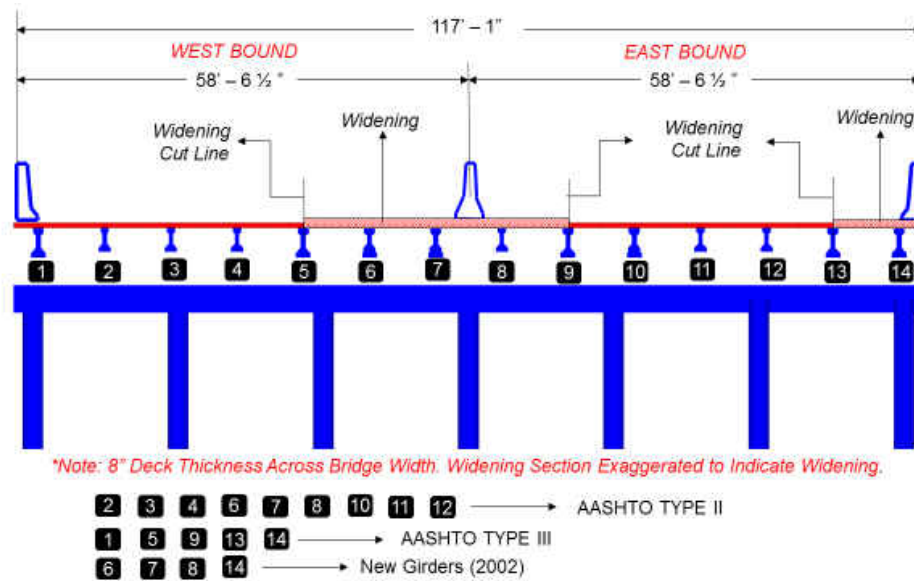
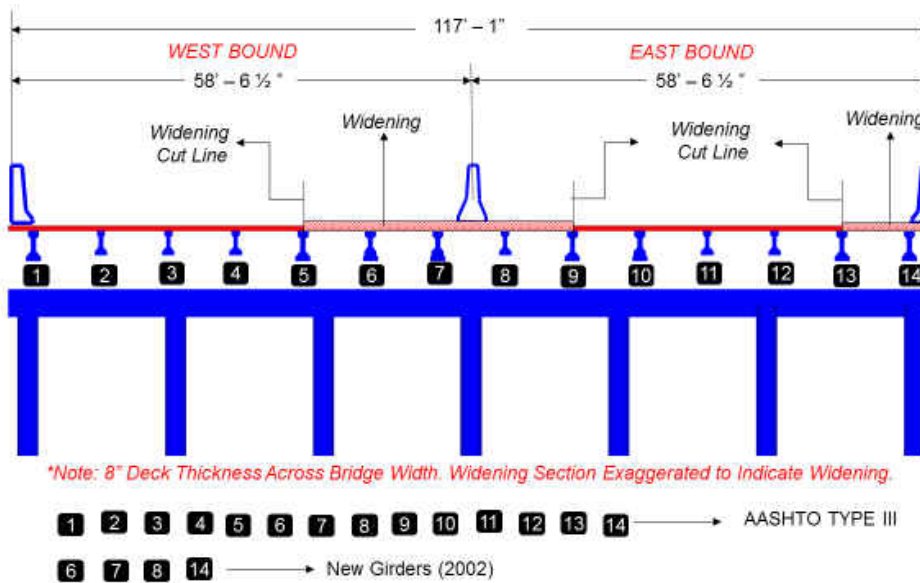


Figure 19: Bridge Plan indicating significant segment



Spans 1 & 4



Spans 2 & 3

Figure 20: Bridge Cross – Section indicating New and Existing Girders

The segment should be representative, in that many other segments in the fleet share the same dimensions, loading, materials, and other design features. The present study is expected to provide insight into the structural behavior of the bridge systems, and to serve as a baseline to

establish methodology for analytical investigation of the bridge systems. With the bridge considered for this research having no skews, it serves a reasonable baseline, with curved spans (skews) recommended for future studies.

Secondary Selection Criteria

Boundary conditions should be considered – curved approach will affect behavior on a straight span and hence only straight segments with straight approaches are considered.

Existing documentation is a final consideration as the availability of design documentation facilitates the development of the finite element model and provides insight into the thinking of the original design engineers. Fortunately, the segments in the system have excellent documentation in the form of design drawings and calculations documenting the design methodology.

Software Considerations

Finite-element software was chosen by considering a variety of constraints and objectives. The first requirement was the ability of the software to accurately represent structural behavior, especially geometric and material nonlinearity as well as bridge response. Usability in practice was considered, and an attempt was made to balance this consideration with advanced analysis capabilities (usability in research). These two goals conflict in some ways; more advanced

analysis capabilities may be provided by software that is prohibitively difficult to learn, such that it would never be implemented in professional practice. It is intended in this research to establish a benchmark for an analytical investigation, such that this approach may be adopted by practicing engineers using conventional software under conventional constraints of project schedules and limited budgets.

Consequently, as discussed in the literature review, a complicate approach is not required for this analysis hence the software should not be prohibitively complicated. Since the elastic behavior is generally accepted as a valid assumption for analysis of prestressed concrete structures under service loads a software within these constraints should be capable and acceptable.

CSi Bridge by Computers and Structures, Inc. (Berkeley, CA) and Nonlinear Analysis Program (NAP) [46] were chosen for this research. CSi bridge meets the previously defined goals and objectives; it is widely used in practice and has robust analysis capabilities, except material nonlinearity, which will be accommodated by NAP.

CSiBridge has the capability to permute all the possible vehicular loading patterns once a set of lanes is defined. First, the entire bridge response due to a single lane loaded, without the application of the Multiple Presence Factor (MPF), can be easily obtained by arbitrarily defining a lane of any width within the bridge. Then, lane configurations that would generate the maximum shear and moment effects would be defined, and the MPF would be defined. The cases where one lane is loaded are important for fatigue design; in addition, the cases where one lane is loaded may control the cases where two lanes are loaded. Therefore, the cases where one lane is loaded are separated from the permutation and are defined, based on a single lane of the whole

bridge width [31].

The NAP software models the cross-section of the member to be investigated, incorporating the elements and materials. Figure 21 shows the simplified structure of NAP, and Figure 22 shows the defined base classes (element, section and material).

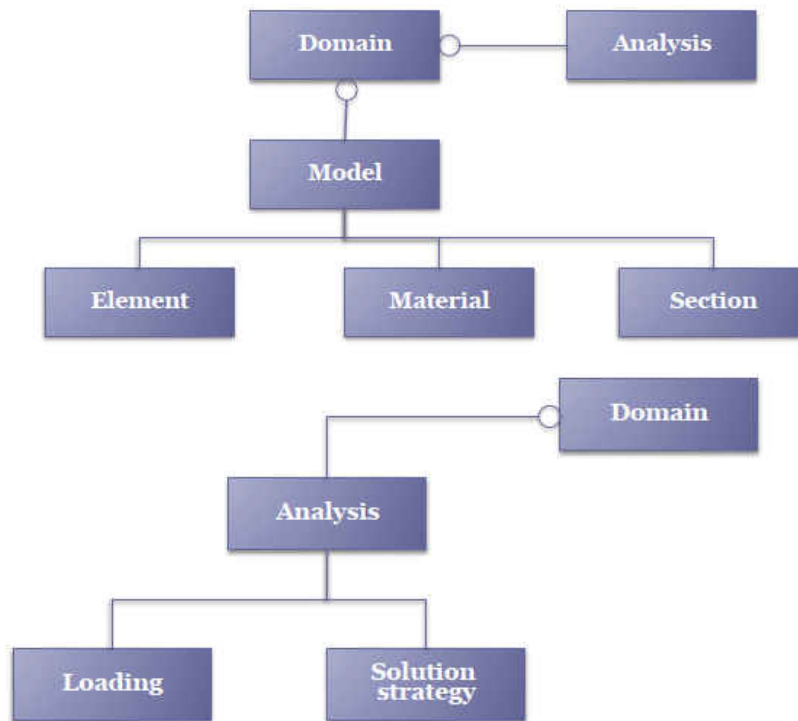
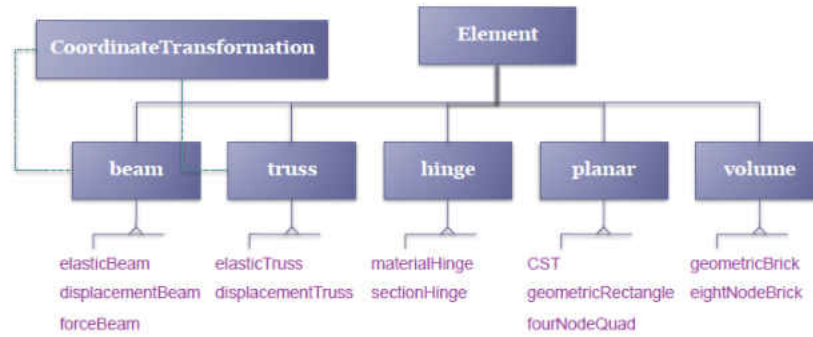
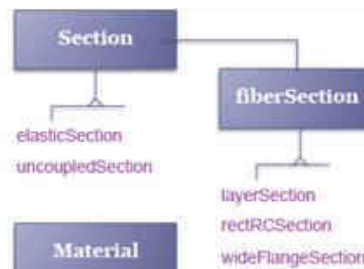


Figure 21: Simplified Structure (NAP)

- Element base class



- Section base class



- Material base class

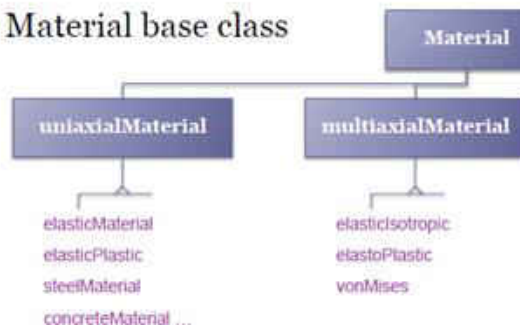


Figure 22: NAP Classes

The architecture of the NAP input files is reminiscent of FEDEASlab. The front matter defines the problem title that appears on the screen and in the output file. This can be any text string, and has no impact on the solution process [37].

At this point, the Matlab – based interpreter which translate the high – level commands into low – level machine instructions construct the functions added in the file, and it serves as a convenient platform for making a single input file that can take on a variety of possible

realizations. NAP also allows the use of existing templates without creating new models or codes from scratch (file tweaking versus new file creation).

A key advantage of NAP is its capability of solving both linear and nonlinear problems. This allows for a benchmark analysis using its linear capabilities with different linear software like CSi Bridge.

Preliminary Models and Benchmark Studies

It is useful to develop several models of simpler structural systems, or systems with adequate analyzed information and results, before attempting to model the actual models one intends to analyze or investigate, like the four-span bridges before and after widening. Benchmark studies help verify accuracy of the software, acquaint the author with intricacies of the software, and assess the sensitivity of model outputs to various model parameters.

A finite-element model was developed for a structural bridge system with known experimental results and analyzed data. Special attention was paid to the incorporation of material properties, bridge modeling tools, moving-load analysis, and prestressing tools. There is ongoing evaluation inaccuracy, due to the unknown assumptions made by the authors of the benchmark model, as well as the tools and software used, which may include modeling, user, software, discretization, or numerical error. Preliminary model development is a parallel effort with model visualization. Details of the benchmark model incorporated in this research by Lubin Gao are presented here. The benchmark bridge to be modeled is an existing bridge, which was analyzed by the author, and is part of his textbook [38].

Benchmark Background Information and Input

The benchmark bridge is an example problem (Example 7.3) from the author's text - Load Rating Highway Bridges in accordance with Load and Resistance Factor Rating Method.

The structural condition for the 1980 bridge is as follows;

- o From the most current inspection, Superstructure Condition Rating (SI & A Item 59) is 6.
- o The section loss is minimal.
- o There is no shear distress noted.
- o The thickness of overlay was field-measured/verified.

The bridge characteristics and data are provided below, along with accompanying illustrations (see Figure 23, Figure 24, Figure 25, Figure 26 and Figure 27).

- A three-span simple span continuous precast, prestressed concrete AASHTO Type V girder bridge.
- Only an interior girder is rated for the design load, HL- 93.
 - o Straight alignment without skew (similar to bridge for analysis/research)
 - o Span length: Each span is 100 ft (Three Spans).
 - o Four (4) AASHTO/PCI Type V precast PC I girders spaced at 8 ft.
 - o Depth of concrete deck: 8 in.
 - o Overhang width: 3 ft.
 - o Out-to-out width of the concrete deck: 30 ft.

- o Curb-to-curb width of the concrete deck: 27 ft.
- o Overlay: 2 ½ inches

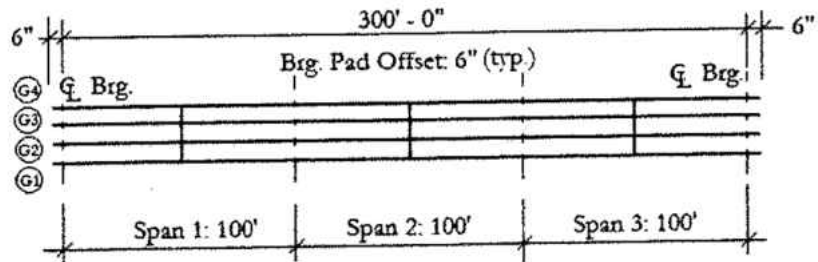


Figure 23: Benchmark Bridge – Framing Plan

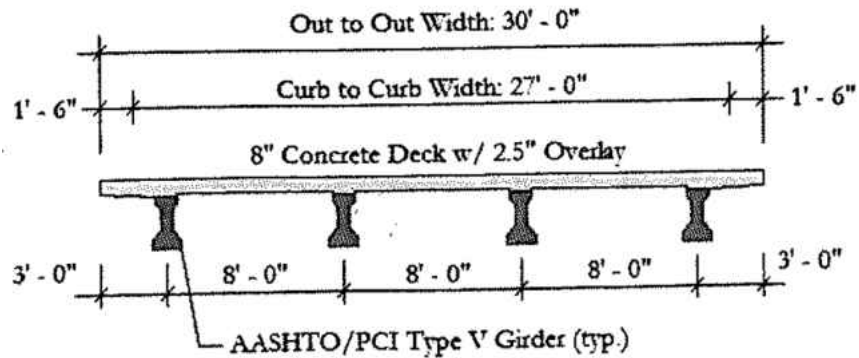


Figure 24: Benchmark Bridge Typical Cross Section

I BEAM PROPERTIES				
BEAM TYPE	WEIGHT (k/ft.)	AREA (in. ²)	DISTANCE FROM C.G. TO BOTTOM (in.)	MOMENT OF INERTIA I _x (in. ⁴)
I	0.288	276	12.59	22750
II	0.384	369	15.83	50980
III	0.583	560	20.27	125390
VJ	0.822	789	24.73	260730
V	1.055	1013	31.96	521180
VI	1.130	1085	36.38	733320

Figure 25: Benchmark AASHTO Type V Girder Section Dimensions & Properties

The strand profile with 44 strands, provided in eight layers deflected at 0.3 points, are

also provided here, including the composite section properties shown in Table 5. Benchmark material properties are shown in Table 6.

Table 5: Benchmark Composite Section Properties

Section	Composite Section ($n=E_B/E_D = 1.225$)			
	A	Y_{bot}	I_x	S_{bot}
#	(in^2)	(in)	(in^3)	(in^4)
Composite	1640	45.4	1000006.8	22048.2

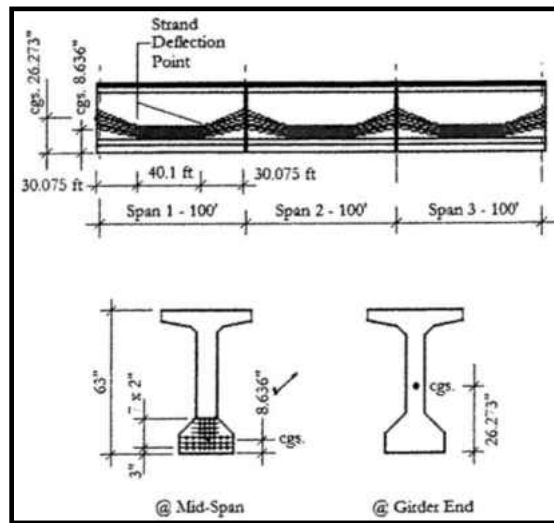


Figure 26: Benchmark Strand Layout

Table 6: Summary – Benchmark Material Properties

Benchmark - Material Properties					
Prestressing Steel		Girder		Deck	
Type	0.5" Dia. Grade 270 Low Relaxation	Type	Precast I	Type	Conc. - Composite
		Comp. Strength	6 ksi	Comp. Strength	4 ksi
Yield Strength	240 ksi	Initial Strength	4.5 ksi	Unit Weight	0.15 kcf
Tensile Strength	270 ksi	Unit Weight	0.15 kcf		
Modulus of Elasticity	28,500 ksi	Modulus of Elasticity	4415 ksi	Modulus of Elasticity	3605 ksi

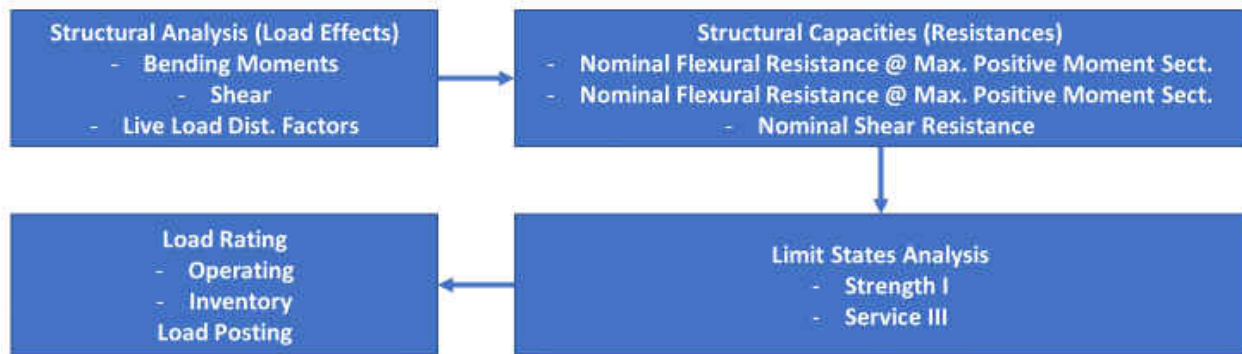


Figure 27: Benchmark Analytical Investigation Flow Chart

Benchmark Three – Span Model

Working with the finite element software, related documentation, and technical support personnel, an observation was made that shell elements would be a good choice to represent the concrete girders of the bridge. Shell elements have the advantage over frame elements of representing local behavior. Although bridge models are often developed with frame elements with equivalent cross-sections representing the deck, the goal in this study was to develop additional resolution to capture local behavior at the connections [48].

A detailed benchmark study was undertaken to understand the details of bridge analysis in CSiBridge. Shell elements are chosen for meshing the bridge deck.

A few figures are presented here for a better understanding of the model process. Figure 28 shows the three-span continuous precast prestressed concrete AASHTO Type V girder bridge. Undulating prestressing tendons are defined within the deck shown in Figure 29.

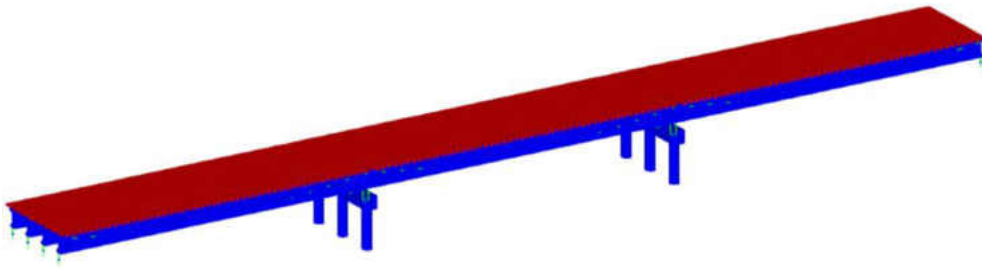


Figure 28: Benchmark Continuous Three – Span Model

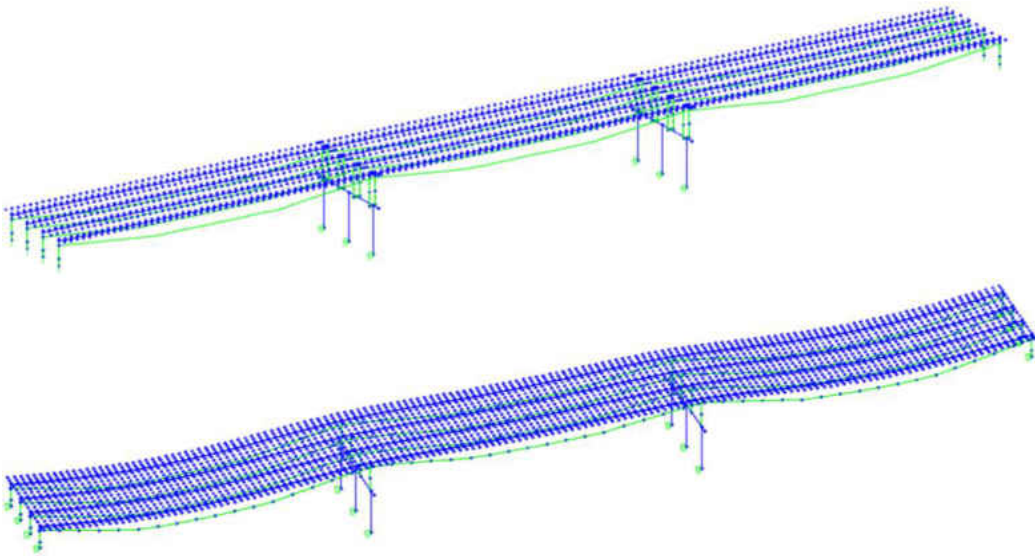


Figure 29: Benchmark Model – Tendons

The model cross – section is also shown in Figure 30 which illustrates subsequent loads which must be predefined as CSi Bridge considers these loads (barrier and wearing surface) as non – composite external loads. These loads are therefore modeled as line loads, which are analyzed and shown in Table 7 with their respective line action positions.

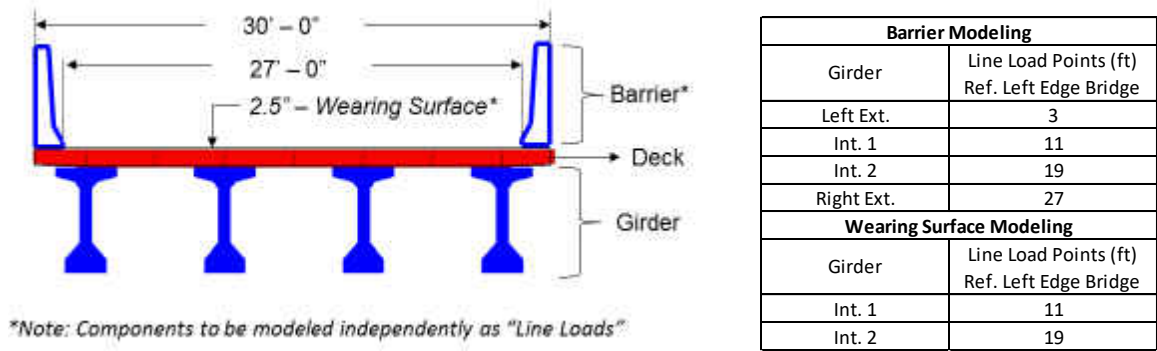


Figure 30: Benchmark Cross – Section Model & Line Loads

Table 7: Benchmark Line Load Analysis

Component	Weight (klf)	Qty	Total Wt. (klf)	# Girders	Weight/Girder (klf)
Barrier	0.335	2	0.67	4	0.1675
<i>Therefore, Line Load = 0.168 klf applied @ girder centers - 3, 11, 19, & 27 ft resp. from deck edge.</i>					
Component	Thickness (in)	Conc. Wt. (kcf)	Beam Sp. (ft)	Wt./Int. Girders (klf)	# Int. Girders
Wearing Surface	0.335	0.15	8	0.25	2
<i>Therefore, Line Load = 0.25 klf applied @ Int. girder centers - 11 & 19 ft resp. from deck edge.</i>					

Figure 31 and Figure 32 show the bridge response/force output from CSi Bridge for dead and live load analysis envelopes. The bridge object response feature is a powerful tool in CSi Bridge that calculates resultant load effects by integrating forces at sections along the length of the bridge object (Computers and Structures Inc. 2015). The moment envelope indicates minimum and maximum values from the moving load analysis. A sample of a loading case is also shown here in Figure 33 with its respective live load distribution factors.

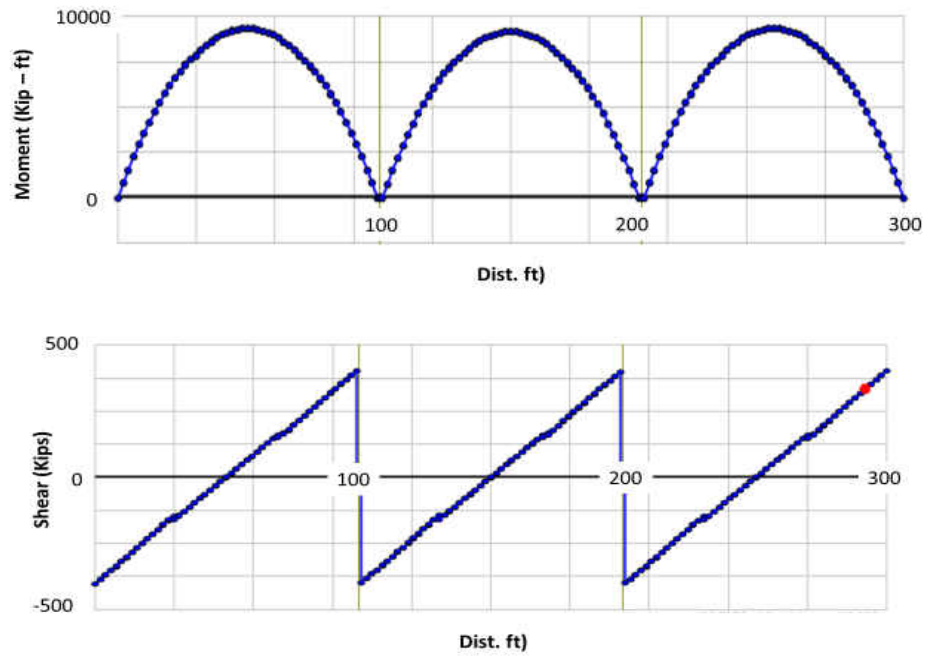


Figure 31: Benchmark Study Dead – Load Moment & Shear Envelopes

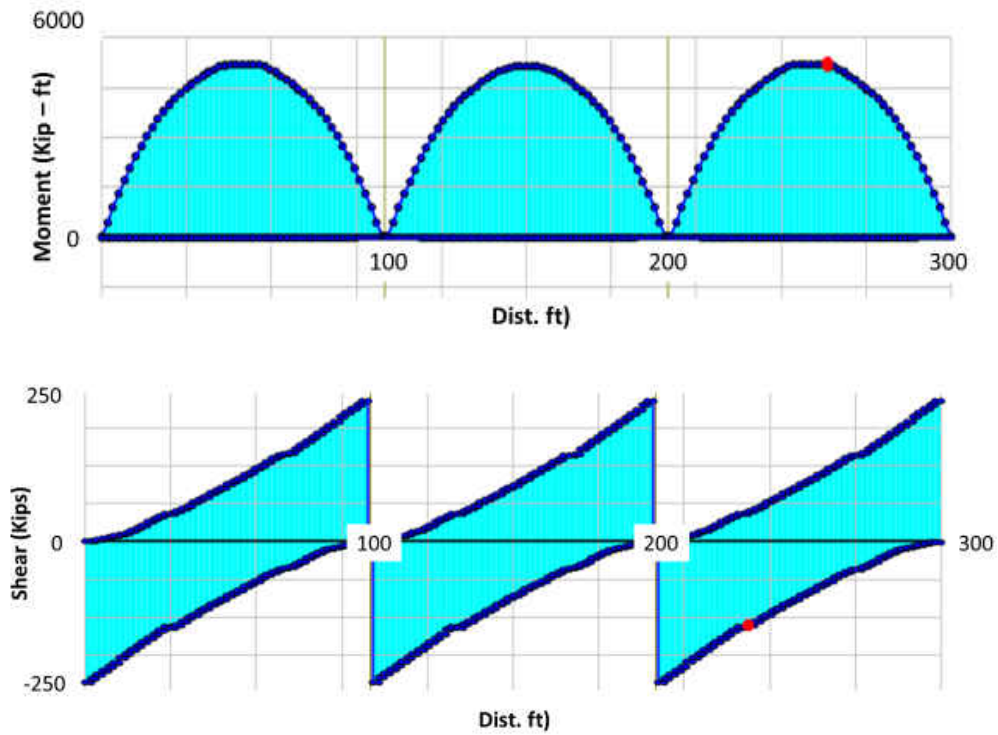


Figure 32: Benchmark Study Live – Load Moment & Shear Envelopes

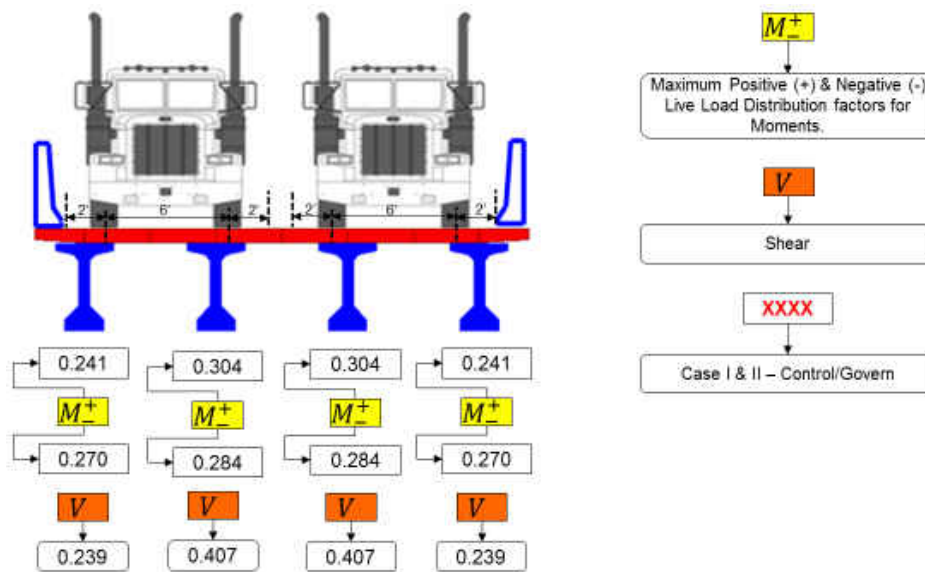


Figure 33: Benchmark Live – Load Distribution Factors Schematics

The first span, which is symmetrical to the other two spans, was used in comparing the textbook dead-loads analysis for both shear and moment, as shown in Figure 34, Figure 35 and Figure 36. The first span gives good dead-loads analysis results, with a 1% to 5% variation in both moment and shear, as also illustrated in Figure 34 and Figure 35.

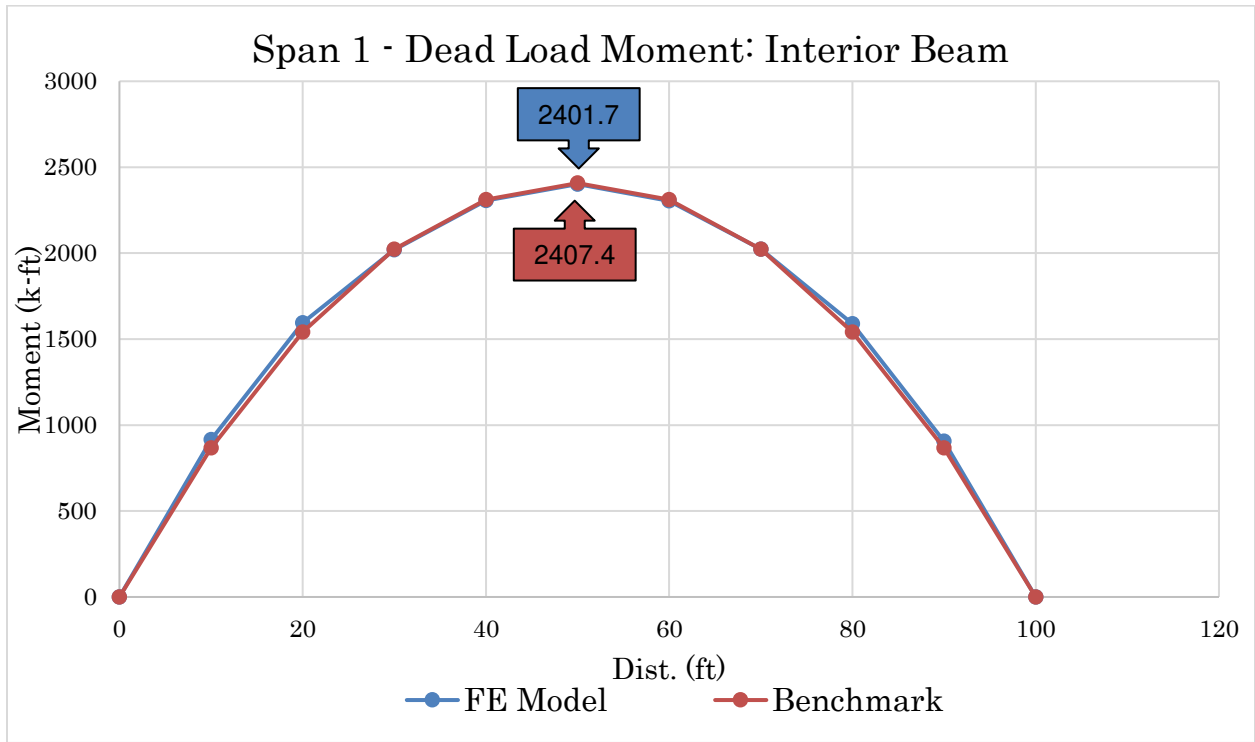


Figure 34: Benchmark Single – Span Moment Comparison

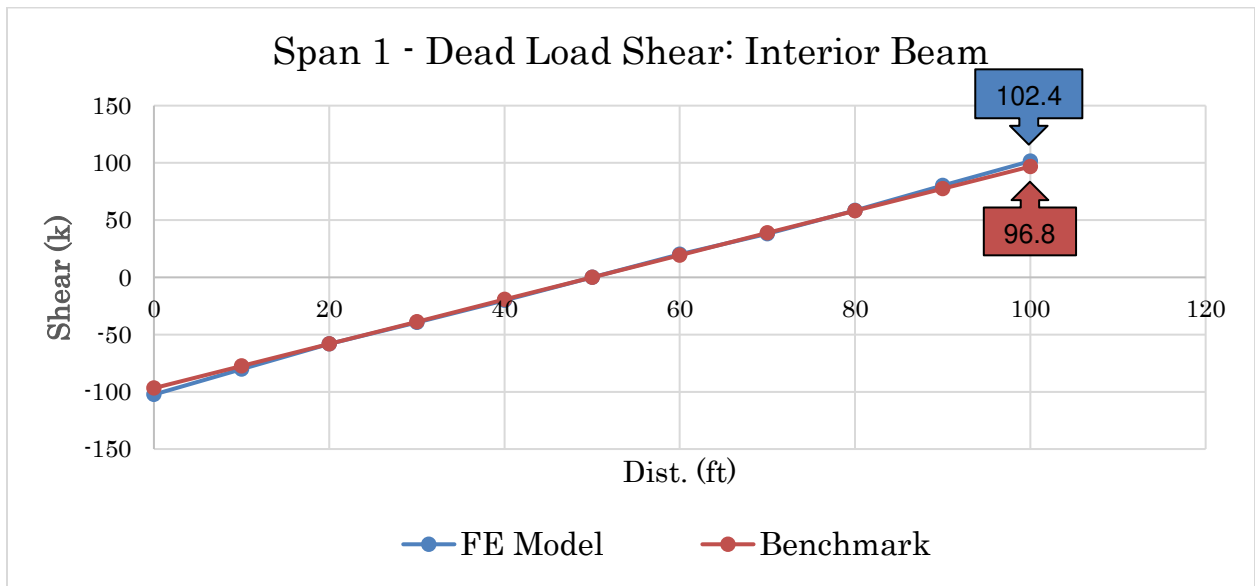


Figure 35: Benchmark Single – Span Shear Comparison

	Max. Moment Loc.	Max. Moment (K - ft)		Max. Shear Loc.	Max. Shear (K)	
Source	(ft)	Girder	Deck	(ft)	Girder	Deck
Benchmark	49.8	1371.2	1036.4	0 , 100	55.1	41.7
FE Model	49.5	*2401.7		0 , 100	*102.4	

**Composite section used in modeling (Deck + Girder)*

Figure 36: Benchmark Single – Span Maximum Points

Benchmark Modal Analysis

Eigenvalue analysis (modal analysis) which determines the undamped free-vibration mode shapes and frequencies of a given structural system was performed on the benchmark bridge. Additionally, the analysis provides the effect of a modeled structure by examining its responses (static and dynamic), flexibility and stiffness, and behavior (global versus local). Figure 37 illustrates the effects of a dynamic analysis, as well as the expected modes for a typical modeled bridge structure.

In CSiBridge, eigenvalue analysis involves the solution of the generalized eigenvalue problem:

$$[K - \Omega^2 M]\Phi = 0$$

Where;

K = the stiffness matrix,

M = the diagonal mass matrix,

Ω^2 = the diagonal matrix of eigenvalues, and

Φ = the matrix of corresponding eigenvectors, or mode shapes

In this research, to determine the structure's natural characteristics (modes, shapes, frequencies, etc.) or physical characteristics (capacity, resistance, etc.), a modal analysis was performed on the finite-element model to verify its natural frequencies and dynamic responses.

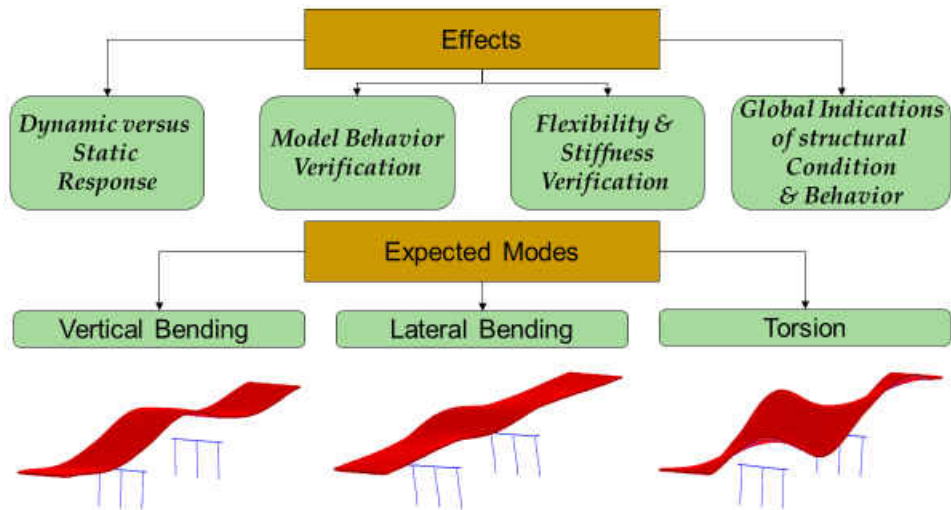


Figure 37: Dynamic Analysis Effects & Modes

The modal analysis case for the benchmark model is defined such that it uses the stiffness at the end of a nonlinear case, accounting for the P-delta effects of the prestress, which also restrains the end supports, thus producing the expected vertical bending first mode. The restraint which prevents motion in the x and y direction (hence creating a fixed connection) is illustrated in the segment shown in Figure 38 (dashed red circles).

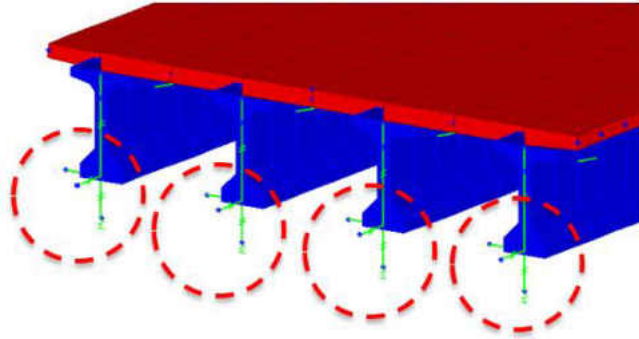


Figure 38: Benchmark End – Connection for Modal Analysis

The frequencies and mode-shape vectors provide the best global indications of structural condition and behavior. Results of the modal analysis may be used to plan a field-verification plan or long-term monitoring program; and in this case, verification checks of the software’s capabilities. For the benchmark model, the following characteristic responses are identified:

1. Vertical beam bending
2. Lateral beam bending
3. Torsion

The eigenvalue analysis of the benchmark model in CSiBridge gives natural frequencies in the range from 5.177 Hz to 19.058 Hz for the first 20 modes of the nominal model. Examples of the first 10 modes are illustrated in Figure 39.

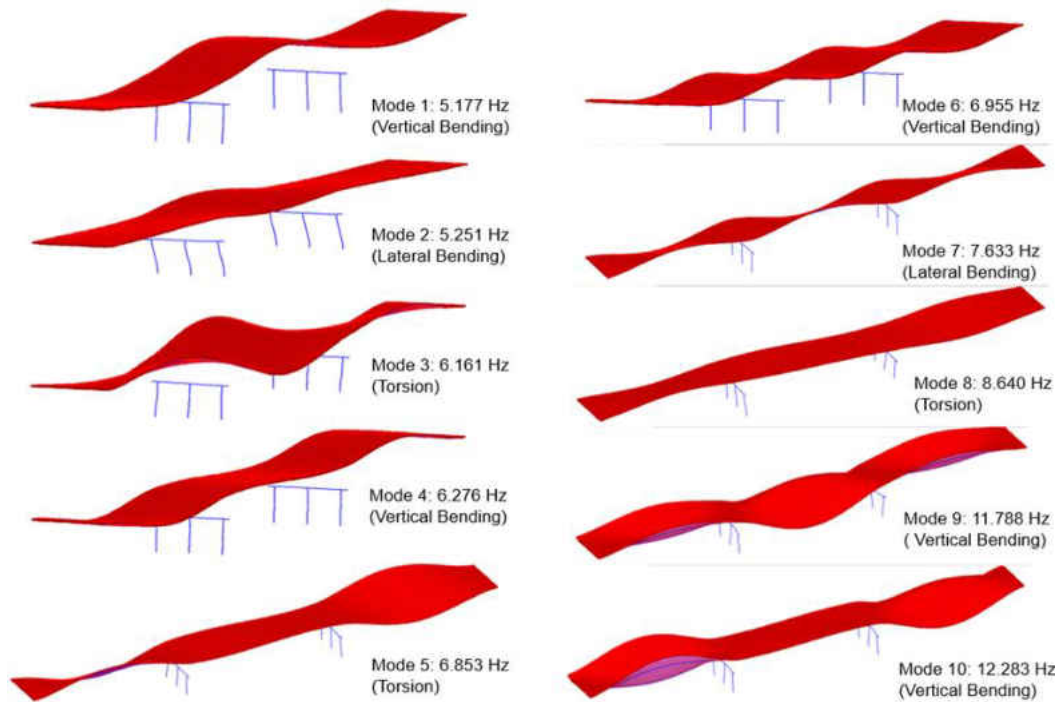


Figure 39: Benchmark Eigen Value Analysis First Modes

Appendix A contains tables with frequencies, along with graphical representations and text descriptions of mode shapes for 16 modes.

Benchmark Discussion

The benchmark results validate the modeled FEM, as well as the software. The moment, shear-load and live-load envelopes were similar to those provided in the textbook, as well as capacity, live-load distribution factors and load-rating values, which will be discussed in detail in later chapters. Consequently, the modal analysis results showed frequencies within the range of magnitude of similar bridges.

CHAPTER FOUR: FOUR – SPAN FINITE – ELEMENT MODEL (1972)

Introduction

A finite element model for the four-span bridge structure is developed as an extension of the benchmark studies (Figure 40 showing the plan and three – dimensional views). Shell elements are used to represent the prestressed concrete girders. Frame elements with nonprismatic cross sections represent columns. The twenty precast beams and associated pre-tensioning were developed and updated with the CSi Bridge Design Module.

The subsequent sections detail certain assumptions and choices made in developing the full four-span continuous model.

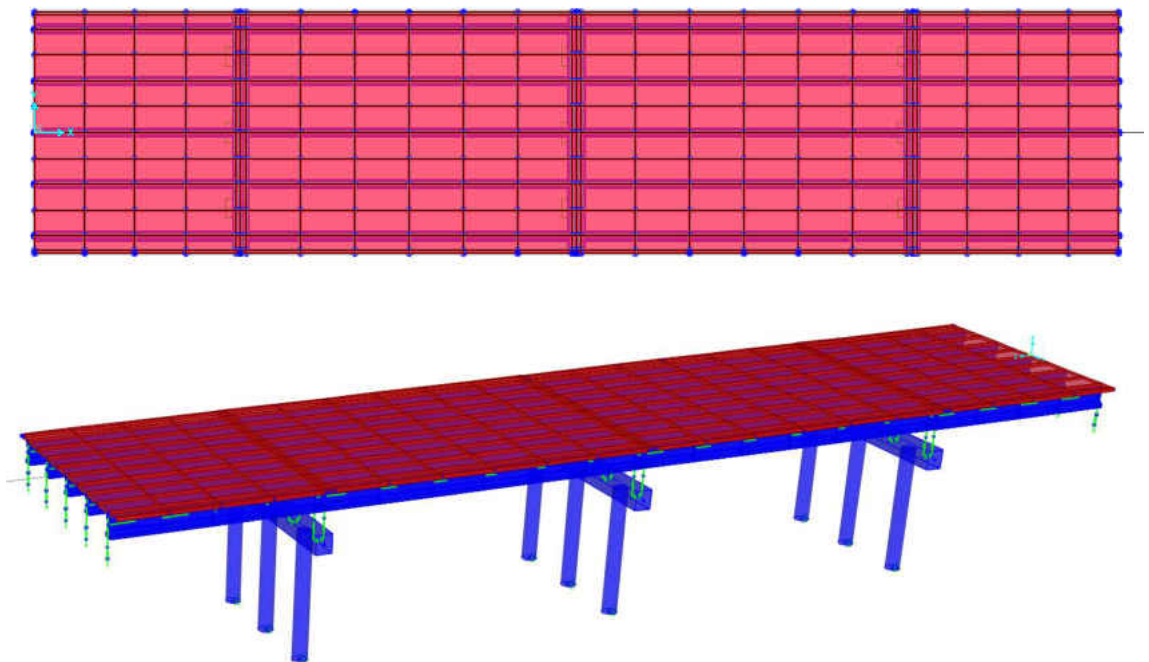


Figure 40: Four – Span Continuous Bridge FEM

Superstructure

The superstructure refers to the section of the bridge receiving vehicular live loads, principally the precast haunched beams and their associated prestressing elements. While many aspects of developing the beam, model have already been discussed, additional items specific to implementation of the full model in CSi Bridge are included in subsequent sections.

Beams

The beam geometry and meshing were developed using the CSi Bridge design module. Shell elements were chosen to represent the beams for reasons discussed in the previous chapter, especially to develop the resolution and smoothness required to capture local behavior at the connections. Shell elements give results at their neutral axis, which can then be integrated by the software to give resultant forces and moments at a section of interest.

The prestressed beam section is selected from the programs data file. The cross-section of the selected beam is shown here (Figure 41).

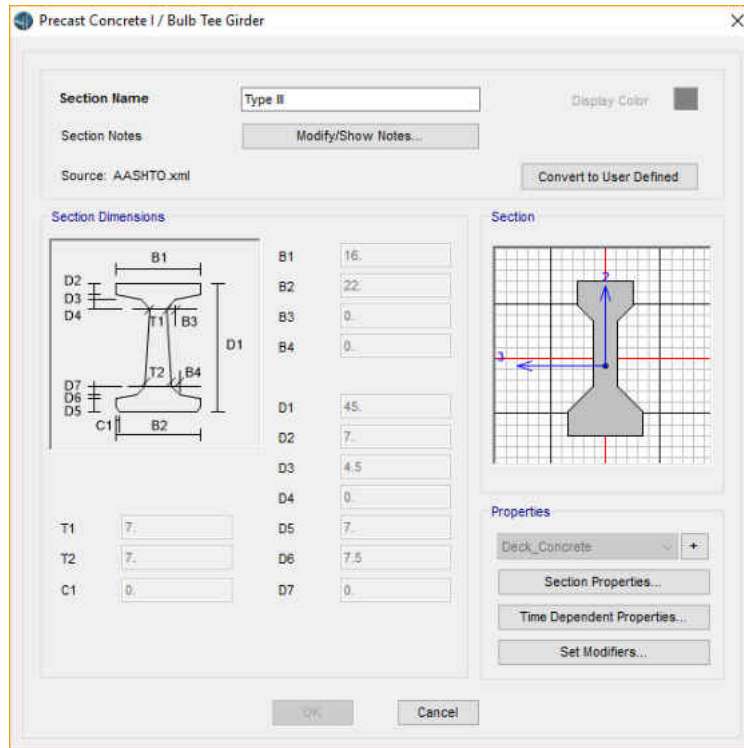


Figure 41: Beam Cross – Section Pre-defined in Program

The beams are meshed by the bridge design module into reasonable segment lengths. An automatic sub-mesh is also assigned which essentially doubles the resolution of the beam models. No shell is longer than 60 in, which follows the recommended guidelines, to limit the aspect ratio.

Prestressing

Two bridge objects were defined in the bridge design module, representing the two sets of prestressed beams (Type II & Type III) in the 1972 model in the four-span continuous bridge. Spans 1 and 4 consist of the same configuration, while spans 2 and 3 have similar configurations, but different from spans 1 and 4. Figure 42 below shows the two bridge objects for the stated configurations.

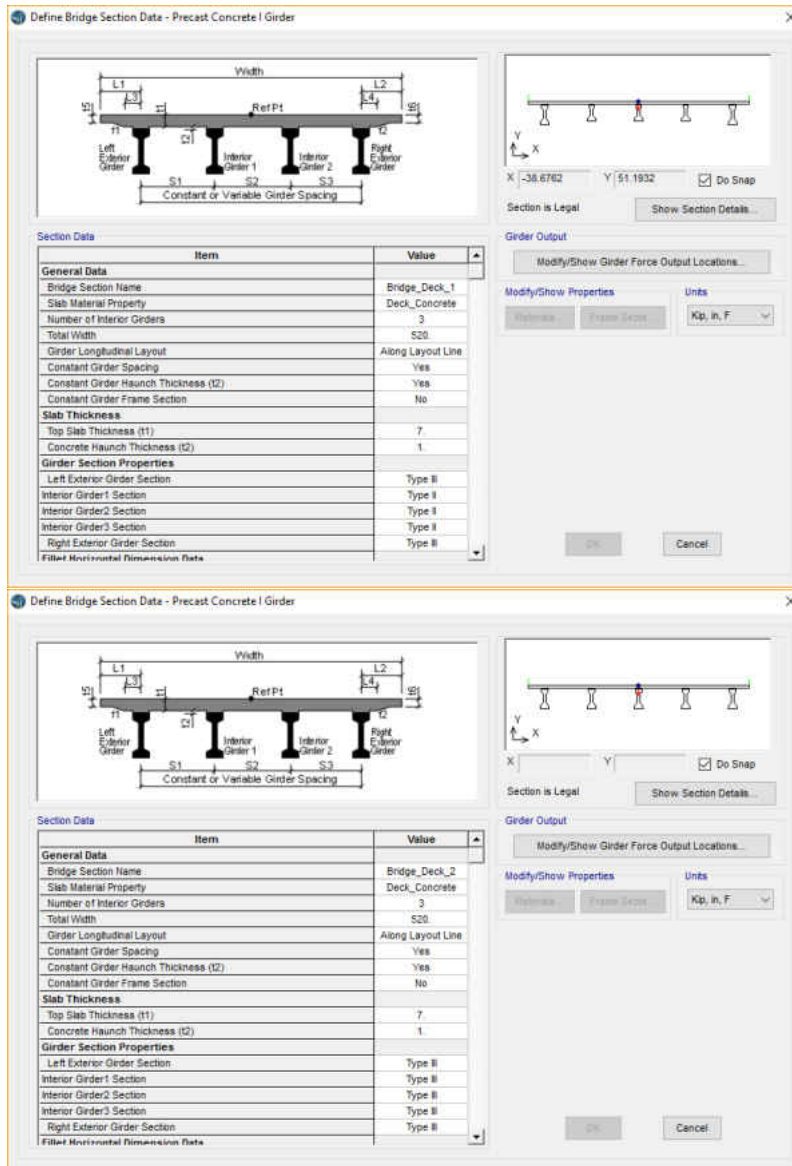


Figure 42: Bridge Object Definitions

A single tendon (with the combined area of all the tendons) is placed at the centroid of the tendon group, and debonded portions of the tendon are accounted for by not modeling the portion of tendon that lies within the debonded region.

The fundamental difference between the bonded pretensioning strands and the bonded

post-tensioning tendons in the bridge is that the pretensioning strands were pulled and set at the plant before the surrounding concrete cures.

Many researchers and professionals choose to neglect the effect of the prestress force on global structural behavior. However, because the prestress force is such an integral and important structural feature in the continuous bridge, the present study considers the effect of the prestress force (and, consequently, prestress loss) on static and dynamic structural behavior.

The resulting stiffness is used as the basis for all static and dynamic analyses. The P-Delta effect of the prestress force (axial compression) has the effect of reducing the effective stiffness of the beams in lateral and vertical bending. The prestress loss parameters are very important to the behavior of the structural model. The prestress loss parameters are defined and discussed in subsequent sections.

Columns

The precast columns are modeled in CSiBridge as frame elements with non-prismatic cross-sections. Non-prismatic cross-sections may be defined for which the properties vary along the element length. The variation of bending stiffness may be linear, parabolic, or cubic over each segment. The axial, shear, torsional, mass, and weight properties all vary linearly over each segment (Computers and Structures Inc., 2015).

The concrete unit weight is taken as 150 pcf from the original structural calculations, and Poisson's ratio is taken as 0.2. The concrete modulus of elasticity, E_c , is an important parameter with significant variability. Treatment of E_c is discussed in subsequent sections.

The column frame elements are discretized to mesh with the bearing shell elements. Rigid links are used to connect the column frame nodes to the centers of the clusters of the

defined bearings.

The precast columns are rigidly connected to pile caps with grouted pipes. The pile caps develop the rigidity of the steel pile foundations. All the columns are considered fixed at the base for the finite element model.

Model Parameters

Technically, all possible parameters relating to the geometric, elastic, and inertial properties, as well as boundary and continuity conditions, should be considered for sensitivity studies and model verification [28]. However, if too many parameters (as compared to the number of measurements available) are considered, the possibility of obtaining an unreliable updated model may increase [40].

In the process of developing the benchmark studies and full four-span FEM, the critical model parameters are noted. Special attention is paid to parameters representing material properties, prestressing force/loss, boundary conditions, and bridge continuity condition over the columns. Some model parameters, such as the length of a beam or the unit weight of concrete, are well-characterized and deterministic. Other parameters, such as the prestress loss or concrete stiffness parameters, have significant uncertainty with their characterization. Different assumptions for these parameters are possible and, in some cases, these assumptions are critical to the behavior of the structural model.

In developing the benchmark model and full four-span models, key parameters were identified that significantly affect the structural response. The finite element model is used for static load analysis, including moving loads as well as eigenvalue modal analysis. The free

vibration modes and frequencies depend on global parameters, including material stiffness, prestress loss, and boundary and continuity conditions. Deflection, moment, and shear from static analysis are sensitive to these parameters as well.

Concrete Modulus of Elasticity

The critical material property for analysis is the concrete stiffness, represented by the modulus of elasticity, E_c . In CSiBridge, the concrete stiffness is controlled through the modulus of elasticity. Additional specified components include the shear modulus and Poisson's ratio. These are shown in the material properties dialogue box (Material Property Data) in Figure 43.

Section	Property	Value
General Data	Material Name and Display Color	Deck_Concrete
	Material Type	Concrete
	Material Notes	Modify/Show Notes...
Weight and Mass	Weight per Unit Volume	8.681E-05
	Mass per Unit Volume	2.248E-07
	Units	Kip, in, F
Isotropic Property Data	Modulus of Elasticity, E	3604.9965
	Poisson	0.2
	Coefficient of Thermal Expansion, A	5.500E-06
	Shear Modulus, G	1502.0819
Other Properties for Concrete Materials	Specified Concrete Compressive Strength, Fc	3
	Lightweight Concrete	<input type="checkbox"/>

Figure 43: Material Property Data

In some engineering materials, such as steel, strength and the stress-strain relationships are independent of the rate and duration of loading, at least within the usual ranges of rate-of-stress, temperature, and other variables. In contrast, effect of the rate of loading on the behavior of concrete is significant. The main reason for this is that concrete creeps under load, while steel does not exhibit creep under conditions prevailing in buildings, bridges, and similar structures [41]. When calculating deformations, a reduced modulus is used for long-term load (dead load). There is no way to simultaneously represent the reduced stiffness induced by long-term loads and the greater stiffness for live-load response in one FEM. Instead, an attempt is made to come up with reasonable values for effective stiffness, which adequately represents the dynamic behavior and moving-load response, but also considers the dead-load influence. It is expected that the appropriate effective concrete modulus for use in the FEM lies somewhere between the instantaneous modulus for live load and the reduced modulus for long-term load.

Many expressions are given for the modulus of elasticity. There are expressions for the instantaneous modulus, as well as expressions that consider long-term loads and curing processes. Many expressions for the concrete modulus were adapted from academic and technical publications [32], [42], [43], [41], [44] and used to establish lower- and upper-bound values. A reasonable nominal value was selected using judgment, and was based on assumptions in the original calculations. Expressions for instantaneous and long-term modulus are generally given in terms of the compressive strength, f'_c . Results of the long-term modulus of elasticity (E_c) and concrete compressive strength (f'_c) analysis are presented in Figure 44 and Figure 45, with detailed computation presented in Appendix D.

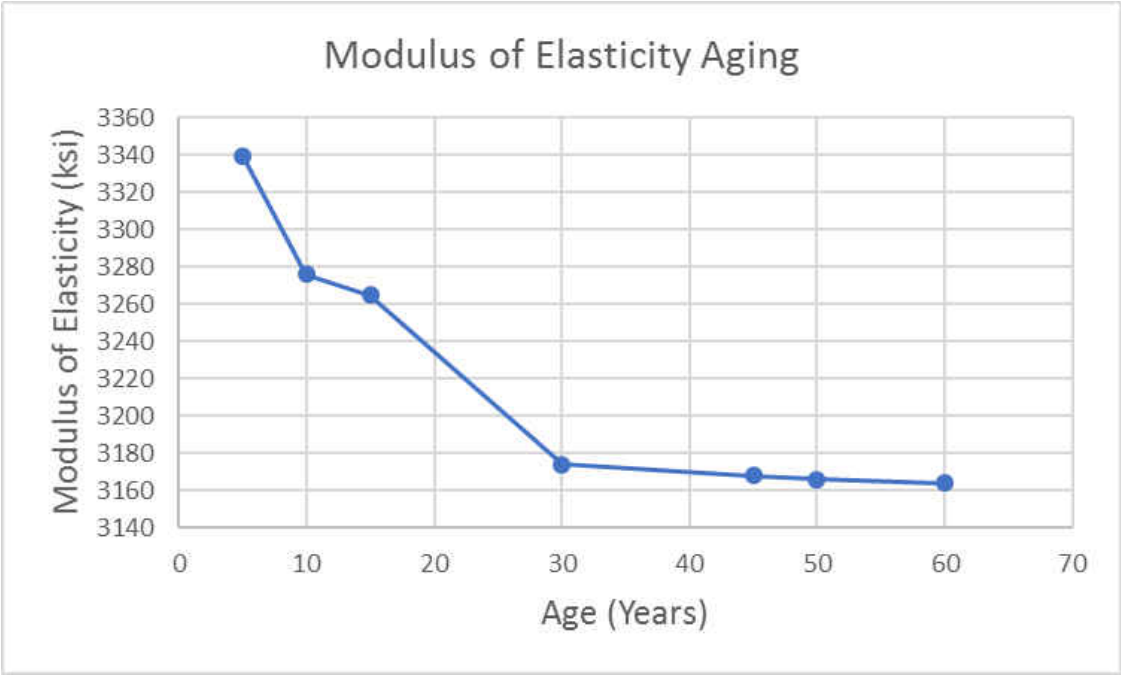


Figure 44: Plot of Long – Term Modulus of Elasticity Aging

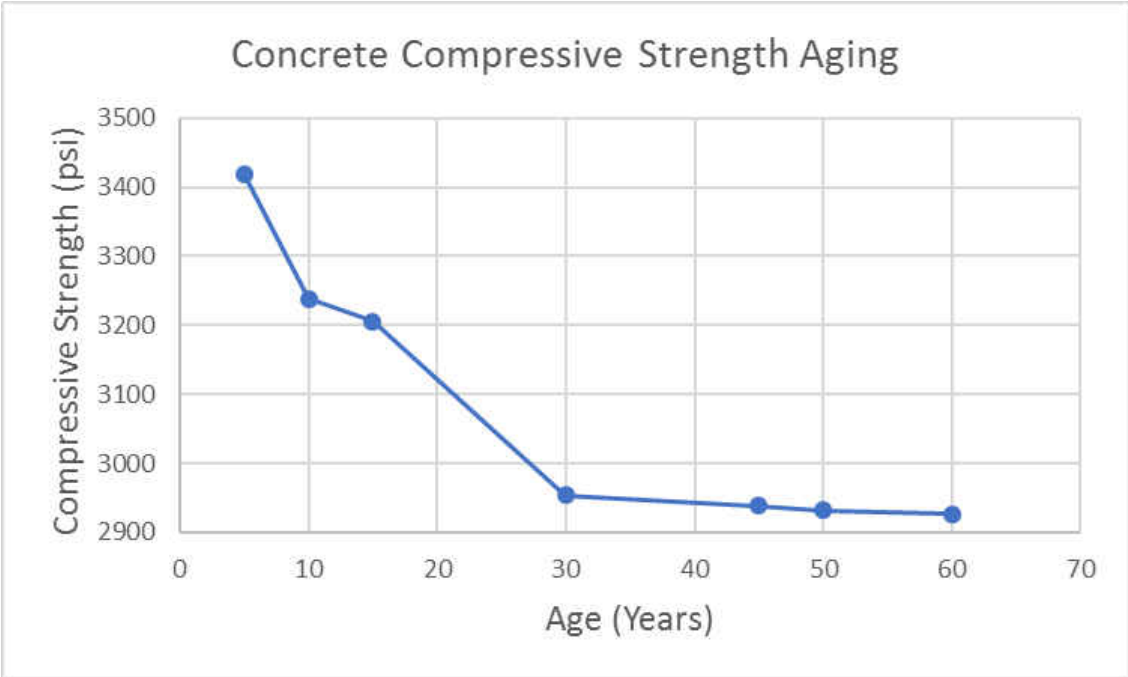


Figure 45: Plot of Long – Term Concrete Compressive Strength Aging

Prestress Loss

It is well-established that the initial prestressing force applied to a concrete element undergoes a progressive process of reduction. Reduction of the prestressing force can be grouped into two categories (also see Figure 46):

1. immediate elastic loss during fabrication and construction, including elastic shortening of the concrete, anchorage losses, and frictional losses (post-tensioning only); and
2. time-dependent losses such as creep, shrinkage, and those due to temperature effects and steel relaxation.

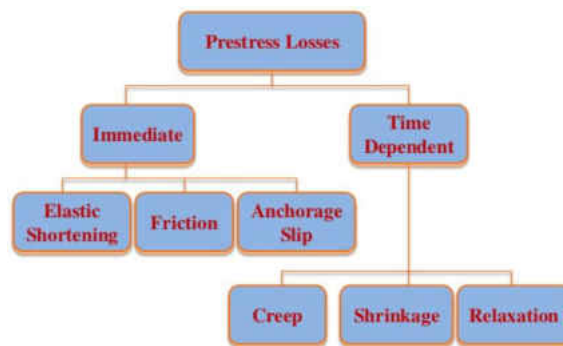


Figure 46: Prestress Losses Analysis Map

An exact determination of these losses is not feasible because of the many interrelated factors, as well as imprecise understanding of their values [43]. Empirical methods for estimating losses are adapted [43], including the author's (Nawy) presentation of AASHTO and PTI methods. Appendix E gives the full set of prestress loss calculations. The loss parameters are constant over the length of the bridge, except for the wobble coefficient, which influences the prestress loss linearly, from zero effect at the jacking end to full effect at the anchored end.

The prestress loss parameters are divided into elastic shortening stress, creep stress, shrinkage stress, and steel relaxation stress, in addition to curvature and wobble coefficient for friction, and anchorage set slip. CSiBridge adds the stress losses algebraically (Computers and Structures Inc., 2015), so it makes no difference how we split up the losses among the categories of elastic shortening, creep, shrinkage, and steel relaxation stress loss.

Using the lump sum of time-dependent losses methodology (LRFD Article 5.9.5.3), the effective prestress after losses was estimated over a long-term period by incorporating the modulus of elasticity and compressive strength losses estimated in the previous section. The results for long-term elastic shortening and its corresponding effective prestress are provided in Figure 47 and Figure 48, with detailed analysis presented in Appendix E.



Figure 47: Plot of Long – Term Elastic Shortening Losses

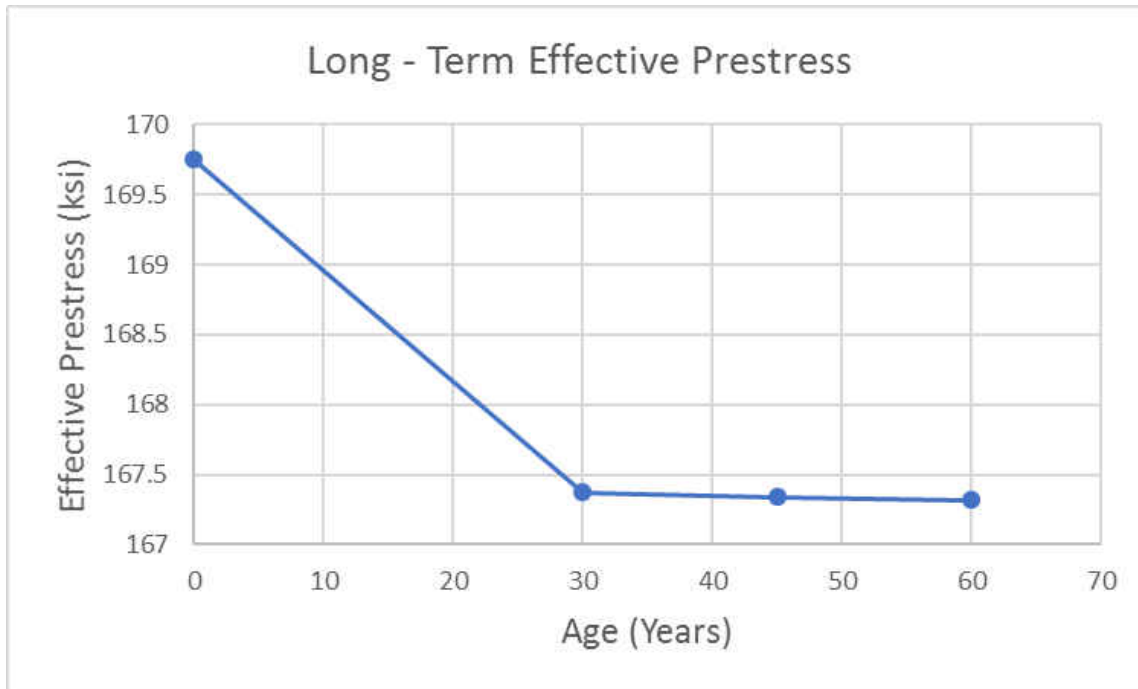


Figure 48: Plot of Long – Term Effective Prestress

Boundary Conditions

The main boundary conditions were developed at the supports for the two main cases, the eigenvalue analysis, and the capacity and live-load analysis. The conditions for the abutments and end bents, were incorporate in the foundation springs. The foundation springs were fixed in the translation vertical, translation normal to skew and rotation about line along skew directions and free in the translation along skew, rotation about vertical and rotation about line normal to skew directions.

Objective

In the absence of experimental data, the analytical investigation will focus on the model (FEM) which will be used for calibration and the results used for the analysis in the section below. The process will also include a comprehensive association and comparison of existing results.

The original 1972 bridge was modeled in this research, since the structure under investigation (the 2002 bridge) was widened from the 1972 bridge. Understanding the behavior and characteristics of this bridge will facilitate the variation and comparison of the existing structure (the 2002 Bridge).

The finite-element model for the four-span bridge structure (developed as an extension of the benchmark studies) will be used for the following studies, with their results presented in the respective chapters:

- Modal Analysis and Parameter Sensitivity (Chapter 6)
- Live-Load Distribution Factors Analysis (Chapter 7)
- Simulations and Load Ratings (Chapter 8)
- Modal Analysis and Loading Ratings Correlations (Chapter 9)
- Load Rating and Reliability Analysis (Chapter 10)
- Nonlinear Simulation and Reliability Analysis (Chapter 11)

It should be noted that for consistency, close approximation of reliability analysis results; and with a focus of component versus system investigation, a single span (consisting of critical

components) will be used in chapters 10 and 11.

System reliability is a major concept in reliability analysis, because individual limit-state functions are assembled together in a system model. The failure conditions are determined by the system model, since failure of one or two members may not be important due to redundancy. On the other hand, there may be critical components (flexure/critical), which must stay intact for the structural integrity of the whole system. Since individual girder components have been investigated through live-load distribution factors and load-ratings analysis, it will be appropriate in this case to focus on the component reliability analysis, which is also less complex compared to a system reliability analysis. The single span to be used for the component reliability analysis is shown in Figure 49. This section is equivalent to spans 2 and 3 in the main structure, which are of equal lengths (60 ft., 3 in.), as illustrated in Figure 50.

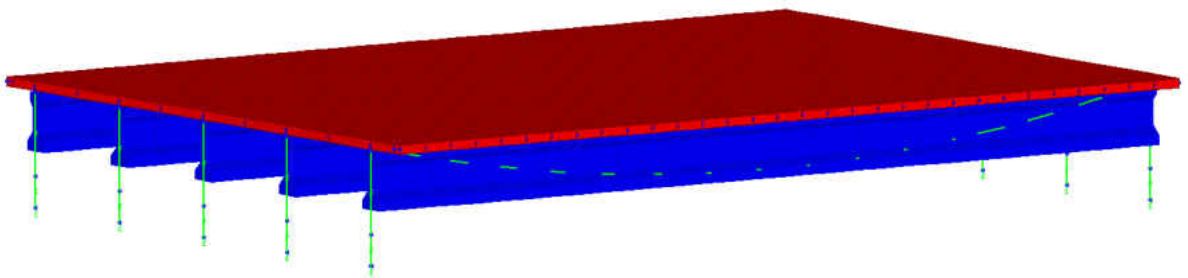


Figure 49: Single – Span 1972 Bridge Model

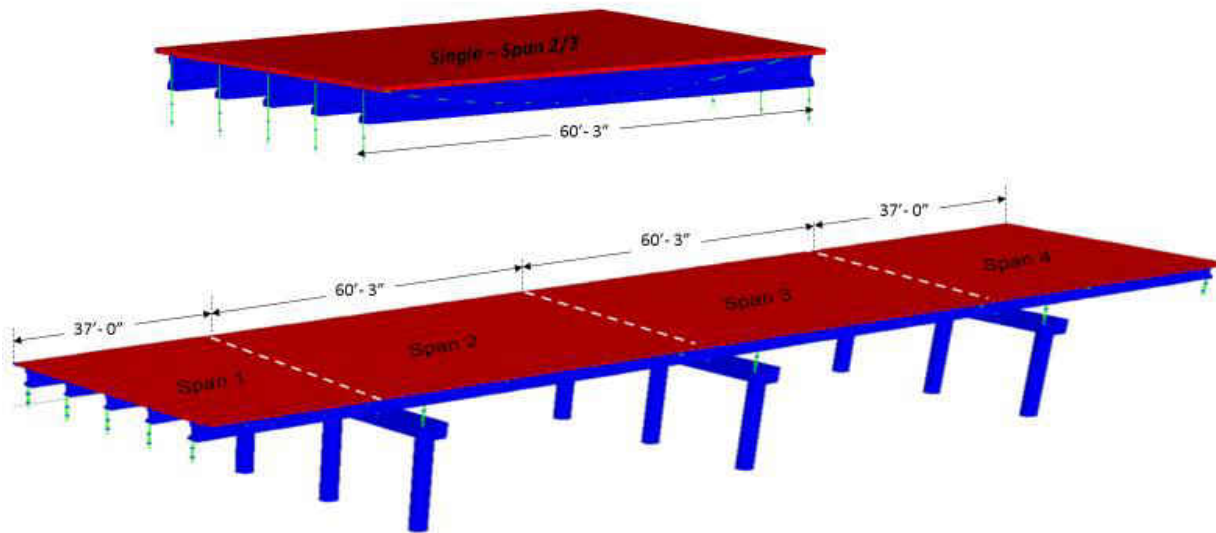


Figure 50: 1972 Bridge Single – Span Illustration

Discussion

Since aging is a key factor in modeling and analyzing this bridge, it was very important to identify the critical parameters to be incorporated into the model. The modulus of elasticity and prestress losses were two critical parameters that affect older bridge components, and were investigated very carefully. Results from these analyses show a rapid loss for the first 30 years, and a minimal, steady loss *after* the first 30 years. These losses will be incorporated in the FEM during aging sensitivity analysis, as well as in the widened bridge model to replicate the existing (2002) bridge.

CHAPTER FIVE: FOUR – SPAN FINITE ELEMENT MODEL (2002)

Introduction

A finite-element model for the four-span widened bridge structure is developed as an extension of both the benchmark studies and the four-span original 1972 bridge (see Figure 51). Shell elements are used to represent the prestressed concrete girders. Frame elements with non-prismatic cross-sections represent columns. The 20 precast beams and associated pre-tensioning were developed and updated with the CSiBridge Design Module.

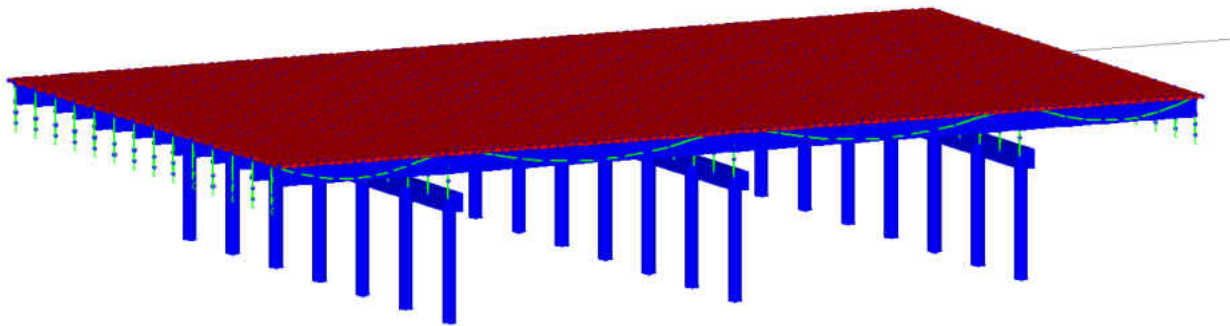


Figure 51: Four – Span Continuous Widened FEM

While the widening connection was not modeled for the four-span continuous bridge unit, the components at the connection were carefully examined. To understand the connection, one must consider the construction process.

Widened decks are typically constructed to match both an existing bridge deck and theoretical grades generated for the outside edge of the widened deck. Field personnel generally develop deck contours for widening. The widening process described here is very specific to the

bridge chosen for this research, the original 1972 bridge that was reconstructed (widened) in 2002.

The following analysis and calculations are carefully made in sections before detailed planning schematics are executed;

- Section I: Geometry
- Section II: Elevations
- Section III: Superstructure Design
 - o Deck
 - o Beam
 - o Bearing
- Section IV: Substructure Design
 - o End Bent
 - o Piers
 - o Foundation Design
- Section V: Retaining Wall Design
- Section VI: Aesthetic Documents

Upon completion of the above calculations, the schematics and detailed planning and drawings are in effect. Since the bridge chosen to be analyzed undergoes an inside as well as outside widening, the steps taken here will follow the procedure and process of an inside and outside widening criteria.

One of the steps is an examination of the cross-section of the bridge to be widened, with the

proposed cross-section to match both the existing bridge deck and the proposed deck.

In their paper Du et al. [45] point out several issues regarding the common practice of widening bridges, in which a new bridge deck is constructed alongside an existing bridge deck, and an *in situ* concrete stitch (also called stitching slab) is cast between the existing and new decks to provide a monolithic connection and continuous riding surface; but no issues regarding load transfers from the deck to its members, which is key to this research, was mentioned. In this paper, engineering issues concerning bridge widening are addressed, and finite-element method-related grillage theory is used to investigate the effect of shrinkage and creep differences between existing and new bridge decks on the internal forces of the structures. The influence of settlement in the substructure of new bridges on widened structures is also investigated. Possible improvement of concrete materials used for connecting existing and new bridge decks is discussed. Thus, it is suggested that the connection time interval between existing and new bridge decks should be determined if possible, to minimize the shrinkage and creep effect. Some feasible measures to enhance the integrity of the widened bridge are also proposed. This is to support the argument that load transfers between the bridge deck and its components were not hindered because the connection was not modeled. Figure 52 demonstrates a typical bridge-widening connection.

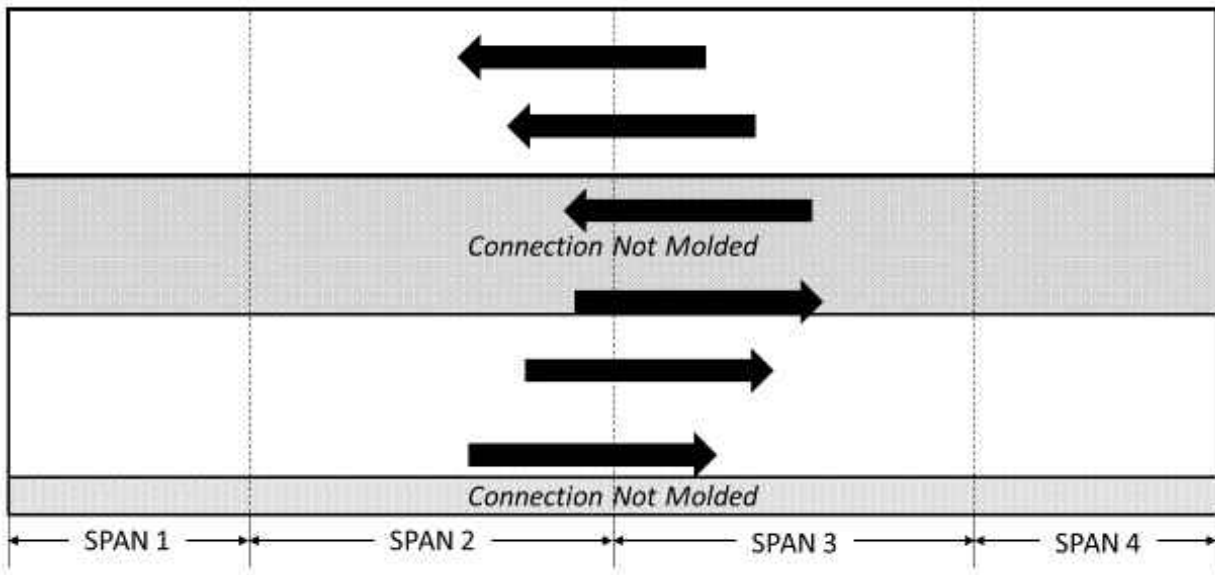


Figure 52: Bridge – Widening Connection

Additionally, it should be noted that the existing bridge girders (1972 Bridge) were modeled to incorporate a reduction in their modulus of elasticity, based on the concrete bound stiffness analysis to replicate their condition and characteristics when the bridge was widened. The existing bridge girders in the widened bridge are shown in Figure 53, along with the corresponding targeted bridge girders focused on in this research.

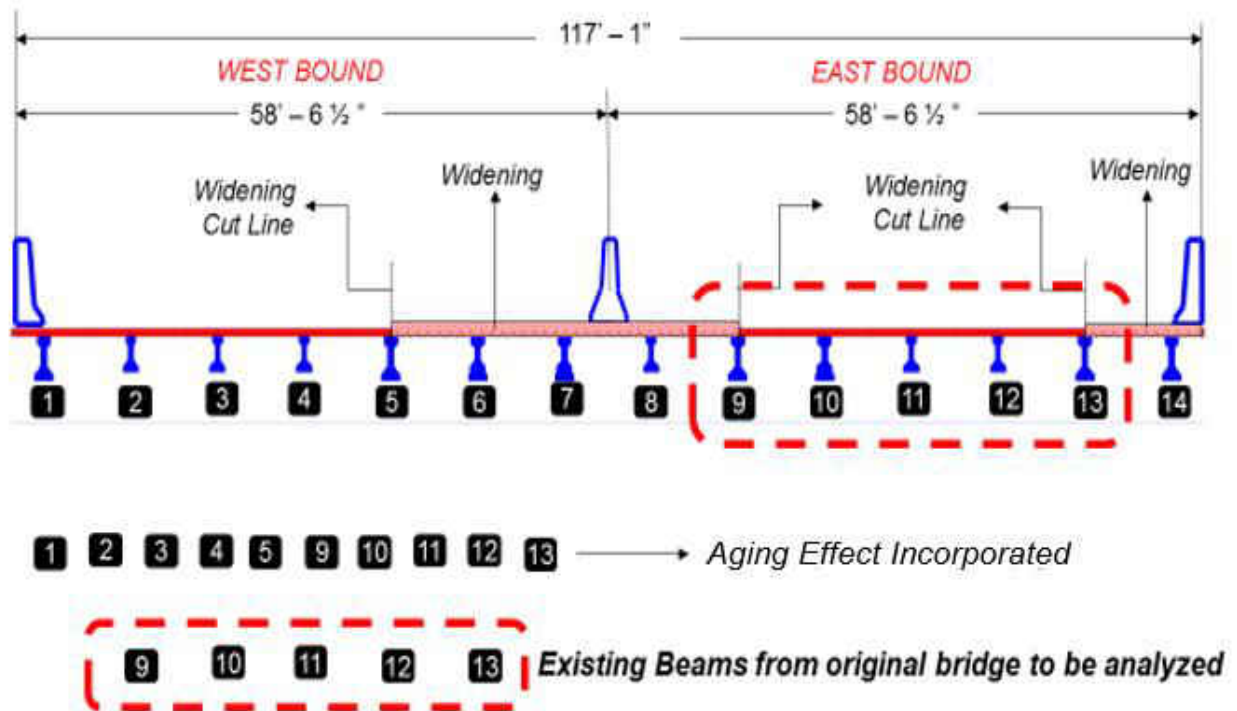


Figure 53: Existing and Targeted Girder in Widened Bridge

Objective

The focus of this research is the behavior and performance of the widened bridge, with emphasis in the following areas:

- Capacity after widening, which investigates the following:
 - o ultimate flexure and shear,
 - o live-load distribution factors,
 - o load ratings, and
 - o reliability

- Interaction between new and existing members, which investigates the following:
 - o modal analysis and
 - o sensitivity analysis

Like the 1972 bridge model, the 2002 widened bridge was modeled in the absence of experimental data; therefore, the analytical investigation will focus on the FEM model, which will be used for calibration. The results will be used for the analysis in the chapter sections listed below. The process will also include a comprehensive association and comparing of existing results.

Understanding the behavior and characteristics of the 2002 widened bridge will facilitate variation and comparison to the original 1972 bridge.

The finite-element model for the 2002 widened four-span bridge, developed as an extension of both the benchmark and 1972 bridge studies, will be used for the following studies (along with their results) in the chapters noted:

- Modal Analysis and Parameter Sensitivity (Chapter 6)
- Live-Load Distribution Factors Analysis (Chapter 7)
- Simulations and Load Ratings (Chapter 8)
- Modal Analysis and Loading Ratings Correlations (Chapter 9)
- Load Rating and Reliability Analysis (Chapter 10)
- Nonlinear Simulation and Reliability Analysis (Chapter 11)

Consequently, it should be noted that for consistency, close approximation of reliability analysis results will be used in chapters 10 and 11, and as shown in Figure 54. These results will

focus on component versus system investigation of a single span (consisting of critical components) on the widened bridge. This section is equivalent to spans 2 and 3 in the widened structure, which are of equal lengths (60 ft., 3 in.), as illustrated in Figure 55.

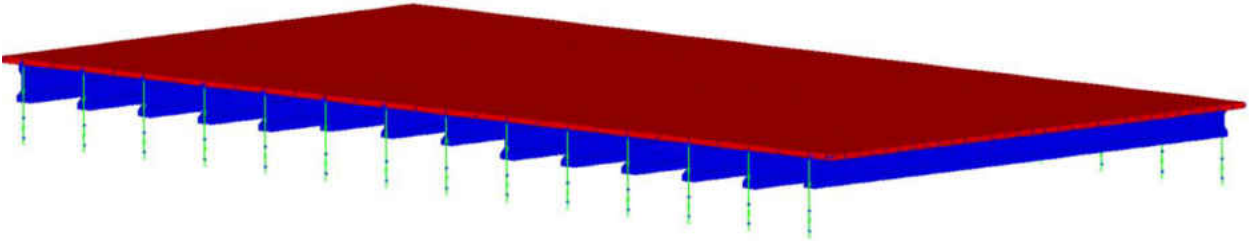


Figure 54: Single – Span 2002 Widened Bridge

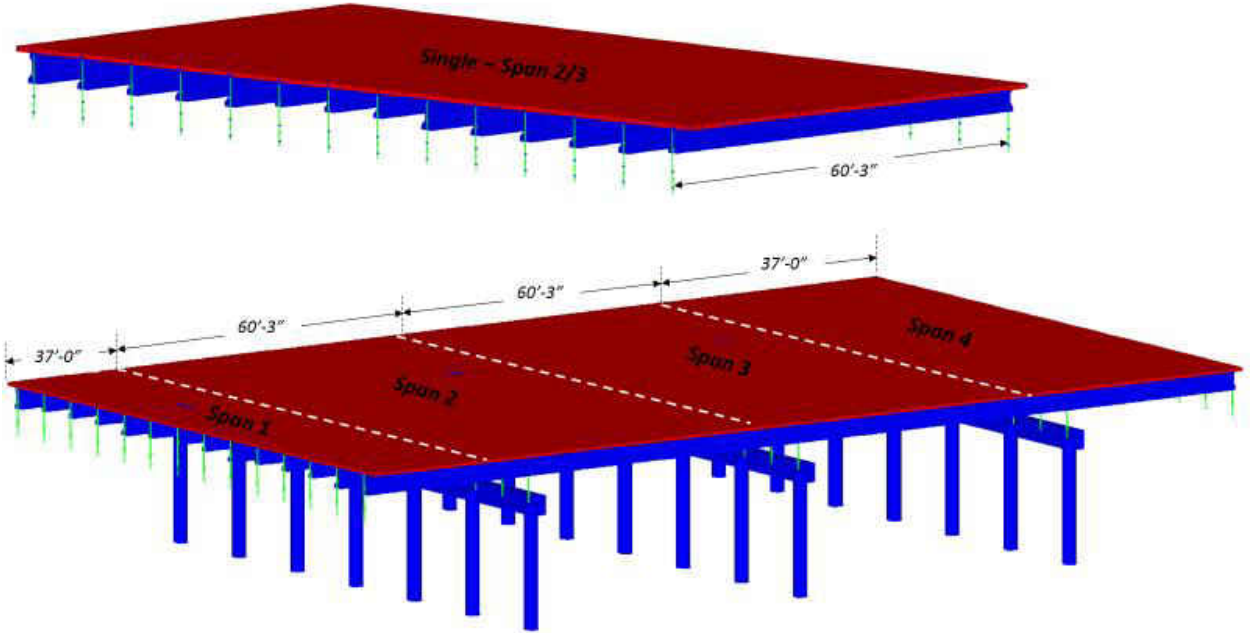


Figure 55: 2002 Widened Bridge Single – Span Illustration

Discussion

The aging parameters previously estimated will be incorporated in this model and its analysis. The modulus of elasticity and prestress losses were the two critical parameters identified, and will be assigned to the existing members in the model. Additionally, the parameters will be varied for different age stages for future prediction of the bridge capacity and its members. For example, an initial investigation immediately after widening might suggest that the new members in the bridge system will have no loss; however, the existing members will be affected by a 30-year loss, and must be incorporated in the model accordingly. This can be done for ages 5, 10, 15, 20 years, etc. after the bridge widening, which means that while the new members will be 5, 10, 15, or 20 years old, their existing counterparts will be 35, 40, 45 or 50 years old. The specific losses will be assigned to the members, per their respective ages. Figure 56 illustrates the schematics and aging progression of the widened bridge, per the individual components.



Figure 56: Aging Progression Schematics of Widened Bridge Members

CHAPTER SIX: MODAL ANALYSIS AND PARAMETER SENSITIVITY

Introduction

As stated earlier (under “Benchmark: Modal Analysis” in Chapter Three), the dynamic characteristics (modes shapes, frequencies, etc.) and physical characteristics (capacity, resistance, etc.) of a bridge structure were obtained numerically in the absence of experimental analysis. Thus, a modal analysis performed on the finite-element model is developed and evaluated for the initial validation of the structure, as well as verification of its dynamic behavior and responses.

Modal analysis is used to measure the impact of parameter variations on the vibration characteristics of a bridge by incrementally changing one parameter at a time, neglecting any cross-sensitivities. The frequencies and mode shape vectors are global indicators of structural condition and structural behavior [46]. Results of the modal analysis may be used to plan a field-verification plan or long-term monitoring program. When dynamic responses obtained from field monitoring studies, finite element models (FEMs) can be updated and calibrated. A flow chart that shows a procedure for manual FEM calibration, using modal analysis, is given in the literature by Aktan [25].

Selection of Modes

Zhang [32] gives practical recommendations for selection of relevant modes. In the case of long-span bridge response to wind excitation, inclusion of the lowest vertical dominant, horizontal-dominant, and torsional-dominant deck modes is recommended. The response of the

bridge can be quite accurately spanned by the lower modes. For seismic response prediction, those modes dominated by motions of the towers or piers should also be considered. In the areas of structural health monitoring and damage detection, it is found that higher modes are more sensitive to local damage. Indeed, it would be ideal to match as many modes as possible between the measurement and FEM predictions. However, it does not seem logical to include higher modes that cannot be obtained reliably from either the measurement or the FEM analysis.

For the present study, enough modes will be reported, such that all the characteristic responses are represented. For the four-span continuous bridge, the following characteristic responses are identified:

1. vertical beam bending,
2. lateral beam bending and
3. torsion.

Results

Eigenvalue analysis of the bridge using CSiBridge program gives natural frequencies in the range from 6.680 Hz to 14.775 Hz, and 10.735 Hz to 15.403 Hz, for the first 16 modes of the nominal model for the original 1972 bridge and widened 2002 bridge, respectively. In general, the mode shapes of the bridge could be classified as exhibiting lateral beam bending, vertical beam bending, and torsion. Example behaviors are shown graphically in Figure 57 and Figure 58, with complete modes presented in Appendix A.

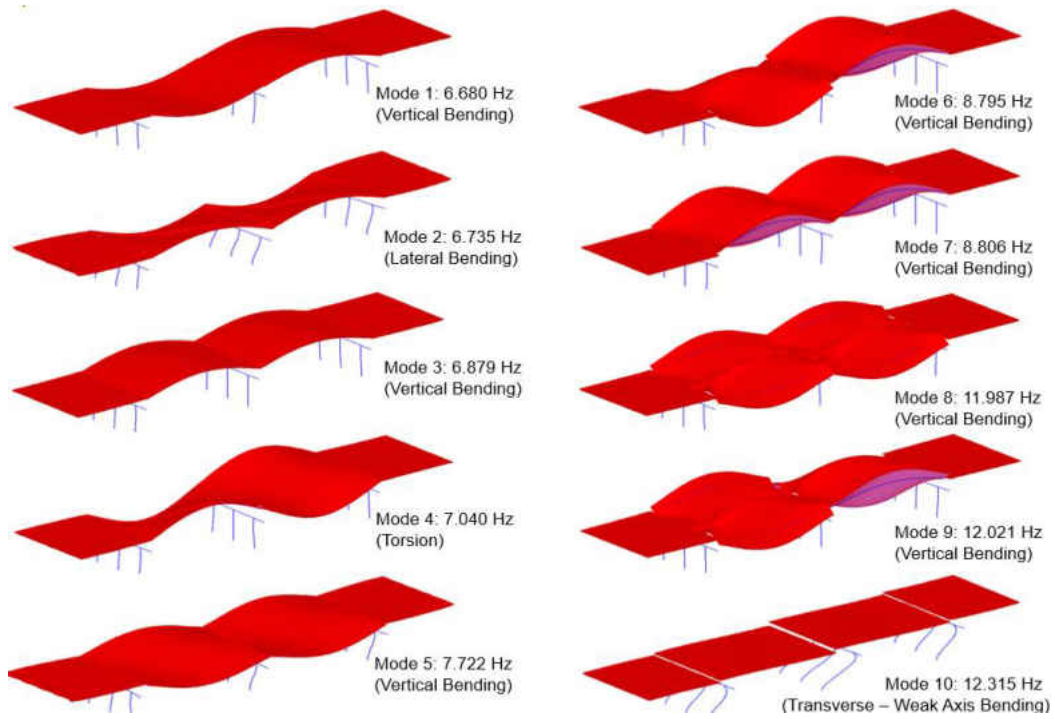


Figure 57: Modal Behavior of 1972 Bridge

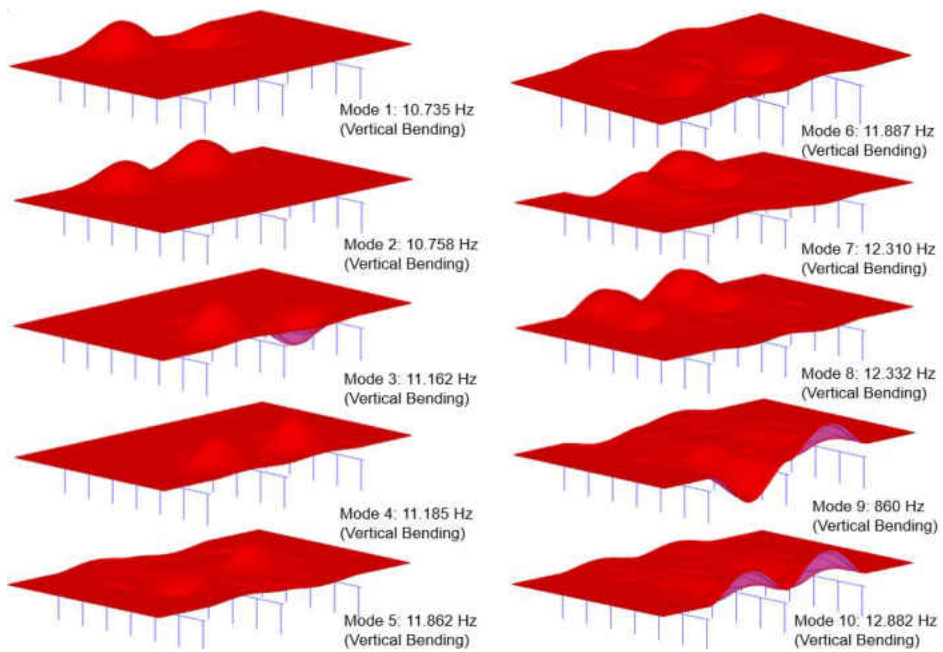


Figure 58: Modal Behavior of 2002 Widened Bridge

Discussion

The results demonstrate significant stiffness shift between the two bridges (original 1972 bridge and 2002 widened bridge). The first mode frequency varies by more than 4.00 Hz, with frequencies of 6.680 Hz and 10.735 Hz for the 1972 and 2002 bridges, respectively. The 2002 widened bridge also seems to exhibit a local behavior, as compared to the original 1972 bridge, which behaves globally. These behaviors are observed in their respective first modes, with the whole system in the 1972 bridge having a dynamic global response, while only part of the system in the 2002 widened bridge reacts to the vibration of the system. It should also be noted that the section of the 2002 widened bridge responding to the vibration constitutes more of the existing old members in the original bridge. Consequently, we can add that the condition of the bridge also has significant effect on the dynamic response. It requires much more energy to overcome the torsion resistance; so, we see the first torsional mode occur at a much higher frequency in the 1972 bridge during the fourth mode at a frequency of 7.04 Hz, and completely absent in the 2002 widened bridge. Also, not only are torsional modes absent in the 2002 widened bridge, but the second lateral mode in the 1972 bridge is also completely absent, leaving vertical bending modes to control and dominate all the modes in the 2002 widened bridge.

It is interesting to note that the above analysis and results are an indication of increased stiffness between the time when the original bridge was built in 1972 and when it was widened in 2002, thus indicating that more stiffness is introduced in the bridge system after widening.

It is recommended that comprehensive modal testing be pursued for a more objective and comprehensive model calibration and validation, which could also include field investigation

and testing.

CHAPTER SEVEN: LIVE LOAD DISTRIBUTION FACTORS ANALYSIS

The finite-element models developed in this study are intended to represent the conditions of both the original 1972 bridge and the existing bridge that was widened in 2002. The live-load moments are the results of the FEM models. However, the live-load distribution factors were estimated in a spreadsheet as a function of the moment of the entire structure, divided by the subsequent individual girder moments, as illustrated in the sample sketch in Figure 59.

$$LLDF = \frac{\text{Moment of Individual Girder}}{\text{Moment of Entire Bridge Span}}$$

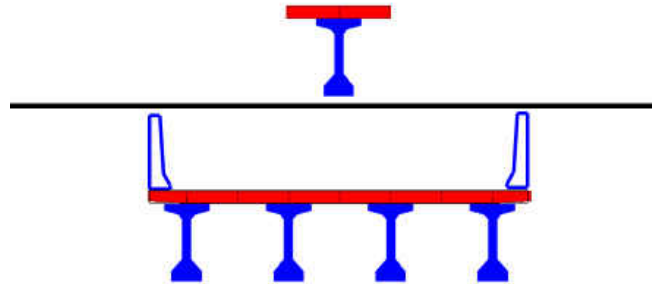


Figure 59: Live Load Distribution Factors Analysis Illustration

Live-load distribution factors are typically how bridges are analyzed for design. These distribution factors result in a simple approximate analysis of bridge superstructures. Live-load distribution factors separate the transverse and longitudinal distribution of force effects in the superstructure. Live-load force effects are assumed to be distributed transversely, by proportioning the design lanes to individual girders through the application of distribution factors. The force effects are subsequently distributed longitudinally between the supports, through the one-dimensional (1-D) structural analysis over the length of the girders.

In simplifying the design process, distribution factors minimize potential modeling errors.

They reduce the necessity of modeling the entire bridge from a two-dimensional (2-D) or three-dimensional (3-D) analysis to a 1-D analysis of a girder.

Benchmark Live Load Distribution Factors

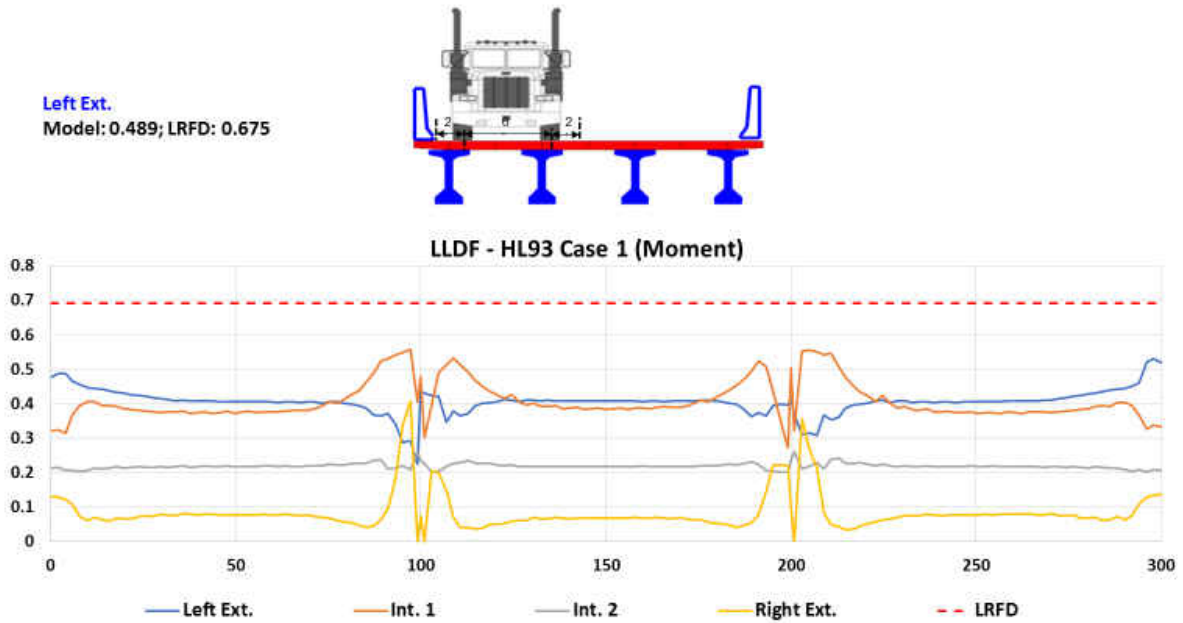
Since the benchmark bridge was designed per LRFD requirements—(and hence, LRFR-rated), this model was also designed per LRFD requirements and, as stated previously, the concept of using the single-girder moment, divided by the moment of the entire structure, was used. The results of the hand calculations using MathCAD are detailed in Appendix B, and are summarized on Table 8.

Table 8: Benchmark Hand Calculations for Distribution Factors

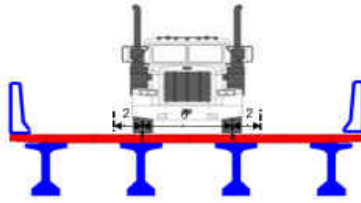
<p><i>Int. Girder (Positive Moment)</i></p> <ul style="list-style-type: none"> ➤ <i>Single Lane = 0.485</i> ➤ <i>Multi Lane = 0.692</i> 	<p>← Controls</p>	<p>➤ <i>Ext. Girder (Positive Moment)</i></p> <ul style="list-style-type: none"> ➤ <i>Single Lane = 0.675</i> ➤ <i>Multi Lane = 0.692</i>
<p><i>Int. Girder (Negative Moment)</i></p> <ul style="list-style-type: none"> ➤ <i>Single Lane = 0.485</i> ➤ <i>Multi Lane = 0.692</i> 		<p>➤ <i>Ext. Girder (Negative Moment)</i></p> <ul style="list-style-type: none"> ➤ <i>Single Lane = 0.746</i> ➤ <i>Multi Lane = 0.556</i>
<p><i>Int. Girder (Shear)</i></p> <ul style="list-style-type: none"> ➤ <i>Single Lane = 0.680</i> ➤ <i>Multi Lane = 0.814</i> 	<p>← Controls</p>	<p><i>Note: Exterior Girder Analysis not computed by Benchmark author since investigated was focused on the controlling interior girder.</i></p>

The results of the live-load distribution factors for the benchmark bridge (for three

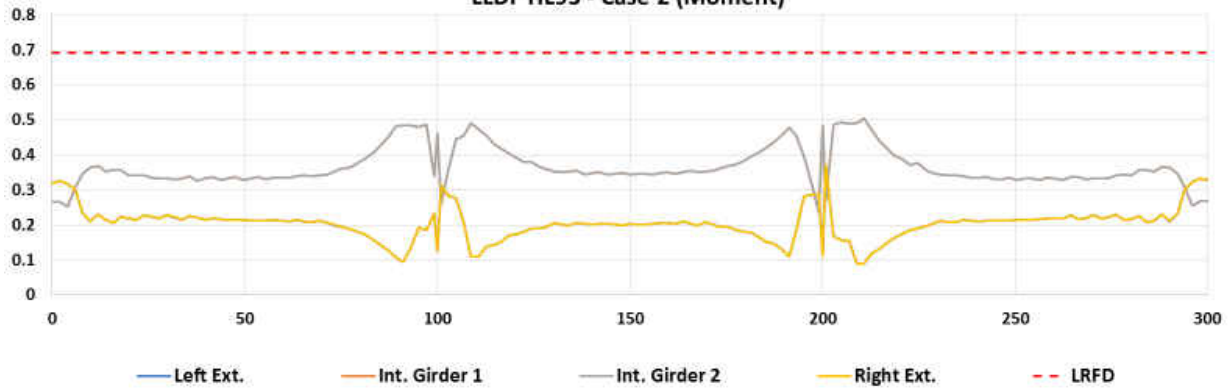
different moment-loading cases and a shear-loading case) are shown in the drawings in Figure 60 and on Table 9. These results are shown with code-estimated distribution, so the margin between the model distribution factors and the code can be observed.



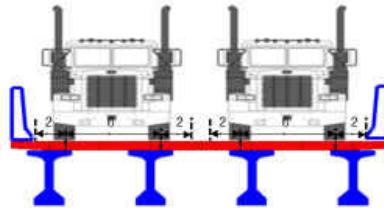
Interior
Model: 0.474; LRFD: 0.485



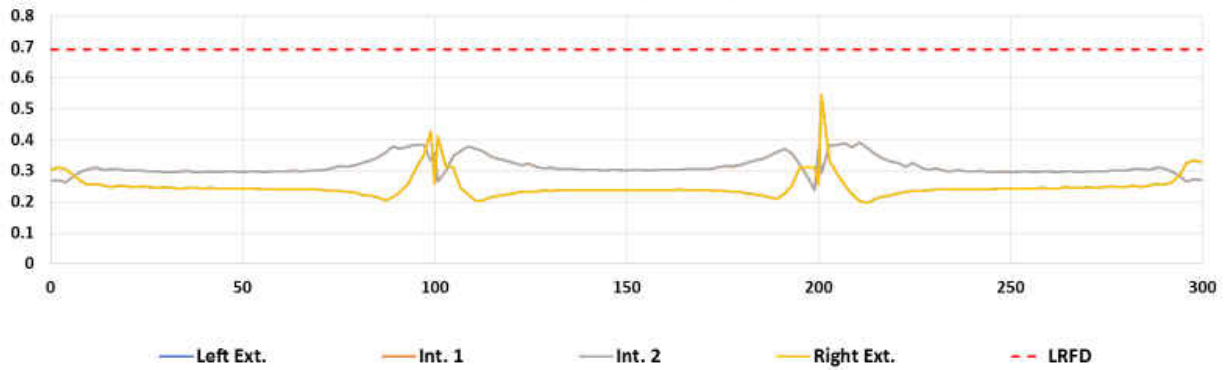
LLDF HL93 - Case 2 (Moment)



Interior
Model: 0.378; LRFD: 0.692



LLDF HL 93 - Case 3 (Moment)



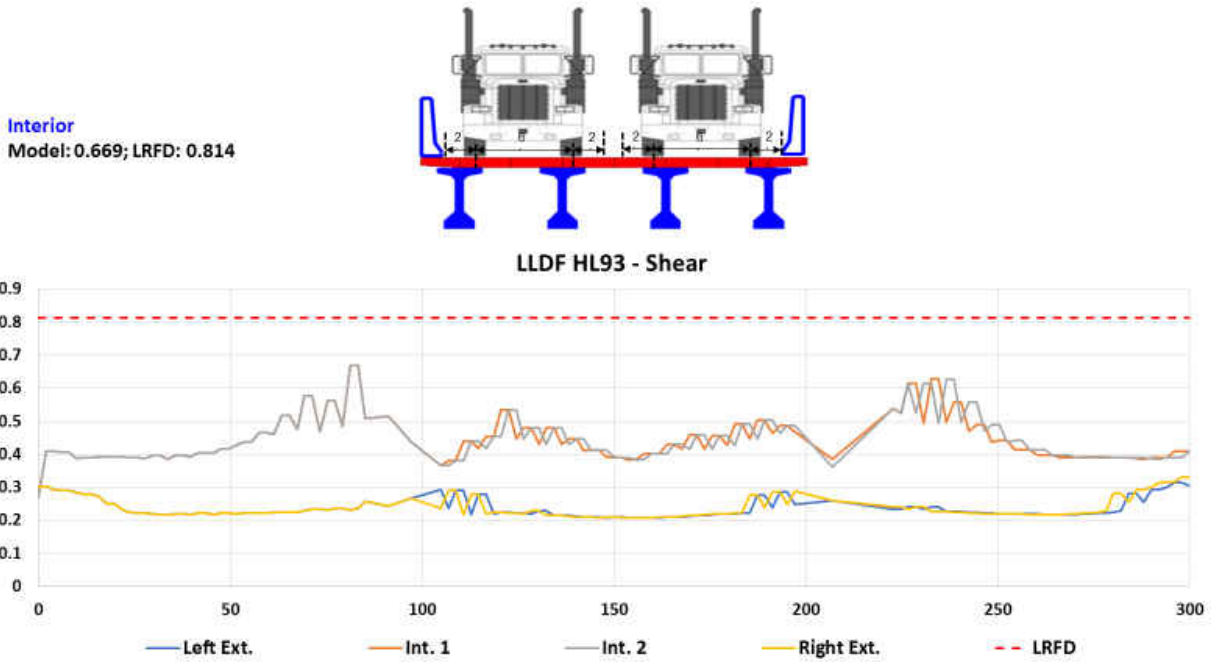


Figure 60: Benchmark Live Load Distribution Factors

Table 9: Moment & Shear Controlling Live Load Distribution Factors

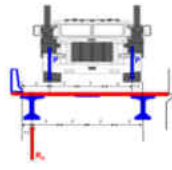
	HL93	
	FEM	LRFD
Moment	0.489	0.692
Shear	0.669	0.814

1972 and 2002 Live Load Distribution Factors

Since the original 1972 bridge was constructed using LFR ratings, and since current codes require that such bridges be assessed by the same ratings, the LFR analysis is considered and evaluated in this research. Similarly, a hand-calculation analysis was done for both the LFD and LRFD for the

1972 and 2002 bridges. A detailed analysis appears in Appendix B, and the results are shown on Table 10.

Table 10: 1972 and 2002 Bridge Hand Calculations for Distribution Factors

	Interior Girder (Positive Moment)	Exterior Girder (Positive Moment)	Interior Girder (Negative Moment)	Exterior Girder (Negative Moment)	
Moment	<ul style="list-style-type: none"> Spans 1 & 4 <ul style="list-style-type: none"> Single Lane = 0.661 Multi Lane = 0.877 Spans 2 & 3 <ul style="list-style-type: none"> Single Lane = 0.555 Multi Lane = 0.768 	<ul style="list-style-type: none"> Spans 1 & 4 <ul style="list-style-type: none"> Single Lane = 0.746 Multi Lane = 0.877 Spans 2 & 3 <ul style="list-style-type: none"> Single Lane = 0.746 Multi Lane = 0.768 	<ul style="list-style-type: none"> Spans 1 & 4 <ul style="list-style-type: none"> Single Lane = 0.661 Multi Lane = 0.877 Spans 2 & 3 <ul style="list-style-type: none"> Single Lane = 0.555 Multi Lane = 0.768 	<ul style="list-style-type: none"> Spans 1 & 4 <ul style="list-style-type: none"> Single Lane = 0.746 Multi Lane = 0.877 Spans 2 & 3 <ul style="list-style-type: none"> Single Lane = 0.746 Multi Lane = 0.768 	
	Shear	<ul style="list-style-type: none"> Interior Girder <ul style="list-style-type: none"> Spans 1 & 4 <ul style="list-style-type: none"> Single Lane = 0.730 Multi Lane = 0.901 Spans 2 & 3 <ul style="list-style-type: none"> Single Lane = 0.730 Multi Lane = 0.901 	<ul style="list-style-type: none"> Exterior Girder <ul style="list-style-type: none"> Spans 1 & 4 <ul style="list-style-type: none"> Single Lane = 0.746 Multi Lane = 0.678 Spans 2 & 3 <ul style="list-style-type: none"> Single Lane = 0.746 Multi Lane = 0.678 	<div style="text-align: right;">  </div>	

Numerous loading cases were investigated for the critical position for each girder within the system. The distribution factors for the 1972 bridge are shown here in Figure 61 and Figure 62 for both moment and shear and their respective controlling factors summarized on Table 11.

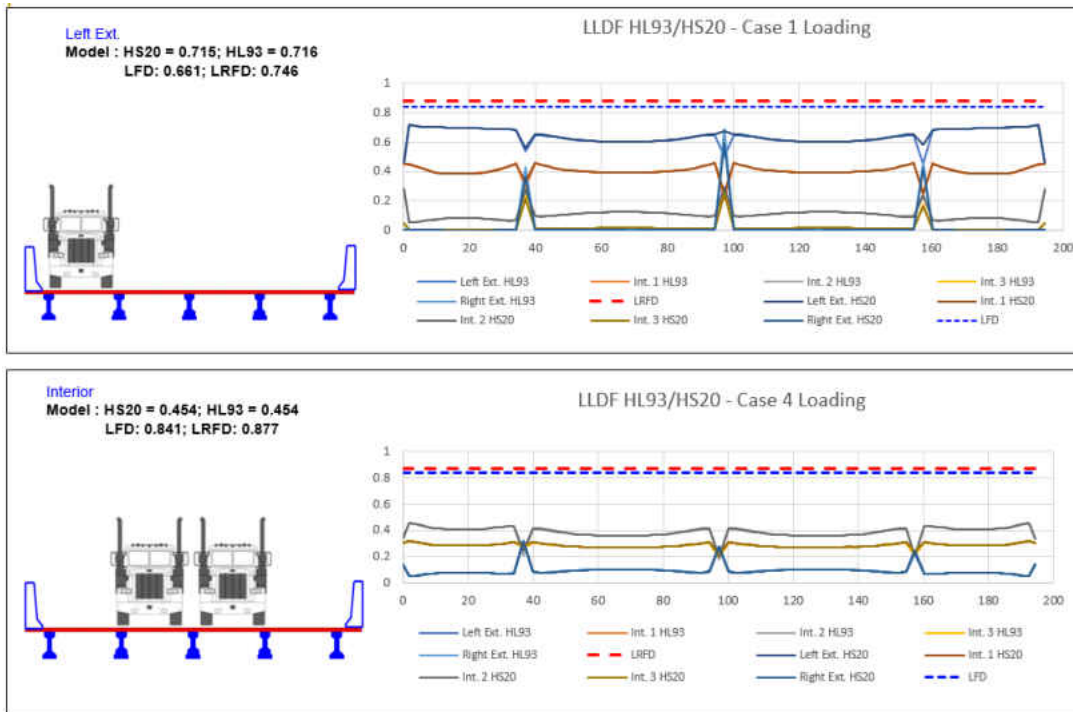


Figure 61: 1972 Bridge Live Load Distribution Factors (Moment)

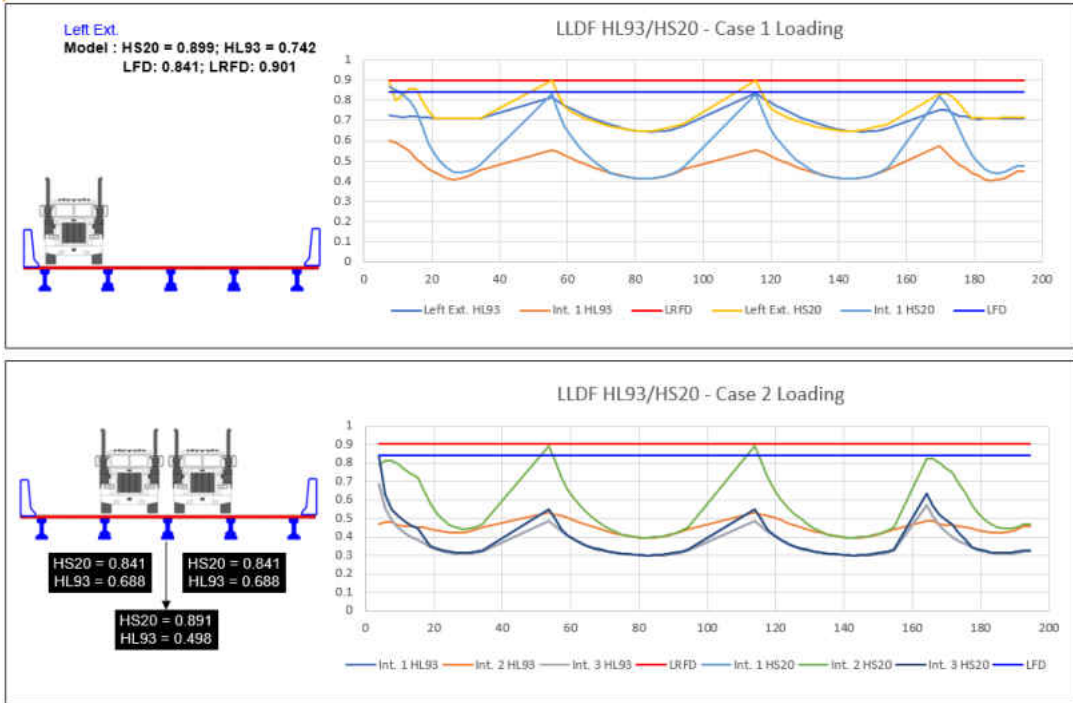


Figure 62: 1972 Bridge Live Load Distribution Factors (Shear)

Table 11: Moment and Shear Controlling Live Load Distribution Factors (1972 Bridge)

	HS20		HL93	
	FEM	LFD	FEM	LRFD
Moment	0.715	0.841	0.716	0.877
Shear	0.899	0.841	0.742	0.901

Consequently, the process was applied to the 2002 bridge. Figure 63 shows the critical case assessment and selection. Figure 64 and Figure 65 show the distribution factors results for both moment and shear, and a summary of the controlling live-load distribution factors is provided on Table 12.

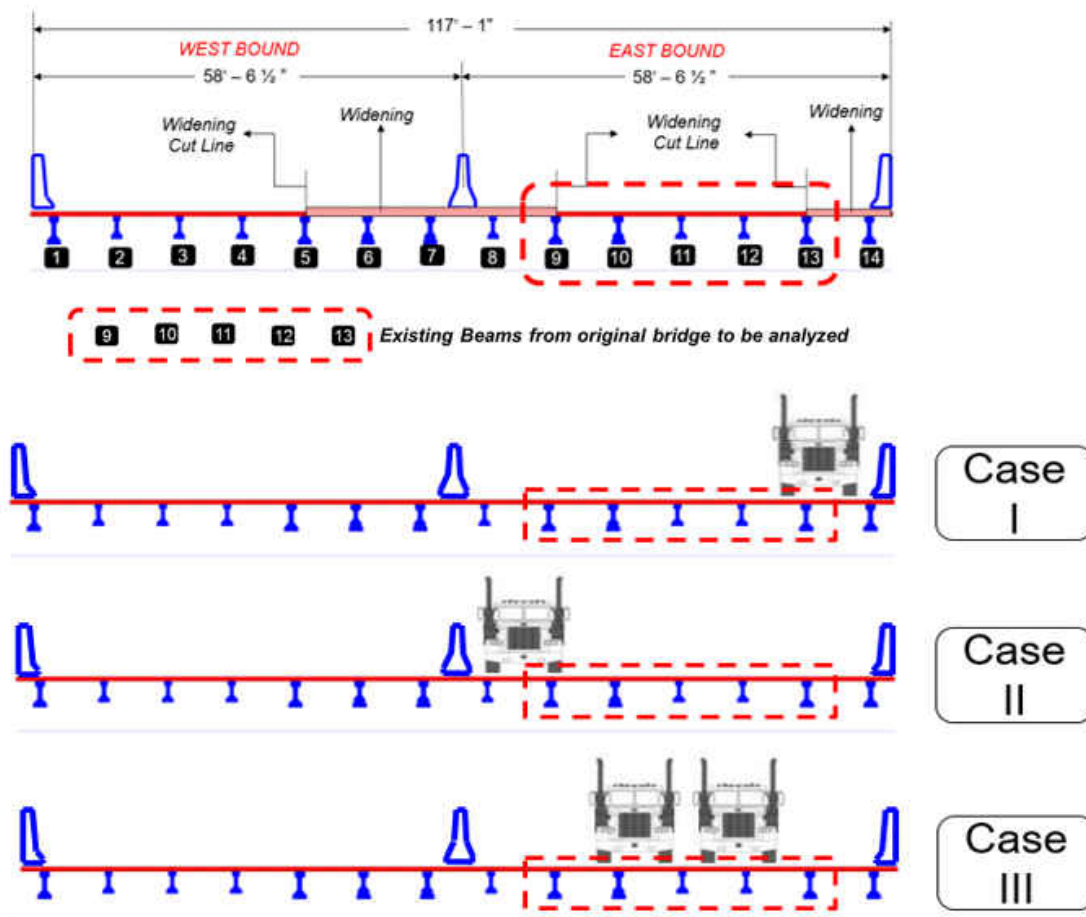


Figure 63: Critical Case Selection for Targeted Components

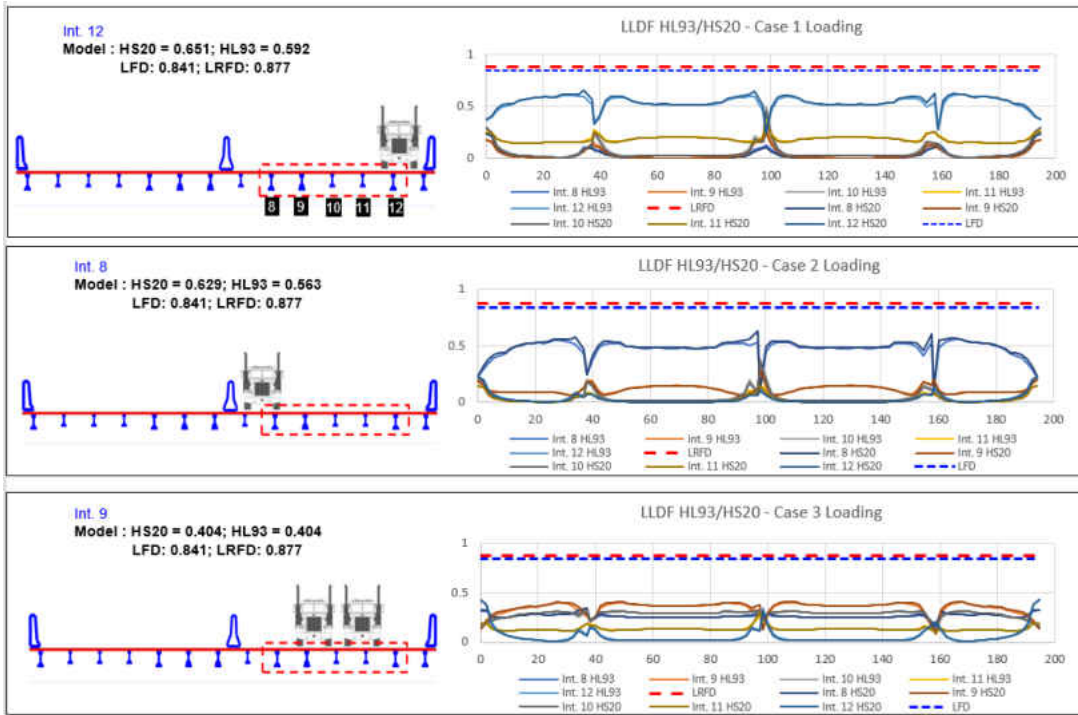


Figure 64: 2002 Bridge Live Load Distribution Factors (Moment)

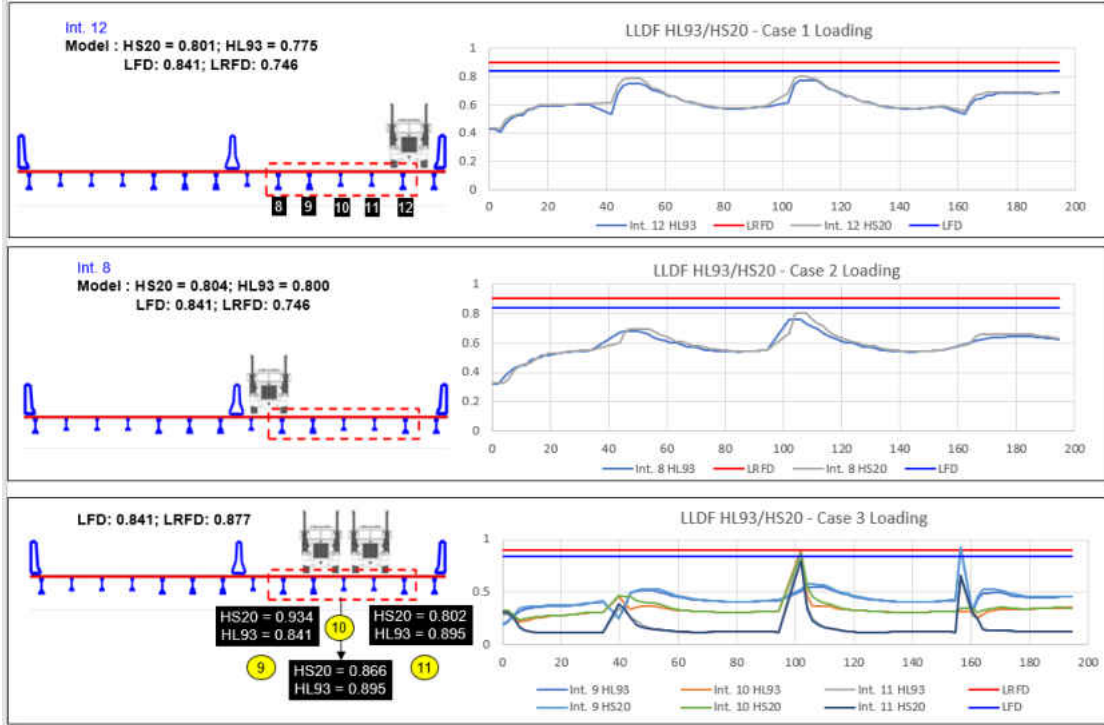


Figure 65: 2002 Bridge Live Load Distribution Factors (Shear)

Table 12: Moment and Shear Controlling Live – Load Distribution Factors (2002 Bridge)

	HS20		HL93	
	FEM	LFD	FEM	LRFD
Moment	0.651	0.841	0.592	0.877
Shear	0.934	0.841	0.895	0.901

Discussion

The live-load distribution factors derived from the model analysis, compared to both the previous and current codes, range from 18% to 33%, and from 1% to 18% for both moment and shear, respectively, as shown on Table 13 and Table 14. The graphs shown in Figure 66 and Figure 67 illustrate the variations between the AASHTO and FEM live-load distribution factors for an HL-93 truck, for both moment and shear.

Table 13: Moment Live – Load Distribution Factors Analysis

Bridge	Live Load Distribution Factors (HL - 93 Truck)		Diff. %
	AASHTO	FEM	
Benchmark	0.692	0.489	29.3
1972	0.877	0.716	18.4
2002	0.877	0.592	32.5

Table 14: Shear Live – Load Distribution Factors Analysis

Bridge	Live Load Distribution Factors (HL - 93 Truck)		Diff. %
	AASHTO	FEM	
Benchmark	0.814	0.669	17.8
1972	0.901	0.742	17.6
2002	0.901	0.895	0.7

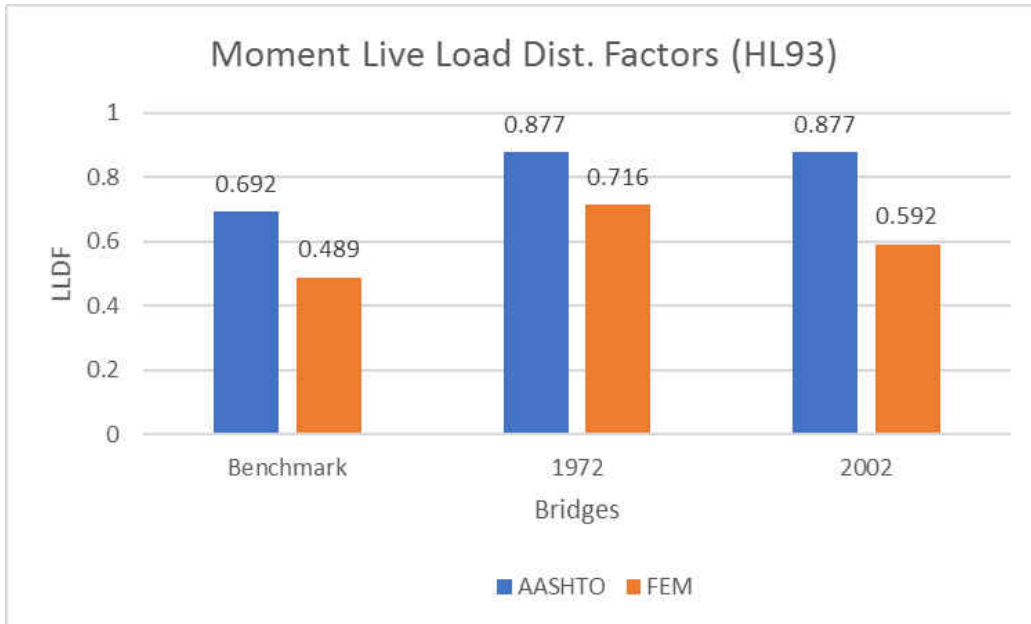


Figure 66: Moment Live – Load Distribution Factors Comparison

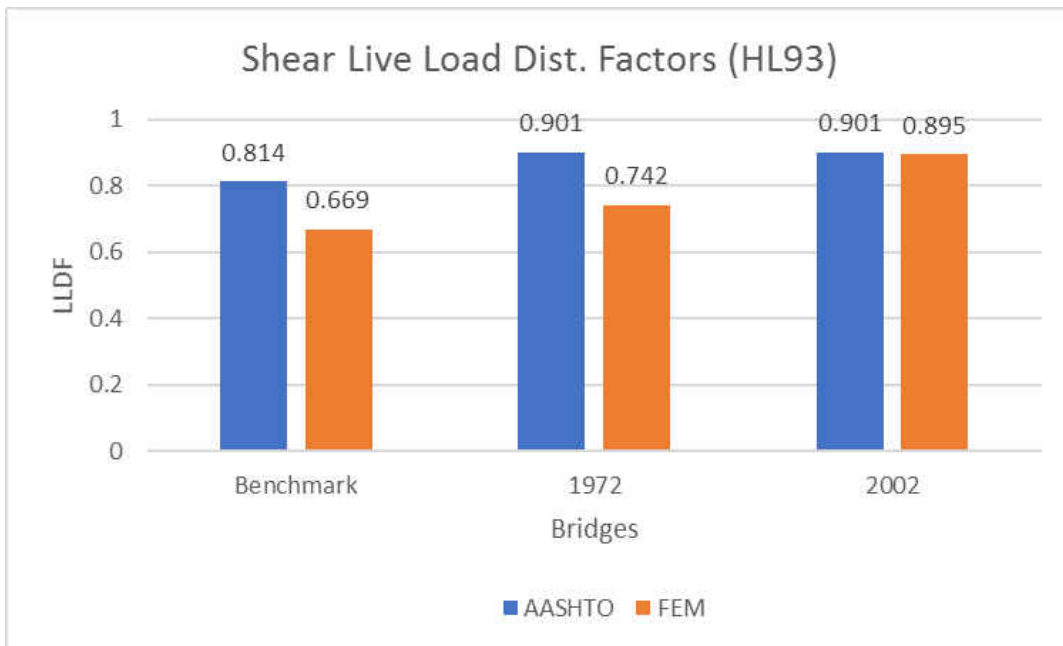


Figure 67: Shear Live – Load Distribution Factors Comparison

The close variation of the shear live-load distribution factors between AASHTO and the FEM is an indication of how critical shear analysis can be in any case. It is also observed that the wider the spans, the closer the variation.

However, there seems to be a wide variation between the moment live-load distribution factors for AASHTO and the FEM, which can be addressed. One possible explanation of this variation in the redistribution of mid-span moment live-load could be the continuity conditions assumed in the FEM. Whereas, there is some flexural resistance offered by the column and crosshead in the FEM, the AASHTO analysis may have assumed pin supports at the ends and rollers between spans of the bridge.

CHAPTER EIGHT: SIMULATIONS AND LOAD RATING (FULL BRIDGE)

Objective

In this chapter, simulations and load-rating results will be presented for the benchmark, 1972 and 2002 bridges, following the AASHTO LFR and LRFR methodology. Resistance calculations are based on the AASHTO LRFD method, which includes analysis outlined in the benchmark study. The objective is to investigate the variations in the load ratings of the bridge before and after widening, which in this case implies investigating and load rating the 1972 bridge model (before widening) and the 2002 bridge model (after widening). The benchmark load rating will once again be used as verification by comparing the FEM results with those provided in the text.

Simulations

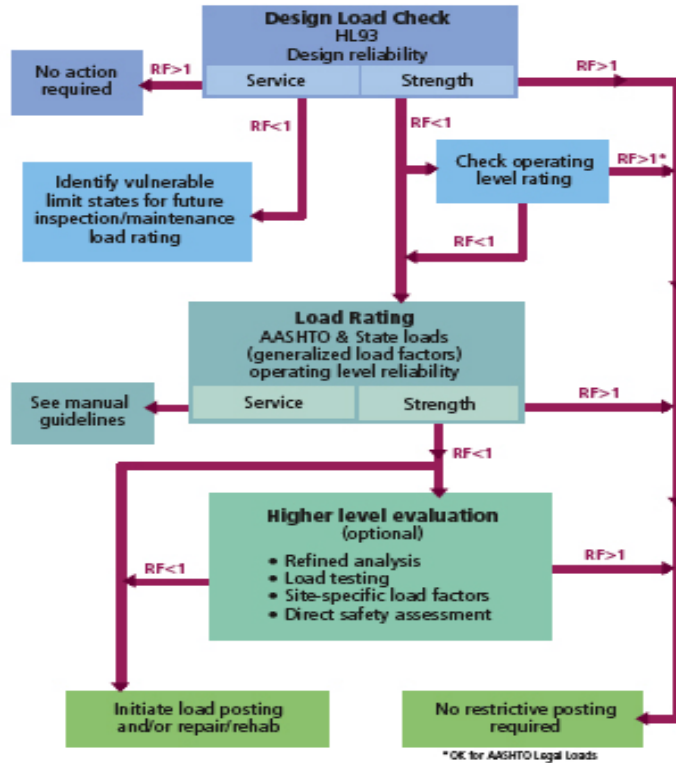
Simulations are conducted using the benchmark model and the two parametric 1972 and 2002 models. Load effects are derived from the FEM output. Critical limit states are identified as well as trends in the data and the physical meaning of the results.

Load Rating

Load rating, which measures the bridge live-load capacity, is analyzed next in this section. It should be noted that the rating for the bridge system is taken as the minimum of the component

ratings. Although the two key focus areas in load rating include operating level (the maximum permissible live-load that can be placed on the bridge) and inventory level (the load that can safely use the bridge for an indefinite period), the initial focus will be on the operating level.

Since the research bridge has a very high likelihood of future widening, only the current acceptable truck (HL-93) will be used for the load-rating analysis. This approach allows assessment of the current components in the bridge for future provisions and its capacity. The equation for load rating is also discussed here; but it should be emphasized that the goal and objective for a component to be considered competent (in the sense of capacity) is for it to have a value greater than, or equal to, 1. This also shows the correlation between load rating and the capacity of a component. The load-rating assessment procedure is illustrated in Figure 68.



The flowchart demonstrates the decisionmaking process involved in the LRFR approach. Source: AASHTO Guide Manual for Condition Evaluation and Load and Resistance Factor Rating (LRFR) of Highway Bridges.

Figure 68: Load Rating Flow Chart

The AASHTO Load and Resistance Factor Rating (LRFR) and the Load Factor Rating (LFR) Manual prescribe three methods for evaluating the safe maximum live-load capacity of bridges (LRFR 6.1.6). It should be noted that in LRFR, “Inventory” and “Operating” ratings are defined in terms of associated reliability indices ($\beta = 3.5$ INV, $\beta = 2.5$ OPR) [58], as follows:

1. load and resistance factor rating of bridges,
2. load rating by load testing, and
3. safety evaluation using structural reliability methods for special cases.

The load and factor rating is given generally as:

$$RF = \frac{C - A_1 * D}{A_2 * L * GDF * (1 + I)}$$

Where;

RF = rating factor

C = capacity (Nominal member resistance – R)

A_1 = Factor for Dead Loads

A_2 = Factor for Live Loads

L = Live Load Effect on member

GDF = Girder Distribution Factor

I = Impact Factor to use with the Live Load Effect

The load and resistance factor rating is given generally as LRFR Eq. (6-1):

$$RF = \frac{C - \gamma_{DC} * DC - \gamma_{DW} * DW \pm \gamma_P * P}{\gamma_{LL} * (LL + IM)}$$

Where;

RF = rating factor

C = capacity (Nominal member resistance – R)

γ_{DC} = LRFD Load Factor for structural components and attachments

γ_{DW} = LRFD Load Factor for wearing surfaces and utilities

γ_P = LRFD Load Factor for permanent loads other than dead loads

γ_{LL} = Evaluation live load factor

DC = Dead load effect due to structural components and attachments

DW = Dead load effect due to wearing surface and utilities

P = Permanent loads other than dead loads

L = Live load effect

IM = Dynamics Load Allowance

This rating factor indicates reserve live-load capacity. It may be simplified conceptually as the capacity minus dead-load demand, all over live-load demand. If there is no reserve live-load capacity, then the rating factor is 1.0. Additional live-load capacity is indicated by rating factors greater than 1.0. The AASHTO load rating is a global expression of capacity, limited by the critical behavior [59].

Load rating will be developed per the AAHSTO LRFR methodology. For design load rating of concrete structures, the LRFR Manual prescribes the following limit states for load rating (LRFR 6.5.4.1): *“The Strength I load combinations shall be checked for reinforced concrete components. The Strength I and Service III load combinations shall be checked for prestressed components.”*

Regarding fatigue, the commentary (C6.5.4.1) states: *“Fatigue is not a concern until cracking is initiated. Hence, prestressed components need not be routinely checked for fatigue.”*

Design vs. Load Rating

Bridge design and rating, though similar in overall approach, differ in important aspects. Bridge ratings generally require the engineer to consider a wider range of variables than is typical in bridge design. Design may adopt a conservative reliability index and require comprehensive

serviceability and durability checks. In rating, the target reliability is reduced and application of the serviceability limit states is done on a more selective basis. The added costs of overly-conservative evaluation standards can be prohibitive as load restrictions, rehabilitation, and replacement become increasingly necessary [47].

The rating procedures presented in the AASHTO Manual for Condition Evaluation and Load and Resistance Factor Rating (LRFR) of Highway Bridges [47] are intended to reflect a balance between safety and economics. As such, a lower target reliability than design has been chosen for load rating at the strength limit state. While the LRFD Code calibration reported $\beta_T = 3.5$, the LRFR Manual adopts a reduced target reliability index, β_T of approximately 2.5, calibrated to past AASHTO operating level load rating. This value was chosen to reflect the reduced exposure period, consideration of site realities, and the economic considerations of rating vs. design [58]. The reduced target reliability is reflected in the reduced live-load factor for Design-Load Rating at the Operating Level for the Strength I Limit State, $\gamma_{LL} = 1.35$ [LRFR 6.4.3.2.2], $\beta_T = 2.5$. This may be compared with the LRFD Code Strength I live load factor, $\gamma_{LL} = 1.75$ [LRFD Table 3.4.1-1], $\beta_T = 3.5$.

Relationship between Load Rating and Reliability

For probabilistic design specifications, such as the LRFD Code, the rating factor and reliability should be highly correlated, because a target reliability index, β_T , is used to calibrate the design and rating factors. While relationships between reliability and rating form the basis of load and resistance factors for bridge components (elements), very good correlation has also been demonstrated between rating factors and reliability indices for bridge systems [20]. To compare

ratings against predicted reliability over the life of the bridges in a network, the authors Akgul and Frangopol [48] calculated rating values and reliabilities over the lifetime, in a continuous manner, based on deterioration and live-load models. Resulting relationships between ratings and reliabilities of existing bridges in a network can be used to determine optimum maintenance strategies at the network level.

Benchmark Verification

Before proceeding with the full set of rating calculations for the 1972 and 2002 bridge parametric models, there was an attempt to verify the results of the calculations for critical load effects and resistance in the nominal model. The most effective way to verify the calculations was to compare them to the benchmark model analysis provided by the author Lubin Gao [38]. Figure 69 shows the FEM model rating of 2.59, compared to 2.79 from the text. This verified the proximity of the model to be used for the ratings of the bridges under investigation (1972 and 2002 bridges).

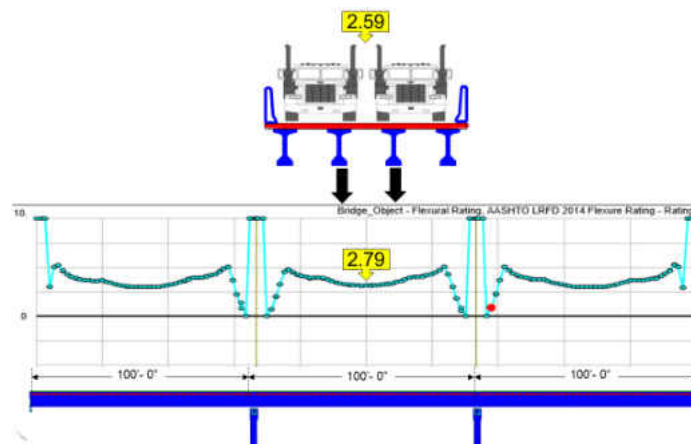


Figure 69: Benchmark Critical Component Rating

1972 Bridge Load Rating Under Aging

Following the benchmark verification load rating, the 1972 was load rated by incorporating the aging effects discussed in previous chapters (modulus of elasticity and prestress losses). Both HS-20 and HL-93 trucks were used to load rate the 1972 bridge. The idea here was that, since the 1972 bridge was designed using the HS-20 truck, its rating results can give us an idea of what its ratings will be if the HS-20 truck were to be used for its rating this present day. It should be noted that the code makes provision for earlier bridges designed using the HS-20 truck to also be rated today (present times) using the HS-20 truck, if unable to rate using the current HL-93 truck. Also, using the HL-93 truck provides a variation and justification of the bridge capacity, depending on whether it rates or not.

Results

A full set of calculations, using the nominal model to find load ratings, is given in Appendix F. The calculations are performed using PTC Mathcad Prime 3.0 (Mathsoft Engineering and Education, Inc., 2015). Once the calculations are laid out for the nominal model, the software facilitates rapid adaptation of the calculations for the parametric models by changing the appropriate inputs. The figures shown here illustrate the ratings for the components in their worst-case loading, and since the 1972 bridge was originally designed using the HS-20 truck, the bridge was evaluated using both HS-20 and HL-93 trucks. Figure 70 shows the load ratings of both trucks for the members.

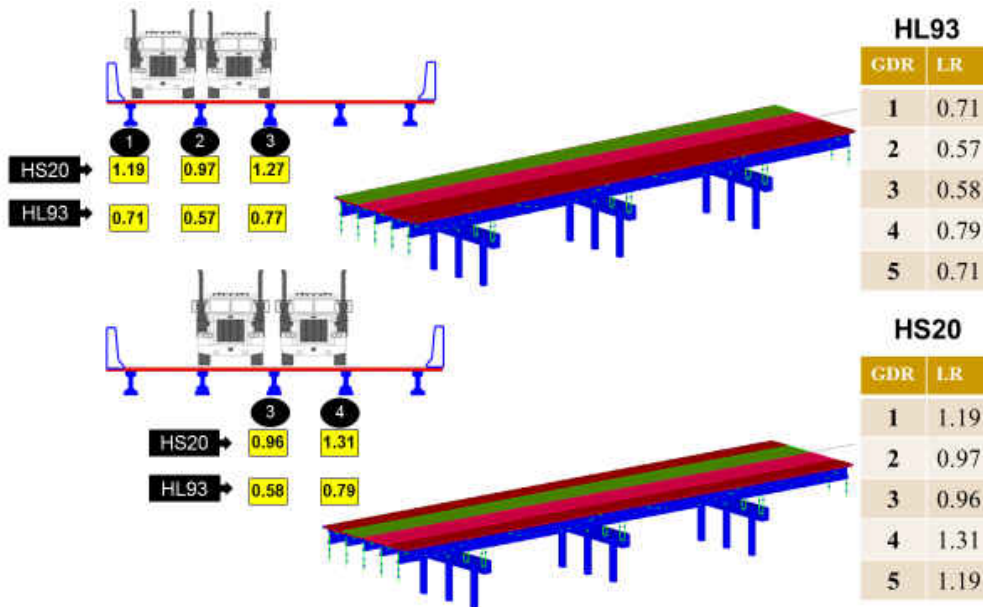


Figure 70: 1972 Bridge Load Ratings

The load ratings results observed from the 1972 bridge show the variation in the HS-20 truck versus the HL-93 truck. The HS-20 truck shows higher rating compared to the HL-93 truck, which is an indication of previous standards and codes not meeting current requirements and standards. The result of the load ratings for the 2002 bridge is discussed in the following chapters.

CHAPTER NINE: MODAL ANALYSIS AND LOAD RATINGS

Introduction

The benchmark bridge, the original four-span 1972 bridge, and the widened 2002 bridge were analyzed and examined to explore a correlation between eigenvalue analysis (modal analysis), which determines the undamped free-vibration mode shapes and frequencies of a given structural system, and load rating, which measures the bridge live-load capacity.

The eigenvalue analysis and load ratings for both single trucks and double trucks (i.e., those towing two trailers in tandem) acting on the central line of the bridge system, with maximum effect on the interior girder, was first performed on the benchmark bridge, as shown in Figure 71. A similar analysis was then performed on both the original 1972 bridge and the 2002 widened bridge, as shown in Figure 72 and Figure 73, respectively. Similar concurrent modes from the eigenvalue analysis were selected for the correlation analysis in this research.

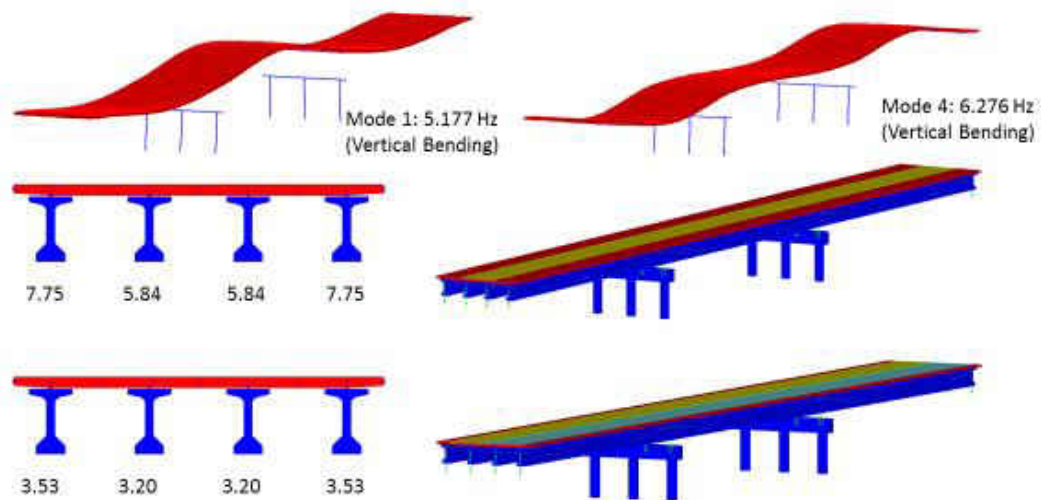


Figure 71: Benchmark Bridge Dynamic Modes and Load Ratings

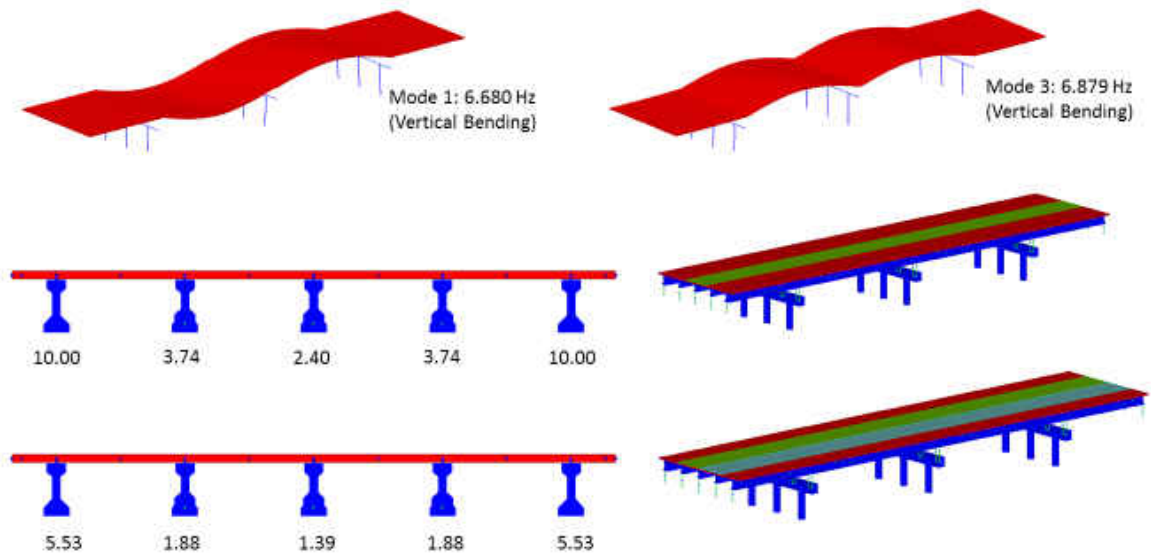


Figure 72: 1972 Bridge Dynamic Modes and Load Ratings (aging not considered)

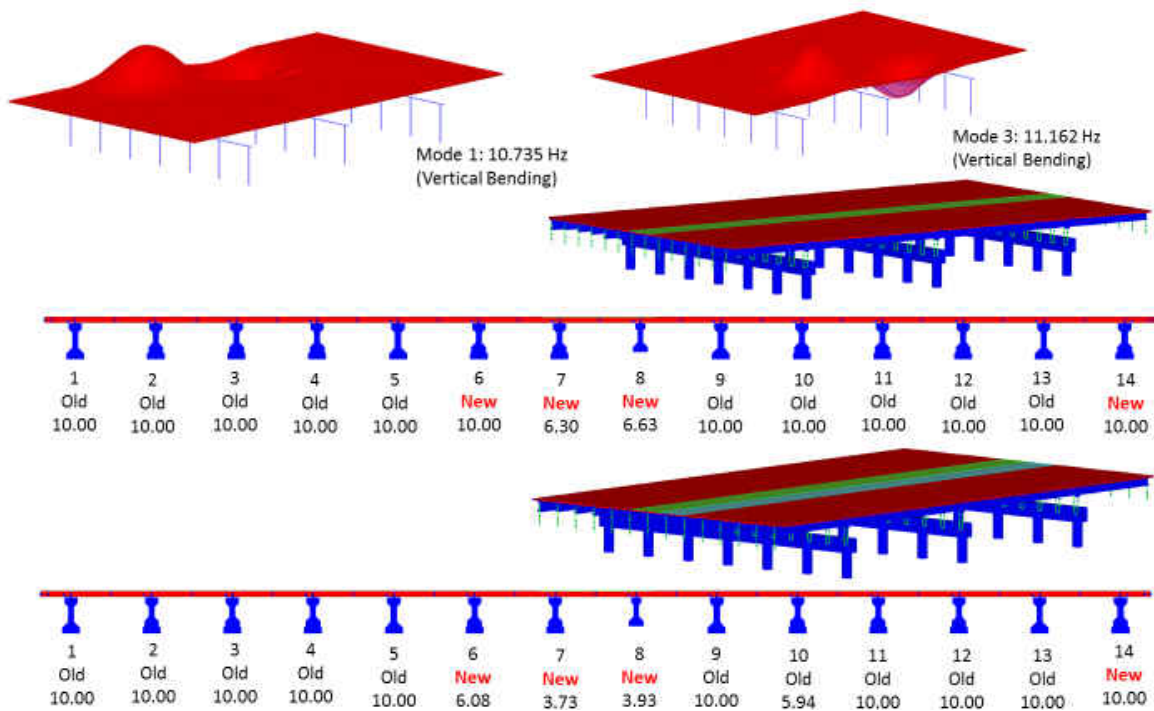


Figure 73: 2002 Bridge Dynamic Modes and Load Ratings

Two sets of analyses were performed for this study;

1. Load ratings versus eigen values plots for all three structures (benchmark, 1972 and 2002 bridges).
2. Load ratings versus eigen values plots for 1972 and 2002 bridges only.

Results

It should be noted that CSiBridge assigns a rating of 10 to all members in the system during analysis that are not affected by the effects of the assigned lane and truck. For the first set of analyses, similar repeating modes were selected for each structure. The load ratings for both single and double trucks were determined for each case, and a scattered plot for all three structures was produced, as shown in Figure 74.

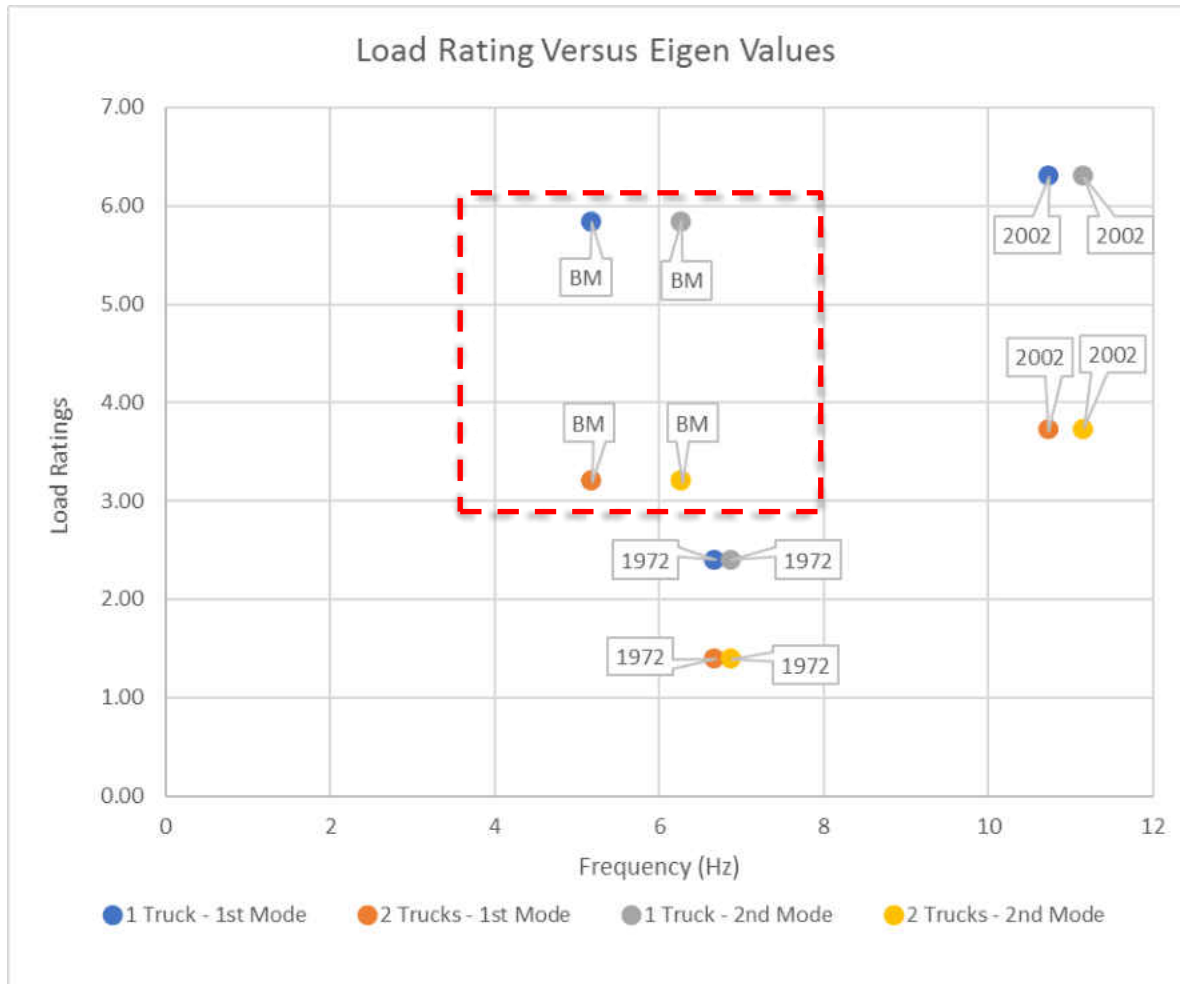


Figure 74: Plot of Loading Ratings Versus Eigen Values (All Structures)

It should be noted that the benchmark (BM) scattered plots do not have a direct correlation with the 1972 and 2002 bridges, due to their different configurations (span lengths and width).

Consequently, the second set of analyses was performed with the same conditions as in the first set. The correlation analysis will focus on the 1972 and 2002 bridges, since they are of similar geometry and characteristics. Since there is a direct correlation between these bridges, it will facilitate the eigenvalues analysis and load ratings correlation investigation to be established.

Initial results from the eigenvalue analysis show signs of increasing strength and stiffness as the frequencies increase from 6.68 Hz for the 1972 bridge to 10.73 Hz for the widened 2002 bridge. Similarly, the load ratings (interior member single-truck ratings) increase from 2.40 for the 1972 bridge to 6.30 for the widened 2002 bridge.

The above observation resulted in the correlation investigation between the eigenvalues and load ratings. The results of this investigation are presented on Table 15.

Table 15: Eigen Values and Load Ratings Results

Bridge	Load Ratings*		Frequency (Hz)		RF – Diff.**	Mode – Diff.***
	1 Truck	2 Trucks	1 st Mode	2 nd Mode		
1972	2.40	1.39	6.68	6.879	1.01	0.199
2002	6.30	3.73	10.735	11.162	2.57	0.427

**Load Ratings of Interior Member*

***Load Rating difference between single and double trucks.*

****Frequency difference between first and second modes*

The following situations were considered as part of this investigation (Load Rating = RF & Eigen Values = EV);

- 1972 (Single Truck RF & 1st Mode EV) versus 2002 (Single Truck RF & 1st Mode EV)
- 1972 (Double Trucks RF & 1st Mode EV) versus 2002 (Double Trucks RF & 1st Mode EV)
- 1972 (Single Truck RF & 2nd Mode EV) versus 2002 (Single Truck RF & 2nd Mode EV)
- 1972 (Double Trucks RF & 2nd Mode EV) versus 2002 (Double Trucks RF & 2nd Mode EV)
- 1972 [RF – Difference (Truck 1 – Truck 2) & EV – Difference (2nd Mode – 1st Mode)] versus 2002 [RF – Difference (Truck 1 – Truck 2) & EV – Difference (2nd Mode – 1st Mode)]

The results for these analyses are shown in Figure 75 and Figure 76.

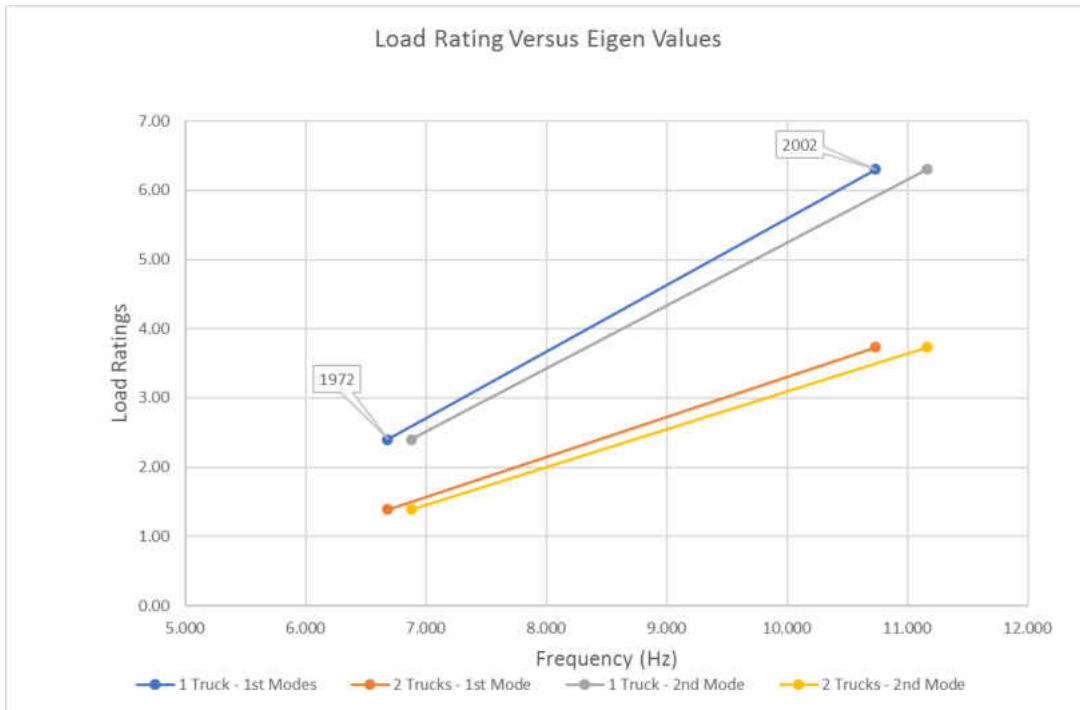


Figure 75: Plot of Load Ratings Versus Eigen Values (1972 and 2002 Bridges)

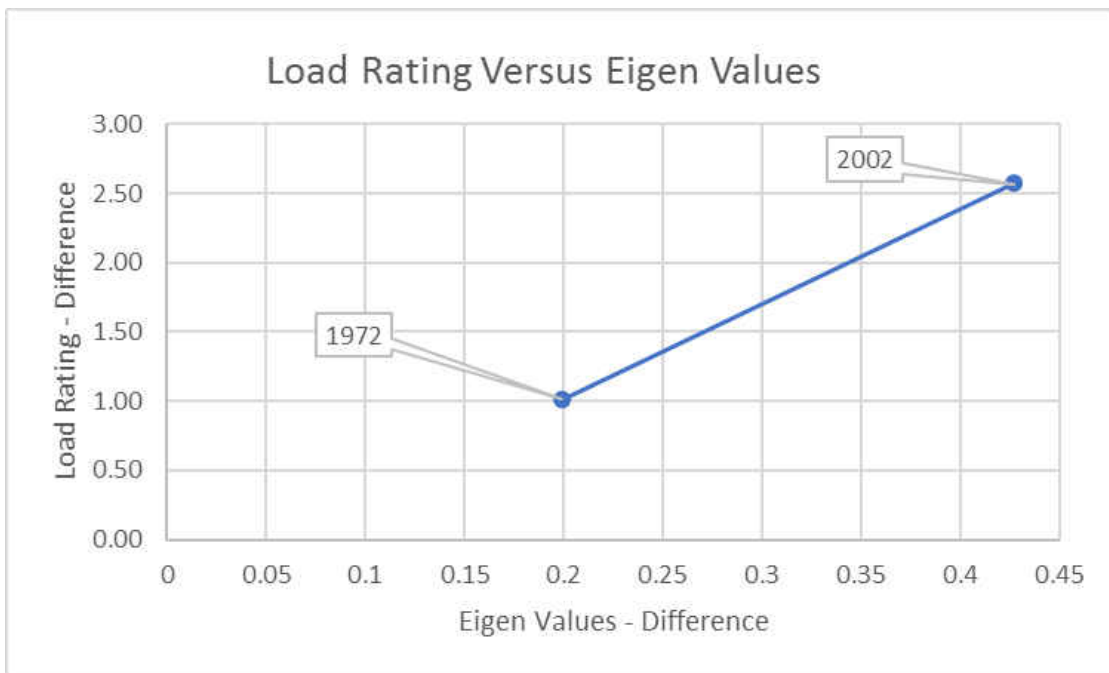


Figure 76: Plot of Load Ratings and Eigen Value Differences (1972 and 2002 Bridges)

Discussion

From the plot for all three structures, it is observed that a much wider spread in the benchmark points, followed by the 1972 and 2002 bridges, respectively. This spread can be attributed to the structures components and stiffness. It should also be noted that the benchmark bridge constitutes Type V girders, while the 1972 and 2002 bridges have Type II & III girders; however, the 2002 widened bridge appears to be much stiffer than the 1972 bridge.

It is seen that there is an increase in eigenvalue and load rating points between the 1972 and 2002 bridges, with the 2002 bridge having the peak points. Consequently, the analysis for only the 1972 and 2002 bridges shows a correlation between the two. It is observed that the essential mode from the eigenvalue analysis and a single-truck load rating dominate all the cases, which also shows that while the first mode is critical to the system (structure), a single-truck load rating is equally as important. (If a system cannot handle a single truck, this can be a critical issue.)

Consequently, the order of investigation importance and criticality (i.e., an investigation of the order of importance) can be drawn from the plot, as follows:

1. 1 truck and 1st mode
2. 1 truck and 2nd mode
3. 2 trucks and 1st mode
4. 2 trucks and 2nd mode

In other words, during an eigenvalue and load-rating investigation, case 1 above should be analyzed first, followed by cases 2, 3 and 4. A simple eigenvalue and load-rating flow chart can be

developed for this exploration, as shown Figure 77.

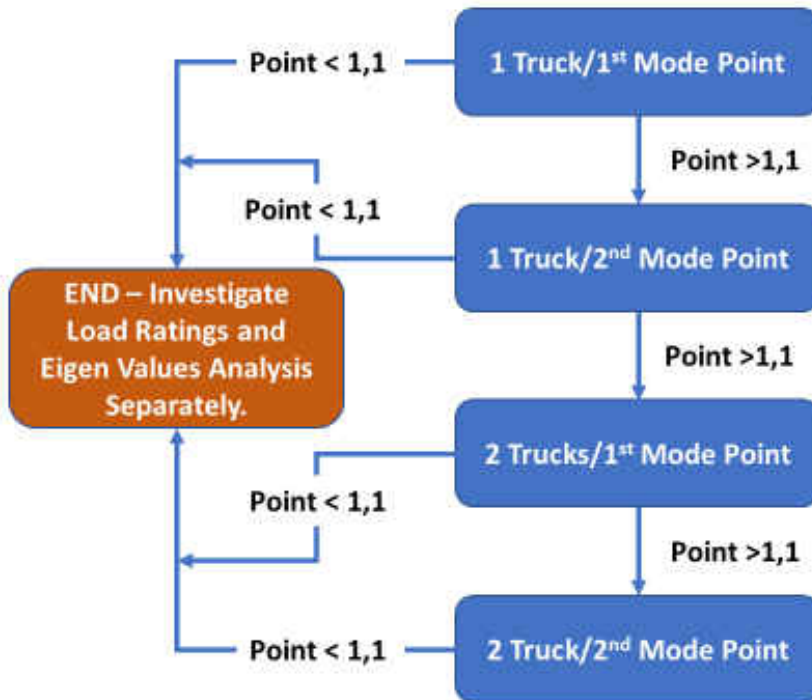


Figure 77: Load Rating & Eigen Value Analysis Flow Chart

CHAPTER TEN: LOAD RATING AND RELIABILITY ANALYSIS (SINGLE SPAN)

Simulations are conducted using a single span system to capture the critical sections within the system and to prevent evaluating and analyzing the whole system which could lead to a complicated system reliability analysis versus a more reliable component reliability analysis.

Introduction

Reliability Index and Probability of Failure

Calibration of the current AASHTO LRFD Bridge Design Specifications (LRFD Code) is based on a reliability analysis procedure [56], [57]. Structural performance is measured in terms of the reliability or probability of failure. In the context, of reliability analysis, failure is defined as the realization of one of several predefined limit states [52]. An alternative method for expressing probability of failure is to use the reliability index, β . For normally distributed random variables R and Q , it can be shown that the probability of failure is related to the reliability index as follows, $P_f = \Phi(-\beta)$. If the random variables are all normally distributed and uncorrelated, then this relationship between β and P_f is exact for a linear limit state function (in the sense that β and P_f are related). Otherwise, this expression provides only an approximate means of relating the probability of failure to the reliability index, β . The reliability index is a common metric used to quantify how close a design code or specification is in achieving its objective [57].

The LRFD Code provisions are formulated such that new structures will have a

consistent and uniform safety level. The basic design formula is:

$$\sum \gamma_i Q_i < \Phi R_n$$

Where;

Q_i = nominal load effect i

γ_i = load factor i

R_n = nominal resistance

Φ = resistance factor

In the LRFD Code calibration, load and resistance are treated as random variables and are described by bias factors (λ) and coefficients of variation (V). Resistance factors, ϕ , are calculated so that the structural reliability is close to the target value $\beta T = 3.5$ [56].

The expression for the reliability index, β , shown here in Figure 78 is used assuming a linear limit state function [57]:

$$\beta := \frac{a_0 + \sum_{i=1}^n (a_i \cdot \mu_{X_i})}{\sqrt{\sum_{i=1}^n (a_i \cdot \sigma_{X_i})^2}}$$

for the linear limit state function of the form,

$$g(X_1, X_2, \dots, X_n) = a_0 + a_1 \cdot X_1 + a_2 \cdot X_2 + \dots + a_n \cdot X_n$$

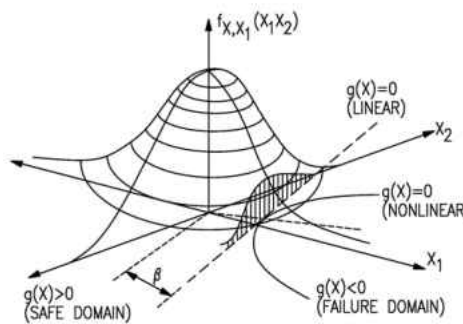
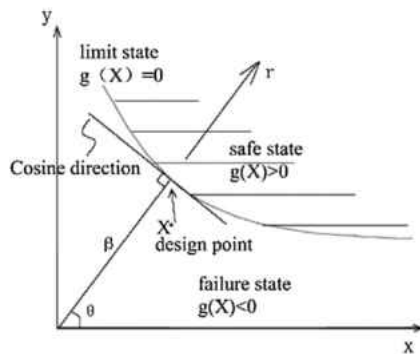


Figure 78: Reliability Index Equation

This expression must be adapted for the current study, considering load effects and resistance in bending. The limit state function is developed in terms of resistance and load effects for the AASHTO Strength I limit state:

$$g(M_{Res}, M_{DL}, M_{LL}) = M_{Res} - M_{DL} - M_{LL}$$

where;

M_{Res} = nominal moment resistance (M_n)

M_{DL} = dead load effect

M_{LL} = live load effect (M_{LL_IM}) impact included

The corresponding reliability index is:

$$\beta = \frac{\mu_R - \mu_{DL} - \mu_{LL}}{\sqrt{\sigma_R^2 + \sigma_{DL}^2 + \sigma_{LL}^2}} \quad (1)$$

Where μ and σ are the means and standard deviations for the resistance, dead load, and live load, respectively.

The limit-state functions are valid if the uncertainties (structure strength/capacity or loads etc.) are incorporated in the failure probability of the structure. Statistical parameters for load and resistance tend to be given in terms of load effects [50], and are available for the present study. A full set of reliability analysis calculations can be found in Appendix F, Load Rating and Reliability Analyses.

For the nonlinear limit-state functions, an approximate answer is obtained by linearizing the nonlinear function using a Taylor series expansion [50]. The result is the equation shown below:

$$g(X_1, X_2, \dots, X_n) \approx g(\mu x_1^*, \mu x_2^*, \dots, \mu x_n^*) + \sum_{i=1}^n (X_i - \mu x_i^*) \frac{\partial g}{\partial X_i} \Big|_{\text{evaluated at } (x_1^*, x_2^*, \dots, x_n^*)}$$

An approximate solution expression for the reliability index, β , is shown here [57];

$$\beta = \frac{g(\mu x_1, \mu x_2, \dots, \mu x_n)}{\sqrt{\sum_{i=1}^n (a_i \sigma_{x_i})^2}} \quad (2)$$

Where;

$$a_i = \frac{\partial g}{\partial X_i} \Big|_{\text{evaluated at mean values}}$$

The reliability index defined in the above equation is called a first-order, second – moment, mean value reliability index where the derivation attributes are as follows;

first order: using first – order terms in the Taylor series expansion;

second moment: only means and variances are needed (mean value because the Taylor series expansion is about the mean values).

A full set of reliability analysis calculations (nonlinear) can be found in Appendix F, Load Rating and Reliability Analyses.

Simulations, Load Rating and Reliability

Once adequate reliability is demonstrated for the resistance calculations and FEM outputs, loading simulations are performed with the two parametric FEMs developed and described in previous chapters. The critical-load effects for dead load and live load were extracted from the

finite element analysis results at critical locations.

Load ratings following the AASHTO LRFR (AASHTO 2010) methodology were calculated, and a reliability analysis was performed. The reliability index, β , was calculated and, assuming normal distribution of random variables, the equivalent probability of failure, P_f was found.

For the reliability analysis, a single span of the bridge, which contains the critical members was examined. From the test cases and recommendations by the author Nowak, the following assumptions were made for the reliability analysis:

- Targeted members only within the bridge single-span system
- Nominal loads to be used (dead, wearing surface and live loads).

Table 16 shows the bias and variation constants used for the analysis in this research taken from Nowak and Collins [50], statistical parameters for load and resistance tables.

Table 16: Statistical Parameters for Load and Resistance

Constants*	
Bias	
Bias Factor for Resistance (λ_R)	1.05
Bias Factor for Live Load (λ_{LL})	1
Bias Factor for Dead Load (λ_{DC})	1.05
Variation	
Coefficient of Variation for Resistance (C_R)	0.075
Coefficient of Variation for Live Load (C_{LL})	0.18
Coefficient of Variation for Dead Load (C_{DC})	0.1

Benchmark

A hand calculation using MathCAD Prime 3.0 software was used to estimate the load ratings, reliability index, and probability of failure for a single and multiple HL-93 trucks. The results of the calculations are presented in Appendix F and on Table 17.

Table 17: Hand Calculation Load Rating and Reliability Results for Single and Multiple HL93

	Single Truck			Multi Trucks		
Case	RF	β	P_F	RF	β	P_F
INT.	1.74	4.89	5.04×10^{-7}	1.23	3.34	4.19×10^{-4}

Similarly, the single-span 1972 bridge was modeled, and an analysis of the load ratings, reliability indices, and probability of failure was performed on the critical interior member. Figure 79 shows the lane assignments, models (and their respective load ratings), reliability indices, and probability of failures for single and multiple HL-93 truck loadings.

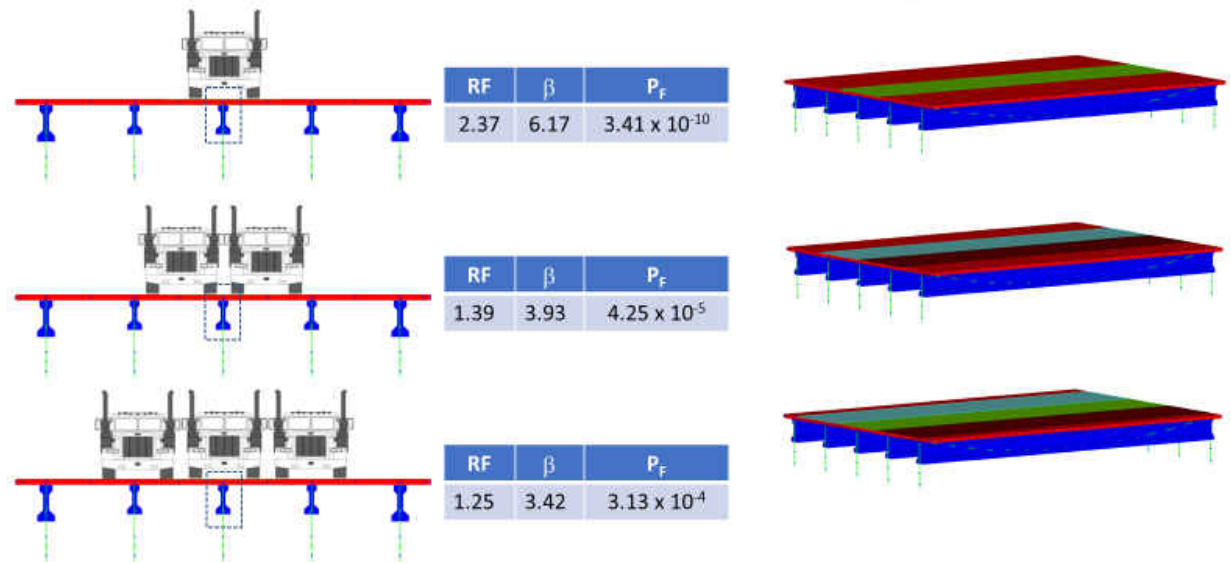


Figure 79: 1972 Single Span Bridge for Load Ratings and Reliability Analysis

Discussion

From the above results, a comparison of the hand calculations and FEM results for the load ratings and reliability analysis indices were established for both single and multiple HL-93 trucks. Figure 80 shows a comparison of the results from both the hand calculations and the FEM of the single span system.

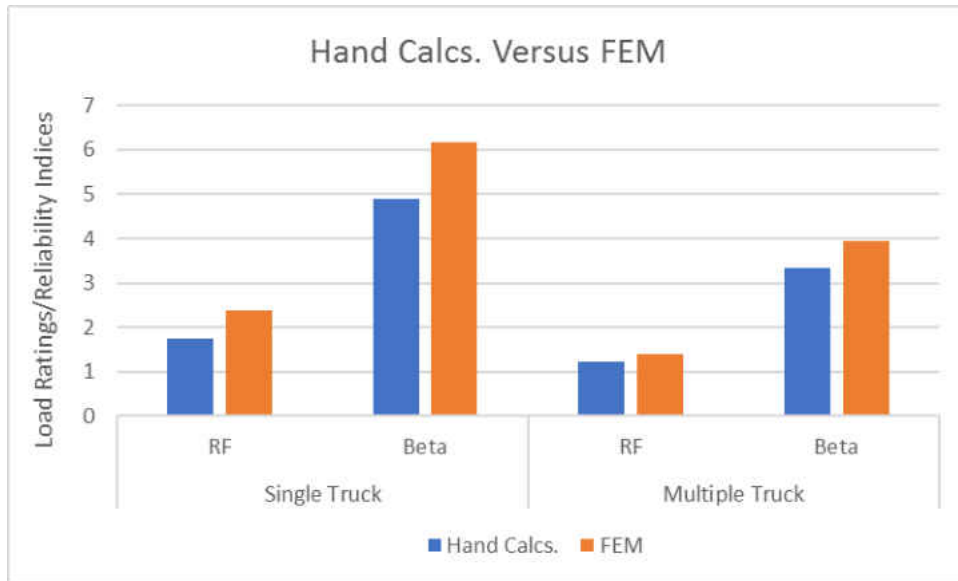


Figure 80: Hand Calculations and FEM Comparison

The difference between the two analyses were within the range of 0.16 (RF Multiple Trucks: Hand Calculations = 1.23 and FEM = 1.39) and 0.63 (RF Single Truck: Hand Calculations = 1.74 and FEM = 2.37). The difference between the two analyses, although close enough to justify use of the FEM for further analysis, could stem from a complete bridge system used in the FEM, versus the component used in the hand calculations, with an estimated effective length of the contribution deck weight on the component girder.

Sensitivity – Load Rating & Reliability Analysis

Introduction

A sensitivity analysis was performed on single span of the 2002 widened bridge by

incorporating aging and materials property losses. Three cases were examined for the sensitivity analysis, as follows:

- Case I: system with no losses.
- Case II: long-term losses (30 years or more), including time-dependent properties such as creep, shrinkage, tendon relaxation and Young's Modulus (E) of all the members.
- Case III: differential losses for new and old girders (0-29 years and 30 + years, respectively), including time-dependent properties such as creep, shrinkage, tendon relaxation and Young's Modulus (E) for selected members (i.e., original members from the 1972 bridge which remain in the widened 2002 bridge).

Results

Results for Case I of the sensitivity analysis, with no losses in material properties, are shown in Figure 81, which includes the load ratings, reliability index, and probability of failure. The analysis focuses on a member within the system that was part of the original 1972 bridge, and which remained in the 2002 bridge widening.

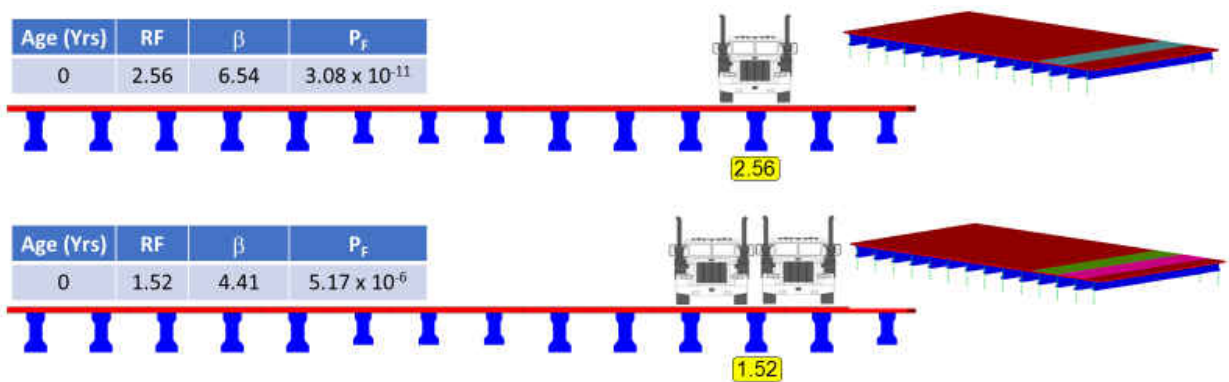


Figure 81: Case I – Sensitivity Analysis (No Losses)

For Cases II & III (with material property losses), an elastic modulus time-dependent analysis and a prestress loss analysis were performed using the “Approximate Lump Sum of Time-Dependent Losses” approach (LRFD Article 5.9.5.3). This approach for standard precast, pretensioned members (subject to normal loading and environmental conditions) and pretensioned members (with low relaxation strands) considers the long-term prestress loss due to creep of concrete, shrinkage of concrete, and relaxation of steel. A detailed analysis of both modulus of elasticity and prestress losses is provided in Appendix D.

Following the analysis and time-dependent material property, the results for both cases are illustrated in Figure 82 and Figure 83, respectively.

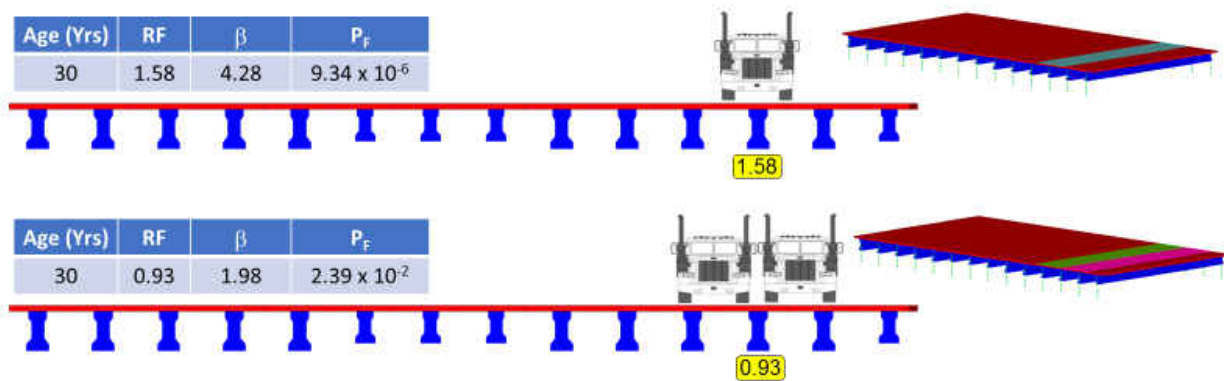


Figure 82: Case II – Sensitivity Analysis (Losses – All Members)

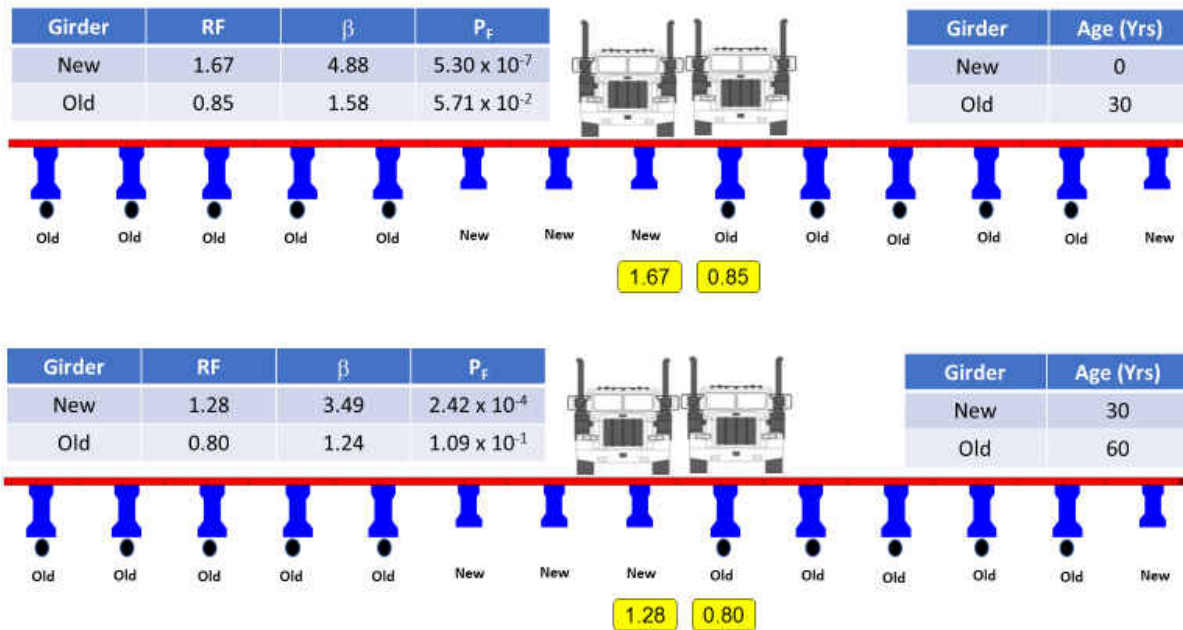


Figure 83: Case III: Sensitivity Analysis (Losses – Selected Members)

Discussion

The goal to examine these three cases is to establish a long-term correlation among members in a widened bridge, since there is a combination of both old and new components. The results can be broken into two main components:

1. aging rating consistency and
2. load-carrying capacity consistency.

Cases I and II reveal that, with everything remaining the same, the system can carry its adequate loads, as is expected of a new bridge; and in 30 years, the bridge shows the same targeted member carrying its loads (HL-93). However, the decrease and the percentage difference in rating should be noted. Table 19 shows that as the system ages, the loading capacity is reduced. Also, the

variation in capacity between Case I and Case II (with respect to single and double truck loadings) also gets closer as the bridges age. As an example, there was a 1.04 rating difference between the targeted member rating of one and two trucks, but this gap is reduced 30 years later to 0.65. As shown in Table 18, the aging difference for one truck at 0 years, versus one truck for 30 years, is 0.98; and the aging difference for two trucks at 0 years, versus two trucks at 30 years, is 0.59.

Table 18: Case I & II Load – Rating Summary Chart

Case	Age (Yrs)	# Truck	RF	Load Diff.	Aging Diff.	
I	0	1	2.56	1.04	1 Truck (0 years)	0.98
		2	1.52		1 Truck (30 years)	
II	30	1	1.58	0.65	2 Trucks (0 years)	0.59
		2	0.93		2 Truck (30 years)	

In Case III, where there is a combination of old and new members (as shown in Figure 89 previously), a similar pattern is observed. The new member has a margin of 0.39, while the old member has a margin of 0.05. This is an indication that, at some point, the ratings will be approximately equal for both old and new members. Table 19 shows the correlation between the old and new members in the system.

Table 19: Case III Load Rating Summary Chart

Girder	Age (Yrs.)	RF	Aging Diff.
New	0	1.67	0.39
New	30	1.28	
Old	30	0.85	0.05
Old	60	0.80	

CHAPTER ELEVEN: NONLINEAR SIMULATION & RELIABILITY ANALYSIS

Introduction

A nonlinear analysis is very critical to this research, as the linear analysis alone does not reveal the ultimate capacities of the components within the system. Consequently, the Nonlinear Analysis Program (NAP) [37], described earlier in chapter three, is employed in this research.

The nonlinear analysis simulation and sensitivity analysis will focus on the critical members within the systems. The nonlinear analysis tool allows for nonlinear loading, varying boundary conditions and material characteristic variations. These in turn imply that NAP is adequate for both material and loading sensitivity analysis.

Model

The initial stage of the nonlinear modeling is to identify and model the critical component (i.e., section) of the bridge that will be a close replicate of the members. Since the span lengths of both the 1972 and 2002 bridges did not change, the critical section identified will be the same in both cases. In this case the section is an interior member within the long span of the bridge, as seen in previous linear analyses. Therefore, the initial modeling process begins with the boundary conditions, elements, and connectivity considerations.

A cross-section of the critical component/section is shown in Figure 90. The effective width of the deck carried by the section is first estimated before constructing the composite cross-section. Appendix F provides a detailed computation for the effective width estimate.

The model is discretized to have a replicate load effect similar to the actual member by defining deck/girder elements and prestress truss elements. These two components are connected by rigid elements to form the composite beam illustrated in Figure 84, which also gives a detailed description of all the components, elements, nodes, cross section and applied loading cases.

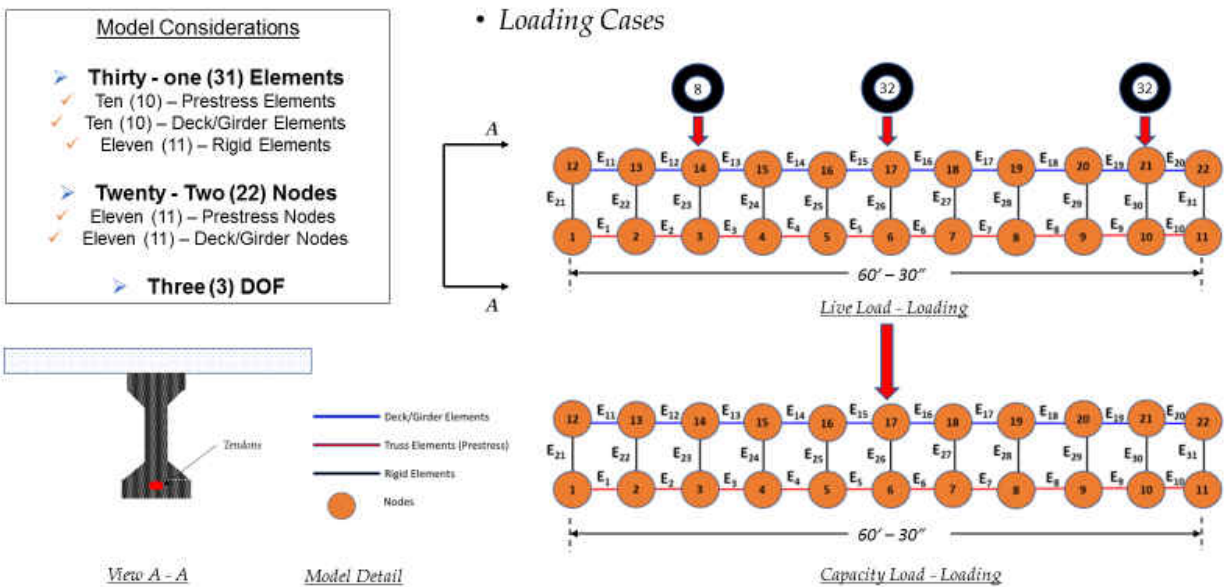


Figure 84: Detailed Schematics of Nonlinear Model

The modeling strategy includes using 1D macro elements that are based on the differential equations for the component resultant forces. Due to the discretization of the elements/nodes, the displacement formulation is adopted. Based on the assumption that plane sections remain plane,

the prestress effect cannot be fully modeled; hence the need to go with the rigid links to offset the physical location of the tendons and (potentially) allow them to move relative to the cross-sectional strains. Also, it should be mentioned that debonding of the strands (slipping) was not considered.

Benchmark

A hand calculated analysis was used as a benchmark verification for the NAP model. Similar geometry and material properties were considered for close approximations and comparisons. Details of the hand calculations and the results from the NAP model used for the analysis are presented in Appendix F. The unfactored load ratings for both the hand calculations and NAP are shown on Table 20. The results between the hand calculations and the NAP model were close enough for the NAP model to be used for further analysis and investigation.

Table 20: Benchmark Results and Comparison

Case	Unfactored Load Rating
Hand Calculations	2.381
NAP	2.584

Analysis

The model in NAP was set – up to have two loading cases as shown in Figure 84.

- Case I: Live Load carrying load points with three nodes for the axle of the HL93 truck (8kips, 32kips, 32kips).

- Case II: Capacity single load point node.

The analysis will also include the following test and sensitivity analysis study with similar boundary conditions (Pin – Pin connections);

1. Load Rating and Reliability Analysis – Linear Limit State Function
2. Load Rating, Reliability and Sensitivity Analysis – Nonlinear Limit State Function

Loading cases I & II were first performed to attain the live load moments due to a single HL39 truck and the capacity of the beam model. Results from this analysis will be used for the Linear Limit State Function reliability analysis and load ratings. Consequently, a sensitivity analysis is performed on the following random variables to attain variation for the nonlinear limit state analysis. The random variables identified in this case are the area of prestress steel (A_{ps}), prestressing tendon (f_{ps}) and the applied load effect (Q). The detailed variability analysis is presented in Appendix F.

A variability analysis was also performed to establish the correlation among the random variables since the normal random variable is the most important distribution in structural reliability theory. The general concept follows the analogy that if for example D (demand) and R (resistance or capacity) are normally distributed with means μ_D and μ_R with standard deviations σ_D and σ_R respectively, their limit state function g will be normally distributed for a linear limit state function. The variability plots showing the normal distribution curves for the linear, nonlinear and limit state functions are presented in Appendix F.

A virtual loading test is also performed by increasing the axle loads of the HL-93 truck by a factor of 0.5, as shown in Figure 85, and load-rating the corresponding cases. Three load-rating scenarios were performed to investigate the correlation and capacity of the nonlinear model, per

the AASHTO and FEM live-load distribution factors (Table 21 – distribution factors used for single and multiple lanes) and the un-factored load as obtained directly from the capacity analysis.

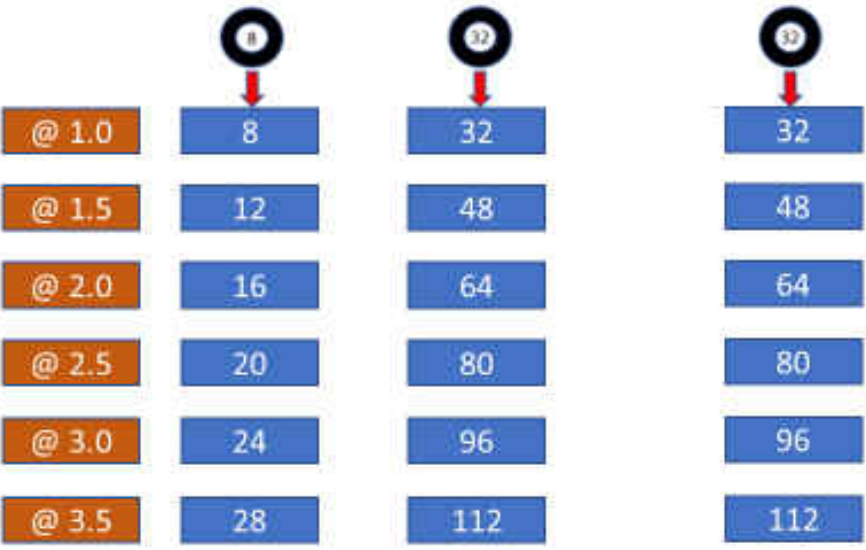


Figure 85: Virtual Loading Schematics

Table 21: Single and Multiple Lanes Distribution Factors (AASHTO/FEM)

AASHTO (Single)	0.555
AASHTO (Multi.)	0.768
FEM (Single)	0.546
FEM (Multi.)	0.716

Results

The results from NAP used for both linear and nonlinear analysis are shown in Table 22 and Table 23 respectively. Table 22 shows the nominal values used for the linear state function analysis and Table 23 shows the variation in the random variables used for the nonlinear limit state function analysis. For the variation in the dead load analysis for both the linear and

nonlinear limit state functions, the self-weight for the system was used for the capacity analysis and the slab thickness varied for the variation. Detailed dead load (self-weight) analysis is presented in the “Nonlinear Load Rating & Reliability Analysis” MathCAD File in Appendix F.

Table 22: Nominal Parameters Load Analysis Results

NAP - Run 1	Nominal Values	Live Load (1)	Capacity (2)
Area (Aps)	2.45	10890	28940
Prestress (fps)	250	10890	28940
Live Load (Q)	$8 + 32 + 32 = 72$	10890	28940

Table 23: Variable Parameters Load Analysis Results

NAP - Run 2	Variable Area	Live Load (1)	Capacity (2)	NAP - Run 3	Variable Area	Live Load (1)	Capacity (2)
Area (Aps)	2.44	10910	28870	Area (Aps)	2.46	10860	28760
Prestress (fps)	250	10910	28870	Prestress (fps)	250	10860	28760
Live Load (Q)	$8 + 32 + 32 = 72$	10910	28870	Live Load (Q)	$8 + 32 + 32 = 72$	10860	28760
NAP - Run 4	Variable Prestress	Live Load (1)	Capacity (2)	NAP - Run 5	Variable Prestress	Live Load (1)	Capacity (2)
Area (Aps)	2.45	11070	28680	Area (Aps)	2.45	10700	29070
Prestress (fps)	240	11070	28680	Prestress (fps)	260	10700	29070
Live Load (Q)	$8 + 32 + 32 = 72$	11070	28680	Live Load (Q)	$8 + 32 + 32 = 72$	10700	29070
NAP - Run 6	Variable Live Load	Live Load (1)	Capacity (2)	NAP - Run 7	Variable Live Load	Live Load (1)	Capacity (2)
Area (Aps)	2.45	10850	28940	Area (Aps)	2.45	10920	28940
Prestress (fps)	250	10850	28940	Prestress (fps)	250	10920	28940
Live Load (Q)	$7.9 + 31.9 + 31.9 = 71.7$	10850	28940	Live Load (Q)	$8.1 + 32.1 + 32.1 = 72.3$	10920	28940

The reliability indices for both the linear and nonlinear limit state functions are shown in Table 24. The details used for this analysis including bias and coefficient variation assumptions are presented in Appendix F under the “Linear Load Rating & Reliability Analysis” and “Nonlinear Load Rating & Reliability Analysis” MathCAD spreadsheets respectively.

Table 24: Linear and Nonlinear Limit State Function Reliability Indices

Case	Reliability Index (β)
Linear Limit State Function	6.202
Nonlinear Limit State Function	4.368

It should be noted that the result from the hand calculated linear analysis showed a rating of 5.696 compared to 6.202 from the NAP model which are also close.

The results for the virtual load test is also presented here in Table 25 and Figure 86 with the detailed computation also presented in Appendix F.

Table 25: Virtual Load Rating Results

Load Factors	Axle -1	Axle -2	Axle -3	Moment (k-in)	RF	RF - AASHTO	RF - FEM
1.0	8	32	32	10700	2.62	4.72	4.80
1.5	12	48	48	14830	1.89	2.46	2.64
2.0	16	64	64	18920	1.48	1.93	2.07
2.5	20	80	80	22950	1.22	1.59	1.71
3.0	24	96	96	27060	1.04	1.35	1.45
3.5	28	112	112	FAIL	---	---	---

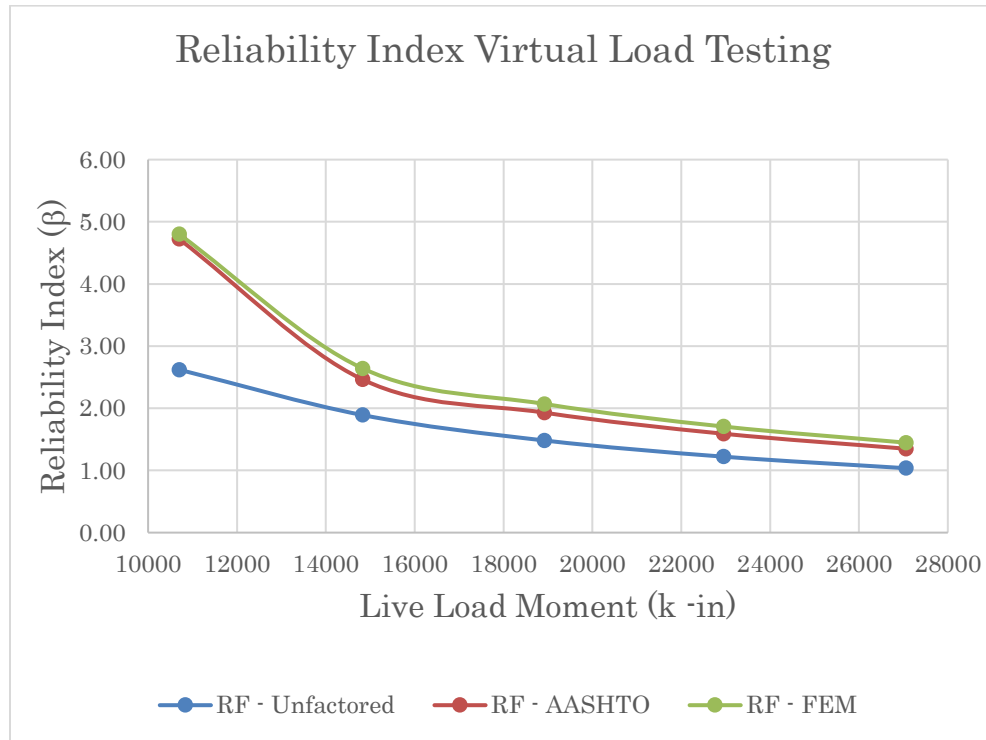


Figure 86: Virtual Load Testing Plots

Discussion

The nonlinear analysis performed on the critical section investigates the capacity of the section beyond the linear state, and shows the variation between its linear and nonlinear state limitations. This analysis clearly shows (by capacity, load ratings and reliability analysis) that the identified critical component/section within the system is far from critical. Although the reliability index during the linear limit state analysis was slightly higher 6.202 based on the assumption that the random variables are all normally distributed and uncorrelated, the nonlinear limit state function which considers the variabilities in the random variables showed only a difference of 1.834 in

reliability index (4.368). It should be noted that the linear limit state function does not use the distribution information about the variable and the limit state function $g()$ is linearized at the mean values of the X_i variables. If $g()$ is non-linear, neglecting of higher order term in Taylor series expansion introduces significant error in the calculation of reliability index (errors are not solely attributed to the first – order expansion). However, the nonlinear limit state function can obtain an approximate answer by linearizing the nonlinear function using a Taylor series expansion (about the mean values).

The modeled section shows results greater than its linear capacity as shown in the virtual loading analysis with a capacity loading of three times the truck live – load capacity. The incremental loads in NAP to determine the section’s behavior under both normal and anticipated peak load conditions to identify the maximum operating capacity showed rating factors ranging between 4.80 to 1.45 before failure.

CONCLUSIONS AND RECOMMENDATIONS

Highlights

- Dynamic performance of a bridge before and after widening.
- Re-distribution of live loads of a bridge before and after widening.
- Linear capacity assessment through load ratings of a bridge before and after widening.
- Reliability assessment of a bridge before and after widening.
- Nonlinear capacity assessment through load ratings of a bridge before and after widening.

Details

Detailed finite element models (linear and nonlinear) were developed to represent the original 1972 single-span bridge and the widened 2002 bridge, a four-span continuous structure. Four-span continuous models were used for the linear analysis investigation for the dynamic behaviors of the modeled bridge structures, and their respective global and local behaviors were observed. Live-load distribution factor and load-rating analyses were also conducted, using several moving-load combinations and standard trucks (HS-20 and HL-93) with the linear model. The linear and nonlinear single-span models were used to investigate critical components within the system, and load-rating and reliability calculations were performed.

It was important to develop procedures for verification and validation of the analysis. Benchmark studies were conducted to validate finite-element models with well-established

solutions. Critical modeling features were incorporated in a few simpler benchmark studies before the single-span 1972 and full four-span widened 2002 models were developed. It is encouraging that the FEM-predicted load effects for the modeled bridge were close to the textbook results. This verifies the model, software and accompanying analysis in a qualitative sense. A comprehensive test plan (or monitoring program) to capture frequencies, mode shapes, and deflections is recommended for objective validation of the FEM. This can lead to model calibration using experimental data and an objective understanding of the measured structural behavior.

The dynamic behavior was evaluated with respect to continuity conditions. Eigenvalue analysis in CSiBridge gives natural frequencies in the range of 5.18 Hz to 12.28 Hz, 6.68 Hz to 12.32 Hz and 10.74 Hz to 12.88 Hz for the first 10 modes of the benchmark, 1972 and 2002 bridge nominal models, respectively. The mode shapes of the bridges were categorized in terms of pure modal behaviors, including lateral beam bending, vertical beam bending, and torsion. The boundary condition has significant effect on the longitudinal modes, and dramatically increases the energy required to achieve the first longitudinal mode. The eigenvalue analysis is the first indication of the stiffness and strength increase in a widened bridge structure.

Live-load distribution factors, which determine the maximum number of loaded lanes that an individual girder of the superstructure will be expected to carry, was evaluated next. This investigation was important to this research, not only to verify any conservativeness, but also to understand the distributions between the original and widened bridges. The controlling moment live-load distribution factors (LLDF) for the 1972 and 2002 bridges were 0.716 and 0.592, respectively. These factors were based on the FEM, using the HL-93 truck. The controlling moment LLDF (using the AASHTO LRFD code) is 0.877 for both bridges. While these results

indicate the decrease in distribution factors for widened bridges, they also show the conservativeness in the code. Similarly, the HS-20 trucks showed controlling moment LLDF of 0.715 and 0.651 for the 1972 and 2002 bridges, respectively, and FEM of 0.841 for both bridges, using the AASHTO LFD code. The load ratings which measure the bridge live-load capacity were also evaluated. The HS-20 and HL-93 trucks used for the LLDF analysis were also employed for the full 1972 Bridge model. The 1972 bridge model showed with aging showed less than acceptable load rating especially under HL93 truck loading, which was not the design load for the original bridge. However, the ratings for the widened 2002 bridge model increased, which shows the increased load carrying capacity of the widened bridge.

For a better understanding of the load rating and reliability analysis correlation, a single-span model was developed for both the 1972 and 2002 bridges. These models are the longer spans within the structure and contain the critical component (interior beam). A linear FEM was developed for both bridges, and a nonlinear model to replicate the critical member was created. The 1972 and 2002 bridges rated at 2.37 and 2.56, respectively, for a single truck, and had reliability indices of 6.17 and 6.54, respectively. For multiple trucks, their respective ratings and reliability indices were $RF = 1.39$, $\beta = 3.93$ (1972 bridge) and $RF = 1.52$, $\beta = 4.41$ (2002 bridge). Since the widened 2002 bridge has a combination of old and new members, a sensitivity (aging) analysis was performed on the model. The model was first investigated assuming a 30-year aging for all the members in order to establish a benchmark. The investigated material properties used for the aging process include the modulus of elasticity (E_c) and prestress losses. The rating and reliability indices for a targeted member were $RF = 1.58$ and $\beta = 4.28$ (single truck) and $RF = 0.93$ and $\beta = 1.98$ (multiple trucks). With these benchmark values, the 2002 bridge model (with the

combination of both old and new members) was investigated.

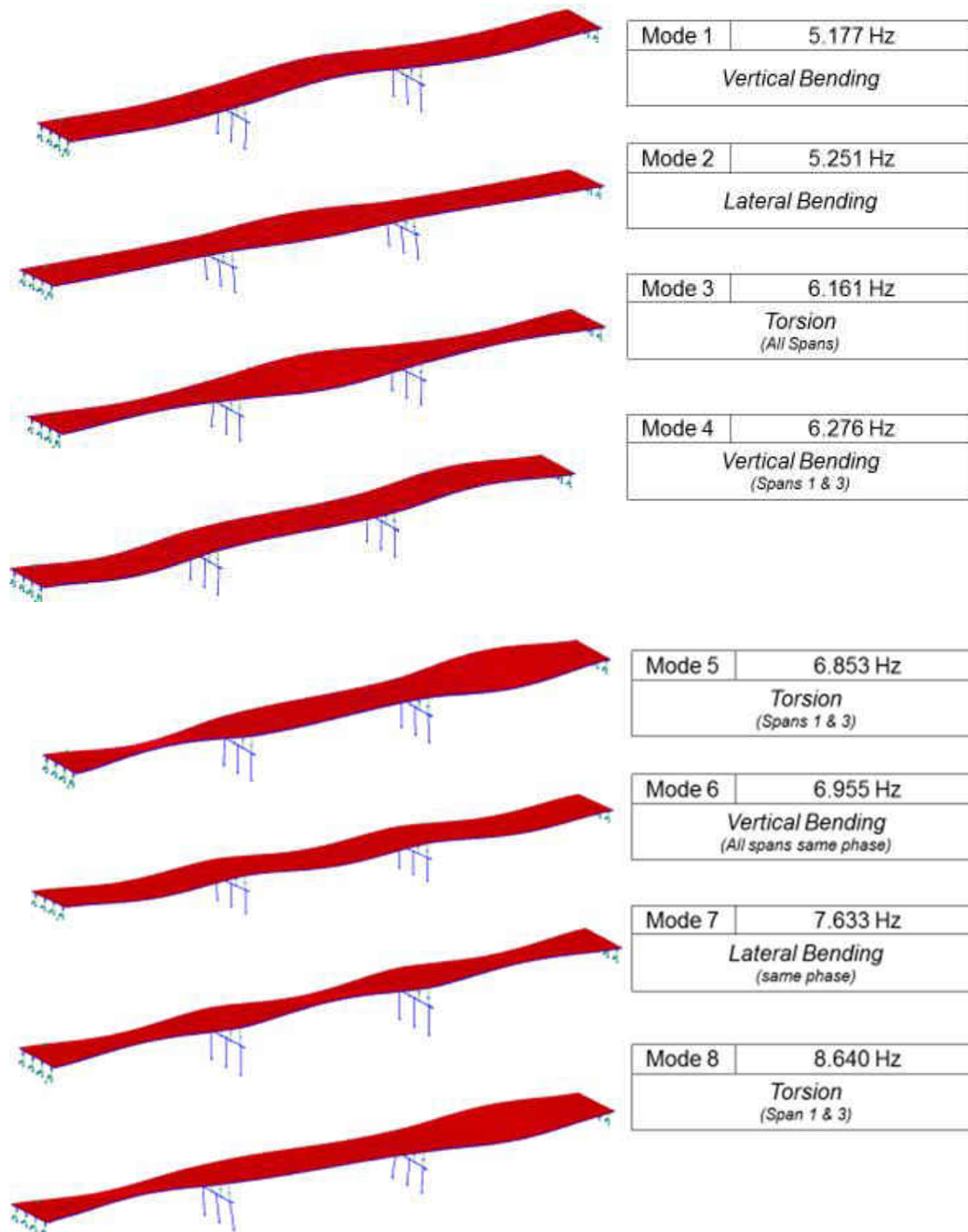
The first case with the new member at zero years and the old member at 30 years showed load ratings and reliability indices as $RF = 1.67$ and $\beta = 4.88$ (new) and $RF = 0.85$ and $\beta = 1.58$ (old). The second case with the new member at 30 years and the old member at 60 years showed load ratings and reliability indices as $RF = 1.28$ and $\beta = 3.49$ (new) and $RF = 0.80$ and $\beta = 1.24$ (old). The results show the correlation of both old and new members in the widened bridge. For the nonlinear model, the linear limit state function produced reliability indices of $\beta = 6.202$ and $\beta = 4.368$ for the nonlinear limit state function with similar boundary conditions.

Finally, a virtual load-test analysis to determine the ultimate capacity of the girders using the nonlinear model was performed by means of incrementally increasing the applied axle loads. The ratings showed a 3.5 times factor of the axle loads ($8 \times 3.5 = 28$ kips, $32 \times 3.5 = 112$ kips, and $32 \times 3.5 = 112$ kips) for load ratings greater than 1. The results for this loading were $RF = 1.04$ (no LLDF), $RF = 1.35$ (AASHTO LLDF) and $RF = 1.45$ (FEM LLDF).

In conclusion, the following characteristics were immediately observed for a widened bridge: increased overall capacity, lower distribution factors, and higher ratings and reliability indices. Additionally, it was also observed that a member within the system may be highly underestimated if analyzed linearly. The information generated from these analyses can be considered for better understanding the load rating improvement for widened bridges.

APPENDIX A: FREQUENCIES AND MODE SHAPES

Benchmark Bridge Modes



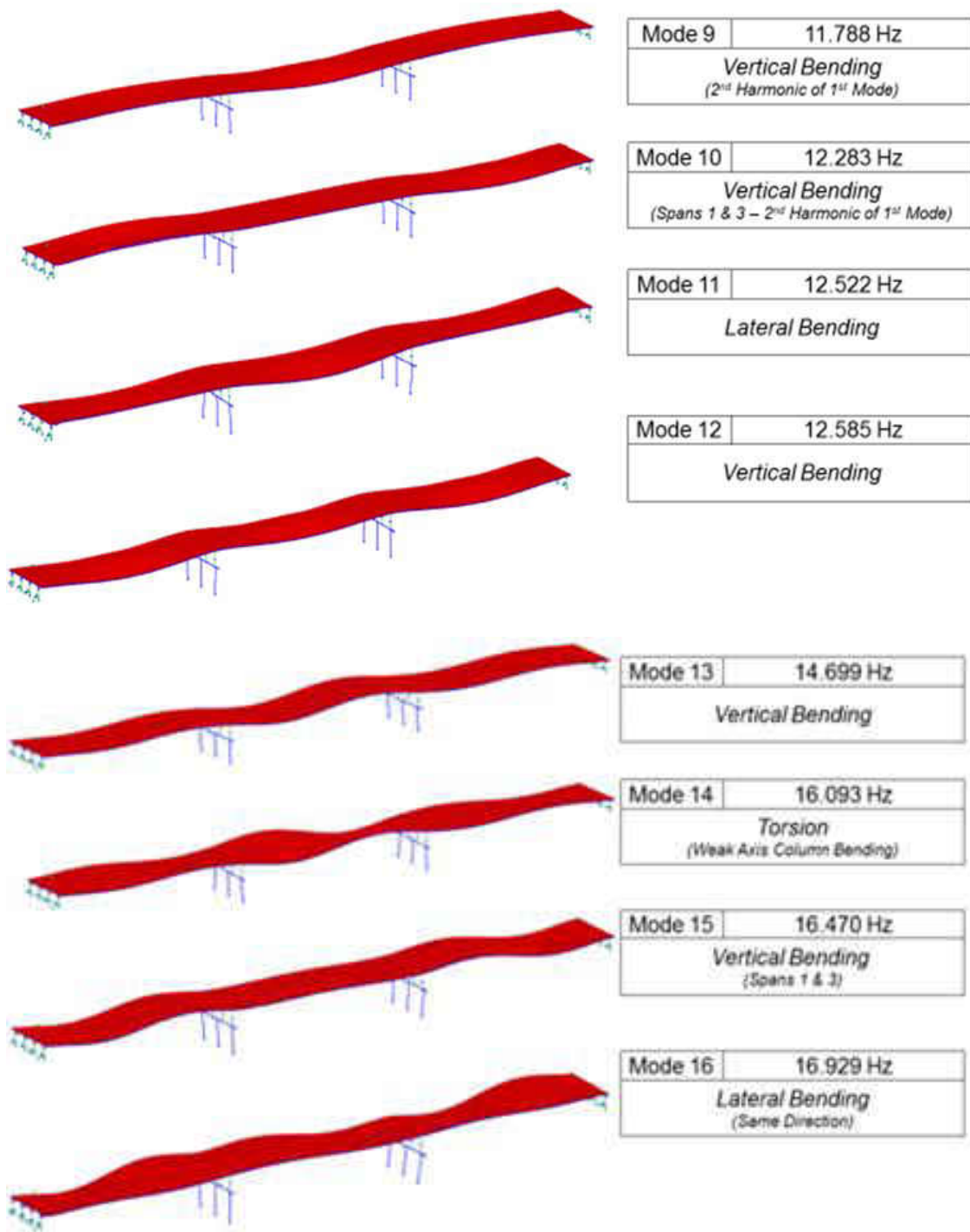
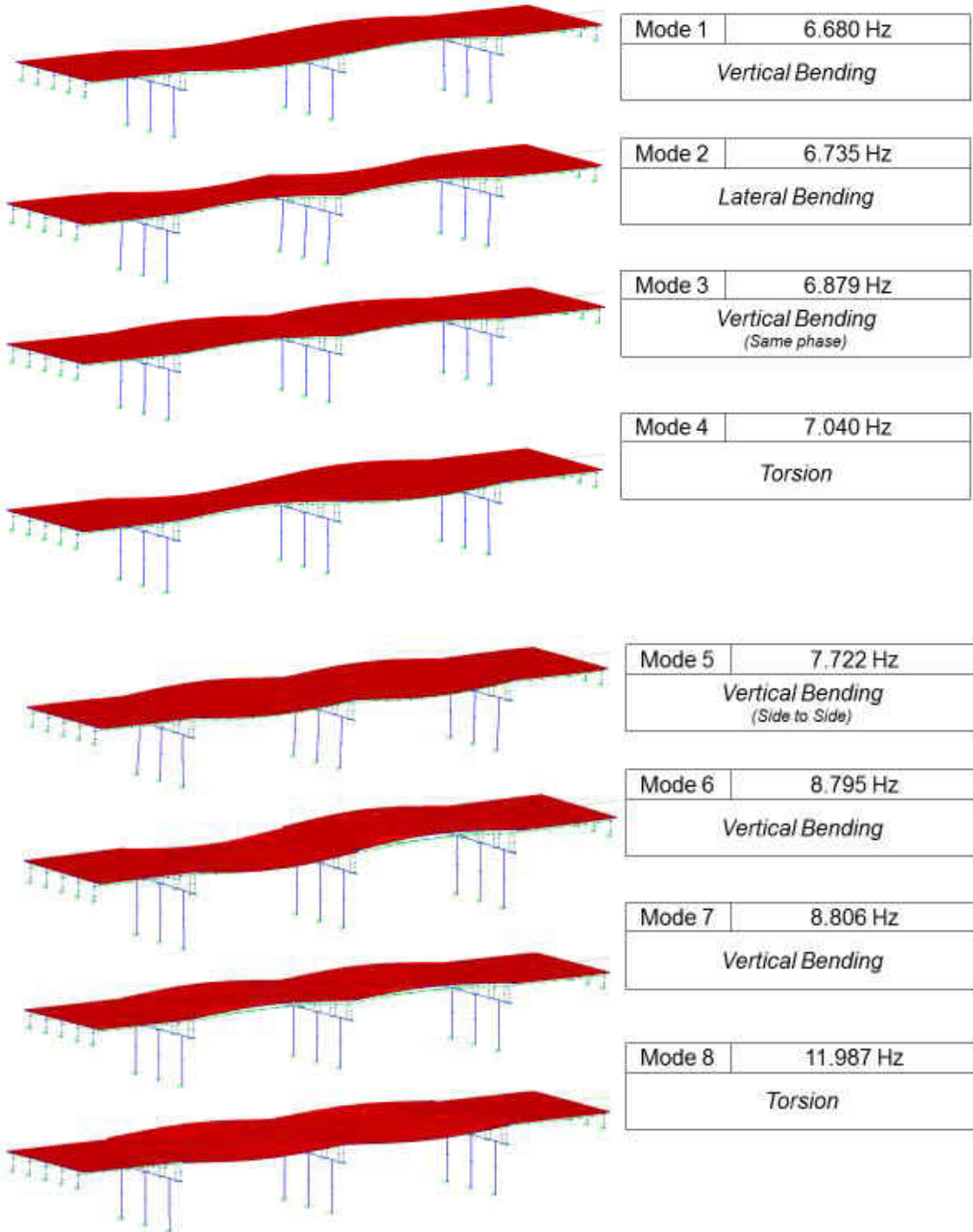


Figure 87: Benchmark Modes

1972 Bridge Modes



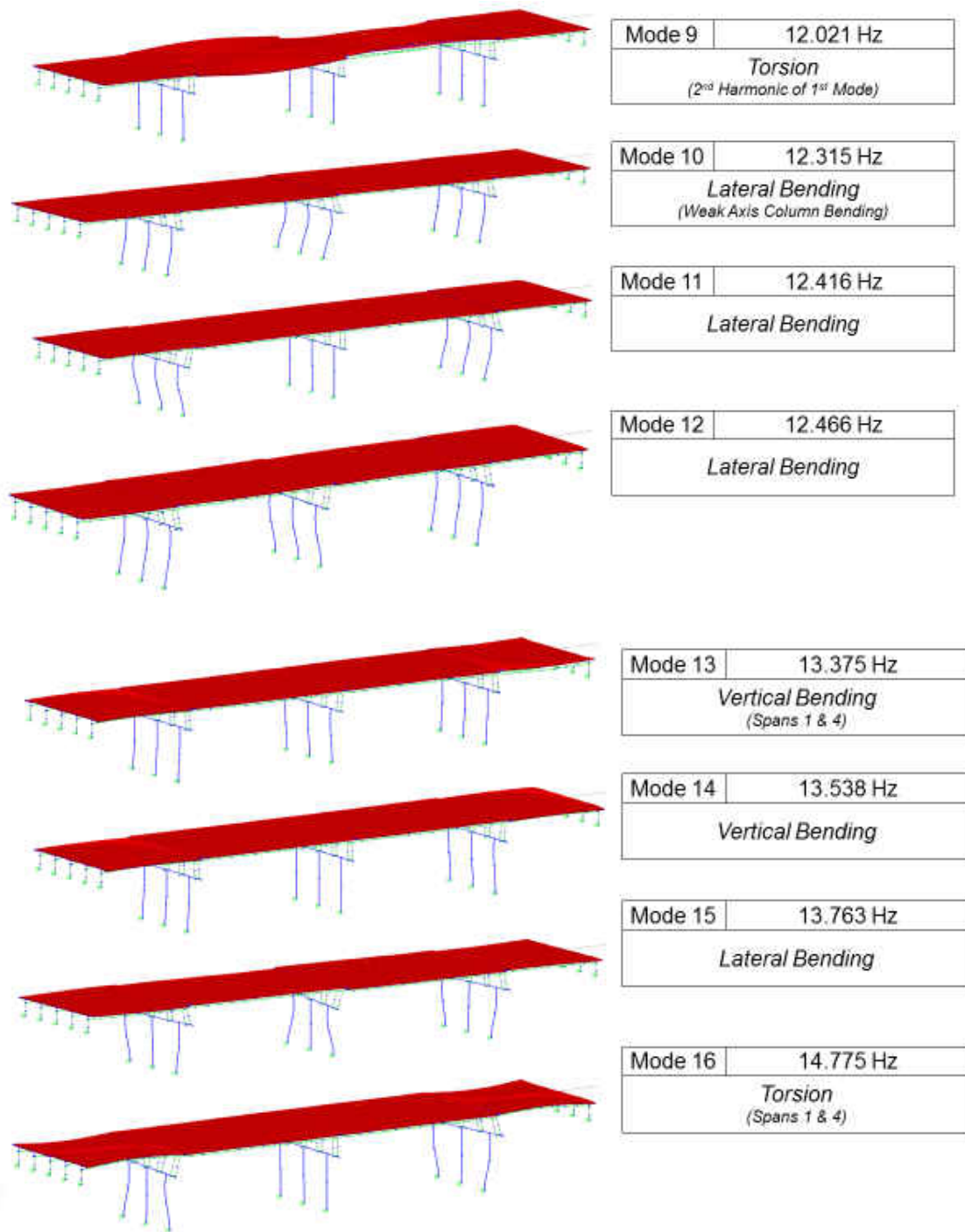
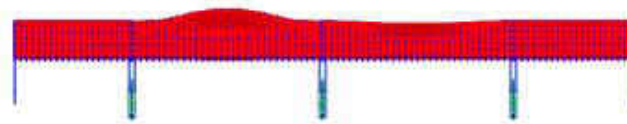
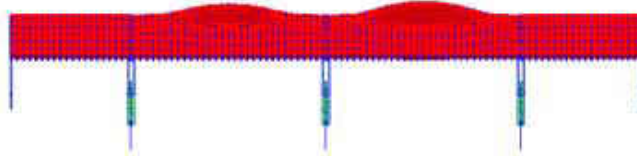


Figure 88: 1972 Bridge Modes

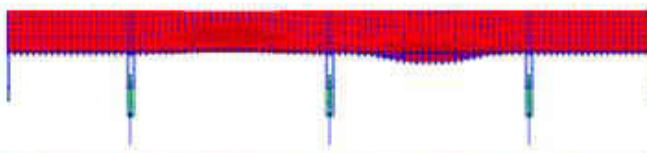
2002 Bridge Modes



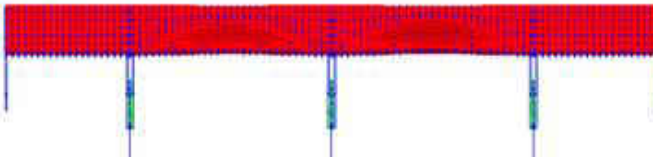
Mode 1	10.735 Hz
<i>Vertical Bending</i>	



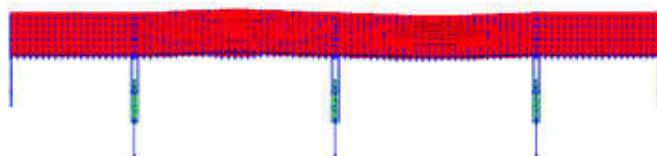
Mode 2	10.758 Hz
<i>Vertical Bending</i>	



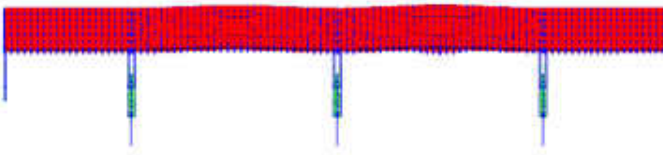
Mode 3	11.162 Hz
<i>Vertical Bending</i>	



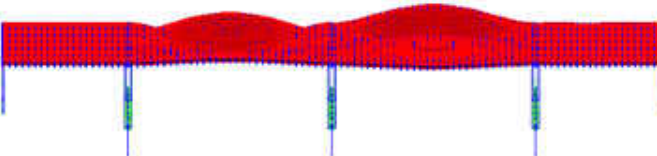
Mode 4	11.185 Hz
<i>Torsion</i>	



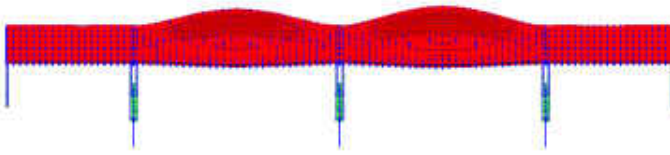
Mode 5	11.862 Hz
<i>Vertical Bending (Side to Side)</i>	



Mode 6	11.887 Hz
<i>Vertical Bending</i>	



Mode 7	12.310 Hz
<i>Vertical Bending (same phase)</i>	



Mode 8	12.333 Hz
<i>Torsion</i>	

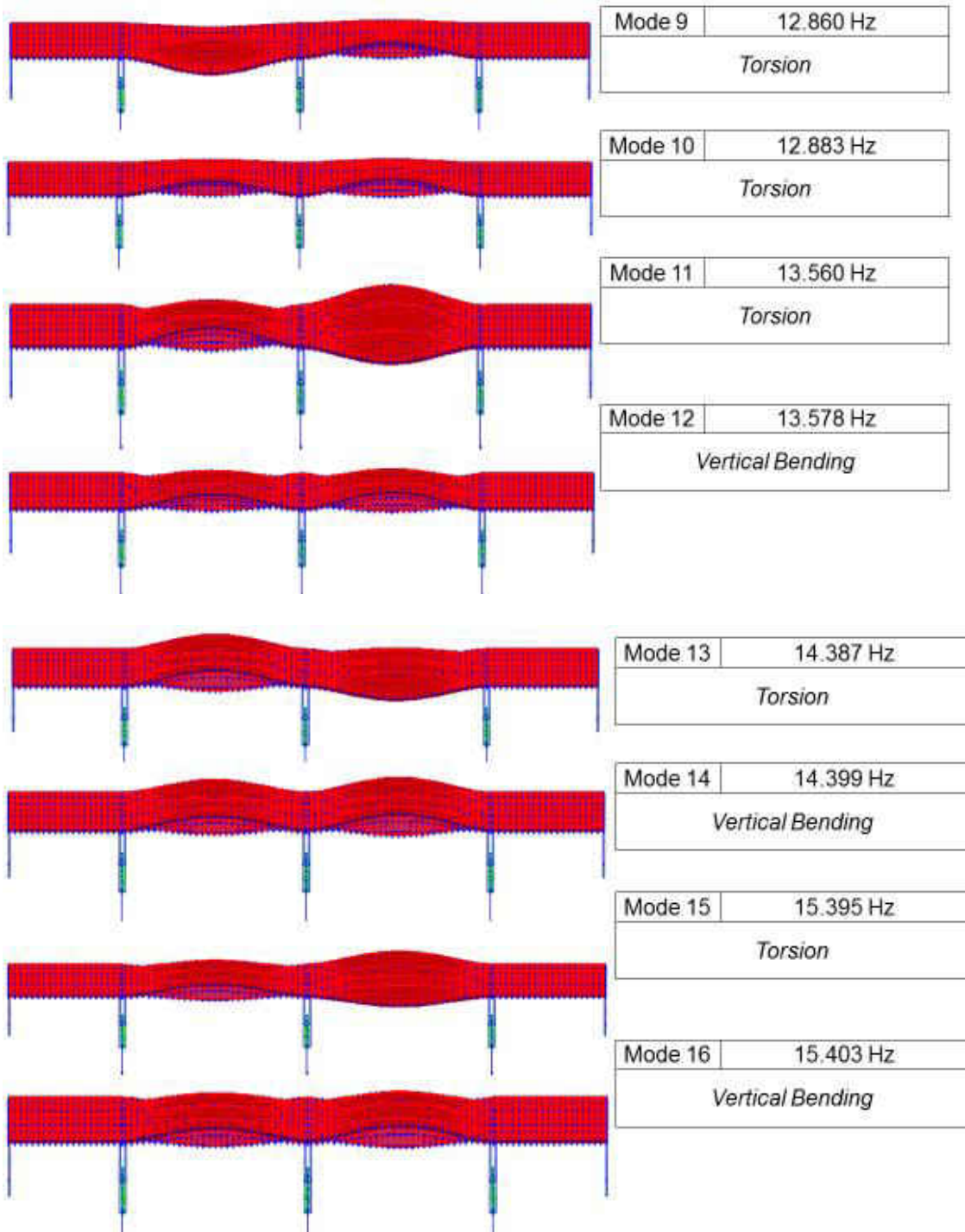


Figure 89: 2002 Bridge Modes

APPENDIX B: LIVE LOAD DISTRIBUTION FACTORS ANALYSIS

*Live Load Distribution Factor for Positive Moment (Interior Girder) - Benchmark
(LRFD Table 4.6.2.2.2b-1.) - SPANS 1/2/3*

Span Length (1,2,3);	$psi := \frac{lb}{in^2}$	$Span_L := 100.00 \cdot ft$
Girder Spacing (Interior Girders);		$Girder_S := 8 \cdot ft$
Deck Thickness		$t_s := 8 \cdot in$
Number of Beams (Girders)		$N_b := 4$
Depth of Girder (Type V - Interior)		$d_G := 63 \cdot in$
Area of Girder (Type V - Interior)		$A_G := 1013 \cdot in^2$
Moment of Inertia (Type V - Interior)		$I_G := 521180 \cdot in^4$
Girder center of gravity from bottom in the y - direction		$y_b := 31.96 \cdot in$
Distance between center of gravity of the girder and concrete deck;		$e_g := (d_G - y_b) + \frac{t_s}{2}$
Compressive strength of Precast Concrete;	$f_{cp} := 6000 \cdot psi$	
For the Modulus Elasticity analysis used fcpp;	$f_{cpp} := 6000$	
Therefore the Modulus Elasticity (Precast Concrete)	$E_B := ((57) \cdot \sqrt{f_{cpp}}) \cdot 1000 \cdot psi$	
Compressive strength of Concrete Deck;	$f_{cd} := 4000 \cdot psi$	
For the Modulus Elasticity analysis used fcdd;	$f_{cdd} := 4000$	
Therefore Modulus of Elasticity (Deck Concrete);	$E_D := 57 \cdot \sqrt{f_{cdd}} \cdot 1000 \cdot psi$	
Modular Ratio	$n := \frac{E_B}{E_D} \quad n = 1.225$	
Longitudinal stiffness parameter, Kg (LRFD Eq. 4.6.2.2.1 - 1)	$K_g := n \cdot (I_G + A_G \cdot (e_g)^2)$	

The number of design lanes is equal to the integer portion of the roadway width divided by 3600mm.

Clear roadway width	$RW_{width} := 40 \cdot ft$
	$RW_{width} = (1.219 \cdot 10^4) \text{ mm}$
Therefore Number of Design Lanes	$N_L := \frac{RW_{width}}{3600 \cdot mm}$

The command "floor" returns "integer" component

$$\text{floor}(N_L) = 3$$

Check Range of Applicability

$$Girder_S = (2.438 \cdot 10^3) \text{ mm} \quad 1100\text{mm} \leq S \leq 4900\text{mm} \quad \text{OK}$$

$$t_s = 203.2 \text{ mm} \quad 110\text{mm} \leq t_s \leq 300\text{mm} \quad \text{OK}$$

$$Span_L = (3.048 \cdot 10^4) \text{ mm} \quad 6000\text{mm} \leq L \leq 73000\text{mm} \quad \text{OK}$$

$$N_b = 4 \quad \text{Number of beams} \geq 4 \quad \text{OK}$$

Note that if "S" exceeds 4900mm we would use the lever rule to compute all the live load distribution factors and if Nb is equal to 3 additional considerations are required.

Naming: mgSI_{momPos} → mg (multiple presence), S (Single Lane), I (Interior), mom (moment), Pos = +

Naming: mgMEslr → mg (multiple presence), M (Multiple Lane), E (Exterior), slr (shear)

Single Lane Loaded:

Distribution Factor (Moment Interior) Multiple Presence Factor - included.

Note: "ts" is not converted into feet (ft) in these equations;

Use unitless dimensions;

$$\text{Let_Girder_Spacing } G_S := \frac{\text{Girder}_S}{\text{ft}} \quad \text{Let_Span_Length } S_L := \frac{\text{Span}_L}{\text{ft}}$$

$$\text{Let_Stiffness_Parameter } KG := \frac{K_g}{\text{in}^4} \quad \text{Let_Slab_Thickness } TS := \frac{t_s}{\text{in}}$$

$$mgSI_{momPos} := 0.06 + \left(\frac{G_S}{14}\right)^{0.4} \cdot \left(\frac{G_S}{S_L}\right)^{0.3} \cdot \left(\frac{KG}{12 \cdot S_L \cdot (TS)^3}\right)^{0.1} \quad mgSI_{momPos} = 0.485$$

Two or More Lanes Loaded:

Distribution Factor (Moment Interior) Multiple Presence Factor - included.

$$mgMI_{momPos} := 0.075 + \left(\frac{G_S}{9.5}\right)^{0.6} \cdot \left(\frac{G_S}{S_L}\right)^{0.2} \cdot \left(\frac{KG}{12 \cdot S_L \cdot (TS)^3}\right)^{0.1} \quad mgMI_{momPos} = 0.692$$

Live Load Distribution Factor for Negative Moment (Interior Girder) - Benchmark (LRFD Table 4.6.2.2.2b-1.) - SPANS 1/2/3

The same Live Load Distribution Factors used for Positive Moments will be used ...

Live Load Distribution Factor for Positive Moment (Exterior Girder) - Benchmark
(LRFD Table 4.6.2.2.2b-1.) - SPANS 1/2/3

Note: The two axle wheels (P) denoted here with the "Blue" arrows and the reaction (RA) denoted by the "Red" arrow.

Let the distance between the barrier & first wheel

$$D_1 := 2 \cdot ft$$

Let the distance between both wheels

$$D_2 := 6 \cdot ft$$

Let the distance between the 2nd wheel & Center of Interior girder

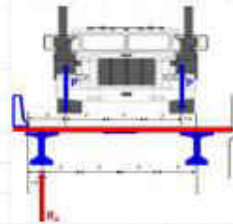
$$D_3 := 1 \cdot ft + 6 \cdot in$$

Let the distance between the barrier & Center of Exterior girder

$$D_4 := 1 \cdot ft + 6 \cdot in$$

Let the distance between the Center of Exterior girder & Center of Interior girder

$$D_5 := 8 \cdot ft + 0 \cdot in$$



Therefore using Statics and taking moments about the centerline of the Interior Girder;

$$P \cdot (D_2 + D_3) + P \cdot (D_3) - R_A \cdot D_5 = 0 \xrightarrow{\text{solve, } R_A} \frac{3 \cdot P \cdot in + 2 \cdot P \cdot ft}{2 \cdot ft}$$

Which implies $R_A(P) := \frac{3 \cdot P \cdot in + 2 \cdot P \cdot ft}{2 \cdot ft}$

Therefore lane fraction carried by the Exterior Girder; $Lane_{fraction} := \frac{R_A(P)}{2 \cdot P}$

$$Lane_f := \frac{(3 \cdot in + 2 \cdot ft)}{2}$$

$$Lane_f = 0.563$$

The multiple presence factor - one lane loaded

$$MPF_1 := 1.2$$

The multiple presence factor - two lane loaded

$$MPF_2 := 1.0$$

The multiple presence factor - three lane loaded

$$MPF_3 := 0.85$$

The multiple presence factor - More than three lane loaded

$$MPF_{3plus} := 0.65$$

Single Lane Loaded:

Therefore the Distribution Factor for a One design lane loaded (Using Lever Rule)

$$mgSE_{momPos1,4} := MPF_1 \cdot Lane_f$$

$$mgSE_{momPos1,4} = 0.675$$

Note, LRFD requires the use of Lever Rule for "One - Lane Design Load" Exterior Girder.

Two or More Lanes Loaded:

The distribution factor for moment in the exterior girder for multiple lanes loaded requires an adjustment factor "e"

Bridge Deck Cantilever

$$BD_{cant} := 3 \cdot ft + 0 \cdot in$$

Barrier Width

$$Barrier_W := 1 \cdot ft + 6 \cdot in$$

Therefore, the clear distance between centerline of girder to the edge of barrier;

$$d_e := BD_{cant} - Barrier_W$$

d_e = Distance from the center of the exterior girder to the location of the centroid of the outermost wheel group (feet). NCHRP

From LRFD - 4.6.2.2.2d-1, the adjustment factor "e" $e_{adj} := 0.77 + \frac{d_e}{2800 \cdot mm}$ $e_{adj} = 0.933$

Since this value has to be greater or equal to one, we will use 1.

Therefore;

$$MOM e_{adj} := 1.0$$

Therefore the Distribution Factor for the multiple design lane loaded (moment - exterior) = Adjustment Factor for the moment multiplied by the factor for the interior girder (multiple).

Therefore recall from "Interior Girder" Multiple Lanes;

Span Length (1-3);

$$Span_L := 100 \cdot ft$$

Girder Spacing (Interior Girders);

$$Girder_S := 8 \cdot ft$$

Deck Thickness

$$t_s := 8 \cdot in$$

Number of Beams (Girders)

$$N_b := 4$$

Depth of Girder (Type V - Interior)

$$d_G := 63 \cdot in$$

Area of Girder (Type V - Interior)

$$A_G := 1013 \cdot in^2$$

Moment of Inertia (Type V - Interior)

$$I_G := 521180 \cdot in^4$$

Girder center of gravity from bottom in the y - direction

$$y_b := 31.96 \cdot in$$

Distance between center of gravity of the girder and concrete deck;

$$e_g := (d_G - y_b) + \frac{t_s}{2}$$

Compressive strength of Precast Concrete; $f_{cp} := 6000 \cdot \frac{lb}{in^2}$

For the Modulus Elasticity analysis used f_{cpp} ; $f_{cpp} := 6000$

Therefore the Modulus Elasticity (Precast Concrete) $E_B := ((57) \cdot \sqrt{f_{cpp}}) \cdot 1000 \cdot \frac{lb}{in^2}$

Compressive strength of Concrete Deck; $f_{cd} := 4000 \cdot \frac{lb}{in^2}$

For the Modulus Elasticity analysis used f_{cdd} ; $f_{cdd} := 4000$

Therefore Modulus of Elasticity (Deck Concrete); $E_D := 57 \cdot \sqrt{f_{cdd}} \cdot 1000 \cdot \frac{lb}{in^2}$

Modular Ratio $n := \frac{E_B}{E_D} \quad n = 1.225$

Longitudinal stiffness parameter, K_g (LRFD Eq. 4.6.2.2.1 - 1) $K_g := n \cdot (I_G + A_G \cdot (e_g)^2)$

$K_g = (2.162 \cdot 10^6) \text{ in}^4$

Two or More Lanes Loaded;

Note: "ts" is not converted into feet (ft) in these equations;

Use unitless dimensions;

Let Girder Spacing $G_S := \frac{Girders_g}{ft}$ Let Span Length $S_L := \frac{Span_L}{ft}$

Let Stiffness Parameter $KG := \frac{K_g}{in^4}$ Let Slab Thickness $TS := \frac{t_s}{in}$

Distribution Factor (Moment Interior) Multiple Presence Factor - included.

$mgMI_{momPos} := 0.075 + \left(\frac{G_S}{9.5}\right)^{0.6} \cdot \left(\frac{G_S}{S_L}\right)^{0.2} \cdot \left(\frac{KG}{12 \cdot S_L \cdot (TS^3)}\right)^{0.1}$ $mgMI_{momPos} = 0.692$

Hence the Distribution Factor for the multiple design lane loaded (moment - exterior) = Adjustment Factor for the moment multiplied by the factor for the interior girder (multiple).

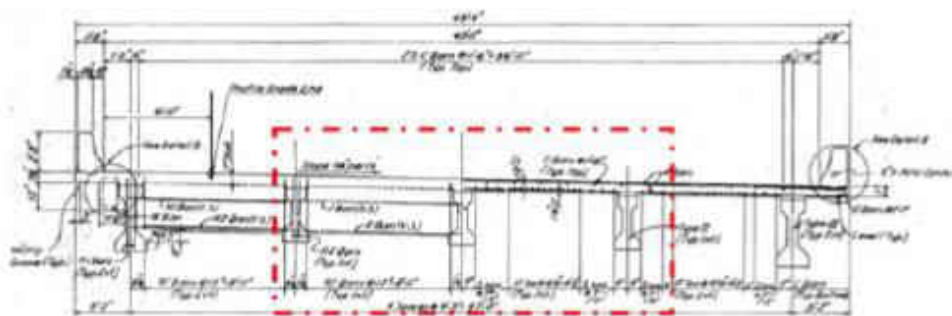
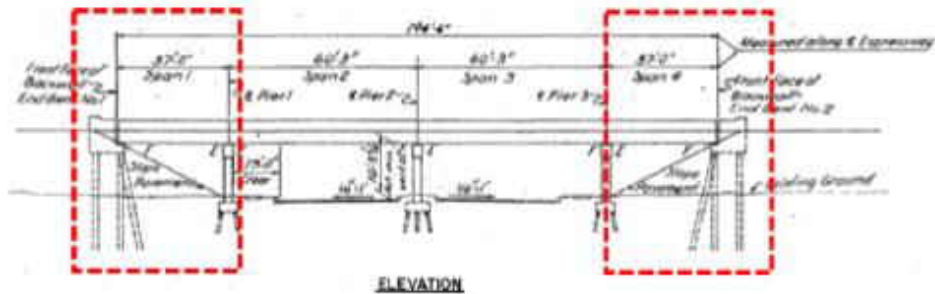
$mgME_{momPos} := MOMe_{adj} \cdot mgMI_{momPos}$ $mgME_{momPos} = 0.692$

Live Load Distribution Factor for Shear (Interior Girder) - Benchmark
(LRFD Table 4.6.2.2.2b-1.) - SPANS 1/2/3

Span Length (Same);	$Span_L := 100 \cdot ft$	Depth of Girder (Type V)	$d_G := 63 \cdot in$
Girder Spacing ;	$Girder_S := 8 \cdot ft$	Area of Girder (Type V)	$A_G := 1013 \cdot in^2$
Deck Thickness	$t_s := 8 \cdot in$	Moment of Inertia (Type V)	$I_G := 521180 \cdot in^4$
Number of Beams (Girders)	$N_b := 4$	Girder center of gravity from bottom in the y - direction	$y_b := 31.96 \cdot in$
Distance between center of gravity of the girder and concrete deck;	$e_g := (d_G - y_b) + \frac{t_s}{2}$		
Compressive strength of Precast Concrete;	$f_{cp} := 6000 \cdot \frac{lb}{in^2}$		
For the Modulus Elasticity analysis used fcpp;	$f_{cpp} := 6000$		
Therefore the Modulus Elasticity (Precast Concrete)	$E_B := ((57) \cdot \sqrt{f_{cpp}}) \cdot 1000 \cdot \frac{lb}{in^2}$		
Compressive strength of Concrete Deck;	$f_{cd} := 4000 \cdot \frac{lb}{in^2}$		
For the Modulus Elasticity analysis used fodd;	$f_{odd} := 4000$		
Therefore Modulus of Elasticity (Deck Concrete);	$E_D := 57 \cdot \sqrt{f_{odd}} \cdot 1000 \cdot \frac{lb}{in^2}$		
Modular Ratio	$n := \frac{E_B}{E_D} \quad n = 1.225$		
Longitudinal stiffness parameter, Kg (LRFD Eq. 4.6.2.2.1 - 1)	$K_g := n \cdot (I_G + A_G \cdot (e_g)^2)$		
Clear roadway width	$RW_{width} := 30 \cdot ft$		
<i>The number of design lanes is equal to the integer portion of the roadway width divided by 3600mm.</i>			
Therefore Number of Design Lanes	$N_L := \frac{RW_{width}}{3600 \cdot mm} \quad \text{floor}(N_L) = 2$		
<u>Single Lane Loaded;</u>			
Distribution Factor	$mgSI_{shr1,4} := 0.36 + \frac{Girder_S}{25 \cdot ft}$	$mgSI_{shr1,4} = 0.68$	
<u>Two Lanes Loaded;</u>			
Distribution Factor	$mgMI_{shr1,4} := 0.2 + \left(\frac{Girder_S}{12 \cdot ft} \right) - \left(\frac{Girder_S}{35 \cdot ft} \right)^2$	$mgMI_{shr1,4} = 0.814$	

Since the LLDF Analysis for Shear are independent of the Span Lengths, the LLDF will be the same for ALL Spans.

Live Load Distribution Factor for Positive Moment (Interior Girder) - 1972 Bridge
(LRFD Table 4.6.2.2.2b-1) - SPANS 1/4



Span Length (1 & 4);	$Span_{L1,4} := 37.00 \cdot ft$
Girder Spacing (Interior Girders);	$Girder_S := 9.25 \cdot ft$
Deck Thickness	$t_s := 7 \cdot in$
Number of Beams (Girders)	$N_b := 5$
Depth of Girder (Type II - Interior)	$d_G := 36 \cdot in$
Area of Girder (Type II - Interior)	$A_G := 369 \cdot in^2$
Moment of Inertia (Type II - Interior)	$I_G := 50980 \cdot in^4$
Girder center of gravity from bottom in the y - direction	$y_b := 15.83 \cdot in$
Distance between center of gravity of the girder and concrete deck;	$e_g := (d_G - y_b) + \frac{t_s}{2}$
	$e_g = 23.67 \cdot in$

Compressive strength of Precast Concrete;	$f_{cp} := 6000 \cdot \frac{lb}{in^2}$
For the Modulus Elasticity analysis used fcpp;	$f_{cpp} := 6000$
Therefore the Modulus Elasticity (Precast Concrete)	$E_B := ((57) \cdot \sqrt{f_{cpp}}) \cdot 1000 \cdot \frac{lb}{in^2}$
Compressive strength of Concrete Deck;	$f_{cd} := 4000 \cdot \frac{lb}{in^2}$
For the Modulus Elasticity analysis used fcdd;	$f_{cdd} := 4000$
Therefore Modulus of Elasticity (Deck Concrete);	$E_D := 57 \cdot \sqrt{f_{cdd}} \cdot 1000 \cdot \frac{lb}{in^2}$
Modular Ratio	$n := \frac{E_B}{E_D} \quad n = 1.225$
Longitudinal stiffness parameter, Kg (LRFD Eq. 4.6.2.2.1 - 1)	$K_g := n \cdot (I_G + A_G \cdot (e_g)^2)$
Clear roadway width	$RW_{width} := 40 \cdot ft$
Therefore Number of Design Lanes	$N_L := \frac{RW_{width}}{3600 \cdot mm} \quad \text{floor}(N_L) = 3$

Check Range of Applicability

$Girder_S = (2.819 \cdot 10^3) \text{ mm}$	$1100mm \leq S \leq 4900mm$	OK
$t_s = 177.8 \text{ mm}$	$110mm \leq t_s \leq 300mm$	OK
$Span_{L1,4} = (1.128 \cdot 10^4) \text{ mm}$	$6000mm \leq L \leq 73000mm$	OK
$N_b = 5$	Number of beams ≥ 4	OK

Note that if "S" exceeds 4900mm we would use the lever rule to compute all the live load distribution factors and if Nb is equal to 3 additional considerations are required.

Naming: mgSImom -> mg (multiple presence), S (Single Lane), I (Interior), mom (moment), Pos = +
 Naming: mgMEshr -> mg (multiple presence), M (Multiple Lane), E (Exterior), shr (shear)

Single Lane Loaded:

Let Girder Spacing	$G_S := \frac{Girder_S}{ft}$	Let Stiffness Parameter	$KG := \frac{K_g}{in^4}$
Let Span Length	$S_L := \frac{Span_{L1,4}}{ft}$	Let Slab Thickness	$TS := \frac{t_s}{in}$

Distribution Factor (Moment Interior) Multiple Presence Factor - included.

$$mgSI_{momPos1_4} := 0.06 + \left(\frac{G_S}{14}\right)^{0.4} \cdot \left(\frac{G_S}{S_L}\right)^{0.3} \cdot \left(\frac{KG}{12 \cdot S_L \cdot (TS^3)}\right)^{0.1} \quad mgSI_{momPos1_4} = 0.661$$

Two or More Lanes Loaded:

Distribution Factor (Moment Interior) Multiple Presence Factor - included.

$$mgMI_{momPos1_4} := 0.075 + \left(\frac{G_S}{9.5}\right)^{0.6} \cdot \left(\frac{G_S}{S_L}\right)^{0.2} \cdot \left(\frac{KG}{12 \cdot S_L \cdot (TS^3)}\right)^{0.1} \quad mgMI_{momPos1_4} = 0.877$$

Live Load Distribution Factor for Positive Moment (Interior Girder) - 1972 Bridge
(LRFD Table 4.6.2.2.2b-1.) - SPANS 2/3

Span Length (2 & 3); $Span_{L2,3} := 60.25 \cdot ft$ Area of Girder (Type III) $A_{G3} := 560 \cdot in^2$

Depth of Girder (Type III) $d_{G3} := 45 \cdot in$ Moment of Inertia (Type III) $I_{G3} := 125390 \cdot in^4$

Girder center of gravity from bottom in the y - direction $y_{b3} := 20.27 \cdot in$

Distance between center of gravity of the girder and concrete deck; $e_{g3} := (d_{G3} - y_{b3}) + \frac{t_s}{2}$

Longitudinal stiffness parameter, Kg (LRFD Eq. 4.6.2.2.1 - 1) $K_{g3} := n \cdot (I_{G3} + A_{G3} \cdot (e_{g3})^2)$

Single Lane Loaded:

Let Girder Spacing $G_S := \frac{Girder_S}{ft}$ Let Stiffness Parameter $KG3 := \frac{K_{g3}}{in^4}$

Let Span Length $S_{L2} := \frac{Span_{L2,3}}{ft}$ Let Slab Thickness $TS := \frac{t_s}{in}$

Distribution Factor (Moment Interior) Multiple Presence Factor - included.

$$mgSI_{momPos2_3} := 0.06 + \left(\frac{G_S}{14}\right)^{0.4} \cdot \left(\frac{G_S}{S_{L2}}\right)^{0.3} \cdot \left(\frac{KG3}{12 \cdot S_{L2} \cdot (TS^3)}\right)^{0.1} \quad mgSI_{momPos2_3} = 0.596$$

Two or More Lanes Loaded:

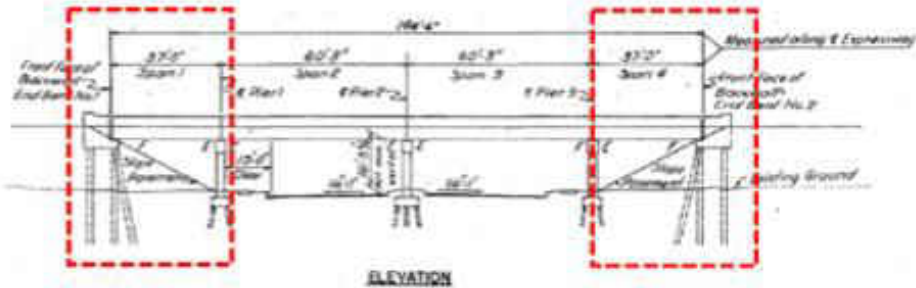
Distribution Factor (Moment Interior) Multiple Presence Factor - included.

$$mgMI_{momPos2_3} := 0.075 + \left(\frac{G_S}{9.5}\right)^{0.6} \cdot \left(\frac{G_S}{S_{L2}}\right)^{0.2} \cdot \left(\frac{KG3}{12 \cdot S_{L2} \cdot (TS^3)}\right)^{0.1} \quad mgMI_{momPos2_3} = 0.826$$

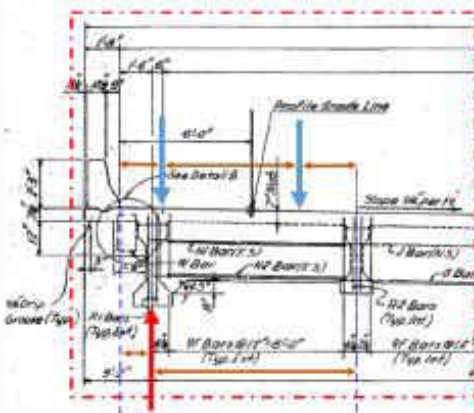
Live Load Distribution Factor for Negative Moment (Interior Girder) - 1972 OBT Bridge
(LRFD Table 4.6.2.2.2b-1.) - SPANS 1/4

The same Live Load Distribution Factors used for Positive Moments will be used ...

Live Load Distribution Factor for Positive Moment (Exterior Girder) - 1972 OBT Bridge
(LRFD Table 4.6.2.2.2b-1.) - SPANS 1/4



Note: The two axle wheels (P) denoted here with the "Blue" arrows and the reaction (RA) denoted by the "Red" arrow.



- Let the distance between the barrier & first wheel $D_1 := 2 \cdot ft$
- Let the distance between both wheels $D_2 := 6 \cdot ft$
- Let the distance between the 2nd wheel & Center of Interior girder $D_3 := 2 \cdot ft + 9 \cdot in$
- Let the distance between the barrier & Center of Exterior girder $D_4 := 1 \cdot ft + 6 \cdot in$
- Let the distance between the Center of Exterior girder & Center of Interior girder $D_5 := 9 \cdot ft + 3 \cdot in$

Therefore using Statics and taking moments about the centerline of the Interior Girder;

$$P \cdot (D_2 + D_3) + P \cdot (D_3) - R_A \cdot D_5 = 0 \xrightarrow{\text{solve, } R_A} \frac{18 \cdot P \cdot in + 10 \cdot P \cdot ft}{3 \cdot in + 9 \cdot ft}$$

Which implies $R_A(P) := \frac{18 \cdot P \cdot in + 10 \cdot P \cdot ft}{3 \cdot in + 9 \cdot ft}$

Therefore lane fraction carried by the Exterior Girder; $Lane_{fraction} := \frac{R_A(P)}{2 \cdot P}$ $Lane_f := \frac{(18 \cdot in + 10 \cdot ft)}{2}$

The multiple presence factor - one lane loaded $MPF_1 := 1.2$

The multiple presence factor - three lane loaded $MPF_3 := 0.85$

The multiple presence factor - two lane loaded $MPF_2 := 1.0$

The multiple presence factor - More than three lane loaded $MPF_{3plus} := 0.65$

Single Lane Loaded:

Therefore the Distribution Factor for a One design lane loaded (Using Lever Rule)

$$mgSE_{momPce1,4} = 0.746$$

Note, LRFD requires the use of Lever Rule for "One - Lane Design Load" Exterior Girder.

Two or More Lanes Loaded:

Therefore;

$$MOM e_{adj} = 1.0$$

Therefore the Distribution Factor for the multiple design lane loaded (moment - exterior) = Adjustment Factor for the moment multiplied by the factor for the interior girder (multiple).

Therefore recall from "Interior Girder" Multiple Lanes:

Span Length (1 & 4);	$Span_{L1,4} := 37.00 \cdot ft$	Depth of Girder (Type II)	$d_G := 36 \cdot in$
Girder Spacing (Girders);	$Girder_S := 9.25 \cdot ft$	Area of Girder (Type II)	$A_G := 369 \cdot in^2$
Deck Thickness	$t_s := 7 \cdot in$	Moment of Inertia (Type II)	$I_G := 50980 \cdot in^4$
Number of Beams (Girders)	$N_b := 5$	Girder center of gravity from bottom in the y - direction	$y_b := 15.83 \cdot in$
Distance between center of gravity of the girder and concrete deck;			$e_g := (d_G - y_b) + \frac{t_s}{2}$
Compressive strength of Precast Concrete;			$f_{cp} := 6000 \cdot \frac{lb}{in^2}$
For the Modulus Elasticity analysis used fcpp;			$f_{cpp} := 6000$
Therefore the Modulus Elasticity (Precast Concrete)			$E_B := (57) \cdot \sqrt{f_{cpp}} \cdot 1000 \cdot \frac{lb}{in^2}$
Compressive strength of Concrete Deck;			$f_{cd} := 4000 \cdot \frac{lb}{in^2}$
For the Modulus Elasticity analysis used fcdd;			$f_{cdd} := 4000$
Therefore Modulus of Elasticity (Deck Concrete);			$E_D := 57 \cdot \sqrt{f_{cdd}} \cdot 1000 \cdot \frac{lb}{in^2}$
Modular Ratio			$n := \frac{E_B}{E_D} \quad n = 1.225$
Longitudinal stiffness parameter, Kg (LRFD Eq. 4.6.2.2.1 - 1)			$K_g := n \cdot (I_G + A_G \cdot (e_g)^2)$

$$\text{Let_Girder_Spacing} \quad G_S := \frac{\text{Girder}_S}{\text{ft}} \quad \text{Let_Stiffness_Parameter} \quad KG := \frac{K_g}{\text{in}^4}$$

$$\text{Let_Span_Length} \quad S_L := \frac{\text{Span}_{L1,4}}{\text{ft}} \quad \text{Let_Slab_Thickness} \quad TS := \frac{t_s}{\text{in}}$$

Two or More Lanes Loaded:

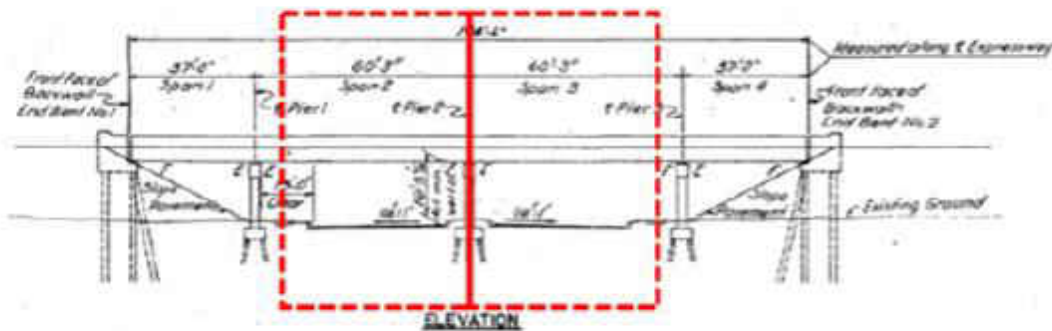
Distribution Factor (Moment Interior) Multiple Presence Factor - included.

$$mgMI_{momPos1,4} := 0.075 + \left(\frac{G_S}{9.5}\right)^{0.6} \cdot \left(\frac{G_S}{S_L}\right)^{0.2} \cdot \left(\frac{KG}{12 \cdot S_L \cdot (TS^3)}\right)^{0.1} \quad mgMI_{momPos1,4} = 0.877$$

Hence the Distribution Factor for the multiple design lane loaded (moment - exterior) = Adjustment Factor for the moment multiplied by the factor for the interior girder (multiple).

$$mgME_{momPos1,4} := MOMe_{adj} \cdot mgMI_{momPos1,4} \quad mgME_{momPos1,4} = 0.877$$

Live Load Distribution Factor for Positive Moment (Exterior Girder) - 1973 OBT Bridge (LRFD Table 4.6.2.2.2b-1.) - SPANS 2/3



Span Length (2 & 3):

$$\text{Span}_{L2,3} := 60.25 \cdot \text{ft}$$

Let_Span_Length_2_3

$$S_{L1} := \frac{\text{Span}_{L2,3}}{\text{ft}}$$

$$S_{L1} = 60.25$$

Depth of Girder (Type III - Interior)

$$d_{G3} := 45 \cdot \text{in}$$

Area of Girder (Type III - Interior)

$$A_{G3} := 560 \cdot \text{in}^2$$

Moment of Inertia (Type III - Interior)

$$I_{G3} := 125390 \cdot \text{in}^4$$

Girder center of gravity from bottom in the y - direction

$$y_{b3} := 20.27 \cdot \text{in}$$

Distance between center of gravity of the girder and concrete deck; $e_{g3} := (d_{G3} - y_{b3}) + \frac{t_s}{2}$

Longitudinal stiffness parameter, Kg (LRFD Eq. 4.6.2.2.1 - 1) $K_{g3} := n \cdot (I_{G3} + A_{G3} \cdot (e_{g3})^2)$

Let Stiffness Parameter $KG3 := \frac{K_{g3}}{\text{in}^4}$ $KG3 = 7.002 \cdot 10^5$

Single Lane Loaded: (Similar to One Design Lane Loaded for Span 1 & 4)

Distribution Factor (Moment Exterior) Multiple Presence Factor - included.

$$mgSE_{momPos2,3} := mgSE_{momPos1,4} \quad mgSE_{momPos2,3} = 0.746$$

Two or More Lanes Loaded:

Distribution Factor (Moment Interior) Multiple Presence Factor - included.

$$mgMI_{momPos2,3} := 0.075 + \left(\frac{G_S}{9.5}\right)^{0.6} \cdot \left(\frac{G_S}{S_{L1}}\right)^{0.2} \cdot \left(\frac{KG3}{12 \cdot S_{L1} \cdot (TS^3)}\right)^{0.1} \quad mgMI_{momPos2,3} = 0.826$$

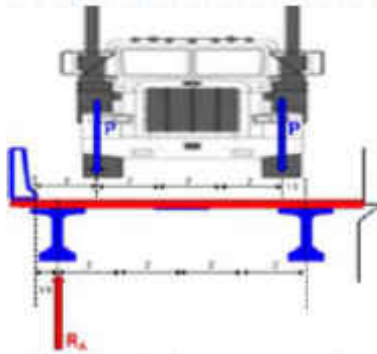
Hence the Distribution Factor for the multiple design lane loaded (moment - exterior) = Adjustment Factor for the moment multiplied by the factor for the interior girder (multiple).

$$mgME_{momPos2,3} := MOMe_{adj} \cdot mgMI_{momPos2,3} \quad mgME_{momPos2,3} = 0.826$$

Note: Since this bridge does not have skewed piers, the span length parameter L does not figure into the calculation of live load distribution factors in exterior beams. As such, the live load distribution factors for negative moment are exactly the same as for positive moment.

Live Load Distribution Factor for Shear (Exterior Girder) - 1972 Bridge
(LRFD Table 4.6.2.2.2b-1.) - SPANS 1/2/3

Note: The two axle wheels (P) denoted here with the "Blue" arrows and the reaction (RA) denoted by the "Red" arrow.



- Let the distance between the barrier & first wheel $D_1 := 2 \cdot ft$
- Let the distance between both wheels $D_2 := 6 \cdot ft$
- Let the distance between the 2nd wheel & Center of Interior girder $D_3 := 2 \cdot ft + 9 \cdot in$
- Let the distance between the barrier & Center of Exterior girder $D_4 := 1 \cdot ft + 6 \cdot in$
- Let the distance between the Center of Exterior girder & Center of Interior girder $D_5 := 9 \cdot ft + 3 \cdot in$

Therefore using Statics and taking moments about the centerline of the Interior Girder;

$$P \cdot (D_2 + D_3) + P \cdot (D_3) - R_A \cdot D_5 = 0 \xrightarrow{\text{solve, } R_A} \frac{18 \cdot P \cdot in + 10 \cdot P \cdot ft}{3 \cdot in + 9 \cdot ft}$$

Which implies $R_A \quad R_A(P) := \frac{18 \cdot P \cdot in + 10 \cdot P \cdot ft}{3 \cdot in + 9 \cdot ft}$

Therefore lane fraction carried by the Exterior Girder; $Lane_{fraction} := \frac{R_A(P)}{2 \cdot P}$

$$Lane_f := \frac{\left(\frac{18 \cdot in + 10 \cdot ft}{3 \cdot in + 9 \cdot ft} \right)}{2} \quad Lane_f = 0.622$$

The multiple presence factor - one lane loaded $MPF_1 := 1.2$

The multiple presence factor - two lane loaded $MPF_2 := 1.0$

The multiple presence factor - three lane loaded $MPF_3 := 0.85$

The multiple presence factor - More than three lane loaded $MPF_{3plus} := 0.65$

The live load distribution factor for shear in exterior beams for one design lane loaded is determined by the lever rule. This will produce the same results and the distribution factors for negative moment.

Single Lane Loaded:

Therefore the Distribution Factor for a One design lane loaded (Using Lever Rule) $mgSE_{shr1_4} := MPF_1 \cdot Lane_f$

$$mgSE_{shr1_4} = 0.746$$

CONTROLS

Note, LRFD requires the use of Lever Rule for "One - Lane Design Load" Exterior Girder.

Two or More Lanes Loaded:

The distribution factor for moment in the exterior girder for multiple lanes loaded requires an adjustment factor "e"

Bridge Deck Cantilever $BD_{cant} := 3 \cdot ft + 2 \cdot in$

Barrier Width $Barrier_W := 1 \cdot ft + 8 \cdot in$

Therefore, the clear distance between centerline of girder to the edge of barrier; $d_e := BD_{cant} - Barrier_W$
 $d_e = 457.2 \text{ mm}$

The distribution factor for shear in the exterior girder for multiple lanes loaded requires an adjustment factor "e"

$$SHEARe_{adj} := 0.6 + \frac{d_e}{3000 \cdot mm} \quad SHEARe_{adj} = 0.752$$

Therefore the Distribution Factor for the multiple design lane loaded (shear - exterior) = Adjustment Factor for the shear multiplied by the factor for the interior girder (multiple).

Recall: Interior girder analysis for shear "See LLDF_Shear_INT_1972"

Girder Spacing (Interior Girders); $Girder_S := 9.25 \cdot ft$

Let Girder Spacing $G_S := \frac{Girder_S}{ft} \quad G_S = 9.25$

Two Lanes Loaded:

Distribution Factor $mgMI_{shr1_4} := 0.2 + \left(\frac{G_S}{12}\right) - \left(\frac{G_S}{35}\right)^2 \quad mgMI_{shr1_4} = 0.901$

Therefore;

$$mgME_{shr1_4} := SHEARe_{adj} \cdot mgMI_{shr1_4} \quad mgME_{shr1_4} = 0.678$$

Since the LLDF Analysis for Shear are independent of the Span Lengths, the LLDF will be the same for ALL Spans.

APPENDIX C: CAPACITY ANALYSIS

Maximum Load Placement for HL93 Truck

(Finding Maximum Moment: Determining HL93 Truck Position on Simple Spans - Cory L. Shipman)

Span Length (Input) $L_{span} = 60.25 \cdot ft$ Uniformly Distributed Lane Load: $w_{span} = 640 \cdot \frac{lb}{ft}$

Therefore the resultant for the truck from the 2nd axle $x_2 := \left(\frac{\left(\frac{L_{span}}{ft} \right)}{2} - \frac{447.2}{0.64 \cdot \left(\frac{L_{span}}{ft} \right) + 191.5} \right) \cdot ft$ $x_2 = 28.181 \cdot ft$

Solving the PCI (2003) Equations: $M_T := \left(\frac{\left(\frac{72 \cdot \frac{x_2}{ft} \cdot \left(\frac{L_{span} - x_2}{ft} \right) - 4.67}{\frac{L_{span}}{ft}} \right) - 112}{\frac{L_{span}}{ft}} \right) \cdot 10^3 \cdot lb \cdot ft$
(kip-ft/lane)

$$M_L := \frac{w_{span} \cdot x_2}{2} \cdot (L_{span} - x_2) \quad M_L = (2.892 \cdot 10^5) \cdot lb \cdot ft \quad M_T = (8.107 \cdot 10^5) \cdot lb \cdot ft$$

Therefore applying the dynamic load allowance $M_{LLI} := (M_T + M_L)$

& the summing the moments - Live Load

Moment for HL93 Truck per lane:

$$M_{LLI} = (1.32 \cdot 10^7) \cdot lb \cdot in$$

Nominal Flexural Load Analysis (Dead Load - DC & DW)

Effective_Width $b_{eff} = 104 \cdot in$ TypeIII_Weight $W_{III} = 583 \cdot \frac{lb}{ft}$

Weight_Conc $C_{wt} = 150 \cdot \frac{lb}{ft^3}$ Deck_Thickness $t_s = 8 \cdot in$

WS_Thickness $WS_t = 2 \cdot in$

Wearing_Surface $DW := WS_t \cdot C_{wt} \cdot b_{eff}$ $DW = 216.667 \cdot \frac{lb}{ft}$

DeadLoad_Girder_Deck $DC := W_{III} + (t_s \cdot C_{wt} \cdot b_{eff})$ $DC = (1.45 \cdot 10^3) \cdot \frac{lb}{ft}$

DC_Moment $M_{DC1} := \frac{DC \cdot L_{span}^2}{8}$ $M_{DC1} = (6.578 \cdot 10^5) \cdot lb \cdot ft$

DW_Moment $M_{DW} := \frac{DW \cdot L_{span}^2}{8}$ $M_{DW} = (9.831 \cdot 10^4) \cdot lb \cdot ft$

Total_Dead_Load $M_{DC} := M_{DC1} + M_{DW}$ $M_{DC} = (9.073 \cdot 10^5) \cdot lb \cdot in$

Nominal Flexural Resistance at Maximum Positive Moment Section

Span where maximum positive moments occurs: **Spans 2 & 3**

Girder Type: **AASHTO Type III**

Procedure specified in **LRFD 5.7.3** will be used to compute the flexural resistance.

Prestressed Steel Information:

For the Type III Beam - 16 - 1/2" ϕ strands, Grade 270, low relaxation (Bottom)

(See 252A Bridge Calcs)

Yield Strength	$f_{py} := 240000 \cdot \frac{lb}{in^2}$	Tensile Strength	$f_{pu} := 270000 \cdot \frac{lb}{in^2}$
Value of "k" (LRFD Table C5.7.3.1.1-1) for Low - relaxation strand			$k_{L,R} := 0.28$
Area of 1/2" Strand (Caltrans - LRFD Bridge Design Aids 6 - 4) June 2012			$A_{p12} := 0.153 \cdot in^2$
Number of 1/2" Strands (see 11/139 - 252A Bridge Design Calcs)			$N_{12} := 16$
Total Area of prestressed strands	$A_{ps} := (N_{12} \cdot A_{p12})$		$A_{ps} = 2.448 \cdot in^2$
Compressive strength of Concrete Deck:			$f_{cd} := 4500 \cdot \frac{lb}{in^2}$
For the β_1 analysis used f_{cdd} ;			$f_{cdd} := 4.5$
The β_1 factor for the stress block since $f_c' > 4$ ksi		$\beta_1 := 0.85 - 0.05 \cdot (f_{cdd} - 4)$	$\beta_1 = 0.825$
Deck Thickness	$t_s := 8 \cdot in$	Area of Girder (Type III)	$A_G := 560 \cdot in^2$
Depth of Girder (Type III)	$d_G := 45 \cdot in$	Moment of Inertia (Type III)	$I_G := 125390 \cdot in^4$
Therefore the c.g. of prestressed strands concentration (Eccentricity @ C.L. see 11/139 - 252A Bridge Calcs)			$PS_{cg} := 3 \cdot in$
And hence the depth of prestressed strands	$d_p := d_G + t_s - PS_{cg}$		$d_p = 50 \cdot in$
Girder Spacing "b" (max. spacing 9' - 3") - Using Effective Area			$Girder_S := 9.25 \cdot ft$

Assume that NA is located in the concrete deck, i.e. a rectangular section:

Therefore the distance from extreme compression fiber to neutral axis:

$$c_{\text{defined}} := \frac{A_{ps} \cdot f_{pu}}{0.85 \cdot f_{cd} \cdot \beta_1 \cdot \text{Girder}_S + k_{LR} \cdot \frac{A_{ps} \cdot f_{pu}}{d_p}} = 1.867 \text{ in}$$

$$c := \frac{2.448 \cdot 270}{0.85 \cdot 4.5 \cdot 0.825 \cdot 111 + 0.28 \cdot 2.448 \cdot \frac{270}{50}} \cdot \text{in} = 1.867 \text{ in} < 8'' \text{ (Rect. Sect.)}$$

Therefore the depth of equivalent rectangular stress block $a := \beta_1 \cdot c$ $a = 1.54 \text{ in}$

Hence the stress in prestressed reinforcement at nominal strength:

$$f_{ps} := f_{pu} \cdot \left(1 - k_{LR} \cdot \frac{c}{d_p}\right) \quad f_{ps} = (2.672 \cdot 10^5) \frac{\text{lb}}{\text{in}^2}$$

The nominal flexural resistance is: $M_{n\text{flex}} := A_{ps} \cdot f_{ps} \cdot \left(d_p - \frac{a}{2}\right)$ $M_{n\text{flex}} = (3.22 \cdot 10^7) \text{ lb} \cdot \text{in}$

APPENDIX D: MODULUS OF ELASTICITY ANALYSIS

FIND THE IMMEDIATE AND LONG - TERM MODULUS OF ELASTICITY FOR CONCRETE

Specify the time (age) for concrete for the analysis;

$$\text{TIME} := 50 \cdot \text{yr}$$

The approach to this problem will be to find expressions for the immediate (upper-bound) modulus and the long-term, ultimate modulus (lower-bound), considering effects of creep under long-term dead load. The values for E_c are based on the nominal concrete strength, f_c .

Precast Beams

$$\text{psi} := \frac{\text{lb}}{\text{in}^2} \qquad \text{pcf} := \frac{\text{lb}}{\text{ft}^3}$$

Nominal Concrete Strength

$$f_{cp} := 5500 \cdot \text{psi}$$

Concrete Weight

$$w_c := 150 \cdot \text{pcf}$$

Upper-Bound Modulus

For upper-bound behavior, we look at the immediate modulus without any reductions for long-term creep. Navy gives expressions for high-strength concrete modulus (Navy 2010, p. 38), where high-strength concrete is defined as concrete with compressive strength between 6,000 and 12,000psi,

$$\text{Modulus of Elasticity } E_c := \left[40000 \cdot \left(\frac{f_{cp} \cdot \text{in}^2}{\text{lb}} \right)^{0.5} + 10^6 \right] \cdot \left(\frac{w_c \cdot \text{ft}^3}{145 \cdot \text{lb}} \right)^{1.5} \cdot \frac{\text{lb}}{\text{in}^2}$$

For normal - weight concrete, ACI 318 - 02 gives the following expression (Sect. 8.5.1),

$$E_{cN} := 57000 \cdot \sqrt{\frac{f_{cp} \cdot \text{in}^2}{\text{lb}}} \cdot \frac{\text{lb}}{\text{in}^2}$$

Lower - Bound Modulus

For lower-bound behavior, consider the effects of long-term creep with expressions from Navy [61] and Barker [57].

The following expression is given for ultimate effective modulus (Navy 2010, p. 42);

This is bound by upper and lower values, based on relative humidity;

Usually for Southeast Regional Climate, $RH = 72.5$

$$RH := 72.5$$

Correction factor for relative humidity of ambient air (Upper Bound);

$$\gamma_{hu} := 1.75 + 2.25 \cdot \left(\frac{100 - RH}{65} \right)$$

$$\gamma_W := \text{round}(\gamma_{hu}) = 3$$

Correction factor for relative humidity
of ambient air (Lower Bound);

$$\gamma_{ul} := 0.75 + 0.75 \cdot \left(\frac{100 - RH}{50} \right) \quad \gamma_{ul} := \text{round}(\gamma_{ul}) = 1$$

Ultimate Effective Modulus w.r.t t_u $E_{cnUpper} := \frac{E_c}{1 + \gamma_{tu}} \quad E_{cnUpper} = [1.127 \cdot 10^6] \frac{lb}{in^2}$

Let; $E_{cLT1} := E_{cnUpper}$

Ultimate Effective Modulus w.r.t t_l $E_{cnLower} := \frac{E_c}{1 + \gamma_{ul}} \quad E_{cnLower} = [1.93 \cdot 10^6] \frac{lb}{in^2}$

Let; $E_{cLT2} := E_{cnLower}$

To account for the increase in strain due to creep under permanent loads, Barker [57] gives an expression for a reduced long-term modulus of elasticity that considers humidity, time to permanent load, and volume-to-surface ratio,

Assume the following for permanent loading;

" t_i " is age of concrete in days when $t_i := 1 \cdot \text{day}$ Current_time $t := \text{TIME}$
the permanent load is applied;

See "Prestress Loss" Analysis for Volume-Surface Area Computation; $VS := 5.14 \text{ in}$ $VS = 130.556 \text{ mm}$

Use " t " and " VS " values to estimate Correction Factor - Creep Factor for the effect of the volume/surface area taken from Barker Fig. 7.13 (AASHTO Fig. 5.4.2.3.2-1). $k_c := 0.2$

$f_{cp_into_Pascal}$ $f_{cpPS} := 5500 \cdot \frac{lb}{in^2} \quad f_{cpPS} = 37.921 \text{ MPa}$

Correction Factor; $k_f := \frac{62 \cdot \text{MPa}}{42 \cdot \text{MPa} + f_{cpPS}} \quad k_f = 0.776 \quad k_f := \text{round}(k_f) = 1$

In AASHTO [A5.4.2.3.2], an empirical equation taken from Collins and Mitchell (1991) is given for the creep coefficient;

$$\psi := 3.5 \cdot k_c \cdot k_f \cdot \left(1.58 - \frac{RH}{120} \right) \cdot \left(\frac{t_i}{\text{day}} \right)^{-0.118} \cdot \frac{(t - t_i)^{0.6}}{10 \cdot \text{day}^{0.6} + (t - t_i)^{0.6}} \quad \psi = 0.516$$

Therefore; $E_{eLT3} := \frac{E_c}{1 + \Psi}$ $E_{eLT3} = [2.754 \cdot 10^6] \frac{lb}{in^2}$

Try the Barker method with a much longer t_i , to get a higher E_c ;

New_Time $t_{i2} := 60 \cdot \text{day}$

$$\Psi_2 := 3.5 \cdot k_c \cdot k_f \cdot \left(1.58 - \frac{RH}{120}\right) \cdot \left(\frac{t_{i2}}{\text{day}}\right)^{-0.118} \cdot \frac{(t - t_{i2})^{0.6}}{10 \cdot \text{day}^{0.6} + (t - t_{i2})^{0.6}} \quad \Psi_2 = 0.318$$

Therefore; $E_{eLT4} := \frac{E_c}{1 + \Psi_2}$ $E_{eLT4} = [3.166 \cdot 10^6] \frac{lb}{in^2}$

Finally, AASHTO recommends the following simple expression for the modulus of elasticity for permanent loads Barker [57].

$$E_{eLT5} := \frac{E_c}{3} \quad E_{eLT5} = [1.391 \cdot 10^6] \frac{lb}{in^2}$$

Summary;

Upper_Bound; $E_c = [4.173 \cdot 10^6] \frac{lb}{in^2}$

Lower_Bound; $E_{eLT1} = [1.127 \cdot 10^6] \frac{lb}{in^2}$ Ignore - short period (long term modulus recommended).

$$E_{eLT2} = [1.93 \cdot 10^6] \frac{lb}{in^2} \quad E_{eLT4} = [3.166 \cdot 10^6] \frac{lb}{in^2}$$

$$E_{eLT3} = [2.754 \cdot 10^6] \frac{lb}{in^2} \quad E_{eLT5} = [1.391 \cdot 10^6] \frac{lb}{in^2}$$

Final Modulus of Elasticity to be used for analysis after loss;

$$\max(E_{eLT2}, E_{eLT3}, E_{eLT4}, E_{eLT5}) = [3.166 \cdot 10^6] \frac{lb}{in^2}$$

Time Dependent - Elastic Shortening Losses

Estimating f_c' : $w_c := 145$

Tensile Strength

$f_{pm} := 270$

5 years $Ec1 := 3339 \cdot 10^3$ $kc1 := 0.17$ $f_{cp1} := \left(\frac{\frac{Ec1}{\left(\frac{w_c}{145}\right)^{1.5}} - 10^6}{40000} \right)^2$ $f_{cp1} = 3.419 \cdot 10^3$

10 years $Ec2 := 3276 \cdot 10^3$ $kc2 := 0.18$ $f_{cp2} := \left(\frac{\frac{Ec2}{\left(\frac{w_c}{145}\right)^{1.5}} - 10^6}{40000} \right)^2$ $f_{cp2} = 3.238 \cdot 10^3$

15 years $Ec3 := 3265 \cdot 10^3$ $kc3 := 0.18$ $f_{cp3} := \left(\frac{\frac{Ec3}{\left(\frac{w_c}{145}\right)^{1.5}} - 10^6}{40000} \right)^2$ $f_{cp3} = 3.206 \cdot 10^3$

30 years $Ec4 := 3174 \cdot 10^3$ $kc4 := 0.2$ $f_{cp4} := \left(\frac{\frac{Ec4}{\left(\frac{w_c}{145}\right)^{1.5}} - 10^6}{40000} \right)^2$ $f_{cp4} = 2.954 \cdot 10^3$

45 years $Ec5 := 3168 \cdot 10^3$ $kc4 := 0.2$ $f_{cp5} := \left(\frac{\frac{Ec5}{\left(\frac{w_c}{145}\right)^{1.5}} - 10^6}{40000} \right)^2$ $f_{cp5} = 2.938 \cdot 10^3$

50 years $Ec6 := 3166 \cdot 10^3$ $kc4 := 0.2$ $f_{cp6} := \left(\frac{\frac{Ec6}{\left(\frac{w_c}{145}\right)^{1.5}} - 10^6}{40000} \right)^2$ $f_{cp6} = 2.932 \cdot 10^3$

60 years $Ec7 := 3164 \cdot 10^3$ $kc4 := 0.2$ $f_{cp7} := \left(\frac{\frac{Ec7}{\left(\frac{w_c}{145}\right)^{1.5}} - 10^6}{40000} \right)^2$ $f_{cp7} = 2.927 \cdot 10^3$

APPENDIX E: PRESTRESS LOSS ANALYSIS

Calculating Effective Prestressing

(Approx. Lump Sum of Time-Dependent Losses - LRFD Article 5.9.5.3)

Prestressed Steel Information;

0.5" ϕ strands, Grade 270, low relaxation;

INPUT VALUES

Yield Strength $f_{py} := 240000 \cdot \frac{lb}{in^2}$

Tensile Strength

$f_{pu} := 270000 \cdot \frac{lb}{in^2}$

Modulus of Elasticity $E_p := 28000000 \cdot \frac{lb}{in^2}$

Span Length

$S_L := 60.25 \cdot ft$

Weight of Concrete $w_c := 150 \cdot \frac{lb}{ft^3}$

At transfer,

$f_{ci} := 4.5 \cdot 10^3 \cdot \frac{lb}{in^2}$

Modulus of Elasticity @ transfer: $E_{ct} := \left(57 \cdot \sqrt{f_{ci} \cdot \frac{in^2}{lb}} \right) \cdot 10^3 \cdot \frac{lb}{in^2}$

Initial prestress immediately prior to transfer, $f_i := 0.75 \cdot f_{pu}$ $f_i = (2.025 \cdot 10^5) \frac{lb}{in^2}$

Prestress immediately after transfer, $f_t := 0.93 \cdot f_i$ $f_t = (1.883 \cdot 10^5) \frac{lb}{in^2}$

Area of Prestress

$A_{ps} := 2.45 \cdot in^2$

Area of Girder

$A_G := 560 \cdot in^2$

Moment of Inertia (Girder)

$I_G := 125390 \cdot in^4$

Eccentricity (Girder)

$e_G := 16.27 \cdot in$

Moment (Girder)

$$M_{DC1} := \frac{w_c \cdot A_G \cdot S_L^2}{8}$$

Initial Prestressing force before stress losses

$$P_i := A_{ps} \cdot f_t$$

$P_i = (4.614 \cdot 10^5) lb$

The concrete stress at the center of gravity of prestressing tendons due to the prestressing force immediately after transfer

$$f_{cgp} := \frac{P_i}{A_G} + P_i \cdot \frac{e_G^2}{I_G} - M_{DC1} \cdot \frac{e_G}{I_G}$$

and the self-weight of the member at the section of maximum moment (ksi) - f_{cgp} .

$f_{cgp} = (1.386 \cdot 10^3) \frac{lb}{in^2}$

Calculate Prestress Loss Due to Elastic Shortening;

$$\Delta f_{pES} := \frac{E_p}{E_{ct}} \cdot f_{cgp} \quad \Delta f_{pES} = (1.015 \cdot 10^4) \frac{lb}{in^2}$$

Check: Prestress Immediately after transfer;

$$0.75 \cdot f_{pu} - \Delta f_{pES} = (1.924 \cdot 10^5) \frac{lb}{in^2} > f_t = (1.883 \cdot 10^5) \frac{lb}{in^2} \quad \text{OK}$$

Calculate Approximate Lump Sum of Time - Dependent Losses; (LRFD Article 5.9.5.3)

Assume Annual Average Relative Humidity, $RH = 60\%$

$$H = 60$$

Let the Humidity Constant

$$\gamma_h := 1.7 - 0.01 \cdot H \quad \gamma_h = 1.1$$

Let the Stress Constant (where $f_c' = 4.5 \text{ksi}$)

$$\gamma_{st} := \frac{5}{(1 + 4.5)} \quad \gamma_{st} = 0.909$$

The Prestress Loss Due to Relaxation of Prestressing steel for low relaxation strands (see Lubin Gao - Page 534)

$$\Delta f_{pR} := 2.4 \cdot 10^3 \cdot \frac{lb}{in^2}$$

$$APS := \frac{A_{ps}}{in^2} \quad APS = 2.45$$

$$FPR := \Delta f_{pR} \cdot \frac{in^2}{10^3 lb} \quad FPR = 2.4$$

$$AG := \frac{A_G}{in^2} \quad AG = 560$$

$$FT := f_t \cdot \frac{in^2}{10^3 lb} \quad FT = 188.325$$

Therefore the long-term losses of prestressing approximately;

$$\Delta f_{pLT} := \left(10.0 \cdot FT \cdot \frac{APS}{AG} \cdot \gamma_h \cdot \gamma_{st} + 12.0 \cdot \gamma_h \cdot \gamma_{st} + FPR \right) \cdot 10^3 \cdot \frac{lb}{in^2}$$

$$\Delta f_{pLT} = (2.264 \cdot 10^4) \frac{lb}{in^2}$$

Total Prestress Loss;

$$\Delta f_{pT} := \Delta f_{pES} + \Delta f_{pLT}$$

Therefore, the effective prestress;

$$f_{pe} := 0.75 \cdot f_{pu} - \Delta f_{pT}$$

$$f_{pe} = (1.697 \cdot 10^5) \frac{lb}{in^2}$$

Assume the following constants;

Prestress Modulus of Elasticity;

$$E_p := 28000$$

The concrete stress at the center of gravity of prestressing tendons due to the prestressing force immediately after transfer and the self-weight of the member at the section of maximum moment (ksi) - f_{cgp} .

$$f_{cgp} := 1.386$$

Lump Sum Time Dependent Losses - For standard precast, pretensioned members subject to normal loading and environmental conditions and pretensioned with low relaxation strands, the long-term prestress loss, due to creep of concrete, shrinkage of concrete, and relaxation of steel.

$$\Delta f_{pLT} := 22.6$$

Estimating E_{ct} based on Time Dependent f_{ci} ;

$$@ t = 0 \text{ years} \quad f_{ci,0} := 4500 \quad E_{ct,0} := 57 \cdot \sqrt{f_{ci,0}} = 3.824 \cdot 10^3$$

$$@ t = 30 \text{ years} \quad f_{ci,30} := f_{cp4} \quad E_{ct,30} := 57 \cdot \sqrt{f_{ci,30}} = 3.098 \cdot 10^3$$

$$@ t = 45 \text{ years} \quad f_{ci,45} := f_{cp5} \quad E_{ct,45} := 57 \cdot \sqrt{f_{ci,45}} = 3.089 \cdot 10^3$$

$$@ t = 60 \text{ years} \quad f_{ci,60} := f_{cp7} \quad E_{ct,60} := 57 \cdot \sqrt{f_{ci,60}} = 3.084 \cdot 10^3$$

Therefore Elastic Shortening Loss;

$$@ t = 0 \text{ years} \quad \Delta f_{pES,0} := \frac{E_p}{E_{ct,0}} \cdot f_{cgp} = 10.149 \quad @ t = 45 \text{ years} \quad \Delta f_{pES,45} := \frac{E_p}{E_{ct,45}} \cdot f_{cgp} = 12.562$$

$$@ t = 30 \text{ years} \quad \Delta f_{pES,30} := \frac{E_p}{E_{ct,30}} \cdot f_{cgp} = 12.527 \quad @ t = 60 \text{ years} \quad \Delta f_{pES,60} := \frac{E_p}{E_{ct,60}} \cdot f_{cgp} = 12.585$$

Therefore Total Prestress Losses & Effective Prestresses;

$$@ t = 0 \text{ years} \quad \Delta f_{pT,0} := \Delta f_{pES,0} + \Delta f_{pLT} = 32.749 \quad f_{pe,0} := 0.75 \cdot f_{pu} - \Delta f_{pT,0} = 169.751$$

$$@ t = 30 \text{ years} \quad \Delta f_{pT,30} := \Delta f_{pES,30} + \Delta f_{pLT} = 35.127 \quad f_{pe,30} := 0.75 \cdot f_{pu} - \Delta f_{pT,30} = 167.373$$

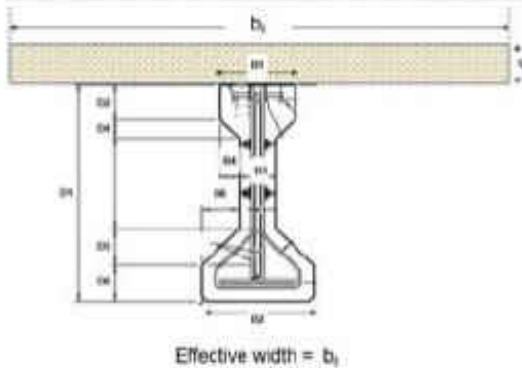
$$@ t = 45 \text{ years} \quad \Delta f_{pT,45} := \Delta f_{pES,45} + \Delta f_{pLT} = 35.162 \quad f_{pe,45} := 0.75 \cdot f_{pu} - \Delta f_{pT,45} = 167.338$$

$$@ t = 60 \text{ years} \quad \Delta f_{pT,60} := \Delta f_{pES,60} + \Delta f_{pLT} = 35.185 \quad f_{pe,60} := 0.75 \cdot f_{pu} - \Delta f_{pT,60} = 167.315$$

APPENDIX F: LOAD RATING & RELIABILITY ANALYSIS

General Information & Analysis (For Non-Linear Modeling)

Beam Section Dimensions



$$D1 := 45 \cdot \text{in} \quad B1 := 16 \cdot \text{in}$$

$$D2 := 7 \cdot \text{in} \quad B2 := 22 \cdot \text{in}$$

$$D3 := 0 \cdot \text{in} \quad B3 := 7.0 \cdot \text{in}$$

$$D4 := 4.5 \cdot \text{in} \quad B4 := 4.5 \cdot \text{in}$$

$$D5 := 7.5 \cdot \text{in} \quad B5 := 0 \cdot \text{in}$$

$$D6 := 7.0 \cdot \text{in} \quad B6 := 7.5 \cdot \text{in}$$

Section Properties (AASHTO) Type III Girder;

Cross - Section Area

$$A_{III} := 560 \cdot \text{in}^2$$

Distance from the center of gravity of the non-composite section to the bottom of the beam (in)

$$y_b := 20.27 \cdot \text{in}$$

Distance from the center of gravity of the non-composite section to the top of the beam (in)

$$y_t := D1 - y_b$$

$$y_t = 24.73 \text{ in}$$

Moment of Inertia

$$I_{III} := 125390 \cdot \text{in}^4$$

Perimeter Analysis;

$$S_1 := B1 \quad S_2 := 2 \cdot D2 \quad S_3 := (\sqrt{B4^2 + D4^2}) \cdot 2 \quad S_4 := (\sqrt{B6^2 + D5^2}) \cdot 2$$

$$S_5 := 2 \cdot (D1 - D2 - D4 - D5 - D6) \quad S_6 := 2 \cdot D6 \quad S_7 := B2$$

$$S := S_1 + S_2 + S_3 + S_4 + S_5 + S_6 + S_7 \quad S = 137.941 \text{ in}$$

Effective Flange Width Analysis - Interior Beam

Effective Span Length	$Span_L := 60 \cdot ft + 3 \cdot in$
Girder Spacing	$Girder_S := 9 \cdot ft + 3 \cdot in$
Average Thickness of Slab	$Slab_T := 8 \cdot in$
Web Thickness	$Web_T := B3$
Top Flange of Girder	$Flange_T := B1$

Analysis:

A) 1/4 of Effective Span Length $EFW_1 := \left(\frac{1}{4}\right) \cdot Span_L$ $EFW_1 = 180.75 \text{ in}$

B) a. Web Thickness $EFW_{2a} := Web_T$ b. 1/2 of top flange $EFW_{2b} := \left(\frac{1}{2}\right) \cdot Flange_T$

Therefore, $12 \cdot \text{Avg. Thk. of Slab} + \text{Greater of } 2a \text{ \& } 2b$

$$EFW_2 := 12 \cdot Slab_T + \max(EFW_{2a}, EFW_{2b})$$
 $EFW_2 = 104 \text{ in}$

C) Average Spacing of adjacent girders $EFW_3 := Girder_S$

$EFW_3 = 111 \text{ in}$

Therefore the Effective Flange Width $EFW := \min(EFW_1, EFW_2, EFW_3)$

$EFW = 104 \text{ in}$

Roadway Width $R_W := 114 \cdot ft$

Number Lanes $N_L := \frac{R_W}{3600 \cdot mm}$

$N_L = 9.652$

Hand Calculated Load Rating & Reliability Analysis

Maximum Load Placement for HL93 Truck

(Finding Maximum Moment: Determining HL93 Truck Position on Simple Spans - Cory L. Shipman)

Span Length (Input) $L_{span} := 60.25 \cdot ft$ Uniformly Distributed Lane Load: $w_{span} := 640 \cdot \frac{lb}{ft}$

Therefore the resultant for the truck from the 2nd axle $x_2 := \left(\frac{\left(\frac{L_{span}}{ft} \right)}{2} - \frac{447.2}{0.64 \cdot \left(\frac{L_{span}}{ft} \right) + 191.5} \right) \cdot ft$ $x_2 = 28.181 \cdot ft$

Solving the PCI (2003) Equations; $M_T := \left(\frac{\left(72 \cdot \frac{x_2}{ft} \cdot \left(\frac{L_{span} - x_2}{ft} \right) - 4.67 \right)}{\frac{L_{span}}{ft}} - 112 \right) \cdot 10^3 \cdot lb \cdot ft$
(kip-ft/lane)

$$M_L := \frac{w_{span} \cdot x_2}{2} \cdot (L_{span} - x_2) \quad M_L = (2.892 \cdot 10^5) \cdot lb \cdot ft \quad M_T = (8.107 \cdot 10^5) \cdot lb \cdot ft$$

Therefore applying the dynamic load allowance & the summing the moments - Live Load Moment for HL93 Truck per lane: $M_{LLI} := (M_T + M_L)$ $M_{LLI} = (1.32 \cdot 10^7) \cdot lb \cdot in$

Nominal Flexural Load Analysis (Dead Load - DC)

Effective_Width $b_{eff} := 111 \cdot in$ Future_Wearing_Surface $FW := 2.0 \cdot in$

Weight_Conc $C_{wt} := 150 \cdot \frac{lb}{ft^3}$ Deck_Thickness $t_s := 8 \cdot in$

Girder Spacing "b" (max. spacing 9' - 3") - Using Effective Area $Girder_s := 9.25 \cdot ft$

Traditionally, dead load positive and negative moments in the deck, except for the overhang, for a unit width strip of the deck are calculated using the following approach; $M = wl^2/c$.

Where;

M = Dead load positive or negative moment in the deck for a unit width strip (k-ft/ft)

w = Dead load per unit area of the deck (ksf)

l = Girder spacing (ft)

c = Constant, typically taken as 10 or 12 (Dead load moment due to the self weight will be assumed to be 10)

Therefore;	Constant	$Const := 10$
	Self - Weight of Deck	$D_{SW} := (t_s \cdot C_{wt}) = 100 \frac{lb}{ft^2}$
	Unfactored self weight positive or negative moment	$M_{SW} := \frac{D_{SW} \cdot (Girder_s^2)}{Const}$
	Unfactored self weight positive or negative moment (full span)	$M_{Deck} := M_{SW} \cdot L_{span}$ $M_{Deck} = (6.186 \cdot 10^5) lb \cdot in$
	Self - Weight of Future Wearing Surface	$F_{SW} := (FW \cdot C_{wt}) = 25 \frac{lb}{ft^2}$
	Unfactored self weight positive or negative moment	$M_{FW} := \frac{F_{SW} \cdot (Girder_s^2)}{Const}$
	Unfactored self weight positive or negative moment (full span)	$M_{FWS} := M_{FW} \cdot L_{span}$ $M_{FWS} = (1.547 \cdot 10^6) lb \cdot in$
Total Dead Load	$M_{DC} := M_{FWS} + M_{Deck}$	$M_{DC} = (7.733 \cdot 10^5) lb \cdot in$
Nominal Flexural Resistance at Maximum Positive Moment Section		
Span where maximum positive moments occurs: Spans 2 & 3		
Girder Type: AASHTO Type III		
Procedure specified in LRFD 5.7.3 will be used to compute the flexural resistance.		
Prestressed Steel Information:		
For the Type III Beam - 16 - 1/2" ϕ strands, Grade 270, low relaxation (Bottom)		
(See 252A Bridge Calcs)		
Yield Strength	$f_{py} := 240000 \cdot \frac{lb}{in^2}$	Tensile Strength
		$f_{pu} := 270000 \cdot \frac{lb}{in^2}$
Value of "k" (LRFD Table C5.7.3.1.1-1) for Low - relaxation strand		$k_{LR} := 0.28$
Area of 1/2" Strand (Caltrans - LRFD Bridge Design Aids 6 - 4) June 2012		$A_{p12} := 0.153 \cdot in^2$

Number of 1/2" Strands (see 11/139 - 252A Bridge Design Calcs)	$N_{12} := 16$
Total Area of prestressed strands $A_{ps} := (N_{12} \cdot A_{p12})$	$A_{ps} = 2.448 \text{ in}^2$
Compressive strength of Concrete Deck;	$f_{cd} := 4500 \cdot \frac{\text{lb}}{\text{in}^2}$
For the β_1 analysis used f_{cdd} ;	$f_{cdd} := 4.5$
The β_1 factor for the stress block since $f_c' > 4\text{ksi}$	$\beta_1 := 0.85 - 0.05 \cdot (f_{cdd} - 4) \quad \beta_1 = 0.825$
Deck Thickness $t_s := 8 \cdot \text{in}$	Area of Girder (Type III) $A_G := 560 \cdot \text{in}^2$
Depth of Girder (Type III) $d_G := 45 \cdot \text{in}$	Moment of Inertia (Type III) $I_G := 125390 \cdot \text{in}^4$
Therefore the c.g. of prestressed strands concentration (Eccentricity @ C.L. see 11/139 - 252A Bridge Calcs)	$PScg := 3 \cdot \text{in}$
And hence the depth of prestressed strands $d_p := d_G + t_s - PScg$	$d_p = 50 \text{ in}$
Assume that NA is located in the concrete deck, i.e. a rectangular section:	
Therefore the distance from extreme compression fiber to neutral axis;	
$c_{\text{defined}} := \frac{A_{ps} \cdot f_{ps}}{0.85 \cdot f_{cd} \cdot \beta_1 \cdot \text{Girder}_S + k_{LR} \cdot \frac{A_{ps} \cdot f_{ps}}{d_p}} = 1.867 \text{ in}$	
$c := \frac{2.448 \cdot 270}{0.85 \cdot 4.5 \cdot 0.825 \cdot 111 + 0.28 \cdot 2.448 \cdot \frac{270}{50}} \cdot \text{in} = 1.867 \text{ in} < 8'' \text{ (Rect. Sect.)}$	
Therefore the depth of equivalent rectangular stress block $a := \beta_1 \cdot c$	$a = 1.54 \text{ in}$
Hence the stress in prestressed reinforcement at nominal strength;	
$f_{ps} := f_{ps} \cdot \left(1 - k_{LR} \cdot \frac{c}{d_p}\right) \quad f_{ps} = (2.672 \cdot 10^5) \frac{\text{lb}}{\text{in}^2}$	
The nominal flexural resistance is;	$M_{nP_{08}} := A_{ps} \cdot f_{ps} \cdot \left(d_p - \frac{a}{2}\right) \quad M_{nP_{08}} = (3.22 \cdot 10^7) \text{ lb} \cdot \text{in}$
	$M_r := M_{nP_{08}}$

Reliability Index, β (HL - 93 - Interior Girder: Critical Section)

Linear Limit State Functions

This expression must be adapted for the current study, considering load effects and resistance in bending:

<i>Bias Factors (λ):</i>		<i>Coefficient of Variations:</i>	
<i>Bias_Factor_for_Resistance</i>	$\lambda_R := 1.05$	<i>Coef._of_var_for_LL</i>	$C_{vLL} := 18\%$
<i>Bias_Factor_for_Live_Load</i>	$\lambda_{LL} := 1.0$	<i>Coef._of_var_for_Resistance</i>	$C_{vR} := 7.5\%$
<i>Bias_Factor_for_Dead_Load</i>	$\lambda_{DC} := 1.05$	<i>Coef._of_var_for_DC</i>	$C_{vDC} := 10\%$

Bias & Coefficient of Variations (COV) Notes:

- Live Load Effect: Assume statistical parameters for "Live Load and Dynamic Load" Table 8.4, page 279 (Nowak and Collins 2013). A range of 1.0 - 1.8 is given for the bias (use 1.0 to be conservative).
- Dead Load Effect: Assume the values for bias and COV of Cast-In-Place components (conservative choice) from Table 8.4, page 279 (Nowak and Collins 2013). These values are adapted from LRFD Calibration (Nowak, 1993).
- Resistance Effect: Assume statistical parameters of resistance from Table 8.5, page 279 for bias and COV of Prestressed (Nowak and Collins 2013).

Analysis:

1. Compute the nominal load and resistance effects:

$$\begin{array}{ll} \text{Live_Load_Effect} & M_{LL} := M_{LLI} \\ \text{Dead_Load_Effect} & M_{DL} := M_{DC} \\ \text{Resistance} & M_R := M_{res} \end{array}$$

2. Compute the means of load and resistance effects:

$$\begin{array}{ll} \text{Mean_Live_Load} & \mu_{LL} := \lambda_{LL} \cdot M_{LL} & \mu_{LL} = (1.1 \cdot 10^6) \text{ lb} \cdot \text{ft} \\ \text{Mean_Dead_Load} & \mu_{DL} := \lambda_{DC} \cdot M_{DL} & \mu_{DL} = (6.766 \cdot 10^4) \text{ lb} \cdot \text{ft} \\ \text{Mean_Resistance} & \mu_R := \lambda_R \cdot M_R & \mu_R = (2.817 \cdot 10^6) \text{ lb} \cdot \text{ft} \end{array}$$

3. Compute the standard deviations of load and resistance effects:

$$\begin{array}{ll} \text{Standard_Deviation_Live_Load} & \sigma_{LL} := C_{vLL} \cdot \mu_{LL} & \sigma_{LL} = (1.98 \cdot 10^5) \text{ lb} \cdot \text{ft} \\ \text{Standard_Deviation_Dead_Load} & \sigma_{DL} := C_{vDC} \cdot \mu_{DL} & \sigma_{DL} = (6.766 \cdot 10^3) \text{ lb} \cdot \text{ft} \end{array}$$

Standard_Deviation_Resistance

$$\sigma_R := C_{vR} \cdot \mu_R$$

$$\sigma_R = (2.113 \cdot 10^5) \text{ lb} \cdot \text{ft}$$

4. Compute the reliability index:

The mean of the loads:

$$\mu_D := \mu_{DL} + \mu_{LL}$$

The mean of the random number g:
(mean of all resistance minus all loads)

$$\mu_g := \mu_R - \mu_D$$

The standard deviation of the
random number g:

$$\sigma_g := \sqrt{\sigma_R^2 + \sigma_{DL}^2 + \sigma_{LL}^2}$$

The reliability index is:

$$\beta := \frac{\mu_g}{\sigma_g} \quad \beta = 5.696$$

Load Rating

$$RF := \frac{M_r - M_{DC}}{M_{LL}}$$

$$RF = 2.381$$

Linear Load Rating & Reliability Analysis

[Nonlinear Analysis Program (NAP) - Dr. Kevin Mackie]

BOUNDARY CONDITION: PIN

Dead Load - NAP

$$M_{DC} := 805.3 \cdot 10^3 \cdot lb \cdot in$$

Live Load Moment (HL93) - NAP

$$M_{LL} := 10890 \cdot 10^3 \cdot lb \cdot in$$

$$M_{LL} := M_{LL}$$

Capacity- NAP

$$M_c := 28940 \cdot 10^3 \cdot lb \cdot in$$

$$M_r := M_c$$

Reliability Index, β (HL - 93 - Interior Girder: Critical Section)

Bias Factors (λ):

Defined as the ratio of the mean value of a variable to its nominal value (i.e., the value specified in a standard or code).

Bias_Factor_for_Resistance

$$\lambda_R := 1.05$$

Bias_Factor_for_Live_Load

$$\lambda_{LL} := 1.0$$

Bias_Factor_for_Dead_Load

$$\lambda_{DC} := 1.05$$

Coefficient of Variations:

Coef._of_variation_for_LL

$$C_{vLL} := 18\%$$

Coef._of_variation_for_Resistance

$$C_{vR} := 7.5\%$$

Coef._of_variation_for_DC

$$C_{vDC} := 10\%$$

Bias & Coefficient of Variations(COV) Notes:

- Live Load Effect: Assume statistical parameters for "Live Load and Dynamic Load" Table 8.4, page 279 (Nowak and Collins 2013). A range of 1.0 - 1.8 is given for the bias (use 1.0 to be conservative).

- Dead Load Effect: Assume the values for bias and COV of Cast-In-Place components (conservative choice) from Table 8.4, page 279 (Nowak and Collins 2013). These values are adapted from LRFD Calibration (Nowak, 1993).

- Resistance Effect: Assume statistical parameters of resistance from Table 8.5, page 279 for bias and COV of Prestressed (Nowak and Collins 2013).

Analysis;

1. Compute the nominal load and resistance effects:

$$\text{Live_Load_Effect} \quad M_{LL} := M_{LL}$$

$$\text{Dead_Load_Effect} \quad M_{DL} := M_{DC}$$

$$\text{Resistance_Load_Effect} \quad M_R := M_r$$

2. Compute the means of load and resistance effects:

$$\text{Mean_Live_Load} \quad \mu_{LL} := \lambda_{LL} \cdot M_{LL} \quad \mu_{LL} = (9.075 \cdot 10^5) \text{ lb} \cdot \text{ft}$$

$$\text{Mean_Dead_Load} \quad \mu_{DL} := \lambda_{DC} \cdot M_{DL} \quad \mu_{DL} = (7.046 \cdot 10^4) \text{ lb} \cdot \text{ft}$$

$$\text{Mean_Resistance} \quad \mu_R := \lambda_R \cdot M_R \quad \mu_R = (3.039 \cdot 10^7) \text{ lb} \cdot \text{in}$$

3. Compute the standard deviations of load and resistance effects:

$$\text{Standard_Deviation_Live_Load} \quad \sigma_{LL} := C_{vLL} \cdot \mu_{LL} \quad \sigma_{LL} = (1.634 \cdot 10^5) \text{ lb} \cdot \text{ft}$$

$$\text{Standard_Deviation_Dead_Load} \quad \sigma_{DL} := C_{vDC} \cdot \mu_{DL} \quad \sigma_{DL} = (7.046 \cdot 10^3) \text{ lb} \cdot \text{ft}$$

$$\text{Standard_Deviation_Resistance} \quad \sigma_R := C_{vR} \cdot \mu_R \quad \sigma_R = (2.279 \cdot 10^6) \text{ lb} \cdot \text{in}$$

4. Compute the reliability index:

The mean of the loads; $\mu_D := \mu_{DL} + \mu_{LL}$

The mean of the random number g;
(mean of all resistance minus all loads) $\mu_g := \mu_R - \mu_D = (1.865 \cdot 10^7) \text{ lb} \cdot \text{in}$

The standard deviation of the random number g: $\sigma_g := \sqrt{\sigma_R^2 + \sigma_{DL}^2 + \sigma_{LL}^2} = (3.007 \cdot 10^6) \text{ lb} \cdot \text{in}$

The reliability index is; $\beta := \frac{\mu_g}{\sigma_g} \quad \beta = 6.202$

Load Rating

$$RF := \frac{M_r - M_{DC}}{M_{LL}} \quad RF = 2.584$$

Nonlinear Load Rating & Reliability Analysis

[Nonlinear Analysis Program (NAP) - Dr. Kevin Mackie]

(The following results obtained using "Load Type 2" in NAP) - see raw data.

Upper Bound Area:	$A_{psU} := 2.46$	Upper Bound Area Capacity:	$AU_c := 911.7$
Mean Area:	$A_{psM} := 2.45$	Mean Area Capacity:	$AM_c := 901.2$
Lower Bound Area:	$A_{psL} := 2.44$	Lower Bound Area Capacity:	$AL_c := 890.6$
Upper Bound Prestress:	$f_{psU} := 260$	Upper Bound Prestress Capacity:	$fU_c := 29070$
Mean Prestress:	$f_{psM} := 250$	Mean Prestress Capacity:	$fM_c := 28940$
Lower Bound Prestress:	$f_{psL} := 240$	Lower Bound Prestress Capacity:	$fL_c := 28680$
Applied Load 1	$L_1 := 10$	Max. Capacity	$MU_c := 28940$
Applied Load 2	$L_2 := 10.1$	Mean Capacity	$M_c := 28860$
Applied Load 3	$L_3 := 9.9$	Min. Capacity	$ML_c := 28850$

For the Dead Load Analysis, the Self Weight of the Girder and Deck were estimated by varying the thickness of the slab $t_s = 10.5"$, $10.0"$ and $9.5"$ for the perturbation... (2" of Wearing Surface added to 8" of Slab)

Effective width $b_{eff} := 111 \cdot \text{in}$ Span Length $L_{span} := 60.25 \cdot \text{ft}$

Weight Conc. $C_w := 150 \cdot \frac{\text{lb}}{\text{ft}^3}$ Weight Type III $W_3 := 583 \cdot \frac{\text{lb}}{\text{ft}}$ Slab Thickness $t_s := \begin{bmatrix} 10.5 \\ 10 \\ 9.5 \end{bmatrix} \cdot \text{in}$

Dead Load - Self Weight $DL := (W_3 + (t_s \cdot C_w \cdot b_{eff})) \cdot L_{span} = \begin{bmatrix} 1.083 \cdot 10^6 \\ 1.048 \cdot 10^6 \\ 1.013 \cdot 10^6 \end{bmatrix} \text{ lb}$

Upper Bound DL; (For $t_s = 10.5"$)	$D_u := 108.3$ $D_1 := 10.5$	Upper Bound DL Capacity:	$DU_c := 785$
Mean DL; (For $t_s = 10.0"$)	$D_m := 104.8$ $D_2 := 10.0$	Mean DL:	$DM_c := 805.3$
Lower Bound DL; (For $t_s = 9.5"$)	$D_l := 101.3$ $D_1 := 9.5$	Lower Bound DL:	$DL_c := 828$

(The following results obtained using "Load Type 1" in NAP) - see raw data.

Upper Bound Applied Load:	$Q_{MU} := 8.1 + 32.1 + 32.1$	Upper Bound Applied Load; $Q_U := 0.1$	$QU_c := 10920$
Mean Applied Load:	$Q_M := 8 + 32 + 32$	Mean Applied Load; $Q_m := 0.0$	$QM_c := 10890$
Lower Bound Applied Load:	$Q_{ML} := 7.9 + 31.9 + 31.9$	Lower Bound Applied Load; $Q_L := -0.1$	$QL_c := 10860$

Perturbations (h)

Area:	$h_A := A_{psU} - A_{psM} = 0.01$	Prestress:	$h_f := f_{psU} - f_{psM} = 10$
Load:	$h_Q := Q_U - Q_m = 0.1$	Dead Load:	$h_D := D_1 - D_2 = -0.5$
Cap/Resist:	$h_R := L_1 - L_2 = -0.1$		

Bias & Coefficient of Variations(COV) Notes (CAPACITY):

- Resistance Effect: Assume statistical parameters of resistance from Table 8.5, page 279 for bias and COV of Prestressed (Nowak and Collins 2013).

Bias_Factor_for_Resist. $\lambda_R := 1.05$ Coef._of_variation_for_Resist. $C_{vR} := 7.5\%$

Mean_Resistance $\mu_R := \lambda_R \cdot L_2 = 10.605$ Std_Resistance $S_R := C_{vR} \cdot \mu_R = 0.795$

Bias & Coefficient of Variations(COV) Notes (LIVE LOAD):

-Live Load Effect: Assume statistical parameters for "Live Load and Dynamic Load" Table 8.4, page 279 (Nowak and Collins 2013). A range of 1.0 - 1.8 is given for the bias (use 1.0 to be conservative) and 0.18 for coefficient of variation.

Bias_Factor_for_Live_Load $\lambda_{LL} := 1.0$ Coef._of_variation_for_LL $C_{vLL} := 18\%$

Mean_Live_Load $\mu_{LL} := \lambda_{LL} \cdot Q_M$ Std_Live_Load $S_Q := C_{vLL} \cdot \mu_{LL}$

Bias & Coefficient of Variations(COV) Notes (DEAD LOAD):

-Dead Load Effect: Assume the values for bias and COV of Cast-In-Place components (conservative choice) from Table 8.4, page 279 (Nowak and Collins 2013). These values are adapted from LRFD Calibration (Nowak, 1993).

Bias_Factor_for_Dead_Load $\lambda_{DC} := 1.05$ Coef._of_variation_for_DC $C_{vDC} := 10\%$

Mean_Dead_Load $\mu_{DL} := \lambda_{DC} \cdot D_m$ Std_Dead_Load $S_{DL} := C_{vDC} \cdot \mu_{DL}$

Bias & Coefficient of Variations(COV) Notes (PRESTRESS):

Source for A_{ps} & f_{ps} - Uncertainties in Material Strength, Geometric, and Load Variables - Hess P., Bruchman D., Assakkaf I., & Ayyub B.

Coef._of_var._fps $C_{vf} := 0.075$ Mean_fps $\mu_f := 1.05 \cdot f_{psM}$ Std_fps $S_f := C_{vf} \cdot \mu_f$

Bias & Coefficient of Variations(COV) Notes (AREA):

Reliability - based sensitivity analysis for prestressed concrete girder bridges - Rakoczy A. and Nowak A.

Coef._of_var._Aps $C_{vA} := 0.015$ Mean_Aps $\mu_A := A_{psM}$ Std_Aps $S_A := C_{vA} \cdot \mu_A$

The Partial Derivatives;

Area: $g(x+h)$ $A_{xh} := AU_c$ $g(x)$ $A_x := AM_c$

$$\frac{g(x+h) - g(x)}{h} \quad \sigma_A := \frac{A_{xh} - A_x}{h_A} \quad \sigma_A = 1.05 \cdot 10^3$$

Prestress: $g(x+h)$ $f_{xh} := fU_c$ $g(x)$ $f_x := fM_c$

$$\frac{g(x+h) - g(x)}{h} \quad \sigma_f := \frac{f_{xh} - f_x}{h_f} \quad \sigma_f = 13$$

Live Load: $g(x+h)$ $Q_{xh} := QM_c$ $g(x)$ $Q_x := QL_c$

$$\frac{g(x+h) - g(x)}{h} \quad \sigma_Q := \left(\frac{Q_{xh} - Q_x}{h_Q} \right) \quad \sigma_Q = 300$$

Dead Load: $g(x+h)$ $D_{xh} := DM_c$ $g(x)$ $D_x := DL_c$

$$\frac{g(x+h) - g(x)}{h} \quad \sigma_D := \left(\frac{D_{xh} - D_x}{h_D} \right) \quad \sigma_D = 45.4$$

Cap/ Resist: $g(x+h)$ $R_{xh} := ML_c$ $g(x)$ $R_x := M_c$

$$\frac{g(x+h) - g(x)}{h} \quad \sigma_R := \left(\frac{R_{xh} - R_x}{h_R} \right) \quad \sigma_R = 100$$

Compute the reliability index:

To calculate β , the partial derivatives must be determined and the limit state function must be evaluated at the mean values of the random variables:

$$g_{rv} := M_c - QM_c - DM_c = 1.716 \cdot 10^4$$

$$\sigma_g := \sqrt{(S_A \cdot \sigma_A)^2 + (S_f \cdot \sigma_f)^2 + (S_Q \cdot \sigma_Q)^2 + (S_{DL} \cdot \sigma_D)^2 + (S_R \cdot \sigma_R)^2} = 3.929 \cdot 10^3$$

The reliability index is:

$$\beta := \frac{g_{rv}}{\sigma_g}$$

$$\beta = 4.368$$

$$RF := \frac{MU_c - DM_c}{QM_c} = 2.584$$

$$RF = 2.584$$

Linear & Nonlinear Variability Analysis and Plots

[Capacity/Resistance & Limit State Function Means & Standard Deviations]

If D and R are normally distributed with a mean of μ_D and μ_R , and a standard deviation of σ_D and σ_R , g will be normally distributed too.

The capacity and demand are random variables. The normal distribution is typically adequate to describe both capacity and force demand, considering the upper tail of the demand probability density curve and the lower tail of the capacity probability density curve. The probability density function of the capacity and demand can be expressed as follows;

$$f(R) := \frac{1}{\sigma_R \cdot \sqrt{2 \cdot \pi}} \cdot e^{-\left(\frac{1}{2} \cdot \left(\frac{R - \mu_R}{\sigma_R}\right)^2\right)} \quad \sigma_R := 1 \quad \mu_R := 1$$

From the mean and standard deviation results, the normal plots were investigated since the normal random variable is the most important distribution in structural reliability theory.

Normal random variable PDF is symmetrical about the mean.

*Capacity/Resistance Mean & Standard Deviation
(from Linear Limit State Function Analysis)*

$$\mu_{CR, Lin} := 3.039 \cdot 10^7$$

$$\sigma_{CR, Lin} := 2.279 \cdot 10^6$$

*Limit State Function Mean & Standard Deviation
(from Linear Limit State Function Analysis)*

$$\mu_{g, Lin} := 1.865 \cdot 10^7$$

$$\sigma_{g, Lin} := 3.007 \cdot 10^6$$

*Capacity/Resistance Mean & Standard Deviation
(from Nonlinear Limit State Function Analysis)*

$$\mu_{CR, NonLin} := 3.03 \cdot 10^7$$

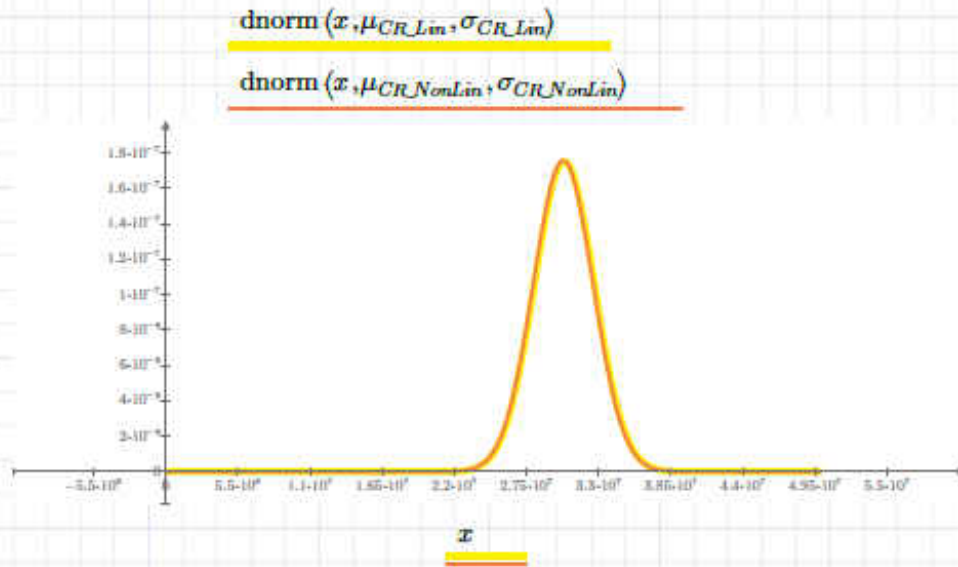
$$\sigma_{CR, NonLin} := 2.273 \cdot 10^6$$

*Limit State Function Mean & Standard Deviation
(from Nonlinear Limit State Function Analysis)*

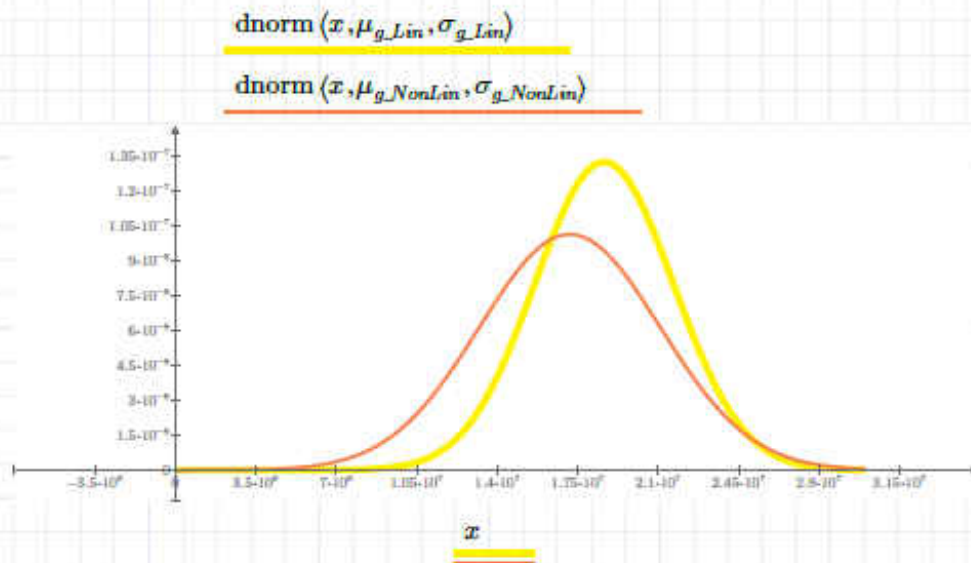
$$\mu_{g, NonLin} := 1.716 \cdot 10^7$$

$$\sigma_{g, NonLin} := 3.929 \cdot 10^6$$

Linear & Nonlinear Capacity/Resistance Plots



Linear & Nonlinear Limit State Function Plots



NAP Nonlinear Variability Analysis

NAP - Run 1	Nominal Values	Live Load (1)	Capacity (2)
Area (Aps)	2.45		
Prestress (fps)	250		
Live Load (Q)	$8 + 32 + 32 = 72$		

Area

```

Editor - C:\Users\Chris\Dropbox\Adjah Mackie\NAP_v1r6\Chris_bridge_simple_firstv3A.m
elasticBeam.m Chris_bridge_simple_firstv3A.m
232 - ElData(i).coordTransf = 'linearTransformation';
233 - end
234
235 % truss elements for pre-stressing tendons
236 - Aps = 2.45;
237 - % pre-stressing force
238 % need to figure out the pre-stressing force (not the capacity)
239 - epsps = fps/Ep/2;
240
241 - trusseln=[1 2 3 4 5 6 7 8 9 10];
242
243 - for i = trusseln,

```

Prestress

```

Editor - C:\Users\Chris\Dropbox\Adjah Mackie\NAP_v1r6\Chris_bridge_simple_firstv3A.m
elasticBeam.m Chris_bridge_simple_firstv3A.m
155 % Member properties
156 - Astop = 1e-4; % area of top steel
157 - Asbot = 1e-4; % area of bottom steel
158 - Asslab = 1e-4; % area of slab steel
159
160 - Ep = 30000; % prestress elastic modulus [kin^2]
161 - fps = 250; % prestress strength
162 - fy = 60; % steel yield strength
163 - Eh = 0.0015; % hardening ratio
164 - Ed = 3605; % deck elastic modulus [kin^2]
165 - fcd = 4; % deck compressive strength
166 - epsd0 = 2*fcd/Ed;

```

Live Load

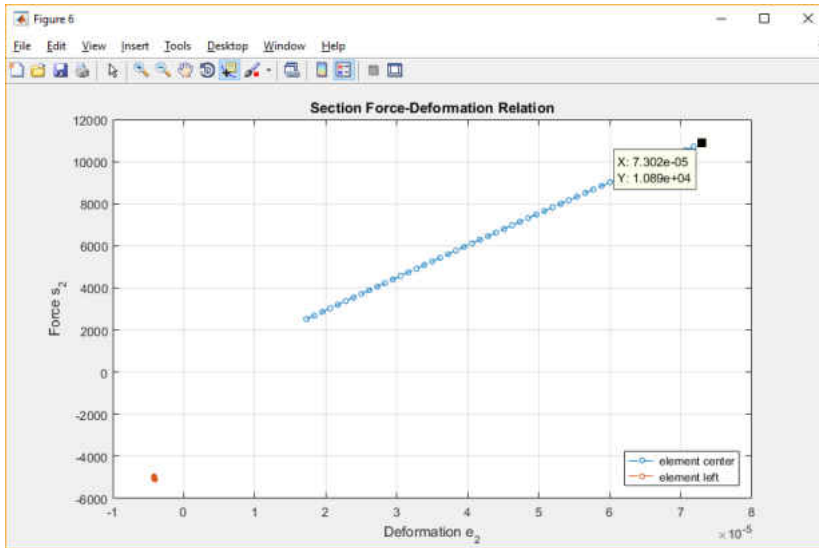
```

Editor - C:\Users\Chris\Dropbox\Adjah Mackie\NAP_v1r6\Chris_bridge_simple_firstv3A.m
elasticBeam.m Chris_bridge_simple_firstv3A.m
286 % Ue(8,1) = -40;
287
288 - if LOAD_TYPE == 1
289 - scale = 1;
290 - Pe(14,2) = -8 * scale;
291 - Pe(16,2) = -32 * scale;
292 - Pe(18,2) = -32 * scale;
293 - elseif LOAD_TYPE == 2
294 - %Pe(center_node,2) = -225;
295 - Ue(center_node,2) = -10.0e-0;
296 - end
297

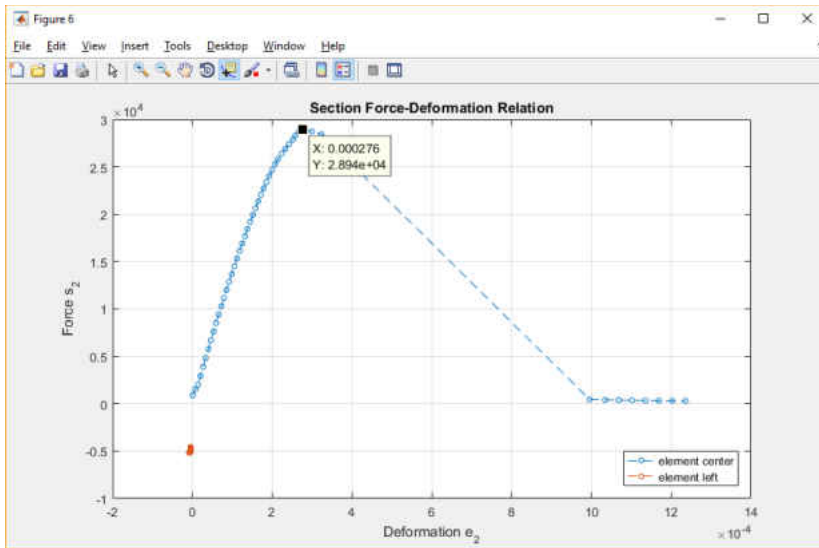
```

Results

Live Load (when LOAD TYPE = 1)



Capacity (when LOAD TYPE = 2)



NAP - Run 1	Nominal Values	Live Load (1)	Capacity (2)
Area (Aps)	2.45	10890	28940
Prestress (fps)	250	10890	28940
Live Load (Q)	8 + 32 + 32 = 72	10890	28940

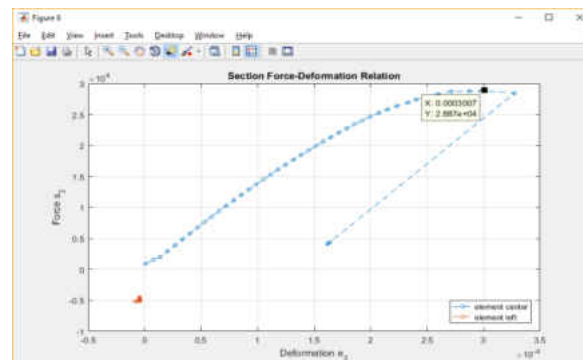
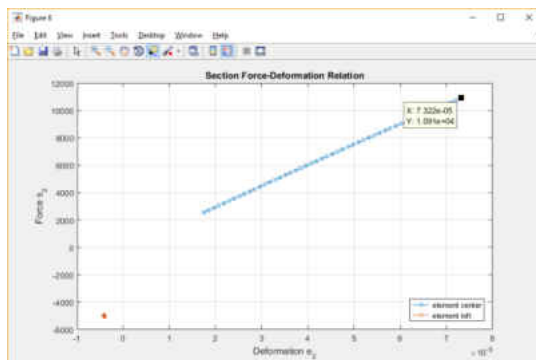
NAP - Run 2	Variable Area	Live Load (1)	Capacity (2)
Area (Aps)	2.44		
Prestress (fps)	250		
Live Load (Q)	8 + 32 + 32 = 72		

```

Editor - C:\Users\Chris\Dropbox\Adjah Mackie\NAP_v1r6\Chris_bridge_simple_firstv3A.m
elasticBeam.m  Chris_bridge_simple_firstv3A.m
231 -         end;
232 -         ElData(i).coordTransf = 'linearTransformation';
233 -     end
234
235 - % truss elements for pre-stressing tendons
236 - Aps = 2.44;
237 -     eps = sqrt(Aps);
238 - % need to figure out the pre-stressing force (not the capacity)
239 -     epsps = fps/Ep/2;
240
241 -     trusseln=[1 2 3 4 5 6 7 8 9 10];
242

```

Live Load/Capacity Plots



NAP - Run 2	Variable Area	Live Load (1)	Capacity (2)
Area (Aps)	2.44	10910	28870
Prestress (fps)	250	10910	28870
Live Load (Q)	8 + 32 + 32 = 72	10910	28870

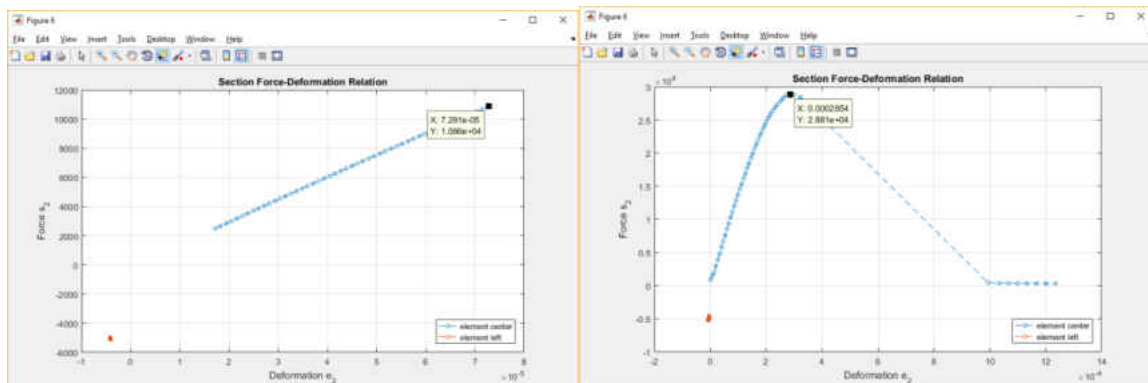
NAP - Run 3	Variable Area	Live Load (1)	Capacity (2)
Area (Aps)	2.46		
Prestress (fps)	250		
Live Load (Q)	$8 + 32 + 32 = 72$		

```

Editor - C:\Users\Chris\Dropbox\Adjah Mackie\NAP_v1r0\Chris_bridge_simple_firstv3A.m*
elasticBeam.m  Chris_bridge_simple_firstv3A.m*
231 -         end;
232 -         ElData{1}.coordTransf = 'linearTransformation';
233 -     end
234 -
235 -     % truss elements for pre-stressing tendons
236 -     Aps = 2.46;
237 -     eps = sqrt(Aps);
238 -     % need to figure out the pre-stressing force (not the capac
239 -     epsps = fps/Ep/2;
240 -
241 -     trusseln=[1 2 3 4 5 6 7 8 9 10];
242 -

```

Live Load/Capacity Plots



NAP - Run 3	Variable Area	Live Load (1)	Capacity (2)
Area (Aps)	2.46	10860	28810
Prestress (fps)	250	10860	28810
Live Load (Q)	$8 + 32 + 32 = 72$	10860	28810

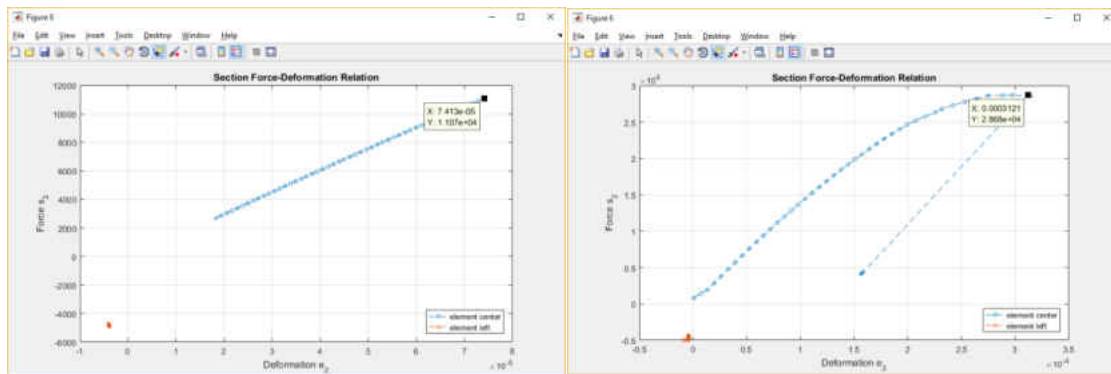
NAP - Run 4	Variable Prestress	Live Load (1)	Capacity (2)
Area (Aps)	2.45		
Prestress (fps)	240		
Live Load (Q)	8 + 32 + 32 = 72		

```

Editor - C:\Users\Chris\Dropbox\Adjah Mackie\NAP_v1r6\Chris_bridge_simple_firstv3A.m*
elasticBeam.m  Chris_bridge_simple_firstv3A.m*
154
155  % Member properties -----
156 - Astop = 1e-4;           % area of top steel
157 - Asbot = 1e-4;         % area of bottom steel
158 - Asslab = 1e-4;        % area of slab steel
159
160 - Ep = 28000;           % prestress elastic modulus [kin^2]
161 - fps = 240;           % prestress strength
162 - fy = 60;             % steel yield strength
163 - Eh = 0.0015;         % hardening ratio
164 - Ed = 3605;           % deck elastic modulus [kin^2]
165 - fcd = 4;             % deck compressive strength

```

Live Load/Capacity Plots



NAP - Run 4	Variable Prestress	Live Load (1)	Capacity (2)
Area (Aps)	2.45	11070	28680
Prestress (fps)	240	11070	28680
Live Load (Q)	8 + 32 + 32 = 72	11070	28680

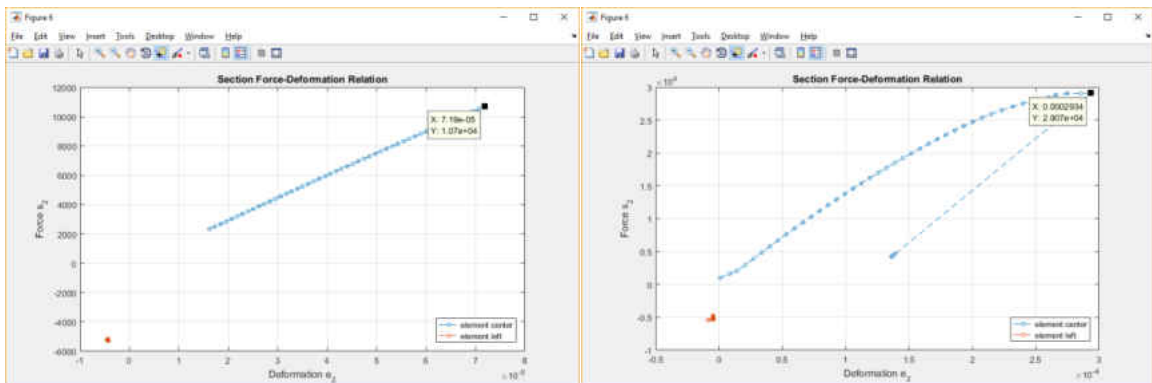
NAP - Run 5	Variable Prestress	Live Load (1)	Capacity (2)
Area (Aps)	2.45		
Prestress (fps)	260		
Live Load (Q)	8 + 32 + 32 = 72		

```

Editor - C:\Users\Chris\Dropbox\Adjah Mackie\NAP_v1r6\Chris_bridge_simple_firstv3A.m
elasticBeam.m  Chris_bridge_simple_firstv3A.m
% member properties
156 - Astop = 1e-4;           % area of top steel
157 - Asbot = 1e-4;         % area of bottom steel
158 - Asslab = 1e-4;        % area of slab steel
159
160 - Ep = 28000;           % prestress elastic modulus [kin^2]
161 - fps = 260;           % prestress strength
162 - fy = 60;             % steel yield strength
163 - Eh = 0.0015;         % hardening ratio
164 - Ed = 3605;           % deck elastic modulus [kin^2]
165 - fcd = 4;             % deck compressive strength
166 - epsd0 = 2*fcd/Ed;
167 - epsdu = 0.004;

```

Live Load/Capacity Plots



NAP - Run 5	Variable Prestress	Live Load (1)	Capacity (2)
Area (Aps)	2.45	10700	29070
Prestress (fps)	260	10700	29070
Live Load (Q)	8 + 32 + 32 = 72	10700	29070

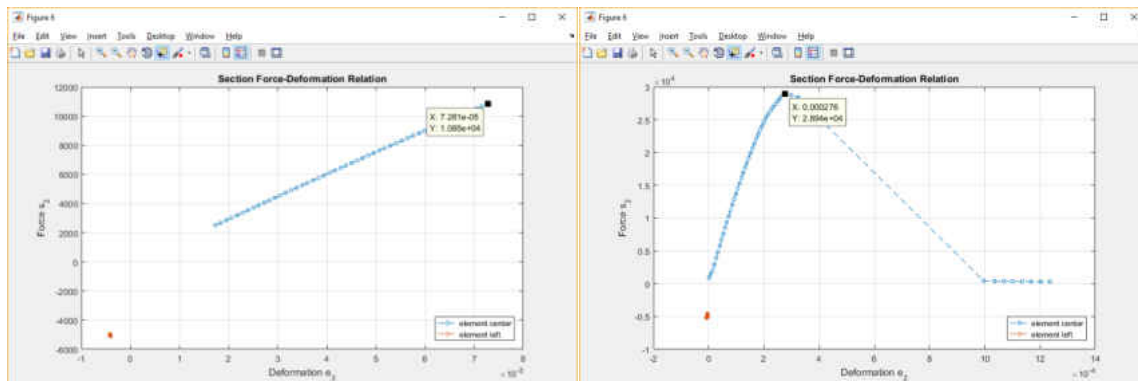
NAP - Run 6	Variable Live Load	Live Load (1)	Capacity (2)
Area (Aps)	2.45		
Prestress (fps)	250		
Live Load (Q)	7.9 + 31.9 + 31.9 = 71.7		

```

Editor - C:\Users\Chris\Dropbox\Adjah Mackie\NAP_v1r6\Chris_bridge_simple_firstv3A.m*
elasticBeam.m Chris_bridge_simple_firstv3A.m*
286 % Ue(0,1) = -40;
287
288 if LOAD_TYPE == 1
289     scale = 1;
290     Pe(14,2) = -7.9 * scale;
291     Pe(16,2) = -31.9 * scale;
292     Pe(18,2) = -31.9 * scale;
293 elseif LOAD_TYPE == 2
294     %Pe(center_node,2) = -225;
295     Ue(center_node,2) = -10.0e-0;
296 end
297

```

Live Load/Capacity Plots



NAP - Run 6	Variable Live Load	LiveLoad (1)	Capacity (2)
Area (Aps)	2.45	10850	28940
Prestress (fps)	250	10850	28940
Live Load (Q)	7.9 + 31.9 + 31.9 = 71.7	10850	28940

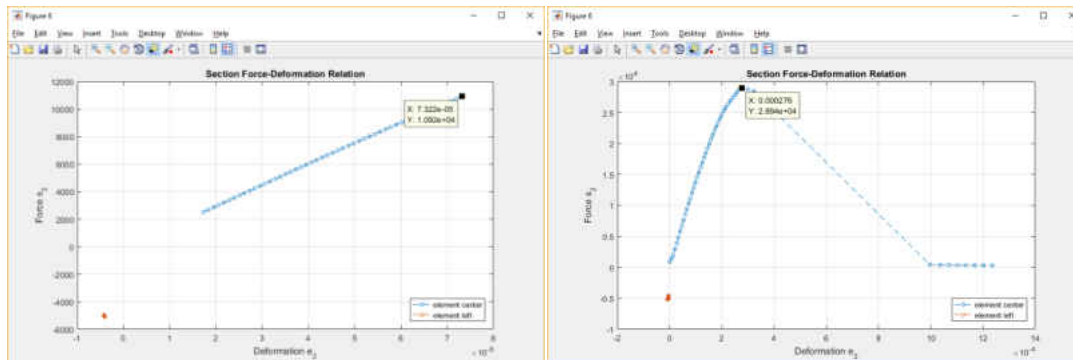
NAP - Run 7	Variable Live Load	Live Load (1)	Capacity (2)
Area (Aps)	2.45		
Prestress (fps)	250		
Live Load (Q)	8.1 + 32.1 + 32.1 = 72.3		

```

Editor - C:\Users\Chris\Dropbox\Adjah Mackie\NAP_v1r6\Chris_bridge_simple_firstv3A.m*
elasticBeam.m  Chris_bridge_simple_firstv3A.m*
286  % Ue(8,1) = -40;
287
288  if LOAD_TYPE == 1
289      scale = 1;
290      Pe(14,2) = -8.1 * scale;
291      Pe(16,2) = -32.1 * scale;
292      Pe(18,2) = -32.1 * scale;
293  elseif LOAD_TYPE == 2
294      %Pe(center_node,2) = -225;
295      Ue(center_node,2) = -10.0e-0;
296  end
297

```

Live Load/Capacity Plots



NAP - Run 7	Variable Live Load	Live Load (1)	Capacity (2)
Area (Aps)	2.45	10920	28940
Prestress (fps)	250	10920	28940
Live Load (Q)	8.1 + 32.1 + 32.1 = 72.3	10920	28940

LIST OF REFERENCES

- [1] National Economic Council, An Economic Analysis of Transportation Infrastructure Investment, Washington DC: The White House, 2014.
- [2] American Society of Civil Engineers, Report Card for America's Infrastructure, ASCE, 2017..
- [3] Central Florida Expressway Authority Authority, "Central Florida Expressway Authority," Central Florida Expressway Authority, 16 June 2015. [Online]. Available: <https://www.cfxway.com/TravelersExpressways/Expressways/CurrentExpressways/408EastWestExpressway/ConstructionProjects/tabid/348/Article/73/sr-408-widening-initiative.aspx>. [Accessed 20 August 2016]..
- [4] National Bridge Inventory Data, "UglyBridges.com," National Bridge Inventory Information, 18 January 2016. [Online]. Available: <http://uglybridges.com/1085616>. [Accessed 18 January 2017].
- [5] Hooke, R. "As The Extension, So The Force," 15 December 2016. [Online]. Available: <http://utsv.net/prestressed-concrete/pre-tensioning-vs-post-tensioning>. [Accessed 5 December 2016].
- [6] Post Tensioning Institute, "What is post - tensioning," PTI, Arizona, 2000.
- [7] Hussien, O. F., Elafandy, T. H. K, Abdelrahman A. A., Abdel Baky S.A. and Nasr, E. A., "Behavior of bonded and unbonded prestressed normal and high strength concrete beams," Housing and Building National Research Center (HBRC) Journal, vol. 8, no. 1, pp. 239 - 251, 2012.
- [8] Abdalla O. A., Ramirez J. A., and Lee R. H., "Strand Debonding in Pretensioned Beams - Precast Prestressed Concrete Bridge Girders with Debonded Strands," Indiana Department of Transportation, Indiana, 1993.
- [9] California Department of Transportation (Caltrans), "Bridge Design Specifications," Caltrans, California, 2000.
- [10] Florida Department of Transportation, "Bridge Load Rating Manual," FDOT, Florida, 2015.
- [11] Zokaie T. A. and Imbsen R., "Distribution of wheel loads on highway bridges," Transportation Research Board, Washington D.C., 1991.
- [12] Chen Y. and Aswad A., "Stretching span capability of prestressed concrete bridges under AASHTO LRFD," Journal of Bridge Engineering, vol. 3, no. 1, pp. 112 - 120, 1996.
- [13] Dennis M., "Simplified Live Load Distribution Factor Equations," National Cooperative Highway Research Program (NCHRP report 5920), Washington D. C. , 2007.
- [14] Eamon Christopher D., Parra - Montesinos Gustavo and Chehab Alaa, "Evaluation of Prestressed Concrete Beams In Shear," Michigan Department of Transportation,

- Michigan, 2014.
- [15] AASHTO, "LRFD Bridge Design Specifications," American Association of State Highway and Transportation Officials, Washington D.C., 2012.
- [16] The Democrat, "Tallahassee Democrat," USA Today Network, 10 December 2015. [Online]. Available: <http://data.tallahassee.com/bridge/florida/orange/sr-408-orange-blossom-trail/12-750238/>. [Accessed 15 December 2016].
- [17] Florida Department of Transportation, "Bridge and Other Structures Inspection and Reporting," Department of Transportation, Florida, 2014.
- [18] Sonnenberg A., "Load Capacity Assessment of Bridges," Small Bridges Conference 2014, Sydney Australia, 2014.
- [19] Estes C. A., and Frangopol M. D., "Load Rating versus Reliability Analysis," *Journal of Structural Engineering*, vol. 1, no. 1, p. 1, 2005.
- [20] F. Akgul and F. M. D. and, "Rating and Reliability of Existing Bridges in a Network," *Journal of Bridge Engineering*, vol. 8, no. 1, pp. 383 - 393, 2003.
- [21] R. Z. Shmerling, "Structural Condition Assessment of Prestressed Concrete Transit Guideways," University of Central Florida, Orlando, 2005.
- [22] C. R. Farrar and G. H. I. and James, "Identification of Dynamic Properties from Ambient Vibration Measurements," Pacific Conference on Earthquake Engineering, Melbourne, 1995.
- [23] Y. L. K. J. M. Xu and W. S. and Zhang, "Vibration Studies of Tsing Ma Suspension Bridge," *Journal of Bridge Engineering*, vol. 1, no. 1, pp. 149 - 156, 1997.
- [24] Q. W. Zhang, T. T. P. Chang and C. C. and Chang, "Finite - Element Model Updating for the Kap Shui Mun Cable - Stayed Bridge," *Journal of Bridge Engineering*, vol. 4, no. 6, pp. 285 - 293, 2001.
- [25] E. Aktan, N. Catbas and A. a. Z. Z. Turer, "Structural Identification: Analytical Aspects," *Journal of Structural Engineering*, vol. 1, no. 1, pp. 817 - 829, 1998.
- [26] A. Berman, "Validity of Improved Mathematical Models: A Commentary," 16th International Modal Analysis Conference, Schenectady, 1998.
- [27] M. I. Friswell and J. E. and Mottershead, "Finite Element Model Updating in Structural Dynamics," Kluwer Academic, Boston, 1995.
- [28] Q. W. Zhang and T. Y. P. a. C. C. C. Chang, "Finite - Element Model Updating for the Kap Shui Mun Cable - Stayed Bridge," *Journal of Bridge Engineering*, vol. 4, no. 6, pp. 285 - 293, 2001.
- [29] M. R. Biggs, F. W. Barton, J. P. Gomez, P. J. Massarelli and W. T. and Mckeel, "Finite Element Modeling and Analysis of Reinforced Concrete Bridge Decks," Virginia Transportation Research Council - U.S. Department of Transportation Federal Highway Administration, Virginia, 2000.
- [30] C. K. Base, "CSi Bridge," Computers and Structures, Inc., 10 June 2014. [Online]. Available: <https://wiki.csiamerica.com/display/csibrIDGE/Home>. [Accessed 10 June

- 2015].
- [31] Caltrans, "Bridge Design Practice," California Department of Transportation, California, 2015.
 - [32] AASHTO, "LRFD Bridge Design Specifications," American Association of State Highway and Transportation Officials, Washington D.C., 2004.
 - [33] A. C. Scordelis, "Computer Models for Nonlinear Analysis of Reinforced and Prestressed Concrete Structures," *PCI Journal*, vol. 1, no. 1, pp. 116 - 135, 1984.
 - [34] N. El-Mezaini and E. and Citipitioglu, "Finite Element Analysis of Prestressed and Reinforced Concrete Structures," *Journal of Structural Engineering*, vol. 10, no. 117, pp. 2851 - 2864, 1991.
 - [35] M. Arafa and G. and Mehlhorn, "Nonlinear Finite Element Analysis of Concrete Structures with a Special Model," *Computational Modeling of Concrete Structures*, vol. 1, no. 1, pp. 777 - 786, 1998.
 - [36] R. Benaim, *The Design of Prestressed Concrete Bridges - Concepts and Principles*, New York: Taylor & Francis, 2008.
 - [37] K. Mackie, *Nonlinear Analysis Program*, Orlando: University of Central Florida, 2010.
 - [38] L. Gao, *Load Rating Highway Bridges - Load and Resistance Factor Rating Method*, Denver: Outskirts Press Inc., 2013.
 - [39] C. A. Banchik and H. and Jasper, "Riding High in Las Vegas," *Civil Engineering*, vol. 3, no. 73, p. 68, 2001.
 - [40] K. D. Hjelmstad and M. R. and Banan, "On Building Finite Element Models of Structures from Modal Response," *Earthquake Engineering and Structural Dynamics*, vol. 1, no. 24, pp. 53 - 67, 1995.
 - [41] A. H. Nilson, D. Darwin and C. W. and Dolan, *Design of Concrete Structures*, New York: McGraw Hill Higher Education, 2004.
 - [42] R. M. a. P. J. A. Barker, *Design of Highway Bridges*, New York: John Wiley & Sons Inc., 1997.
 - [43] E. G. Nawy, *Prestressed Concrete: A Fundamental Approach*, Upper Saddle River: Pearson Education, 2010.
 - [44] A. C. Institute, "Building Code Requirements for Structural Concrete (ACI 318 - 02)," American Concrete Institute, Farmington Hills, 2002.
 - [45] J. Du, Y. Wang, W. Zuo and S. Yuan, "Investigation of engineering issues in bridge Widening," in *Mechanic Automation and Control Engineering (MACE), 2010 International Conference*, 2010.
 - [46] F. N. Catbas and A. E. and Aktan, "Condition and Damage Assessment: Issues and some promising indices," *Journal of Structural Engineering*, vol. 8, no. 128, pp. 1026 - 1036, 2002.
 - [47] AASHTO, "Manual for Condition Evaluation and Load and Resistance Factor Rating (LRFR) of Highway Bridges," American Association of State Highway and Transportation Officials, Washington D.C., 2005.

- [48] F. Akgul and M. D. and Frangopol, "Bridge Rating and Reliability Correlation: Comprehensive Study for Different Bridge Types," *Journal of Structural Engineering*, vol. 130, no. 1, pp. 1063 - 1074, 2004.
- [49] A. S. Nowak, "Calibration of LRFD Bridge Code," *Journal of Structural Engineering*, vol. 8, no. 121, pp. 1245 - 1251, 1995.
- [50] A. S. Nowak and K. R. and Collins, *Reliability of Structures*, New York: CRC Press, Taylor & Francis Group, 2013.
- [51] American Society of Civil Engineers, *Report Card for America's Infrastructure*, ASCE, 2013.
- [52] California Department of Transportation (Caltrans), "Bridge Design Specifications," Caltrans, California, 2000.
- [53] Barr Paul, Halling Marv, Petty Dave and Osborn Perry, "Shear Capacity of In - Service Prestressed Concrete Bridge Girders," Utah Department of Transportation Research Division, Utah, 2010.
- [54] Cliff F., "Service Life and Sustainability of Concrete Bridges," ASPIRE, Oregon, 2009.
- [55] Beatty T. L., "Life - Cycle Cost Analysis Primer," Federal Highway Administration Office of Asset Management, Washington DC, 2002.
- [56] FDOT, "Structures Design Guidelines," Florida Department of Transportation - Structures Design Engineers, Florida, 2016.
- [57] Aktan E., Chase S., Inman, D., and Pines, D., "Monitoring and Managing the Health of Infrastructure Systems," *Proceeding of the 2001 SPIE Conference on Health Monitoring of Highway Transportation Infrastructure*, Irvine, 2001.
- [58] D. Saydam, M. D. Frangopol and Y. and Doug, "Assessment of Risk Using Bridge Element Condition Rating," *Journal of Infrastructure Systems*, vol. 19, no. 1, pp. 252 - 265, 2013.
- [59] D. Ngo and A. C. and Scordelis, "Finite Element Analysis of Reinforced Concrete Beams," *ACI Journal*, vol. 3, no. 64, pp. 152 - 163, 1967.
- [60] DOT, "Notes to Designers for Prestressed Girders," Idaho Department of Transportation, Idaho, 2015.
- [61] C. & S. Inc., "CSi Bridge," Computers & Structures Inc., 1 January 2017. [Online]. Available: <https://www.csiamerica.com/products/csibrige> . [Accessed 22 January 2017].
- [62] C. S. Cai and M. and Shahawy, "Understanding Capacity Rating of Bridges from Load Tests," *ASCE Practice Periodical on Structural Design and Construction*, vol. 4, no. 8, pp. 209 - 216, 2003.
- [63] S. C. D. o. Transportation, *Structural Analysis and Evaluation*, South Carolina: SCDOT, 2006.